The Role of Permanent Carbon Dioxide Removal in the Power Sector

A thesis submitted for the degree of
Doctor of Philosophy (PhD)

by

Augustin Leonardo Prado

Centre for Environmental Policy

Centre for Process Systems Engineering

Imperial College London

May 2023

Supervision: Prof. Niall Mac Dowell – Financial support: Total Energies

Statement of Originality

I declare that this thesis, entitled *The Role of Permanent Carbon Dioxide Removal in the Power Sector*, is entirely my work and that where any material could be construed as the work of others, it is fully cited and referenced and with appropriate acknowledgement given.

Copyright Declaration

The copyright of this thesis rests with the author. Unless otherwise indicated, its contents are licensed under a Creative Commons Attribution-Non Commercial 4.0 International Licence (CC BY-NC). Under this licence, you may copy and redistribute the material in any medium or format. You may also create and distribute modified versions of the work. This is on the condition that: you credit the author and do not use it, or any derivative works, for a commercial purpose. When reusing or sharing this work, ensure you make the licence terms clear to others by naming the licence and linking to the licence text. Where a work has been adapted, you should indicate that the work has been changed and describe those changes. Please seek permission from the copyright holder for uses of this work that are not included in this licence or permitted under UK Copyright Law.

Abstract

In light of the current climate crisis context, utmost effort should be directed towards climate mitigation activities. Amongst them, the sustainable and cost-effective deployment of Carbon Dioxide Removal (CDR) solutions is integral to meeting global climate goals. As some CDR will have direct interaction with power, either by consuming or by producing it, it is imperative to measure the different impacts that CDR operations may have on the energy, and more specifically, the power system. Additionally, the fervour surrounding carbon removal frequently disregards one of its most significant facets: its permanence. Because of the long life of carbon dioxide (CO_2) in the atmosphere, politics, with the help of the scientific community, needs to incorporate the long-term effects of CO_2 emissions in today's decisions. Equivalently, fungibility between removals and emissions must be carefully monitored.

In this thesis, we propose a framework for co-optimizing the power and CDR sectors, using the UK as a case study. We identify techno-economically and biogeophysically feasible pathways to meeting the net zero targets through the deployment of a range of CDR methods. We find that biomass availability is crucial to meet national targets, through the deployment of BECCS and biochar. When biomass is abundant, BECCS plays a significant role in achieving net zero targets, and natural gas with CCS and intermittent renewables are less important. Furthermore, we propose a climate repair value metric to assess the permanent cost of each CDR solution. Through this metric, geological storage demonstrates significantly greater permanence when compared to less secure CDR methods, such as biochar or afforestation.

This thesis aims to convey clear messages to policymakers and corporations operating in the CDR or energy sector by offering valuable insights into the implementation of a permanent CDR portfolio to achieve climate commitments and their implications in the national power mix.

Acknowledgement

I would like to express my sincere gratitude to my supervisor, Niall, for his guidance, support, and encouragement throughout my research. His expertise and feedback have been invaluable to me, and I am truly grateful for his mentorship.

I would also like to thank my colleagues, in particular Mai, Nixon, Solene, Mathilde, Piera, Yoga, Marwan, Matthias, Ro, for their contributions, insights, and discussions that have been instrumental in shaping my ideas and perspectives on my thesis topic. Also, to CEP people for creating a friendly, collaborative, and inspiring research environment.

My family and friends have been a constant source of support and motivation, and I cannot thank them enough for their encouragement and understanding during this challenging period of my academic career.

I would also like to extend my appreciation to Total Energies for their funding support. Their financial assistance has enabled me to cover my research expenses and participate in various academic conferences and workshops. Moreover, the insightful discussions and meetings with Fabrice have been highly valuable in shaping my research objectives and outcomes.

Finally, I would like to express my gratitude to all those who have contributed to my thesis in any way, be it through providing data, feedback, or simply sharing their ideas and experiences with me. Your contributions have made a significant impact on the quality and depth of my research, and I am deeply grateful for your support.

Table of contents

1. Introduction 20
1.1 Motivation 20
1.1.1 The Paris Agreement, starting point of a (coming) revolution 20
1.1.2 The carbon market, a key actor in the transition to a low-carbon economy 21
1.1.3 Need for CDR and the importance of good wording 22
1.1.4 Energy systems, Policy Stability, and CDR 24
1.1.5 A tonne is not a tonne: the real value of a removal 26
1.1.6 Delivering in time the infrastructure to enable a sustainable and permanent energy transition towards net zero emissions in the UK 28
1.2 Objectives 29
1.3 Structure 29
2 The emergence of Carbon Dioxide Removal solutions 30
2.1 CDR status in Europe and the United Kingdom (UK) 30
2.1.1 CDR in Europe 30
2.1.2 CDR in the United Kingdom (UK) 31
2.2 CDR details 32
2.2.1 Bioenergy with Carbon Capture and Storage (BECCS-power) 34
2.2.1.1 BECCS GHG balance 39
2.2.1.2 BECCS cost balance 42
2.2.1.3 BECCS removal cost 44
2.2.1.4 BECCS power balance 45
2.2.2 Direct Air Carbon Capture and Storage (DACCS) 47
2.2.2.1 DACCS GHG balance 48
2.2.2.2 DACCS cost balance 50
2.2.2.3 DACCS removal cost 51
2.2.2.4 DACCS power balance 51
2.2.3 Afforestation/Reforestation (AF) 52
2.2.3.1 AF GHG balance 55
2.2.3.2 AF cost balance and removal cost 58
2.2.3.3 AF power balance 59
2.2.4 Enhanced Weathering (EW) 59
2.2.4.1 EW GHG balance 62
2.2.4.2 EW cost balance 66
2.2.4.3 EW power balance 67
2.2.5 Biochar (BC) 69
2.2.5.1 BC GHG balance 71

2.2.5.2 BC cost balance 74
2.2.5.3 BC removal cost 74
2.2.5.4 BC energy balance 75
2.3 Comparative assessment of CDR 76
2.3.1 Characteristics of CDR deployment in the UK 76
2.3.2 Energy services and requirements 77
2.3.3 Electricity price variation 79
2.3.4 Land use efficiency 80
2.4 MONET optimisation 82
3 Power sector model and interaction with MONET 85
3.1 Electricity System Optimisation 86
3.2 ESO first results 88
3.3 The joint ESO-MONET (EM) framework 90
3.3.1 Convergence and constraints of EM framework 90
3.3.2 Impact of CDR deployment on the electricity system 93
3.3.3 Only one CDR available 94
3.3.4 No Biomass and different levels of biomass available 94
3.4 ESO-MONET Sensitivity Analysis to the availability of imported pellet and AF expansion rate 99
4 Permanence considerations 103
4.1 The case of predictably leaky CDR 104
4.1.1 The BC example 104
4.2 Climate Repair Value (CRV) 112
4.3 Cost of Permanent Removal (CPR) 118
4.4 Permanence assessment of CDR 119
5 CDR-power sector interaction, permanence, and final thoughts 125
5.1 Permanence perspectives on the integration of CDR in the power sector 125
5.2 CO_2 transport and storage availability 128
6 Conclusion 130
6.1 Key conclusions and contributions made 130
6.1.1 Optimal CDR portfolio in the UK (today-2050) 131
6.1.2 The optimal power system in the UK (today-2050) 133
6.1.3 How does the power-CDR system integration change the optimal CDR, and power sector in the UK? 134
6.1.4 How do permanence assumptions change the cost of removal, thus the optimal CDR portfolio? 135

6.1.5 Optimal CDR-power sector deployment given practical assumptions 136
6.1.5.1 Permanence horizon assumption 136
6.1.5.2 CCS infrastructure availability 136
6.2 Limitations and future work 137
6.2.1 Limitations 137
6.2.2 Future work 139
6.2.2.1 What is the role of CDR solutions, in a larger economy-wide setting, to meet net-zero targets? 139
6.2.2.2 Investigate the regional deployment of CDR solutions: the ESONE-MONET framework 139
6.2.2.3 What are the risks of investing in CDR solutions at a global scale? 140
References 141
Appendix 151
A. MONET optimisation equations 151
B. Permanence results 159

List of Figures

Figure 1.1: The Society – Climate Change – Energy Trilemma 25
Figure 1.2: The role of CDR solutions within different Earth's biospheres 27
Figure 2.1: The biomass supply chain will be used for BECCS and Biochar modelling. 36
Figure 2.2: Overall Picture of BECCS [52] 39
Figure 2.3: Emissions of the BECCS supply chain that includes three biomass types.[20], [22] 42
Figure 2.4: Removal Cost of BECCS for four biomass types. 45
Figure 2.5: Overall picture of DACCS 48
Figure 2.6: GHG emissions for DACCS (Liquid Solvent and Solid Sorbent) 50
Figure 2.7: Removal cost of DACCS ($/$t_{CO2}$) 51
Figure 2.8: Overall picture of Afforestation 54
Figure 2.9: Reforestation potential in the UK, according to Griscom et al. [3] 55
Figure 2.10: Cumulative Afforestation GHG emissions over 50 years in *Temperate Oceanic* ecological zone. Computed through our afforestation model, replicated from [20]. 58
Figure 2.11: Removal cost ($/$t_{CO2}$) of Afforestation. 59
Figure 2.12: Overall picture of Enhanced Weathering (EW) 61
Figure 2.13: Carbon capture via Enhance Weathering considering four types of rocks, computed with targeted particle size of 10 μm. 64
Figure 2.14: Emissions of Enhanced Weathering process considering four types of rock. 66
Figure 2.15: Cost of Enhanced Weathering process considering five types of rock. 67
Figure 2.16: Overall picture of biochar (BC) 71
Figure 2.17: Cumulative emissions along the biochar supply chain (in t_{CO2} per ha) 73
Figure 2.18: Removal cost of Biochar 75
Figure 2.19: Energy requirements for various CDR pathways. 78
Figure 2.20: CDR removal cost variations with different electricity prices. 79
Figure 2.21: Land-use efficiency of CDR solutions 82
Figure 2.22: NETs deployment in the UK with CCC's 2050 target. 84
Figure 3.1: Least-cost evolution of the UK electricity system from 2020 to 2050 to net zero* 89
Figure 3.2: ESO-MONET Joint-System framework 92
Figure 3.3: ESO-MONET Optimisation in No-Biomass Scenario (2020-2050) 95
Figure 3.4: ESO-MONET Optimisation in All-Low-bio Scenario (2020-2050) 96
Figure 3.5: ESO-MONET Optimisation in All-High-bio Scenario (2020-2050) 97
Figure 3.6: ESO-MONET scenario's cumulative costs 98
Figure 3.7: Power technology variations compared to their generation share in the ESO reference scenario 100
Figure 3.8: ESO-MONET System (EM) evolution in 2050 imported biomass availability 102
Figure 4.1: Decay Kinetics of Biochar 105
Figure 4.2: Annual Sequestration of a predictably leaky CDR 109
Figure 4.3: Cumulative Sequestration of a predictably leaky CDR 110
Figure 4.4: Graphical representation of permanent (blue numbering) versus temporary removal (black numbering) 112
Figure 4.5: Illustration of the climate damage caused by an unmitigated emission. 114

Figure 4.6: Carbon remaining in the atmosphere, under a variety of temporary or permanent removal scenarios. 116
Figure 4.7: CO_2 leakage curves for diverse types of sequestration and times of permanence TP..... 121
Figure 4.8: Cost of permanent removal for a range of CDR pathways as a function of TP. . 122
Figure 5.1: Evolution of the 2050 CDR portfolio and power generation mix with different times of permanence 127
Figure 5.2: Evolution of the 2050 CDR portfolio and power generation mix with different CO_2 T&S infrastructure availabilities..... 129

List of Tables

Table 2.1: Rock Properties..... 63
Table 2.2: Decay Coefficient for different biomass types for study-specific pyrolysis conditions. 74
Table 2.3: Deployment rates and land availability constraints 77
Table 2.4: Carbon budgets and finances 83
Table 3.1: National Emission Target for the power sector in the UK [88] 87
Table 4.1: Coefficients and timescales representing the earth system removals..... 113
Table 4.2: Results for Climate Repair Values (CRV). 117
Table 5.1: Impact in CDR power mix depending on permanence assumptions, and T&S availabilities 129

Nomenclature

Notation	Unit	Descriptions
Indices		
g, g’	-	Regions
l	-	Transport mode (train, truck, ship)
i, i’,i’’	-	Biomass material (raw material, pellets, and chars)
s	-	Silicate source
t	-	Period
ez	-	Ecological zones
c	-	Climate
sp	-	Tree species
sc	-	DACCS type
Sets		
G	-	Set of all domestic regions
H	-	Set of regions with ports
P	-	Set of pellets (miscanthus pellet, poplar pellet, forest residues pellet, crop residues pellet, imported pellet)
B	-	Set of raw biomasses (miscanthus, poplar, forest residues, crop residues)
BC	-	Set of chars (miscanthus char, forest residues char, crop residues char)
L	-	Set of transport mode L = {truck, train, ship}
S	-	Set of silicate rocks
M	-	Set of materials M = S **U** P **U** B
Ez	-	Set of Ecological zones
C	-	Set of climates in the UK C = {Temperate}
Sp	-	Set of tree species Sp = {broadleaf, coniferous}
Sc	-	Set of DACCS plant types = {Liquid Solvent, Solid Sorbent}
Functions		
$pel(.)$	-	1-1 mapping between biomass set and pellet set
$char(.)$	-	1-1 mapping between biomass set and biochar set
General parameters		

$Dist(g, g')$	km	Inter-region Euclidean distance between region g an g'
$Dist_{intra}(g, g')$	km	Intra-region Euclidian distance in region g
α	hours per year	Annual operating hours
r	%	Discount rate
GHG_{elec}^{1kWh}	t_{CO2}/kWh	GHG emissions associated with producing 1kWh of electricity
GHG_{fuel}^{1L}	t_{CO2}/l	GHG emissions associated with using 1 litre of diesel
$GHG_{i,l}^{transp}$	t_{CO2}/tonne/km	GHG emissions associated with transporting material i over 1km
$cost_{elec}^{1kWh}$	\$/t_{CO2}	Cost of producing 1 kWh of electricity
$UTC_{i,l}$	\$ per tonne	Transport cost of product *i* via transport mode *l*
$D(t)$	seconds	Duration of a project since the beginning

Biomass property parameters

HHV_i	MJ/t_{DM}	Higher heating value of biomass *i*
DMR	%	Dry matter rate in pellet
$Cbio_i$	t_C/t_{DM}	Carbon content of dry biomass of type *i*
$Yield_{i,g}$	t_{DM}/ha of harvested land/yr	Yield of biomass *i* in region *g*
$Landa_{g,t}$	ha	Marginal land available in region *g* at time *t*
$BA_{i,g}^{max}$	t_{DM}/yr	Biomass *i* availability

CDR parameters

$TotCost_{CDR}$	\$/$unit_{CDR}$	Total Cost of CDR
$TotCapex_{CDR}$	\$/$unit_{CDR}$	Capital Expenditures of a CDR plant
$TotOpex_{CDR}$	\$/$unit_{CDR}$	Operational Expenditures of CDR
CR_{CDR}	t_{CO2}/$unit_{CDR}$	Carbon removed by CDR
CC_{CDR}	t_{CO2}/$unit_{CDR}$	Carbon captured by CDR
CE_{CDR}	t_{CO2}/$unit_{CDR}$	Carbon emitted by CDR
RC_{CDR}	\$/t_{CO2}	Removal cost of CDR
$unit_{BECCS}$	ha of harvested land.yr	Unit used for BECCS
$unit_{DAC}$	plant.yr	Unit used for DACCS
$unit_{AF}$	ha of forests.yr	Unit used for AF
$unit_{EW}$	t_{rock}	Unit used for EW
$unit_{BC}$	ha of harvested land.yr	Unit used for BC

BECCS parameters

β	%	Carbon capture and storage rate
$Capacity^{BECCS}$	MW/plant	BECCS power plant capacity
$OPEX^{BECCS}$	$/$t_{DM}$	Non-Fuel Operating expenditures of a BECCS plant
$Cost_{raw\ bio,i}$	$/$t_{DM}$	Cost of raw biomass *i*
UPC_i	$/$t_{DM}$	Unit conversion cost of pellet *i*
γ_i	t_{DM}/tonne raw material	Conversion factor of raw material *i* to pellet
$IMPC$	$ per t_{DM}	Imported pellet cost
η_i^{BECCS}	%	Electricity generation efficiency from BECCS plant with fuel *i*
$capfact(t)$	%	BECCS utilisation/capacity factor

Input parameters for optimisation (BECCS)

$CE_{Land,i,g}$	t_{CO2}/ha of harvested land/yr	Emissions from land operations
$CE_{Farm,i.g}$	t_{CO2}/ha of harvested land/yr	Emissions from farming operations
$CE_{Pelleting,i,g}$	t_{CO2}/ha of harvested land/yr	Emissions from biomass/pellet processing
$CE_{transp,i,g}$	t_{CO2}/ha of harvested land/yr	Emissions from biomass/pellet transport
$CE_{CO_2\ T\&S,i,g}$	t_{CO2}/ha of harvested land/yr	Emissions from CO_2 T&S
$Cost_{Pellet,i,g}$	$/ha of harvested land/yr	Cost of biomass pellets
$VarNFOPEX_g^{BECCS}$	$/ha of harvested land/yr	Variable non-fuel OPEX of BECCS plant
$Cost_{CO_2T\&S,i,g}$	$/ha of harvested land/yr	Cost of CO_2 T&S
$Rev_{Power,i,g}$	$/ha of land/yr	Revenues from power generation
$Cost_{PP,i,g}$	$/ha of harvested land/yr	Cost of pellet production (includes marginal land rent, crop management, and harvesting operation costs)
$Cost_{Import,g}$	$/ha of harvested land/yr	Cost of Imported Pellets
$Cost_{transp,i,g}$	$/ha of harvested land/yr	Cost of pellet transport

DACCS parameters

Input parameters for optimisation (DACCS)

$CostEnergy_{DAC,sc}$	$/plant/year	Cost of energy use of DACCS plant

$NonVarOpex_{DAC,sc}$	\$/plant/year	Variable non-fuel OPEX of DACCS plant
$CostT\&S_{DAC,sc}$	\$/plant/year	Cost of CO_2 T&S
$CE_{Energy,sc}$	t_{CO2}/plant/year	Emissions related to energy use of DACCS plant
$CE_{CO_2T\&S,sc}$	t_{CO2}/plant/year	Emissions occurring during the CO_2 T&S supply chain

Afforestation parameters (AF)

$B^{AG}_{Ref,ez,t}$	t_{DM}/ha	Maximum above-ground biomass stock of reference
$T_{Ref,ez}$	years	Growing period of reference
$B^{tot}_{Ref,ez,t}$	t_{DM}/ha	Maximum total biomass stock of reference
$CE^{AF}_{Thinning}$	t_{CO2}/ha	Emissions from thinning
$Freq_{Thin}$	years	Thinning frequency
t_{MMAG}	years	Maximum mean annual growth (MMAG)

Input parameters for optimisation (AF)

$CC_{c,sp}$	t_C/tDM	Carbon content in forest biomass depending on climate c and species sp
CE^{AF}_{RC}	t_{CO2}/ha	Emissions from road construction
CE^{AF}_{GP}	t_{CO2}/ha	Emissions from ground preparation
CE^{AF}_{SPl}	t_{CO2}/ha	Emissions from seedling plantations
CE^{AF}_{Fert}	t_{CO2}/ha	Emissions from fertiliser use
CE^{AF}_{Herb}	t_{CO2}/ha	Emissions from herbicide use
CE^{AF}_{RM}	t_{CO2}/ha	Emissions from road maintenance

Enhanced Weathering parameters (EW)

$R_{CO_2,s}$	t_{CO2}/t_{rock}	Maximum CO_2 capture potential of the silicate material
$Capacity^{mining}$	t_{rock} per year	Capacity of silicate extraction in region *g*
$Capacity^{commin}$	t_{rock} per year	Capacity of silicate comminution in region g
$elec_s^{crushing}$	kWh/t_{rock}	Electricity consumption for silicate extraction
$elec_s^{commin}$	kWh/t_{rock}	Electricity consumption for comminution
$fuel^{EW}_{app}$	l/t_{rock}	Fuel consumption for rock spreading (application)
$p^{max}_{weathered}$	%	Max weathering rate
$p^{int,weathered}_{g,d,s,t}$	%	Intermediate rock weathering rate at time *t*
$p^{weathered}_{g,d,s,t}$	%	Rock weathering rate at time *t*
W_s	kWh/ t_{rock}	Working index for silicate rock s
V_m	$m^3 mol^{-1}$	Molar volume
W_r	$mol.m^{-2}.s^{-1}$	Weathering rate
$C_{temperature,g}$	-	Correction factor related to average soil temperature
$R_{CA,s}$	$t_{silicate}/t_{rock}$	Maximum CDR potential of rock *s*

ω	$mol_{CO_2}/mol_{silicate}$	Molecule of CO_2 removed
E_a	J.mol^{-1}	Activation energy
R	-	Universal gas constant
T_g	°C	Annual average soil temperature
$d_m(d)$	μm	Targeted article diameter
$d_{ini}\ (s)$	μm	Initial particle diameter
$Rocka_{s,g}$	t_{rock}/year	Rock availabilities for rock *s* in region *g*
$Cropa_g$	ha	Cropland availability in region *g*

Input parameters for optimisation (EW)

$Capex_{mining,s}$	\$/t_{rock}	CAPEX related to mining infrastructures
$Capex_{commin,s}$	\$/t_{rock}	CAPEX related to comminution infrastructures
$Cost^{EW}_{fixOM,s}$	\$/t_{rock}	Fixed OPEX
$Cost^{EW}_{elec,s}$	\$/t_{rock}	Cost of electricity
$Cost^{EW}_{transp,s,g}$	\$/t_{rock}	Cost of rock transport
$Cost^{EW}_{app}$	\$/t_{rock}	Cost of rock application
$Cost^{EW}_{mining,s}$	\$/t_{rock}	OPEX related to mining operation
$Cost^{EW}_{Recycling,s}$	\$/t_{rock}	OPEX related to recycling operation
$Cost^{EW}_{Commin,s}$	\$/t_{rock}	OPEX related to comminution operation
$Cost^{EW}_{GA,s}$	\$/t_{rock}	General & administration OPEX
$cost^{EW}_{OM,app}$	\$/t_{rock}	Operating and maintenance cost of silicate rock spreading
$cost^{EW}_{fuel,app}$	\$/t_{rock}	Fuel cost of silicate rock spreading
$CE^{EW}_{elec,s}$	t_{CO2}/t_{rock}	Emissions from electricity use
$CE^{EW}_{fuel,s,g}$	t_{CO2}/t_{rock}	Emissions from fuel use
$CE_{transp,s,g}$	t_{CO2}/t_{rock}	Emission from rock *s* transport in region *g*

Biochar parameters (BC)

$FeedPyP$	t_{DM}/yr	Pyrolysis plant feedstock consumption
$Yield_C_{char}$	%	Biochar carbon yield
	-	
	t_C in biochar/t_C in biomass	
eff_{BC,C_k}	%	Biochar efficiency of pyrolysis
$Stable_C$	%	Proportion of carbon that is permanently fixed in the char
η_{BC,C_k}	%	Power efficiency of pyrolysis

Input parameters for optimisation (BC)

$CE_{biom,i,g}$	t_{CO2}/ha of harvested land/yr	Emissions from the biomass supply chain
$CE_{char,i,g}$	t_{CO2}/ha of harvested land/yr	Emissions from the biochar supply chain
$CE^{BC}_{transp,i,g}$	t_{CO2}/ha of harvested land/yr	Emissions from the biochar transport
$CE^{BC}_{app,i,g}$	t_{CO2}/ha of harvested land/yr	Emissions from the biochar application on croplands
$Cost_{Pellet,i,g}$	$/ha of harvested land/yr	Pellet cost (including land rent, land input, chemicals, and farming operation costs)
$VarNFOPEX_{BC,i,g}$	$/ha of harvested land/yr	pyrolysis non-variable operating costs
$Cost_{App,BC,i,g}$	$/ha of harvested land/yr	Cost of biochar application

Variables

$D_{i,g,t}$	tonne of material per year	Demand of material *i*, in region *g* at time *t*
$P_{i,g,t}$	tonne of material per year	Production of material *i*, in region *g* at time *t*
$Q_{igg'lt}$	tonne of material per year	Flow of material *i*, between region *g* and *g'* at time *t* using transport mode l
$N^{CDR}_{g,t}$	-	Number of *CDR* units built in region g, at time t, for CDR
$ON^{CDR}_{g,t}$	-	Number of *CDR* units operating in region g, at time t, for CDR
$P^{CDR}_{g,t}$	MWh/yr	Power generated by CDR
$Area_used_{i,g,t}$	ha	MAL area used for biomass *i* in region *g* at time *t*

Abbreviations

AF	Afforestation/reforestation
AR6	IPCC Sixth Assessment Report
BC	Biochar
BECCS	Bioenergy with carbon capture and storage
CAPEX	Capital expenditures
CCS	Carbon capture and storage
CDR	Carbon dioxide removal
CH_4	Methane
CO_2	Carbon dioxide
DACCS	Direct air capture with carbon dioxide storage
DM	Dry mass (biomass)
EU	European Union
EW	Enhanced weathering
FAO	Food and Agriculture Organisation
GHG	Greenhouse gas
GWP	Global warming potential
IAM	Integrated assessment model
IPCC	International Panel on Climate Change
IEA	International Energy Agency
ILUC	Indirect land use change
IRF	Impulse Response Function
LUC	Land use change
MAL	Marginal land
MONET	Modelling and Optimisation of Negative Emissions Technologies
MILP	Mixed Integer Linear Programming
NDCs	National determined contributions
NET	Negative emissions technology
NUTS	Nomenclature of territorial units for statistics
N_2O	Nitrous oxide
OPEX	Operating expenditures
RP	Reforestation Potential
SDGs	Sustainable development goals

T&S	Transport and storage
UK	United Kingdom
UNFCCC	United Nations Framework Convention on Climate Change
WM	Wet mass (biomass)

Chapter 1

1. Introduction

1.1 Motivation

Climate change is indeed considered one of the major societal challenges of the modern era. The scientific understanding of climate change has been evolving for many decades, and evidence of its existence can be traced back to earlier times. Callendar et al. provided evidence of the link between rising carbon dioxide (CO_2) and global temperature increase in 1938 [1]. However, it wasn't until the 1970s that climate models estimating the future impacts of anthropogenic CO_2 emissions on Earth's surface temperature began to emerge. These models, based on computer simulations and various climate factors, aimed to project the potential consequences of increased greenhouse gas emissions on global temperatures [2]. Since then, scientific research has continued to advance our knowledge of climate change, including its causes, impacts, and potential solutions. The issue of climate change has gained significant attention in recent decades as its urgency and potential consequences have become more apparent.

Meanwhile, global carbon emissions have always kept increasing, regardless of international agreements and several reports from the Intergovernmental Panel on Climate Change (IPCC) that summarise the findings of the scientific community. Through the publication of the IPCC's last report (AR6) [3], the scientific community has raised an alarm for immediate action, and yet most policy and individual changes are to come. Even though we observe a stabilisation or even a decrease of emissions in Europe and the USA in the last decade, emissions from rapidly developing countries like China, and India, are rising and driving global emissions to an all-time high record, in 2022. These countries, along with other emerging economies, have experienced significant economic growth and industrialization, resulting in increased energy consumption and greenhouse gas emissions.

1.1.1 The Paris Agreement, starting point of a (coming) revolution

The Paris Agreement [4] – ratified by 187 countries in 2015 – has been the starting point of many ambitions to limit global warming to 1.5°C over pre-industrial references.

As of today, there is no credible pathway to reach the 1.5°C target, given the current emissions trajectory [5]. Instead, a credible goal is to limit global temperature to below 2°C and come down to 1.5°C by 2100, through the use of negative emissions. Over the past decades, it has been proven that global temperature rise and CO_2 anthropogenic emissions

are almost linearly correlated, implying that temperature targets can be translated to remaining carbon budget equivalents [6], [7]. Therefore, reaching net-zero CO_2 emissions is considered crucial to halt the temperature increase [8]. However, the temperature outcomes after reaching global net zero CO_2 emissions will also depend on non-CO_2 emissions and emissions of aerosols. Even though CO_2 plays a major role in the determination of temperature rise, focusing on CO_2 emissions only will not provide a complete solution to the problem that global warming poses.

International communication will be a key component of the fight against climate change, as the world's economy will be at stake. The effects of climate change, such as extreme weather events, rising sea levels, and resource scarcity, can have severe economic and social consequences, particularly for vulnerable regions and populations.

Key coming challenges in the international discussion include the question of countries' responsibility and their role in the global temperature rise, thus assigning carbon budgets per region (or per country). These discussions will need a tremendous participatory effort from major historical and current polluters (EU, UK, USA, Russia, China, India), and new players in the emergent ground (Africa, South America) during international meetings. Inclusivity and participation of all countries, both developed and developing, are crucial for achieving effective climate action and addressing the global nature of the challenge. Defining the end-goals, *i.e.*, country-specific targets is a required step, as different countries have different capacities, responsibilities, and circumstances, and their targets should reflect these variations. It is also key to determine the various global and regional economic and financial mechanisms – including carbon markets, fiscal policies, subsidies, and investments in renewable energy and green technologies – to effectively decarbonise the economy, without stumbling into a major financial crisis.

1.1.2 The carbon market, a key actor in the transition to a low-carbon economy

The carbon market is anticipated to play a significant role in enhancing global cooperation by fostering the adoption of low-carbon solutions. In particular, through Article 6 of the Paris Agreement [4], that delineates international carbon policies.

Therefore, a scrupulous deployment of the carbon market is needed to enable a green and economically friendly transition. In Europe, we can distinguish the compliant from the voluntary carbon market.

On the one hand, the compliant carbon market – known as the European Emission Trading Scheme (EU-ETS) –, became operative in 2005. Today it covers the electricity and heat sector, energy-intensive industries (oil refineries, steel, iron, cement), commercial aviation, and will be including shipping emissions by 2024. Governed by a cap-and-trade system, the goal of the EU-ETS is to control European emissions, and eventually reduce them progressively to reach a specific target (*e.g.*, zero-emission target), by providing fewer allowances over time. Critics claim that asymmetrical climate policies can cause carbon leakage, *i.e.*, that some polluting manufacturing operations have been delocalised to other regions to avoid the tax, and that

the EU-ETS is faulty. However, a 2019 study from the Global Trade Analysis Project (GTAP), finds no evidence and concludes that the EU-ETS did not cause carbon leakage [9].

In addition, the European Parliament has proposed a new Carbon Border Adjustment Mechanism (CBAM) to equalize trade competitiveness for EU importers and reduce carbon leakage. From October 2023, EU importers will have to report the amount of embedded Greenhouse Gas (GHG) emissions in their imports from six covered sectors: iron and steel, cement, fertilizers, aluminium, electricity, and hydrogen. From 2026, EU importers will have to purchase CBAM certificates corresponding to embedded emissions – billed as the world's first major carbon border tax levy. CBAM aims to gradually phase-out free allowances for covered sectors under the EU-ETS by 2034. The impact on global trade could be significant, eventually increasing the cost of materials for carbon-intensive producers or disrupting supply chains. However, if implemented on a transparent basis, the EU-ETS might well become an effective tool.

On the other hand, the voluntary carbon market (VCM) is rapidly evolving but is still immature. Certifications to ensure verifiable carbon offset credits are being proposed, but there are no common agreed principles, yet. The Integrity Council for the VCM (ICVCM) is currently working on the draft Core Carbon Principles (CCPs) that will be used to promote and ensure high integrity across different marketplaces. In the draft assessment, the CCPs are enumerated as follows:

A. Program Governance
B. Robust Validation & Verification
C. No Double-Counting
D. Registry
E. Mitigation Activity Information
F. Sustainable Development
G. Additionality
H. Permanence
I. Robust quantification
J. Transition toward Net-Zero Emissions
K. Attributes
L. Alignment with the Paris Agreement

Among the different mitigation activities that are sellable on the VCM, we can distinguish between emissions reductions, and offset, also called carbon dioxide removal (CDR), or negative emissions. Even though CDR credits are not very popular yet, some marketplaces do focus on CDR (*e.g.*, Puro.earth [10], Carbonfuture [11]) and big tech companies have shown interest in these technologies, aiming to reach net zero emissions for some (British Petroleum, Total Energies), mitigate current and past emissions for others (Microsoft), or even reach negative targets (Stripe).

1.1.3 Need for CDR and the importance of good wording

Within the scope of decarbonisation, it is primordial to distinguish two different actions: emissions reduction (or mitigation), and removals. 'Reductions', as explained by the United

Nations Environment Program (UNEP), refer to the "efforts to reduce or prevent the emission of greenhouse gasses". Indeed, emissions reduction practices can be breakdown into different categories:

- Technologies innovation (*e.g.*, renewable energy instead of fossil fuel, green hydrogen fuel)
- Renovate older equipment to make it more efficient. (Building renovation, such as heat pumps installation)
- Behaviour change (*e.g.*, reducing our meat consumption, transport carbon footprint)

Decarbonisation *via* technology innovation and renovation will be needed. It has already started and is fostered by policies (Inflation reduction act in the US, European Green Deal in Europe). For example, in the UK, a high share of the transport and building sector emissions reduction is foreseen *via* electrification. In the last Net Zero Strategy report from the UK Government, the three scenarios estimated different electrification levels, which increased by a factor of 1.88 in the 'High resource scenario' to more than doubling in the 'High electrification scenario' [12]. In the same scenarios, emissions from industries are abated through hydrogen and CCUS pathways, along with massive electrification. The transport sector can be partially decarbonised through electrification, but heavy goods and personal transport will be harder to decarbonise using such a pathway. A possible solution is to tackle some of its emissions with hydrogen if hydrogen production can reach 500 TWh by 2050. Aviation and agriculture, along with heavy transports are considered 'hard-to-abate' sectors, meaning that it is unlikely that we come up with solutions to abate these emissions by the crepuscule of this half-century. Such a scenario is encapsulated in the 'High innovation scenario'.

Although the need for technology innovation is undebatable, whether we will need to drastically change our habits is still part of the ongoing societal debates [13].

Moreover, as said above, if net zero emission is a global or a national goal, the deployment of technologies to abate the 'hard-to-abate' emissions, that are either unforeseeable or too expensive, is inevitable ([12], [14]). This need will most probably be satisfied through the deployment of carbon dioxide removal solutions. 'Removals' stands for the set of all actions that can be deployed to capture greenhouse gases (GHG) and remove them from the atmosphere, storing them in the lithosphere, land, and ocean biosphere, or materials. The set of technologies used are often called Greenhouse Gas Removal (GGR) technologies, Negative Emissions Technologies (NET), or more specifically Carbon Dioxide Removals (CDR), and the latter notion will be mainly used throughout this dissertation. CDR solutions that appear to be the main candidate for large-scale deployment are afforestation/reforestation (AR), bioenergy with carbon capture and storage (BECCS), direct air capture with CCS (DACCS), biochar (BC), enhanced weathering (EW), but also ocean-based CDR such as blue carbon management, ocean alkalinity enhancement, and ocean fertilisation.

Nonetheless, the present study will center on terrestrial-based CDR methods. Primarily, ocean-based approaches tend to have lower TRLs compared to their terrestrial counterparts, typically ranging from 1-5 for ocean fertilisation, and 2-4 for ocean alkalinity [15]. Furthermore, ongoing research endeavors are imperative to mitigate ocean acidification and

ascertain the potential adverse effects these solutions might impose on marine ecosystems. While these approaches may evolve into feasible options for large-scale implementation in the future, they are not explicitly incorporated into this study due to these considerations.

Using global-scale integrated assessment modelling (IAM) tools, the last IPCC reports have provided predictions on their potential deployment from an economy-wide perspective, showing variation depending on assumptions about costs, resource availabilities, and remaining carbon budget constraints. For example, anticipated CDR deployments are estimated in the range of 20-660 Gt_{CO2} in the period 2020-2100 if we were to limit global warming to 1.5°C with no or limited overshoot but fall to 0-290 if we aim at 2°C, instead of 1.5°C [3].

Globally, the required removal anticipated by the IPCC (AR6) is 2 – 10 Gt_{CO2}/yr by 2050 across scenarios limiting warming to 2°C [14]. In the UK, the estimations for CDR deployment are still disputed (75 – 90 Mt_{CO2}/yr by 2050) and will depend on other decarbonisation efforts but it is mainly agreed that large-scale ramp-up rates of CDR infrastructure will be needed in the 2030s and 2040s ([12], [16]) as most options are not fully mature, yet.

A major weakness, often criticized, of these solutions, is the *moral hazard* associated with them, sometimes called *mitigation deterrence*, pointing out the impacts that the *offsetting* solutions will have on developing the *mitigation* solutions. However, critics are acknowledged by members of the CDR community amongst academics, and politics.

Indeed, *removals* may allow big polluters to keep running their polluting daily operations, adding millions of tonnes of CO_2 into the atmosphere, as net zero policies will allow them to do so by offsetting their emissions and being net zero. It becomes clear that various CDR pathways are possible to reach a certain emission target (*e.g.*, net zero emission target), or an equivalent carbon budget, at a certain point in time (*e.g.*, in 2050). The next question for scientists is to determine what the different characteristics between different pathways are, which one is preferable for the environment, including the effect on biodiversity, wildlife, and water scarcity, and which one would avoid the world economy from crashing. We find in this previous question the notions that appear to be 'constraints' in our model. We explore how CDR deployment varies when we activate constraints such as a specific carbon emission target, CDR-specific bio-geophysical or other environmental constraints, such as land, water use, etc.

Finally, the need for Carbon Dioxide Removal (CDR) solutions to compensate for residual emissions is inevitable to limit global warming to 1.5°C by the end of the century, as claimed by the IPCC [14]. They will be used to counterbalance residual emissions from hard-to-abate sectors but will also enable bringing the temperature down to 1.5°C after a temporary overshoot (IPCC 2018). Therefore, it is primordial to explore different CDR solutions to ensure that they effectively remove CO_2 and that we understand the implications of such deployment, in particular potential interactions with other sectors.

1.1.4 Energy systems, Policy Stability, and CDR

The current *climate crisis*, initially caused by human activities, is somehow well correlated with what can be referred to as the *energy crisis*. Indeed, major shifts are foreseen in our future energy mix, due to the withdrawal from fossil fuel and the nascent dependence on renewables, posing the challenges of providing reliable power and heat to an increasing population. In turn, a stable and secure energy supply is essential to the fight against poverty and plays a key role in policies and social stability, at the global scale. These multiple interactions, illustrated in Figure 1.1, show the importance of understanding the causes and consequences of such impacts, and justify the scope of this research, at the intersection between climate change solutions and energy systems.

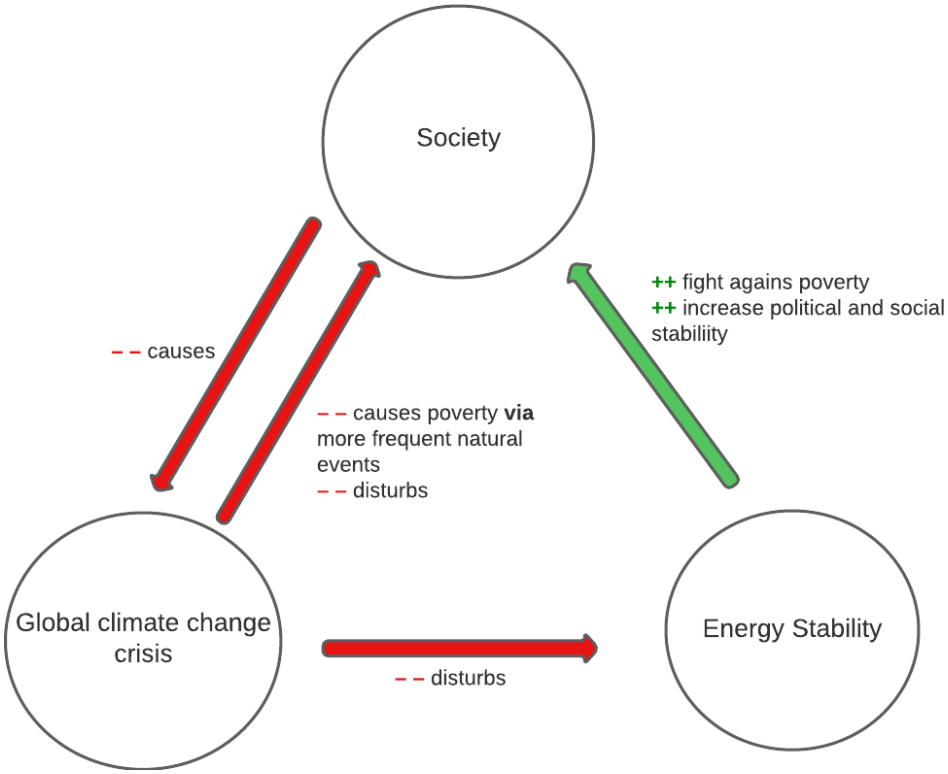


Figure 1.1: The Society – Climate Change – Energy Trilemma

Energy crises can also be provoked or accentuated by conflicts, illustrated by today's war in Ukraine, which fostered geopolitical and climatic tensions in European through the surge of energy prices. To address these challenges, the EU has diversified its energy supply, increasing the levels of liquefied natural gas (LNG), through new commitments with Egypt, Israel, Azerbaijan, and the USA, reduced demand, and established new storage rules [17]. Interestingly, most of the fossil fuel that used to be traded from Eastern to Western Europe has changed directions and is mostly shipped first to Western Europe, before being distributed to the East. Similarly, Russia's new exporting regions have rapidly changed. Both examples show that countries have a remarkable capacity to adapt to unforeseen situations.

Also, politics can be influenced by their countries' interests, or their popularity, sometimes putting their inhabitant finances forward, at the cost of global climate benefits, which are not yet sufficiently integrated into our economic institutions. All the more so as such an observation prove to be true during crisis times. For example, in response to the Russo-Ukrainian conflict, Austria and Germany re-opened a part of their coal power plant fleet to

circumvent the shortage of natural gas, ensuring stable electricity production, yet more polluting.

Transforming the power sector is key in the decarbonisation of the energy sector, and other sectors, *via* their electrification. Power systems have already undergone drastic changes in the past years through the rise of renewables, reaching 28.7% of global electricity generation in 2021 [18] and raising the challenge of supplying a predictable power output at the regional level. The role of nuclear is yet to be determined in the future of power systems, and carbon capture technologies emerge as a solution to keep current infrastructure and supply chains while abating our emissions, although the question of carbon use remains. Both bioenergy power generation coupled with CCS (BECCS) and Direct Air with CCS (DACCS) are tightly linked to the electricity system, the former by producing power, the latter by consuming it. Equivalently, biochar systems have proven to be net-positive energy systems and could play a role in energy system decarbonisation ([19], [20]).

Given the importance of CDR in the prospect of meeting the Paris Agreement targets, their inclusion in the electricity systems, and the role of energy security in policy and societal stability, this dissertation builds on two existing modelling works (CDR & power sectors), to elaborate a new framework that aims at determining an optimal technology deployment from a CDR and power perspective. This contribution includes modelling, coding, and multi-sectoral challenges; it focuses on the UK as a study case, allowing a regional granularity for bio-geophysical resources. Both CDR and power sectors models have a Mixed Integer Linear Programming (MILP) formulation and use off-the-shelf commercial solvers to find an optimal solution:

- *Modelling and Optimisation of Negative Emission Technology* (MONET [21]–[25]) has been used, extended and adapted for this work.
- *Electricity System Optimisation* (ESO [26]–[28]) is used to find the optimal system design and the hourly dispatch of electricity.

Given the important role that CDR might have in the prospect of the energy system, but foremost in the race to net zero emission, we will then compare the efficiency of CDR solutions. As importantly raised by the Climate Change Committee (CCC), a UK-independent body advising the government, “if bad offsets were sold on the voluntary carbon markets, as often seen today, the use of such offsets by businesses would delay the point when net zero is reached” [29]. Thus, the next paragraph will introduce the premise of permanent removals.

1.1.5 A tonne is not a tonne: the real value of a removal

There is a common misconception that all types of carbon removals have similar climate repercussions, resulting in false assertions in scientific studies, and carbon accountings. One reason for this misunderstanding is the neglect of carbon pool considerations.

On Earth, carbon lies in multiple pools, which are the lithosphere, the land, the ocean sphere, and the atmosphere. In the lithosphere, carbon exists under both organic and inorganic forms, in fossil fuels such as coal, oil, natural gases, and methane hydrate, but also in sedimentary rock deposits such as limestone, dolomite, and chalk. The processes governing carbon absorption within these pools last from millions to hundreds of millions of years.

However, carbon can also be dissolved in the land and ocean biosphere, through more rapid mechanisms (from decades to many centuries). For millennia, carbon molecules have naturally flowed between them, following an equilibrium that has been disturbed by human activities, thus increasing the amount of carbon in the atmosphere. When removing carbon from the atmosphere, it will be important to determine in which pool (lithosphere, land, or ocean biosphere) the carbon will be stored, as this will determine the new carbon cycle equilibrium, vital to life on earth.

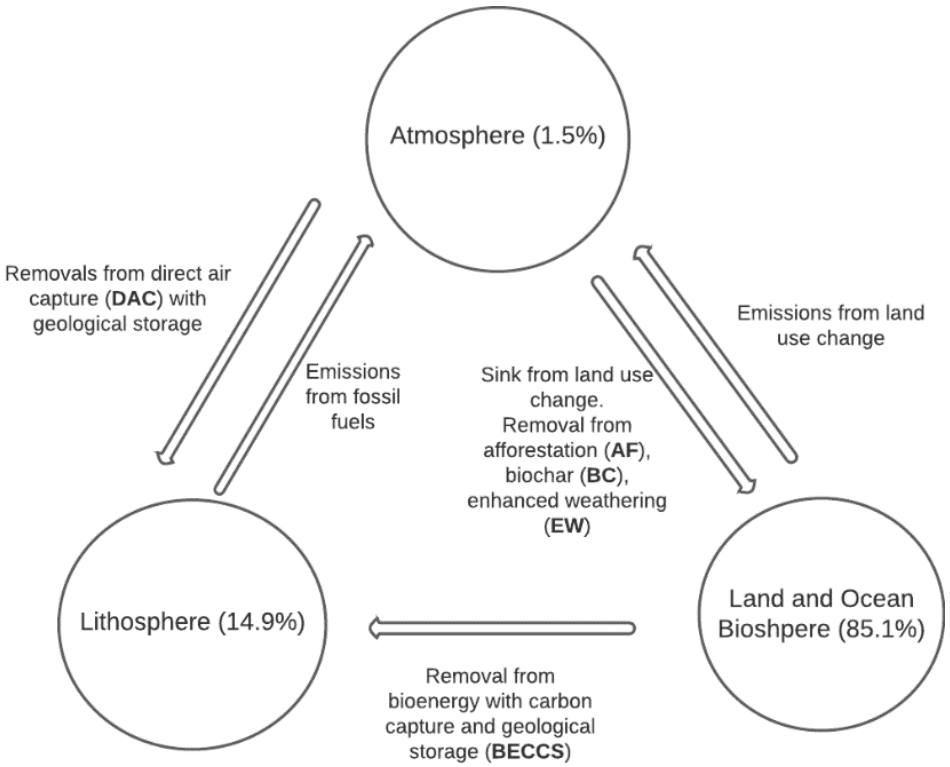


Figure 1.2: The role of CDR solutions within different Earth's biospheres
Inspired from Fankhauser et al. (2022) [30]. In addition, were added the fraction of carbon in each pool (Lal (2010) [31]), as well as the five CDR solutions considered in this dissertation (in bold in Figure 1.2). Note that the absorption of different GHGs (including carbon dioxide) into the different pools has been modelled by earth scientists [32]. For carbon dioxide (CO_2), the absorption of different sinks can be approximated by the Impulse Response Function (IRF), which we will describe in a later section.

Beyond the different carbon pools, the main important aspects of the removal are their permanence and their timing. Permanence can be defined as 'the time of sequestration of the carbon', and timing as 'the rate at which carbon is sequestered'. Indeed, physics is very different when a tonne of CO_2 is sequestered through AF, which takes some time to be captured in a growing tree, and through geological sequestration, which is likely to be more immediate and more permanent. Such physical differences have repercussions in the atmosphere, hence climate outcomes. Thus, the value of both offsets should be differentiated on the market.

Carefulness will be needed to establish a well-regulated, transparent, and global CDR market [33], using financial mechanisms that have been long used by financial institutions that govern us. Today, CDR credits are quite recent on marketplaces (Puro.earth, Pledge, Carbonfuture, Klimate.co, Nori, Salesforce, etc.) and are still poorly regulated. Therefore, this results in

'false' offsets, inaccurate prices, or opportunities to make a profit, being allowed by a vague certification process [34].

The carbon market is still nascent, but the more expanded it will be, the more negative repercussions inaccurate prices will have on the climate. To avoid unwanted impact, a more transparent certification is needed to fill the gap between market pricing and practical climate outcomes.

In Chapter 4 of this dissertation, we expand a novel framework aiming at computing the Climate Repair Value (CRV) of each CDR based on a specific dynamic carbon profile.

1.1.6 Delivering in time the infrastructure to enable a sustainable and permanent energy transition towards net zero emissions in the UK

In most IAMs, CCS is predominant in pathways keeping the global temperature below 2°C [35]. Few modelling studies have considered the eventuality of not having CO_2 transport and storage infrastructure when we will need it, which is likely to occur, according to the IEA [36]. Indeed, estimations show a factor of 10 between realistic CO_2 storage capacity that could be reached (110 Mt_{CO2}/yr) and what is needed by 2030 (1,200 Mt_{CO2}/yr) [36].

In parallel, there is a willingness from governments to invest in CDR technologies using geological storage (*e.g.*, Drax in the UK, and Climeworks in Switzerland). In turn, nature-based solutions struggle to attract the government's attention but are taking advantage of the voluntary carbon market expansion, with more projects having been certified, and supported by individual, or private investors.

On the one hand, this questions us about relying on solutions that might not be functional when needed, thus affecting possible future power and CDR scenarios. On the other hand, by considering longer times of permanence, it has been suggested that permanent solutions must be favoured if we want to avoid pushing back the climate problem for future generations [37].

In this final section, we will try to conciliate both views and provide policy recommendations on CDR and power technologies investments between today and 2050.

Existing modelling and optimisation energy tools such as ESO [27], [28], ESME [38], and eNODE [39], propose an optimal capacity expansion and electricity generation planning, given a set of technological and environmental constraints. Such models enable more realistic national deployment outputs compared to IAMs, providing more details across the spatial and/or temporal dimensions. However, they miss the "whole-system" perspective that IAMs do integrate.

The main contribution of this dissertation, *i.e.*, the integrated ESO-MONET framework, enables sufficient spatiotemporal granularity, from a multi-sectoral approach (in this case power and CDR sectors). Through the lens of this framework, we will discuss the importance of the permanence issue, relative to that of the emergency of deploying CDR solutions in a timely fashion, in a world where CO_2 transport & storage infrastructures do not exist.

1.2 Objectives

The main objectives of this dissertation can be conveyed in the following points:

1. Explore the feasibility, cost, and potentials of different archetypes for BECCS, DACCS, AF, EW, and BC in the UK.

2. Identify an optimal CDR deployment planning for the next decades, evaluate associated limitations and risks, and ascertain the probable implications of such deployment on the electricity sector.

3. Provide a metric to study the permanence of removals, enabling an in-depth comparison of the CDR solutions.

4. Investigate the implications of adopting this innovative permanent approach, with particular emphasis on its effects on CDR strategies and perspectives within the power sector.

This study utilized peer-reviewed journal papers, and their contributions to each chapter are indicated below.

1. Prado, A., Chiquier, S., Fajardy, M., and Mac Dowell, N. (2023). Assessing the impact of carbon dioxide removal on the power system. iScience *26*, 106303. 10.1016/J.ISCI.2023.106303. (Chapter 3)
2. Prado, A., and Mac Dowell, N. (2023). The cost of permanent carbon dioxide removal. Joule. 10.1016/J.JOULE.2023.03.006. (Chapter 4)

1.3 Structure

Chapter 1 expands on the motivation of this work, the objectives, and the structure of the thesis. Chapter 2 gives an overview of the different CDR solutions we will consider in this manuscript. Specifically, subsection 2.1 introduces the status of CDR in Europe with a particular focus on the UK. Subsections 2.2 provides details and assumptions for each CDR, and 2.3 compare their cost, energy balance, and land efficiencies. In Chapter 3, we introduce the electricity system optimisation (ESO) model in 3.1 and present the optimal power generation and capacity expansion outputs in the UK in our reference scenario in 3.2. In subsection 3.3, we describe a system-wide approach that establishes a link with the CDR sector and studies the power sector variations after integrating the link. In Chapter 4, we introduce the notion of climate repair value and reformulate the cost of CDR solution based on this definition. A comparative assessment of CDR solutions using this new metric, and identification of CDR removal cost variations, is explored. In Chapter 5, we examine the effects of various perspectives on permanence in the CDR-power modelling framework outlined in Chapter 3. We further investigate potential pathways that are more practical, such as scenarios that account for possible delays in the development of CO2 transport and storage infrastructure. In light of our discoveries, in Chapter 6, we have arrived at conclusive insights

regarding the technical, economic, and policy-related ramifications. Additionally, we have delved into the constraints of this thesis, while also exploring future areas of research.

Chapter 2

2 The emergence of Carbon Dioxide Removal solutions

2.1 CDR status in Europe and the United Kingdom (UK)

An understanding of current policies in the CDR sector is needed when it comes to modelling multiple CDR solutions. In this section, we highlight the importance of the economic and policy landscape to achieve Paris-agreement-compliant CDR deployment in a sustainable and economically viable way.

Yet, the modelling work, presented in the subsequent section (2.2) exclusively concentrates on carbon dioxide removal (CDR) solutions implemented within the United Kingdom and accounted in UK's carbon budgets. By precluding the option of developing CDR abroad that could be allocated to UK carbon budgets, we forego the utilisation of Article 6, which may enable such allocations in the future through the advent of carbon markets. Consequently, this confines the deployment of CDR solutions within the geographical confines of the UK, thereby assessing only its geographical potential within the UK.

The emphasis on the UK and Europe in this section can be attributed to their geographical closeness and similar policy environments. Being both economic and political allies, they have a historical responsibility in the contribution of climate change. Therefore, it is logical for the countries in these institutions to take the lead in combating climate change, given their historical role as leaders during the industrial revolution in the 1900s.

2.1.1 CDR in Europe

Discussions about the role of CDR in climate policies had started as early as 2001, later followed by the Fifth Assessment Report (2014), and the Paris Agreement ([4], 2015). However, the inclusion of CDR technologies into EU policy is, in fact, quite recent. In November 2022, the European Commission proposed a new Carbon Removal Certification Framework (CRCF) that ambitions to integrate carbon removal into EU climate policies, putting forward the role of Europe to move ahead in this space. The CRCF has faced criticism concerning the crucial lack of details on the outline of CDR rollouts, the role of permanence, or the case of reversals, which could be a major barrier against the successful development of the CDR sector [40].

Even though carbon removal had never been included in EU laws before the CRCF proposal, the concept was not quite new in EU policies. Indeed, both LULUCF and the EU-ETS regulations had implicitly included this concept, highlighting the relevance of CDR, and the prospect of its future integration into EU climate policy.

In 2018, the EU regulation '2018/841' allowed some flexibility in the LULUCF sector through the 'no-debit rule' that stipulates "that accounted emissions from land use are entirely compensated by an equivalent removal of CO_2 from the atmosphere through action in the sector". The flexibility lies in the fact that every additional carbon removal from the LULUCF sector (*e.g.*, from afforestation) could be transferred for compensation in another sector. The EU-ETS scheme, a cap-and-trade scheme first implemented in 2005, provides a framework that could potentially integrate CDR, by linking them to allowances to compensate for positive emissions, as in New Zealand's ETS. However, the integration of CDR has not been implemented in the EU-ETS, yet [41]. As of now, only the EU-ETS Innovation Fund incentivises CDR projects, a first step towards integration.

The European Green Deal [42], first presented by the European Commission in December 2019, represents Europe's vision and leadership for an urgent and fair climate transition. Through this deal, the EU announced to reach net-zero emissions by 2050, and a 'fit for 55' package [43]. Meeting such targets will require the establishment of new CDR policies that ensure the sustainable and economically viable deployment of CDR solutions. However, the EU, along with its current institutions (European Commission, European Parliament, and member states), would need more discussions to set out a precise CDR plan for deployment. In particular, the question of country-specific emission targets, potentially net-positive emissions targets for some countries, and net-negative for others, with final carbon balances adding up to zero by 2050 [44].

2.1.2 CDR in the United Kingdom (UK)

At the national scale, the UK has taken an interesting direction towards the adoption of CDR for national policies. Being separated from the EU in 2015, the UK adopted its own net zero national targets in the laws in 2019, by amending the 2008 Climate Change Act [45]. Like in the EU-ETS, the UK-ETS scheme has not included the possibility of CDR allowances, yet.

The only CDR credit mechanism existing in the UK is associated with forestry. Implemented in 2011, the Woodland Carbon Code (WCC) encourages forest expansion by rewarding forest owners. Such credits were sold at around £17.5 per t_{CO2} (~ $21.5 per t_{CO2}) in 2021, contrasting with the carbon prices of £75 per t_{CO2} (~ $93 per t_{CO2}) from the UK-ETS. The WCC also provides details of monitoring, reporting and verification practices for forest projects. In line with such efforts, an afforestation deployment goal has been set out by the government, aiming at trebling the number of newly planted forests per year by 2024 [46]. Yet, specific guidelines to achieve this goal are missing. A rigorous plan must ensure that these new plantations will not overlap with other types of lands, such as lands for food production, or other natural habitats. Also, advice must be provided about optimal forest location, management, or tree species. Moreover, specific targets for CDR solutions other than afforestation are missing from government reports, as of today.

In the UK, scientific debates, feasibility studies, and societal discussions around CDR emerged early in the century. First named under the term *geoengineering*, in the 2009 Royal Society report "Geoengineering the climate science, Governance, and Uncertainty", CDR solutions were presented, along with one of their major barriers to deployment: societal and ethical

issues. In 2017, the UK government and the UK Research and Innovation (UKRI) launched an initiative to fund R&D projects in CDR. The UK's first CDR capacity was constructed with Drax's BECCS demonstration project in North Yorkshire, in 2019.

Recently, two government initiatives have been launched, following recommendations from the CCC's recent report [47]: The five Greenhouse Gas Removal Technologies Demonstrators and the GGR Directive Hub. Via a £30 million investment, the UKRI initiative explores sustainable routes to achieve large-scale removal of greenhouse gases, investigating a) peatland management, b) enhanced rock weathering (EW), c) biochar, d) large-scale afforestation and e) scale-up of bioenergy dedicated crops such as miscanthus, all of these projects being located across the UK.

Such investments in commercial projects are needed to overcome some difficulties associated with large-scale deployment and the robust quantification of removals, as they lie at the frontier between experimental research and industrial-scale deployment. For example, in the case of enhanced weathering – a technology with a Technology Readiness Level (TRL) 3-4 [14]– multiple modelling approaches have been proposed to reliably quantify the amount of CO_2 stored by EW, but no consensus has been set out by the scientific community. This is due to a high variability of quantification results depending on the measurable signal that is chosen (*e.g.*, total alkalinity or total inorganic carbon).

However, strict guidelines and rules are required for transparent and reliable carbon removal quantification of EW, especially regarding the approach used for quantification. Puro.earth has set out specific requirements that need to be followed and will provide a per-project carbon certification if the methodology proposed is accepted [48]. In particular, the methodology must provide a dynamic simulation, uncertainties relative to removal quantifications, validation of the model based on site-specific empirical data, an open-source model, and monitoring of heavy metals. Undo, a pioneer UK-based company that contributes to the large-scale deployment of EW, has had its methodology approved by the Puro Standards in December 2022 and will be able to sell credit from now on. Such an example illustrates the success of investment in commercial projects, showing the path for other CDR solutions with low TRLs.

Finally, the transparency and robust quantification of the CDR project is primordial for having a legitim national CDR governance system [49]. The UK and Europe have made a step forward to lead in the CDR space. This also serves as a motivation to undertake this study in the UK.

In the next section, we will expand on the methodology used for each CDR solution.

2.2 CDR details

This section aims at presenting, in a streamlined way, the functioning of each CDR *via* equations. Each equation corresponds to either modelling (where equality is used, we tell the system the value of a given parameter), or constraints (where inequality is used, we tell the system not to surpass a limit for a given variable). Both equation types will be used later during optimisation time.

Regarding each CDR solution, we present a comprehensive methodology to ascertain the complete balance of GHG emissions and associated costs, while also considering factors such as energy consumption, land use, and the usage of materials such as biomass and rock. In light of the optimisation of a CDR portfolio, we distinguish *parameters* from *variables*. Parameters are fixed values (*e.g.*, the Euclidian distance between regions $Dist(g, g')$ or the number of hours per year $\alpha = 8760$ hours), whereas variables are values that will be optimised and that constitute the optimisation outputs (biomass/rock supply of type *i* in region *g* at time *t:* $D_{i,g,t}$, in tonne/hr). Both parameters and variable names are defined in the nomenclature table.

A bottom-up (or cradle-to-grave) approach is used for all CDR. This approach aims to provide cost, GHG, energy, and land models, that are as close as possible to reality. We also differentiate between multiple archetypes for each CDR (different biomass types for BECCS and BC, different processes for pyrolysis (BC), ecological zones and climates for AR, DACCS technologies for DACCS, and rock type for EW) to cover as many possibilities as the future can offer, while ensuring that they are deployed sustainably.

The rate of sequestration of each CDR solution needs to be considered, as well as leakages (biochar decay, forest fires or insect outbreaks, geological leakage). In this chapter, we assume a project lifetime of 50 years and a permanence horizon of 100 years, but further permanence considerations will be investigated and discussed in Chapters 4 and 5.

The main components that we will explore in this section are the total cost $TotCost_{CDR}$, and the total carbon (equivalent) removed CR_{CDR} during the operations. We acknowledge that looking only at these metrics restricts the broad impact that CDR could have on the environment and society. Therefore, our discussion will also cover additional impacts like land usage, as well as GHGs beyond CO_2 that are released throughout the supply chain of CDR. However, these topics will not be the primary emphasis of our study. Also, we will have a close look at their energy impact as the aim is to integrate them into the power system model, in a second step.

It is important to note that the cost balance for the next 25 years is uncertain for certain CDR solutions, especially for those with lower TRLs (DACCS, EW, BC). Thus, we adopt a cautious approach by assuming no technological advancement or learning across all CDR methods. This decision is twofold: firstly, it prevents the creation of models that might be unrealistically optimistic, and secondly, it ensures uniform reasoning by assuming no CDR solution will experience cost technological learning. In particular, the costs of DACCS are a topic of debate among scientists. Some believe these costs could go down in the future. Yet, predictions of future costs vary widely, ranging from $80 to $600 per ton of CO_2, and are still very uncertain. Since DACCS is still in early development stages, indicated by its low TRL, its costs could initially increase (*i.e.*, cost escalation) before benefits from technological advancements are realized [50].

The cost and GHG equations common to all CDR are as follows:

Capital Expenditures and Operational costs

The technology-specific total cost can be expressed as the following sum:

$$TotCost_{CDR} = TotCapex_{CDR} + TotOpex_{CDR}, \quad \text{Eq. 1}$$

Carbon removed

The total carbon removed is the carbon emitted CE_{CDR} subtracted to CC_{CDR}:

$$CR_{CDR} = CC_{CDR} - CE_{CDR}. \quad \text{Eq. 2}$$

Removal cost of CDR

Finally, a value of interest for carbon removal investors is the removal cost RC_{CDR}. It is computed as the ratio between the total cost $TotCost_{CDR}$ and the total carbon removed CR_{CDR} :

$$RC_{CDR} = \frac{TotCost_{CDR}}{TotRem_{CDR}}. \quad \text{Eq. 3}$$

In the following sections, we will dive into each of the CDR solutions that were chosen along this research journey, *i.e*, Bioenergy with Carbon Capture and Storage (BECCS), Biochar (BC), Direct Air Capture with CCS (DACCS), Afforestation/Reforestation (AR), and Enhanced Weathering (EW).

Lastly, we also assume that each of these CDR solutions will be deployed on UK ground, and not abroad.

2.2.1 Bioenergy with Carbon Capture and Storage (BECCS-power)

Bioenergy with Carbon Capture and Storage (BECCS) encompasses a range of technologies using biomass fuel to provide energy services and combines it with carbon dioxide (CO_2) capture and storage, most often assumed to be in geological reservoirs.

Considering the Technology Readiness Levels (TRLs) of 7-9 for bioenergy and 4-7 for carbon capture and storage (CCS), as reported in literature [15], Bioenergy with Carbon Capture and Storage (BECCS) has been acknowledged in IPCC reports, alongside afforestation (TRL of 8-9 [15]), as a prominent carbon dioxide removal (CDR) technology significantly influencing the projected CDR portfolio. [14].

Role of BECCS in current IAM frameworks

In IAMs pathways, BECCS provides an important share of the removals required to meet the 1.5°C target. Typically, in IPCC scenarios, BECCS deployment ranging from 0-8 Gt_{CO2}/yr by 2050 are compliant with meeting such a target, with no, limited or high overshoot [14].

In the UK, the Department for Business, Energy & Industrial Strategy's (BEIS) GGR policy report estimates that 50 Mt_{CO2} of BECCS removal per year would be needed by 2050. However, the large-scale deployment of BECCS as assumed by most Paris-agreement – and net-zero –compliant pathways is very unlikely, due to the lack of CO_2 transport, and storage infrastructures. The International Energy Agency (IEA) has estimated that there is a factor 10 between the CO_2 storage capacity that could be reached (110 Mt_{CO2}/yr) and what is needed by 2030 (1,200 Mt_{CO2}/yr), in their Net Zero Scenario [36]. Moreover, we observe that there is another factor 10 between what is needed by 2030 in IEA's Net Zero Scenario, and what is needed according to the IPCC by 2050, highlighting the challenge associated with CO_2 transport and storage infrastructures.

Although BECCS was claimed to be determinant to meet a 1.5°C target by the last IPCC report [14], it faces well-documented controversy in terms of land-use concerns, competition with food production, and cost [51], which could drastically reduce its relevance in global scenarios. Further criticism points out water requirements and potential infringement of Sustainable Deployment Goals (SDGs). According to Fuss et al. (2018), an adjusted more realistic sustainable global deployment of BECCS would rather range between 0.5 and 5 Gt_{CO2}, [52].

Various BECCS pathways

There are multiple variations of BECCS, defined by:

- The land used for biomass production (marginal land, cropland or grassland for bioenergy-dedicated crops, cropland for crop residues, forests for forestry residues).

- The biomass type, with associated physical properties.

- The end-product (bioethanol, biodiesel, hydrogen, electricity, use in the iron or steel industry), additional to the carbon removal service.

Scrutiny in the supply chain is needed when evaluating the sustainability of each pathway. Thus, we use a bottom-up methodology that includes the biomass and CO_2 supply chain. The reader will note that the next paragraphs focus on the biomass supply chain and therefore will be also valid for biochar, although biochar will be detailed in a later subsection.

BECCS – and biochar – biomass supply chain

The understanding of biomass pathways will be key in assessing the economic and environmental viability of biomass-based CDR solutions, *i.e.*, BECCS and biochar. For this reason, we use a bottom-up approach considering all the steps along the biomass supply chain, from land seedlings to the transformation process of biomass into pellets, and transport to their final end-use location. We find out as a modelling direct outcome that the availability of biomass can be a barrier or a key lever for biomass-based CDR deployment, proving the importance of having a detailed representation of biomass supply chains, as illustrated in Figure 2.1.

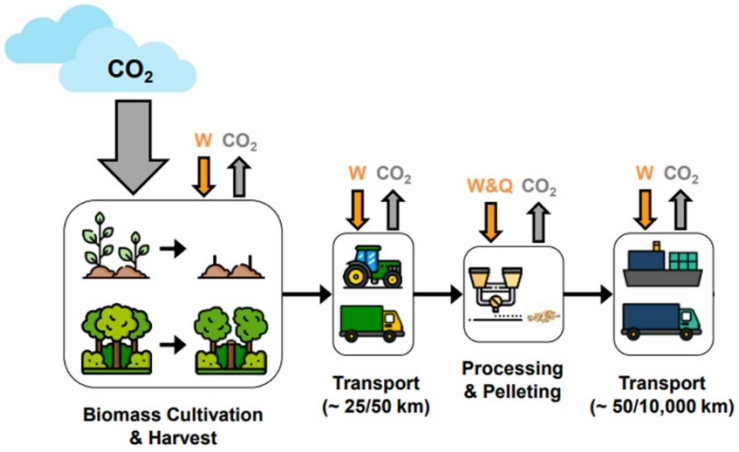


Figure 2.1: The biomass supply chain will be used for BECCS and Biochar modelling. During each step, direct and indirect emissions are accounted for. Adapted from [53].

Assuming that biomass is a carbon-neutral energy source due to the carbon cycle associated with the life of biomass crops is wrong. Indeed, biomass projects suffer an initial carbon debt due to CO_2 emissions associated with the initial land use change and its subsequent emissions. Through a whole-systems analysis of the BECCS value chain, Fajardy et al. have shown that a BECCS project could well cause both carbon-positive and negative outcomes [22].

In particular, the question of land type is crucial for the global viability of a BECCS project [22]. Due to this carbon debt, it can take up to 50 years for BECCS to become a net carbon remover when biomass grows on converted land, previously croplands, grasslands, or managed forests. Thus, we do not consider these possibilities in our BECCS and BC modelling, as they will result in inefficient outcomes. Instead, we consider that bioenergy-dedicated biomass crops (both herbaceous and woody crops) are grown on marginal lands – an economic term designing lands with little agricultural value. These lands are often well-suited for bioenergy crops [54]. Such a choice minimises the emissions related to direct and indirect land-use change (LUC & ILUC).

Moreover, each bioenergy feedstock category (energy crops, agricultural residues, and organic wastes) results in many different thermochemical properties, that greatly impact the way biomass is processed (*via* moisture content, ash content), and effects the overall GHG balance (*via* carbon content), and energy outcome (*via* its energy density, higher heating value (HHV) & lower heating value (LHV)). Therefore, we list different categories of biomass that we consider in this research:

1) Herbaceous crops: miscanthus is considered.

2) Woody crops are grown as short rotation coppices (SRC): willow and poplar.

3) Agricultural residues, wheat straw is considered.

4) Woody biomass extracted from forests (*e.g.*, branches, leftovers) or waste from the wood processing industry (*e.g.,* sawmills), is mentioned as forestry residues in this study.

The availability of these biomass sources can be long debated and is key in our modelling approach, as it will determine the potential of biomass-based CDR solutions. Due to the vast diversity of biomass feedstock supply, forecasting the prospects of future availability is a complex task, fraught with considerable uncertainties. The availability of future feedstock will hinge on various elements, such as policy decisions by governments and market shifts both in the UK and abroad, in addition to the prices that various end users are prepared to offer. In addition, the deployment of technologies such as BECCS depending on biomass fuel could also affect the demand, and the supply, as a consequence. The share of biomass market associated to the UK can be approximated by UK's fraction of global GDP, which is also subject to uncertainties. Such complex trends are being captured by the UK TIMES model [55], from which we base our modelling constraints.

For miscanthus, we assume they are only grown on marginal land (MAL), limited to 2.1 Mha in the UK [56], as detailed in Figure A 1 (Appendix). Such area will be reduced to 1.5 Mha to only account for area with a low water stress index [57].

Agricultural residues, usually by-products of the cereal industry, include wheat, barley, and oats production. They have the advantage of being produced every year, like other energy-dedicated crops.

The availability of crop residues in the UK can be defined by cereal straw production in the range of 10,000 – 13,000 thousand tonnes per year since 2008 [58], thus producing a relatively stable output. However, 82% of this yearly produced straw is used for bedding and feeding animals, and only 6.3% was used or sold as biomass in 2019. It is estimated that the amount of leftover straw from cereal crops and other agricultural residues will remain stable under expected policy and market conditions [55]. Therefore, we make this assumption in our model to limit crop residues availability.

Organic wastes have not been considered in this study. Studies show that waste could play a crucial role in the decarbonisation of the heating sector, by replacing natural gas consumption (up to 25%) [59]. However, this study is limited to the power sector and therefore overlooks waste-to-energy pathways.

Finally, we also assume biomass pellets can be imported from abroad. We assume wood pellets are shipped from the US South to one of the four ports currently used for biomass import (port of Immingham, Tyne, Hull, and Liverpool) in the UK.

BECCS for electricity purposes

When purposed to generate electricity, BECCS can provide a low-carbon dispatchable source of power ([27], [60], [61]). The impact of BECCS on power mix has been studied *via* various lenses in the literature. Often, the case of BECCS is compared with that of DACCS, that also interacts with the energy sector, *via* heat and power requirements.

Different approaches have been undertaken, helping to understand the mutual dependence of BECCS, DACCS and energy systems. In addition to the more traditional *energy per carbon* metrics, or future cost of deployment, it is crucial to investigate the dynamics response of these CDR solutions in intermittent energy systems [62], [63]. Potential synergies between BECCS and DACCS, in a hybrid system, have also been explored and proven to be able to decrease carbon costs, increase the removal, and maximise the effectiveness of limited biomass resources [64].

There are also some potentially important considerations of having BECCS largely deployed in a national electricity mix. For example, Fajardy et al. have shown that inefficient BECCS power generation could be preferred in a national electricity system with a high renewable share, as it was shown to be beneficial from both an environmental and economic perspective [24]. Indeed, a less efficient BECCS plant operating baseload is favoured if the amount of CO_2 removed was to be maximised, raising the dilemma of energy versus carbon removal services [65].

To conclude, the understanding of different BECCS pathway variations and how they can be deployed in a sustainable, economically viable way has been the subject of several studies.

However, although some studies have considered BECCS's synergies with the broader energy system [62]–[64], we aim in this dissertation, to propose a modelling-based framework that quantifies the barriers of BECCS deployment, evaluates its role in delivering negative emissions at the UK level, and examines which power generation technologies the additional share of BECCS would replace within the power mix. These research questions have been addressed and answered in a journal paper (Prado et al. [66]) which discusses the optimal deployment of BECCS within an energy system, encompassing both power generation and carbon removal technologies. The main conclusions of this paper have been reformulated in this dissertation, in chapter 3. In the next subsection, we provide the modelling details of BECCS pathways as implemented in our models.

BECCS-to-power modelling in the UK

In this dissertation, we will focus on BECCS pathways for electricity production *via* direct pulverised combustion of biomass, one of the most mature CDR solutions, and given its dependence, by definition, on the electricity system which is the subject of this dissertation.

In the modelling of BECCS for power generation, we consider the entire BECCS supply chain from land-use change to power generation, including direct and indirect land-use change (LUC & ILUC), seedling and biomass growth, biomass crops transport to pellet plants, pellet drying and densification process, pellet transport to the power plant (BECCS plant) and carbon capture and storage. The big picture of BECCS modelling is illustrated *via* the diagram in Figure 2.2.

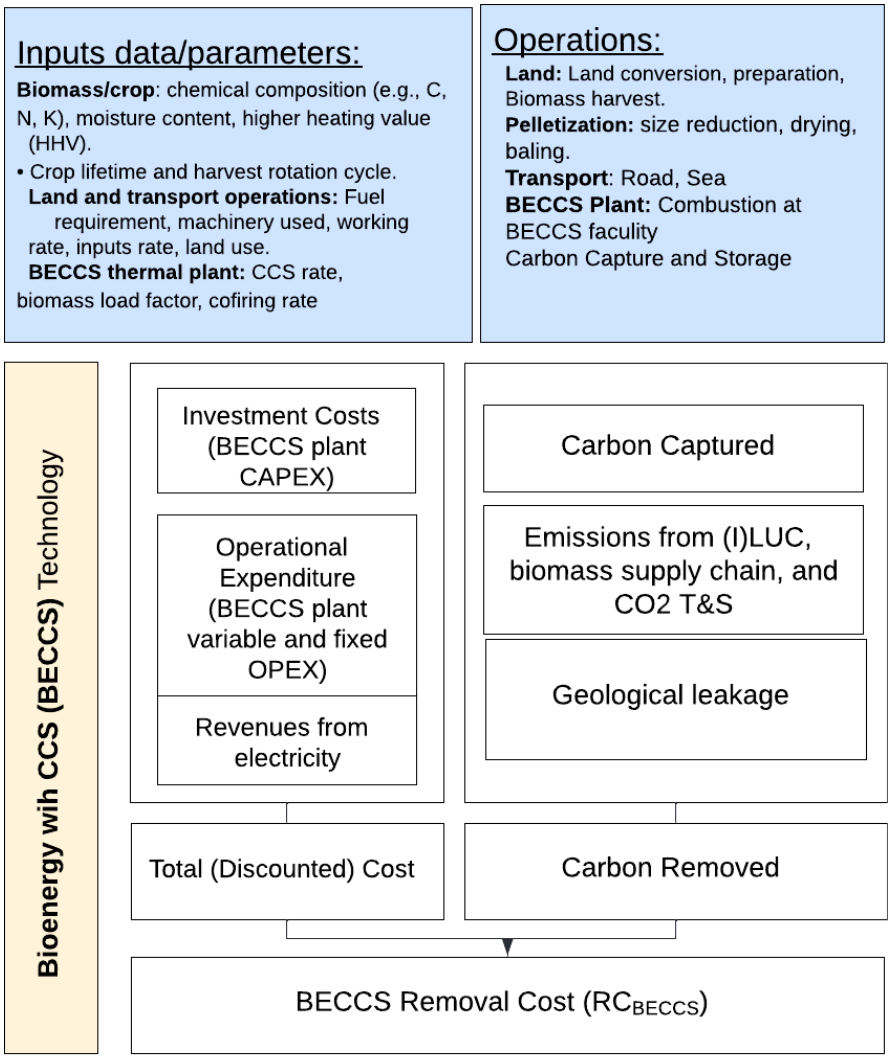


Figure 2.2: Overall Picture of BECCS [53]

The following equations are replicated from a published modelling work [53] and are adapted to the UK level, with its associated spatial granularity (NUTS1 and NUTS3, respectively). Eq. 4 to Eq. 7 incorporate the GHG assessment of the BECCS supply chain. Eq. 8 to Eq. 13 include cost computations. Eq. 14 links the number of BECCS plants built to the power generated by them, through the capacity factor parameter. Eq. 15 and Eq. 16 include pelletisation and generated electricity, respectively.

2.2.1.1 BECCS GHG balance

Applying the GHG balance equation (2) to the BECCS study case, we express the amount of carbon removed by BECCS $CR_{BECCS,i,g}$ as the carbon captured $CC_{BECCS,i,g}$ minus emissions along the supply chain $CE_{BECCS,i,g}$, for each biomass type *i*, and region *g*, expressed in t_{CO2eq}/ha/year:

$$CR_{BECCS,i,g} = CC_{BECCS,i,g} - CE_{BECCS,i,g} \quad \text{Eq. 4}$$

First, we breakdown the carbon captured by BECCS $CC_{BECCS,i,g}$ for biomass i in region g, expressed in t_{CO2eq}/ha/year, as a function of biomass carbon content $Cbio_i$ (in t_{CO2eq} per t_{DM}), carbon capture rate β (in %), and biomass yield $Yield_{i,g}$(in t_{DM} per ha per year):

$$CC_{BECCS,i,g} = \beta * Cbio_i * Yield_{i,g}, \quad \forall\, i \in B, g \in G \qquad \text{Eq. 5}$$

Values used for $Cbio_i$ can be found in Table A 2 (appendix). $Yield_{i,g}$ values are taken from [23]. The value for β is 90% [67].

Emissions from BECCS' supply chain are respectively from land and farming operations, biomass/pellet processing and transport, and CO_2 transport and storage (T&S). The land emissions include land use change (LUC), and indirect LUC (ILUC) and farming operations include planting and harvesting the biomass (expressed in t_{CO2eq}/ha/year):

$$CE_{BECCS,i,g} = CE_{Land,i,g} + CE_{Farm,i,g} + CE_{Pelleting,i,g} + CE_{transp,i,g} * Yield_{i,g} + CE_{CO_2\ T\&S,i,g}, \quad \forall\, i \in P, g \in G \qquad \text{Eq. 6}$$

All terms are expressed in t_{CO2eq}/ha/yr except the emissions from transport $CE_{transp,i,g}$ in t_{CO2eq}/t_{DM}. Transport emissions are the sum of emissions caused by inter-regional and intra-regional transport and are expressed in Eq. A 3 (Appendix).

Geological leakage risk

BECCS includes CO_2 transport and storage to store CO_2 in geological formations. We estimate the risk-probability of carbon leakage, with a linear approximation for well-regulated storage [68] of 0.00063% of leakage per year. This estimation is a threshold that has been validated by 95% of the scenarios simulated via a Monte Carlo analysis in the findings of Alcalde et al. [68].

$$Decay_{(BE)CCS,t} = (1 - 0.00063 * t), \quad \forall\, t \in T \qquad \text{Eq. 7}$$

Given such a leakage rate, the carbon stored in geological formations will leak by 0,063% in 100 years, and 0,63% in 1000 years.

It is important to note that a linear approximation is not representative of reality. Indeed, all available measurements show that leakage rates decrease over time in an approximately exponential manner. In a more practical set-up, the leakage rate would increase linearly from 0% to 100% of the maximum leakage rate, until the end of the injection period. Then, the leakage rate would experience a decay following an exponential decay [68]. However, because the longest available data model lasts for 500 years [69], Alcade et al. recommend not extrapolating the leakage reductions after this timescale, and instead, assuming a constant leakage rate over time. Thus, as we aim at exploring longer timescales (~10,000 years), making a linear approximation does not significantly affect the curve behaviours, nor

does it alter the ranking order of leakage curves, in comparison with other CDR leakage curves (see Chapter 4).

GHG balance modelling results

Looking at the overall GHG emissions for the BECCS supply chain in the UK (Figure 2.3), we observe some variations in the emission balance across biomass types, ranging from 7 t_{CO2eq} per ha for forestry residues to 90 t_{CO2eq} per ha for miscanthus. These results are derived from a BECCS model employed by Fajardy et al. [22] and continued by Chiquier et al. [21]. For further details, we direct the reader to the relevant publications ([21], [22]).

The cumulative GHG emission balance for miscanthus is explained by the higher yield of raw miscanthus per hectare and year compared to that of forestry and crop residues (2 times higher than wheat straw, and 16 times higher than forestry residues [21], [53]), and given the unit chosen for the y-axis.

GHG emissions for miscanthus include a high share of GHG emissions for land inputs (fertilisers, lime, etc.), farming, and biomass drying.

GHG emissions from inputs include emission from land preparation and irrigation, as well as indirect emissions due to use of agrochemicals such as fertiliser, herbicide, lime and seeds. The emissions from inputs for miscanthus amounts to 177 t_{CO2eq} per ha per year. In the case of wheat straw, we only include extra use of agrochemicals, and exclude land preparation or irrigation, resulting to 119 t_{CO2eq} per ha per year. We assume no inputs emissions are associated to forestry residues as no additional inputs are used for forest management.

N_2O emissions directly resulting from the use of nitrogen-based fertilizers in cultivating energy-dedicated crops (or, for agricultural crops, the additional fertilizer use) are also considered.

For forestry residues, residues harvesting (operations, machinery, fuel emissions), and biomass drying constitute the majority of GHG emissions. The minor emission remaining are from road transport, pellet grinding, and CO2 transport and storage. No emissions from size reduction is considered for forestry residues as we assume they are leftovers from forest management operations, including thinning, branches felling, forwarding, and forest residues baling, and storage [53].

We also observe that little emissions are associated with land use change for miscanthus (0.025 t_{CO2eq} per ha), as we assume it is grown on marginal lands. There is logically no land use change associated with forests or crops.

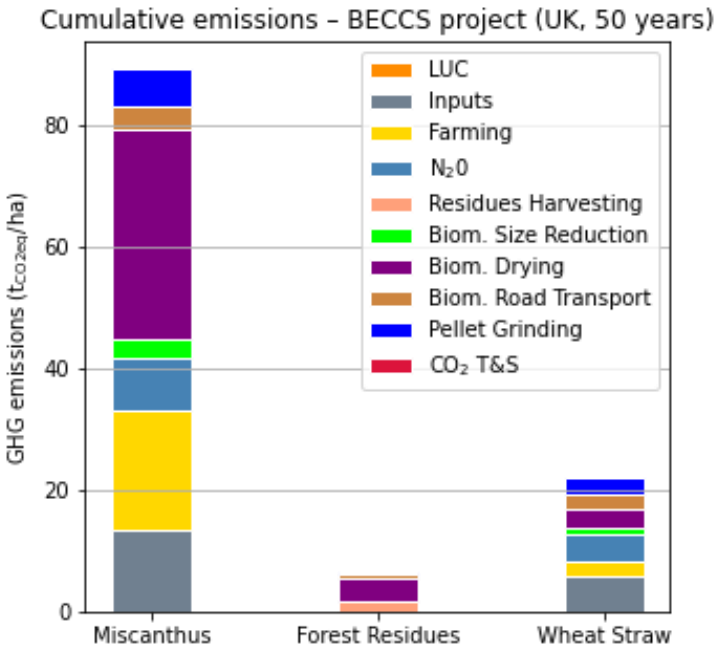


Figure 2.3: Emissions of the BECCS supply chain that includes three biomass types.[21]–[23]

2.2.1.2 BECCS cost balance

Applying the cost equation (1) to BECCS pathways, we express BECCS's total cost in $ per ha per year:

$$TotCost_{BECCS} = TotCapex_{BECCS} + \sum_{i \in B, g \in G} TotOpex_{BECCS,i,g}, \quad \text{Eq. 8}$$

The equation for the capital expenditure is similar to other CDR and is detailed in Eq. A 1 (Appendix).

Operational costs include the cost of fuel (*i.e.*, biomass pellets), BECCS plant non-fuel operating costs (labour, maintenance costs), the cost of transporting and storing CO_2, and the revenues associated with power services:

$$\begin{aligned} TotOpex_{BECCS,i,g} & \quad \text{Eq. 9} \\ &= Cost_{Pellet,i,g} + VarNFOPEX_g^{BECCS} + Cost_{CO_2T\&S,i,g} \\ &- Rev_{Power,i,g} \end{aligned}$$

The cost of the pellets includes the total cost of pellet production $Cost_{PP,i,g}$ (nationally produced), or if applicable, the cost of pellets imported from abroad $Cost_{Import,g}$, and the cost of transporting them to the BECCS facility $Cost_{transp,i,g}$, expressed in $ per ha per year:

$$Cost_{Pellet,i,g} = Cost_{PP,i,g} + Cost_{Import,g} + Cost_{transp,i,g} * Yield_{i,g} \quad \text{Eq. 10}$$

The cost of pellet production $Cost_{PP,i,g}$, expressed in $ per ha per year, includes the cost of the raw biomass, (itself including marginal land rent, crop management, and harvesting operation costs), and the costs of the pelletisation process:

$$Cost_{PP,i,g} = Yield_{i,g} * \left(Cost_{raw\ bio,i} + UPC_i * \gamma_i\right) \quad \text{Eq. 11}$$

where:

- $Yield_{i,g}$ is the biomass yield of biomass *i*, from region g, in t_{DM} per ha per year [23].
- $Cost_{raw\ bio,i}$ is the cost of raw biomass in $ per t_{DM} [23], [25]
- UPC_i is the unit production cost of pellets in $ per t_{pellet} [23], see Table A 3 (Appendix)
- γ_i is the pellet conversion rate ($t_{pellet}/t_{raw\ biomass}$) [23], see Table A 3 (Appendix) [23]

The total cost of imported pellet is expressed as a cost per unit of pellet ($ per tonne of pellet) multiplied by the number of shipped pellets from abroad to region *g'* having a port, at time *t*, $Q_{Imp,out,g',ship,t}$, a variable in our equations:

$$Cost_{Import,Imp,g'} = Q_{Imp,out,g',ship,t} * IMPC \quad \text{Eq. 12}$$

where:

- IMPC is the price of imported pellets (in $/t_{DM}$), set to 150 $/t_{DM}$ [23]

Note that in the case of imported pellet, we don't consider the yield of biomass, neither its conversion rate, instead we assume we directly buy the pellet abroad, at a given cost. Imported biomass pellet's cost cannot be captured in our models, as it will depend on future global market conditions, and will vary with different socioeconomic scenarios of the exporting country, its demand for land for food, which will affect the amount and production cost of biomass.

Finally, alike the GHG balance, the cost of transporting pellets to BECCS plants is divided between inter-regional and intra-regional components and is expressed in Eq. A 4 (Appendix).

We express the total variable non-fuel operational expenditures as a function of the biomass yield $Yield_{i,g}$ and Non-Fuel OPEX of a BECCS plant $OPEX^{BECCS}$:

$$VarNFOPEX_g^{BECCS} = Yield_{i,g} * OPEX^{BECCS} \quad \text{Eq. 13}$$

Cost for CO_2 Transport and Storage (CO_2 T&S)

Based on recent work, the future cost of CO_2 transport and storage will depend on both the transport distance and flow rate [70] and are estimated in the range of $5–$30/t_{CO2}. In 2020, Porthos – a large-scale developing project in which CO_2 is transported from the Port of Rotterdam to gas fields in the North Sea – estimated a cost of 50 euros per t_{CO2e} for transport

and storage [71]. However, based on pre-computations built on Smith et al. [70] and geological storage availabilities in the UK [72], we estimate the cost of transporting and storing CO_2 by a fixed value of \$30/t_{CO2}, which is in the range \$5-45/tCO2 determined by [70]. We provide further details on these calculations in Figure A 4 (Appendix).

Even though today's project costs are significantly more expensive [73], the figure used in our modelling is an average value for the period between today and 2050, *i.e.*, includes that future pipelines capacity will increase (hence decreasing the cost, see Figure A 4), and the potential technology learning, both factors that can decrease of T&S costs.

2.2.1.3 BECCS removal cost

In the cost results for BECCS, provided in Figure 2.4, we compute the costs of different BECCS pathways, with and without extra-revenues from electricity sale. The revenues from electricity generation that we consider are set to 125 \$/MWh, the calculated average annual non-domestic electricity price in the UK in the period 2010-2021[74]

When electricity revenues are included, we observe that forest residues biomass is cheaper (\$140 per t_{CO2}) than other biomass types and that imported biomass is the most expensive (\$210 per t_{CO2}).

The higher carbon content of crop residues (wheat straw) compared to that of forestry residues (44% vs 40%) results in a lower removal cost for BECCS using wheat straw compared to forestry residues if electricity revenues are ignored. However, as its energy density is 23% higher than that of wheat straw, the overall removal cost becomes cheaper for forestry residues (140 \$/t_{CO2}) than for wheat straw (160 \$/t_{CO2}).

The more expensive pathway for BECCS is with imported pellets, due to the assumed cost of pellets, and sea transports representing 10% of its cost.

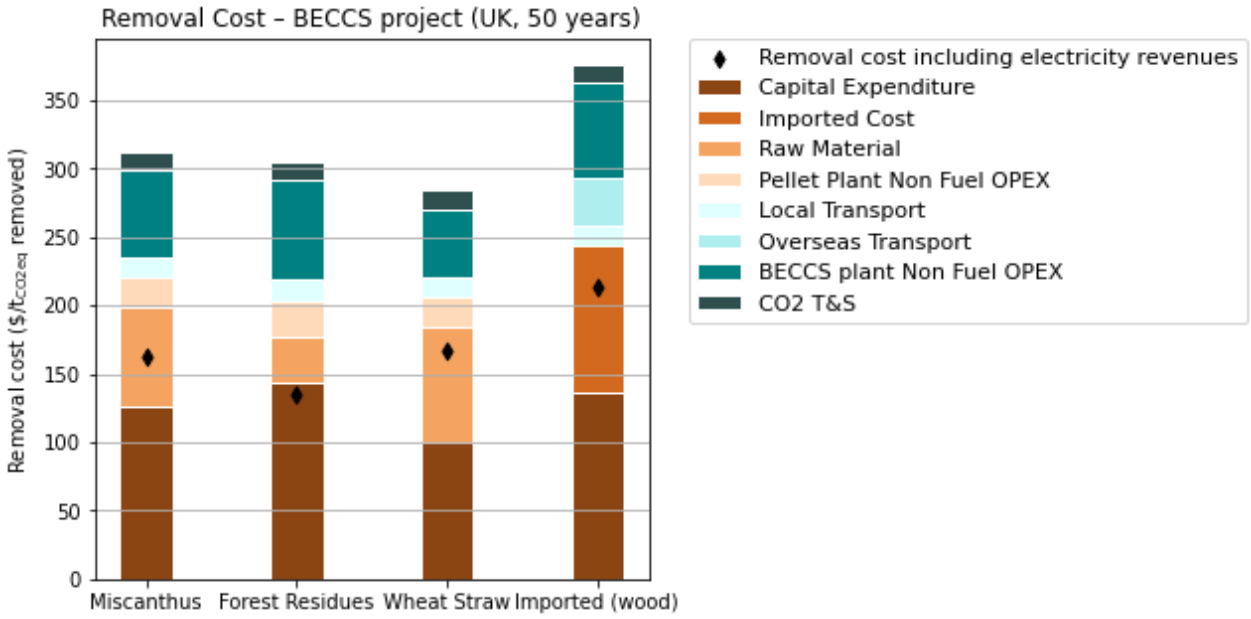


Figure 2.4: Removal Cost of BECCS for four biomass types.
Electricity revenues from power generation are set to 2019 UK electricity prices of 125 $/MWh[74].

Finally, the energy balance of BECCS is a key step of our modelling, as we need to accurately integrate BECCS power balance into the Electricity System Optimisation (ESO) model. As observed in the cost balance Eq. 9 and Figure 2.4, power is a significant source of revenue for BECCS.

2.2.1.4 BECCS power balance

The following equation calculates the power generated by all BECCS plants in region g at time t, based on the number of operating plants, the capacity of BECCS plants $Capacity^{BECCS}$, set to 500MW, and the capacity (or utilisation) factor $capfact(t)$, set to 80% [24]:

$$P_{g,t}^{BECCS} = capfact(t) * Capacity^{BECCS} * ON_{g,t}^{BECCS}, \forall\, g \in G, \forall\, t \in T \qquad \text{Eq. 14}$$

Biomass to pellet conversion

The conversion of raw biomass to biomass pellet through the conversion rate γ_i:

$$P_{pel(i),g,t} = \gamma_i D_{i,g,t}, \forall i \in B\backslash\{Imp\}, \forall\, g \in G, \forall\, t \in T \qquad \text{Eq. 15}$$

Moreover, the number of pellets used is linked to the electricity generated through the following equation:

$$P_{g,t}^{BECCS} = \sum_{i \in Pellet} DMR * HHV_i * \eta_i^{BECCS} * D_{i,g,t}, \quad \forall\, g \in G, \forall\, t \in T \qquad \text{Eq. 16}$$

where:

- $P_{g,t}^{BECCS}$ is the total amount of electricity generated in region *g* at time *t* (in MWh per year)

- DMR is the dry mass rate fixed at 92% [22]

- HHV_i, the higher heating value depends on the biomass type and is assumed to be 49 and 46 MJ/t_{DM} for forest residues and miscanthus respectively [22].

- η_{BECCS}, the power efficiency of BECCS is set to 33%$_{HHV}$ [65], [75]

The power efficiency of BECCS has been shown to vary in the range 26-38%$_{HHV}$ [65], [75]. The lower bound is a baseline scenario computed with the following parameters: biomass pellet at 5% moisture rate, BECCS power plant 90% capture rate. The higher bound comes from Bui et al. [75], that demonstrated the efficiency of BECCS can be enhanced through the utilization of advanced solvents that require less heat duty, alongside the adoption of heat integration strategies, including the recovery of heat from exhaust gases to supply the heat duty needed for solvent regeneration. These modifications have been shown to potentially raise the power generation efficiency of BECCS to 38%$_{HHV}$. In our modelling we chose a middle scenario of 33%$_{HHV}$.

Bio-geophysical constraints for BECCS deployment

Infrastructure equations are detailed in Eq. A 2. Other CDR's infrastructures, such as DACCS, pyrolysis plant, as well as mining and comminution facility (for EW), follow similar equations to BECCS plant infrastructures.

Material balance equation

The biomass balance equation, detailed in Eq. A 5, ensures that traded material between regions is well balanced. Biomass for BC and rock material for EW follow the same equations as that applied to biomass for BECCS.

Biomass ,land use equation and the water concern

Land use for bioenergy-dedicated crops, *i.e.*, miscanthus in the UK is limited by the amount of marginal land (MAL) available, totalling 2.1 Mha, as described and illustrated in Figure A 1 (Appendix). To include water use limitations in the model's constraints, we apply a water stress filter based on the Aqueduct water stress index [57], only conserving lands with an OWR index less or equal to 3 (that precludes biomass growth on lands with high, and very high water risks). Eventually, taking into account these water land limitations, we end up with 1.5 Mha of marginal land available in the UK, with a water stress index lower than 3, or equal. Similarly, availabilities for biomass residues (from croplands & forests) and imported pellets are justified in Eq. A 8 and Eq. A 9 (Appendix).

All biomass types can be used *via* BECCS and Biochar pathways, thus resulting in competition for miscanthus, forestry and crop residues (wheat straw, in this study) due to their limited availabilities.

Although the water concern is a key point for future BECCS large scale deployment, it is not the core of the thesis research question, and water use equations are not explicitly stated in our model. We rather, implicitly include water use limitations by selecting appropriate land, with a low water stress index, for biomass growth. Note that Fajardy found that energy dedicated crops, such as miscanthus, have a lower water footprint than conventional crops (*e.g.*, wheat), because of their low fertilizer inputs, and relatively high yield [76]. However, energy dedicated crop water footprint is also subject to higher uncertainty, echoing from uncertainty in the input data (both yield and fertilizer input). The water footprint of biomass residues, such as wheat straw, can be assumed to be zero, as the entire water withdrawal can be associated to wheat production. In addition, water needs for biomass harvesting is in average 100 times higher than that of operating a BECCS plant. This points out the importance of considering the whole supply chain water consumption, but without minimising the need of reducing power plant consumption.

2.2.2 Direct Air Carbon Capture and Storage (DACCS)

Direct Air Capture and Storage, often abbreviated *DACCS* is a CDR technology that directly captures CO_2 in the air/atmosphere, without the need of being at a CO_2 emission source, and that sequesters it in a geological formation. Unlike other CCS technologies that are usually deployed at power plant locations (like BECCS), the main challenge of DACCS is to capture the very sparse CO_2 in the ambient air, by using chemicals, at a reasonable cost.

Known for its high removal potential at the global scale (due to its low land requirement compared to that of BECCS), DACCS is an energy-intensive process that is still at a relatively early commercial deployment phase [77], with a TRL of 4-7 [15].

DACCS technologies have recently been included in IAMs projections [78]–[81] and their role in IPCC scenarios has increased in the last report AR6 [3]. However, DACCS future projections diverge in the literature. While some confident studies have estimated that DACCS plants could sequester in the range of 10–40 Gt_{CO2}/yr in 2100 [82], broader studies suggest that DACCS sequestration potential rather lies in the range of 0.5–5 Gt_{CO2} annually by 2050 [52].

Yet, its high current cost (~\$1000 per t_{CO2}) makes it a last-resort technology if no other choice is left to meet global targets [83]. Similarly to its potential, cost ranges found in the literature also vary greatly. According to the IEAGHG technical report, first-of-a-kind (FOAK) DACCS plants are likely to cost from \$400 to \$700 per t_{CO2} when global average solar photovoltaic costs are assumed, and even \$350-\$550 per t_{CO2} when lowest renewables costs are assumed [84].

Nowadays, these high costs face scientific debates as they might be subject to a decrease in the future. However, estimated future costs diverge between \$80 and \$600 per t_{CO2} and are still subject to high uncertainties. [50]

Being an energy-intensive process, the other main barrier to DACCS deployment is the availability of a clean energy source, leading to industrial projects located close to clean and

cheap energy resources, such as Climeworks' new Orca, and Mammoth DACCS plants in Iceland [85].

Common technologies used for DACCS are high-temperature liquid solvent (LS), and low-temperature solid sorbent (SS), as we model in our DACCS modelling [86].

DACCS modelling in the UK

DACCS modelling follows that of Chiquier et al. [21]. Both high-temperature liquid solvent (LS) and low-temperature solid sorbent (SS) technologies are considered in this dissertation. The input parameters and operations considered in DACCS modelling are illustrated in a diagram in Figure 2.5.

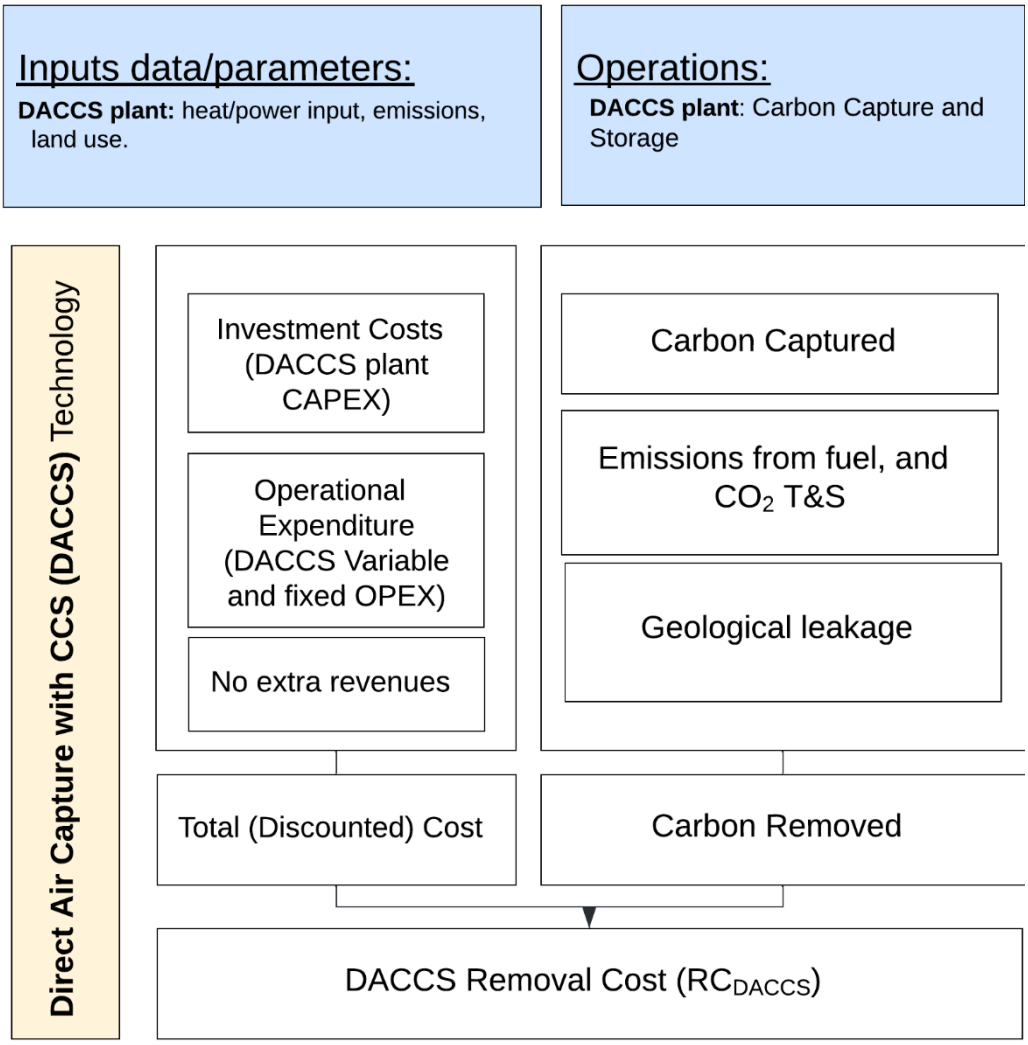


Figure 2.5: Overall picture of DACCS

2.2.2.1 DACCS GHG balance

Using the same general equation as for other CDR solutions, the total carbon removed by DACCS CR_{DACCS} is expressed t_{CO2} per plant per year:

$$CR_{DACCS} = CC_{DACCS} - CE_{DACCS}$$ Eq. 17

DACCS CO_2 capture is assumed to be immediate as it occurs instantaneously when the DACCS plant is operating. The CO_2 capture CC_{DACCS} is constant with time and is assumed to be 110 t_{CO2}/hour [87] for a liquid solvent DACCS plant, and 0.21 t_{CO2}/hour [88] for a solid sorbent DACCS module. These numbers are not representative of respective DACCS technology's efficiencies, as the size and energy need of the plants/modules are not the same for DACCS-LS and DACCS-SS. The CO_2 capture per unit of energy (i.e., implicitly including plant/module size) is 150 t_{CO2}/MJ for DACCS-LS, and 95 t_{CO2}/MJ for DACCS-SS. These calculations are extracted from referenced data in Table A 5 in Appendix.

Emissions during the DACCS process occur along both the DACCS plant/module operation and during the CO_2 T&S supply chain:

$$CE_{DACCS,sc} = CE_{Energy,sc} + CE_{CO_2T\&S,sc}$$ Eq. 18

where:

- $CE_{Energy,sc}$ are the emissions related to energy inputs for the DACCS plant operation (in t_{CO2} per plant per year)

- $CE_{CO_2T\&S,sc}$ are the emissions occurring during the CO_2 T&S supply chain (in t_{CO2} per plant per year)

The input data assumed for DACCS is provided in Table A 5 (Appendix) and is illustrated in Figure 2.6 for two different electricity carbon footprints. It results that emissions are mostly due to energy used during the process, *i.e.*, natural gas and electricity in the case of DACCS liquid solvent, and electricity only in the case of DACCS solid sorbent. Using carbon-free electricity (Figure 2.6, right-hand side), both DACCS types' emissions are drastically reduced but still show a non-zero energy carbon footprint due to natural gas used to meet high-temperature requirements in the case of liquid solvent DACCS.

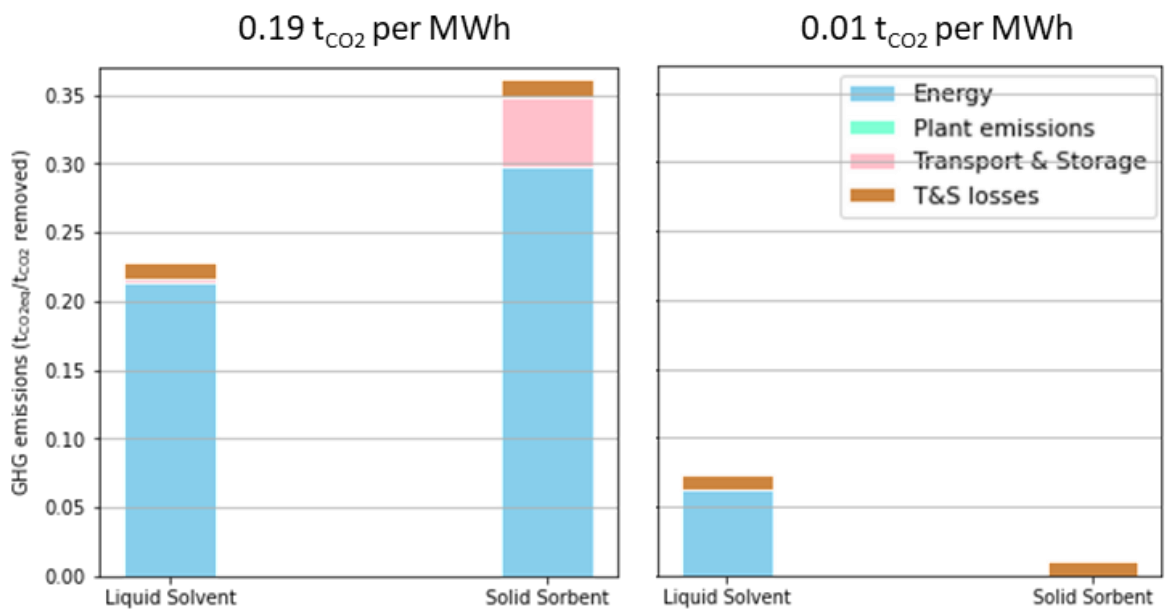


Figure 2.6: GHG emissions for DACCS (Liquid Solvent and Solid Sorbent)
We provide results for two different electricity carbon footprints (from 2021, and a carbon-free power system, as projected in the UK by 2035 [89])

Geological leakage risk

Because DACCS also includes CO_2 transport and storage into geological formations, the leakage probability for CO_2 can be expressed as follow:

$$Decay_{DACCS}(t) = (1 - 0.00063 * t). \quad \text{Eq. 19}$$

Like in the BECCS case, DACCS removal costs will not be affected by geological carbon leakage, as we assume a permanence horizon of 100 years in this section.

2.2.2.2 DACCS cost balance

We incorporate different levels of costs for the operation of DACCS, including capital expenditures, and operational expenditures, expressed in $ per plant per year:

$$TotCost_{DACCS} = TotCapex_{DACCS} + \sum_{sc \in Sc} TotOPEX_{DACCS,sc} \quad \text{Eq. 20}$$

The formula of DACCS plant capital expenditure is expressed in Eq. A 1. Both CAPEX and OPEX cost assumptions are based on [87] for liquid solvent and [88] for solid sorbent and are given in Table A 1 (Appendix).

The operational expenditures are divided into energy costs, non-fuel operating expenses, and CO_2 transport and storage, as follows:

$$TotOPEX_{DACCS,sc} = CostEnergy_{DACCS,sc} + NonVarOpex_{DACCS,sc} + CostT\&S_{DACCS,sc}$$ Eq. 21

2.2.2.3 DACCS removal cost

As illustrated in Figure 2.7, the resulting removal costs of DACCS are \$640 and \$837/t_{CO2} for liquid solvent and solid sorbent respectively, assuming an electricity carbon footprint (CF) of 0.19 t_{CO2} per MWh (2021 UK power system CF) and 0.01 t_{CO2} per MWh, representing a carbon-free power system. We also assume an electricity cost of 125 \$/MWh [74] (2021 values). We find that the removal cost of DACCS with solid sorbent is more dependent on the power carbon footprint, as it is the only energy resource used through its operation, compared to the liquid solvent technology. These removal costs are in line with estimations found in the literature [50].

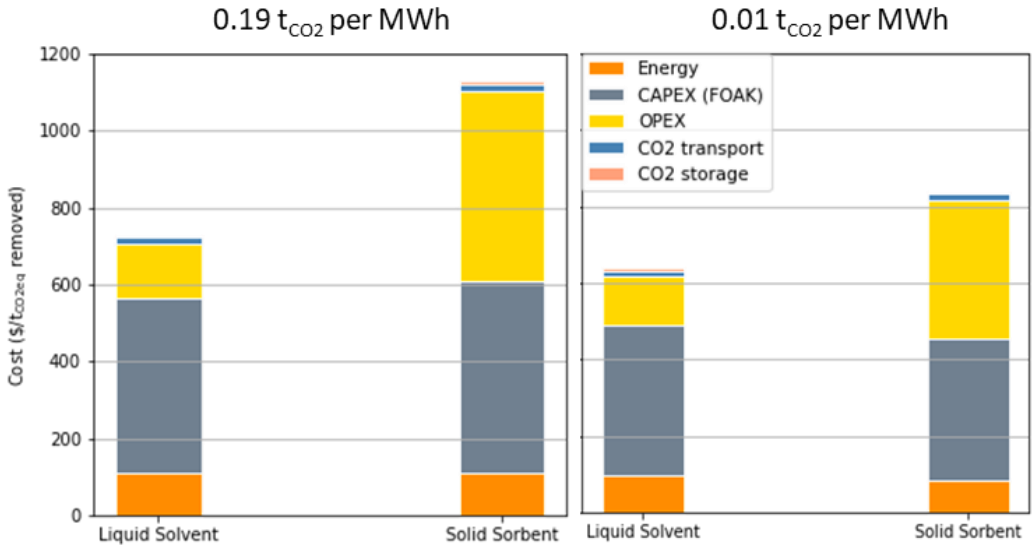


Figure 2.7: Removal cost of DACCS (\$/t_{CO2}).

We make the conservative, but plausible assumption, of powering DACCS from the national grid, as opposed to using waste energy[80], [87], [90], driving its cost to low ranges far from today's DACCS market costs.

2.2.2.4 DACCS power balance

Unlike BECCS, DACCS often requires energy (electricity and/or heat) to remove CO_2 from the atmosphere. The amount of energy needed depends on the DACCS technology used. For high-temperature DACCS-LS, 900°C heat is needed and can be provided *via* either natural gas or hydrogen. DACCS-LS also has power requirements which we set to 366 kWh per t_{CO2} captured, as found in the literature [87].

For low-temperature DACCS-SS, we assume that both heat and power are provided by electricity from the grid, as only heat of 100°C is required for SS. We made our calculations

based on public data for DACCS-SS [88], resulting in electricity consumption of 1434 kWh per t_{CO2} captured.

DACCS land-use

For land-use, we focus on DACCS infrastructure in this work.

More explicitly, we assume DACCS-LS uses 1,370 ha for a capacity equivalent to 1 Mt_{CO2}/yr captured, and DACCS-SS 10 ha for the same capacity [86]. Thus, the solid sorbent archetype is much more efficient than its counterpart. By considering GGR scenario deployments such as anticipated by Vivid Economics [16], DACCS deployment in the UK in 2050 would correspond to 27,400 ha and 200 ha, for DACCS-LS and DACCS-SS, respectively.

Given reasonable area requirements for DACCS, the land footprint of DACCS should not be a barrier to DACCS deployment, if it is assumed that the only space used by DACCS is for the DACCS infrastructure.

However, in a holistic analysis, it may be advantageous to incorporate the land utilized by the electricity infrastructure supporting Direct Air Capture and Carbon Storage (DACCS) operations. Such a consideration is not evaluated in MONET but is included when coupling MONET with the power sector in Chapter 3. As described in the corresponding chapter, the deployment of onshore wind and solar technologies are constrained by environmental constraints, thus limited to 40 GW and 90 GW, as recommended by the CCC [89].

2.2.3 Afforestation/Reforestation (AF)

Afforestation and reforestation (AF) refer to planting trees on land that was previously purposed for other land use, or to the restoration of degraded forests by easing their natural regeneration. The term reforestation is used when a forest was filling the land before another land use occurred, but both terms are usually used together, describing the same solution.

The forest expansion process, when done properly, enables many benefits, including carbon sequestration, greater biodiversity, ecological resilience, and climate regulation benefits. Typically, natural forests with a closed canopy provide more benefits than homogeneous forests destined for timber production [91]. Timber production for bioenergy can also mitigate the use of fossil fuel (*e.g.*, the production of ethanol using gasoline, or the production of electricity using coal, or oil), but faces controversies when it comes to assessing their carbon neutrality, usually *via* life cycle assessments (LCA). Assessing their carbon neutrality is a complex task, and results will vary depending on the feedstock, supply chain emission, but also spatiotemporal assumptions. McKechnie et al. (2011) estimated that payback time (*i.e.*, the time it requires to become carbon neutral, all emissions included) was 16-38 years for electricity production, but as high as 74-100 years for ethanol production, with ranges due to the differentiation between the use of forest residues (low payback time) and standing trees (high) [92]. To illustrate the numerous ways of managing the forest for bioenergy and different carbon reduction impacts, Buchholz et al. (2016) concluded that the payback time of bioenergy forests could vary between 0 to more than 1,000 years [93].

For these reasons, this section will entirely focus on forests destined for carbon sequestration.

Afforestation is the most understood CDR, as forests have surrounded us and been exploited for timber production for a long time. Hence, logically, multiple countries have included forest expansion in their policies, and National Determined Contributions (NDC) [94]. For example, the CCC, an independent body in the UK advising the UK government, suggests increasing the plantation rate of new forests to 50,000 ha per year by 2050 [47].

AF is commonly considered to be the cheapest CDR, with costs ranging from \$10–150/tCO_2 depending on regional assumptions [52]. However, forests face criticism in the scientific community, as it requires space, need to be done in an appropriate climate and region, (*e.g.*, avoiding the albedo effect), does not provide permanent sequestration (*i.e.*, not as permanent as geological storage), and needs to be carefully managed and monitored to ensure the forest effectively becomes a carbon sink during its lifetime.

According Treecoomy – a start-up that tries to enlighten the value brought by forest through AI-based algorithms and modern imagery technologies – today's main barriers to forest expansions, especially for private landowners, are 1) low credit prices associated with the carbon sequestration provided by the forest project, 2) MRV costs, that prevent small landowners to entry the market, 3) the opportunity cost of alternative land use, and 4) slow payment rates, as trees grow slowly [95].

Afforestation modelling in the UK

As said in the last subsection, our modelling investigates afforestation (AR) as a nature-based solution where its management consists in maintaining the forest canopy and carbon stock sustainably, resulting in a net carbon removal operation.

Our AF model is inspired by Chiquier et al.[21], and is composed of five submodels which include forest growth, forest management cycle, biogenic carbon sequestration, fire penalty, and forestry operations [21]. These five components are key to evaluating the cradle-to-grave impact of afforestation. The model is summarized in the diagram in Figure 2.8.

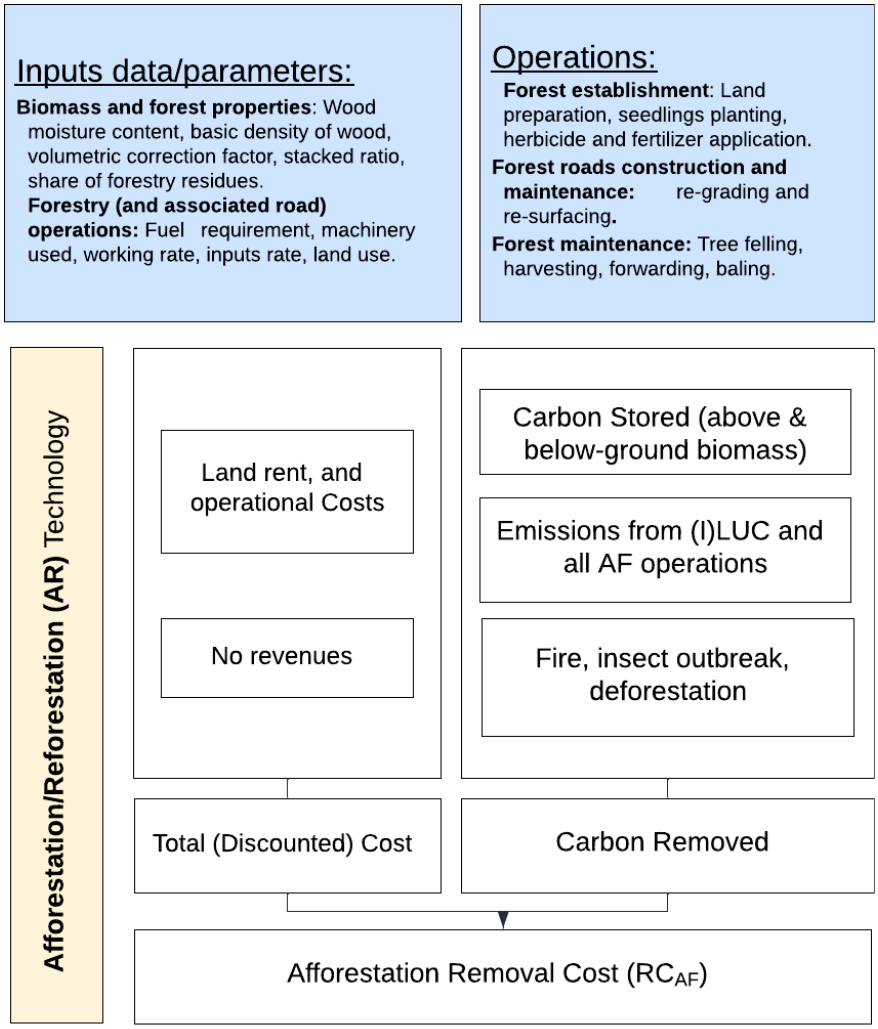


Figure 2.8: Overall picture of Afforestation

We assume our forests are planted on reforestation potential lands, as in the reforestation opportunities dataset provided by Griscom et. al [3] and illustrated in Figure 2.9. Using the same logic as for BECCS, we apply a water stress filter [57] that precludes afforestation projects on lands with high water risks. This afforestation potential will be used as a maximum bound for AF national deployment.

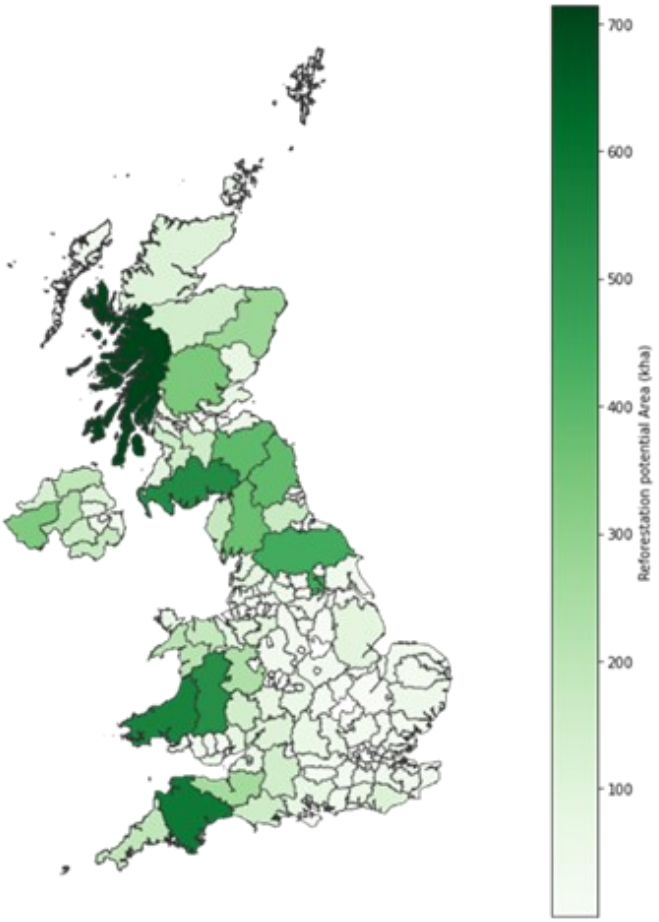


Figure 2.9: Reforestation potential in the UK, according to Griscom et al. [3]

We model afforestation [21] using a spatial resolution at the ecological zone level—an area with homogeneous natural vegetation formations, and similar temperatures and rainfalls [96], [97]. The removal cost of AF depends on the ecological zone forests lie in, which determines the sequestration rate of biomass growth. We assume that management costs are the same throughout the UK. There are four ecological zones in the UK, but 98.6% of potential lands for afforestation in the UK lie within the *temperate mountain systems* and the *temperate oceanic forests* zone, whereas 1.4% lie within the two boreal zones. We, therefore, exclude boreal zones from our modelling.

In the next subsection, we will explore the different high-level equations used in the modelling of AF. For more details regarding the afforestation model that is used in this study, the reader is invited to read Chiquier et al. [21], [53].

2.2.3.1 AF GHG balance

Following the general equation for carbon removal, we can express AF carbon removal in t_{CO2} per ha per year:

$$CR_{AF,ez,t} = CC_{AF,ez,t} - CE_{AF,t} \quad \text{Eq. 22}$$

The carbon captured $CC_{AF,t}$ is proportional to the growth of biomass within the forest, which is determined by a forest growth model [21], parametrised by tree species, ecological zone, thinning frequency and tree density. The main drivers of forest biomass growth can be described by the following sigmoid curve:

$$B^{AG}_{Ref,ez,t} = \frac{B_{Ref,ez}}{1+C*\exp\left(\frac{2*t}{T_{Ref,ez}}-1\right)}, \quad \text{Eq. 23}$$

where:

- $B^{AG}_{Ref,ez,t}$ is the maximum above-ground biomass stock of reference, for which we assume 180 and 100 t_{DM}/ha for temperate oceanic forests (TeDo) and temperate mountains (TeM) climates [98]

- $T_{Ref,ez}$ is the growing period of reference, *i.e.*, the duration for the forest to reach maturity, that is 41 and 34 years, respectively for TeDo and TeM [98]

- C is a constant equal to $C = \frac{100-a_{ref}}{a_{ref}}$ where a_{ref} is the asymptote coefficient of the sigmoid curve, which is set to 99 [21]

Although there are boreal climates in the UK, especially in the northern regions, the reforestation land availability within these regions is negligible, thus we don't consider them in our present study. By only focusing on temperate ecological zones, the immediacy of AF removal, *i.e.*, the length of sequestration before reaching maturity, is 34-41 years.

Then, the above-ground biomass stock $B^{AG}_{Ref,ez,t}$ is then extrapolated to find the total amount of biomass stock in the forest $B^{tot}_{Ref,ez,sp,t}$ through the "root-to-shoot" ratio R, that depends on the ecological zone *ez* and tree species *sp* [98]. The total biomass stock is then used to compute the carbon captured by the forest, following the equation:

$$CC_{AF,ez,sp,t} = B^{tot}_{Ref,ez,sp,t} * CC_{c,sp} * \frac{44}{12}, \quad \text{Eq. 24}$$

where:

- $CC_{AF,ez,sp,t}$ is the carbon removed by AF expressed in t_{CO2}/ha
- $B^{tot}_{Ref,ez,sp,t}(t)$ is the total biomass stock in the forest in t_{DM}
- $CC_{c,sp}$ is the carbon content of trees dependent on climate *c* and the tree species *sp* in t_C/t_{DM}. For temperate climates (UK), it equals 0.48 for broadleaves and 0.51 for conifers, following IPCC values [99]

Emissions related to afforestation depend on the phase of the forest project: establishment, full-vigour, mature, or old-growth phase [21]. During the establishment phase – the first five years – emissions accounted for are road constructions CE^{AF}_{RC}, ground preparation CE^{AF}_{GP},

seeds plantation CE_{SPl}^{AF}, fertilizer CE_{Fert}^{AF}, and herbicide CE_{Herb}^{AF} use. Nitrous oxide emissions (N_2O) resulting from the application of nitrogen-based fertilizers during forest establishment are taken into consideration. During this stage, emissions follow the equation:

$$CE_{AF,t} = CE_{RC}^{AF} + CE_{GP}^{AF} + CE_{SPl}^{AF} + CE_{Fert}^{AF} + CE_{Herb}^{AF}, \text{ if } t \leq 5 \quad \text{Eq. 25}$$

During the full-vigour phase, during which trees growth is increasing every year, emissions are related to road maintenance (CE_{RM}^{AF}), and to thinning ($CE_{Thinning}^{AF}$) assumed to occur every $Freq_{Thin}$ years (equal to 5). This phase lasts between year 15 and when the maximum mean annual growth (MMAG) occurs t_{MMAG}:

$$CE_{AF,t} = CE_{RM}^{AF} + \frac{CE_{Thinning}^{AF}}{Freq_{Thin}} \text{ if } 15 < t \leq t_{MMAG} \quad \text{Eq. 26}$$

Finally, the mature phase occurs after the full-vigour phase, until half of the MMAG is reached (*i.e.*, the forest biomass growth decreases during this phase) and the old-growth phase follows. Emissions during both phases follow the same formula as in Eq. 26, with different thinning frequencies $Freq_{Thin}$ (10 years for the full-vigour phase, 15 during the old-growth phase).

The overall GHG emissions occurring during afforestation in a temperate oceanic ecological zone over 50 years are illustrated in Figure 2.10, for different fractions of biofuel used along forestry operations. We find relatively balanced emissions across the different stages of the AF operations. When no biofuel is used (in this case we assume machinery and vehicles are fuelled with diesel), the highest carbon footprint is associated with thinning operations (1.23 t_{CO2eq} per ha) and the smallest with herbicide application (0.06 t_{CO2eq} per ha), adding up to 3.55 t_{CO2eq} per ha. With biofuel share increasing, we find that emissions related to ground preparation, thinning operations, road construction and maintenance decrease, and total AF emissions reach 1.9 t_{CO2eq} per ha, showing that close to 50% of emissions are related to fuel use in machinery and transports.

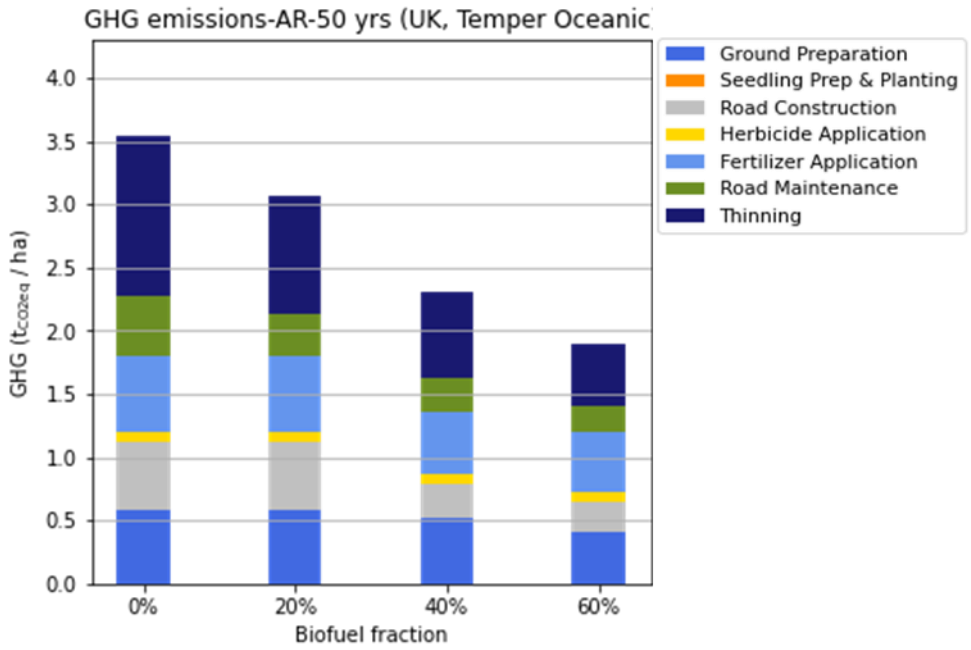


Figure 2.10: Cumulative Afforestation GHG emissions over 50 years in *Temperate Oceanic* ecological zone. Computed through our afforestation model, replicated from [21].

Forest Leakage risk

The fire risk used in this study (Hurteau et al. [100]) is parametrized by two parameters. The average fire-return interval *mFRI* (years), enables us to compute the probability of a fire occurring within a time window specified by an assumed time of permanence TP. The fire regime condition class departure index V_C (%) is the probability of damaging fires, given that a fire event occurs. Both parameters are found in the data provided by the LANDFIRE project[101], and describe the discounted value of forest carbon considering the wildfire risk. The forest-fire probability is thus expressed as [100], [102]:

$$Decay_{AF}(t) = \begin{cases} 0, t < mFRI \\ V_C * \left(1 - \frac{mFRI}{t}\right), t > mFRI \end{cases} \quad \text{Eq. 27}$$

The coefficients are a function of the ecological zone. The values are 424 and 158 years for mFRI for TeDo and TeM, *i.e.*, that the fire probability is zero until the forest's age surpasses these number of years. V_C values are 61% and 51% for TeDo and TeM, respectively. This shows a higher probability of more damaging fires for TeDo zones, whereas the probability of a fire event occurring is smaller.

2.2.3.2 AF cost balance and removal cost

The total cost of forest can be expressed as a sum of capital investment costs, and operating costs:

$$TotCost_{AF} = \sum_{t \in T} TotCapex_{AF,t} + TotOpex_{AF,t} \quad \text{Eq. 28}$$

Where $TotCapex_{AF,t}$ include land costs, ground preparation, seedling preparation & planting, and road construction. Operating costs $TotOpex_{AF,t}$ include herbicide fertilizers, road maintenance, and thinning operations (harvesting). Removal costs for afforestation (Figure 2.11) vary between \$90-120 per t_{CO2} when considering temperate ecological zones. As illustrated in Figure 2.11, boreal climate results in rather expensive AF costs (\$200 – \$350 per t_{CO2}), compared to reported global AF cost ranges (up to \$150 per t_{CO2} [52]). Indeed, boreal climates show a lower amount of carbon sequestered – corresponding to the denominator in Eq. 3, thus increasing the cost of removal. In the rest of the study, we will ignore boreal climates and focus on temperate ecological zones.

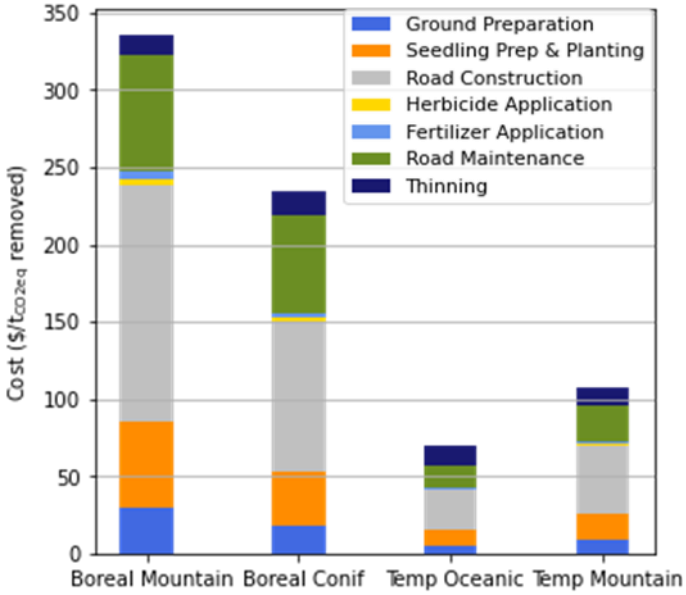


Figure 2.11: Removal cost (\$/t_{CO2}) of Afforestation.
Average cost over 50 years of the four climates existing in the UK.

2.2.3.3 AF power balance

We assume that AF does not use electricity – or too little, *e.g.*, through electric vehicles or machinery for road construction, management, or harvesting processes – in its life cycle. Thus, we have ignored the interaction between AF and the power sector in this dissertation.

2.2.4 Enhanced Weathering (EW)

Enhanced rock weathering (EW or ERW) is a carbon removal solution that has been suggested in the literature for more than 30 years [103], [104]. It is a way of storing carbon dioxide (CO_2) using rocks' chemical reactions. As of today, it is not known exactly how much carbon can be removed *via* this reaction, but good estimates are available and we know that the carbon will be removed permanently over 10,000 years. [3]

One of the main issues with enhanced rock weathering is related to monitoring, reporting and verification (MRV). Indeed, there is no clear way of measuring the carbon that has been sequestered, like in a pipe (CCS) or an idle stock, like in biochar. Three main methods could be used to measure EW, providing a lower, upper bound and one in between, respectively [105]. These methods are 1) measure total alkalinity produced in the leachate waters, 2) measure the remaining rock powder, and 3) measure element flows which may be good estimates for the weathering, or directly measure carbon flows. There is ongoing research work on better measurement methods, to prove that the three methods converge to a single value. For now, this seems to be the bottleneck of EW deployment. However, the marketplace Puro.earth has launched a public consultation to establish a standardised framework enabling EW projects to be commercialised, and the first Puro Standard has been approved in December 2022. An important part of their methodology is to monitor environmental impacts and keep a low level of contaminants in the soil.

EW modelling

Terrestrial enhanced weathering (EW) aims at enhancing the natural carbon sequestration process of silicate dissolution by replicating this process at the land surface [106]. It consists of the spreading of powered silicate minerals in the environment and requires minerals sourcing, crushing, comminution, and transport to application areas such as croplands, forests, marginal lands or coastal areas [52], [107]. Most research has focused so far on terrestrial EW on croplands, due to its high efficiency and potential, and relative ease of application [15]. Thus, this work considers terrestrial EW only and refers to it as EW for simplicity. The modelling of EW used in this study is illustrated in Figure 2.12.

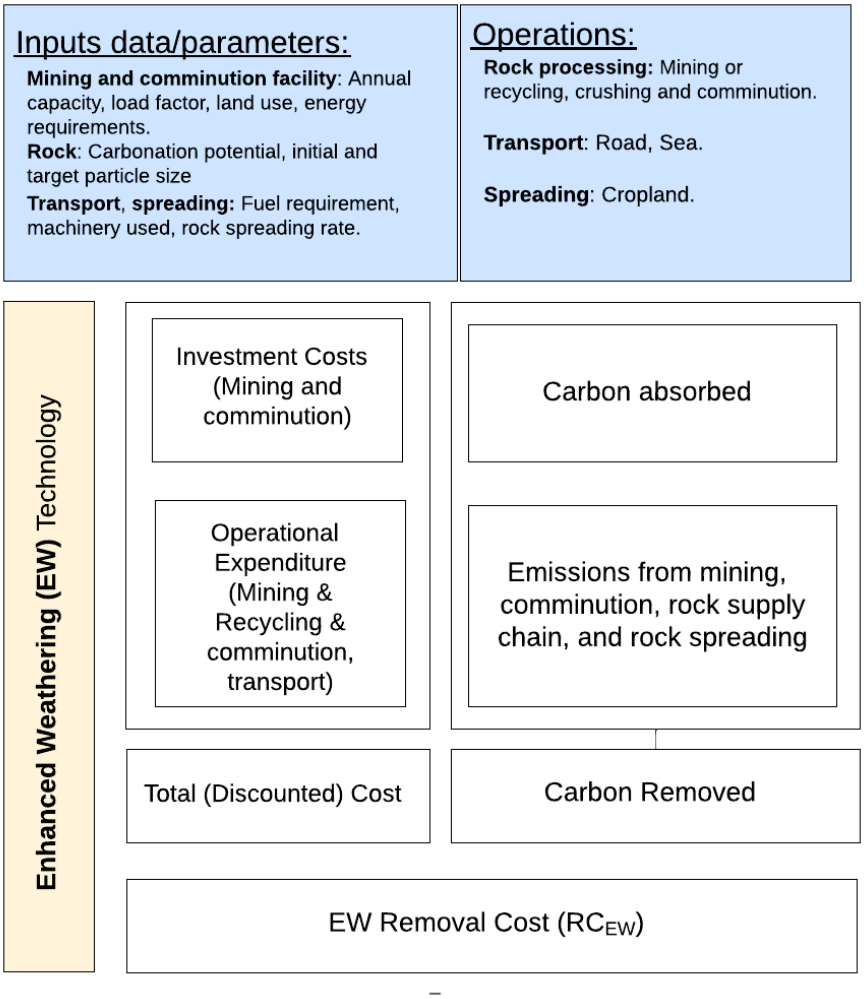


Figure 2.12: Overall picture of Enhanced Weathering (EW)

Different silicate sources can be considered suitable for EW: silicates rock, quarry fines from basaltic rock (fines) and artificial silicate by-products from the industry. Silicate rock needs to be extracted from rock formations. In the UK, Renforth estimates that the utmost quantity of silicates extractable amounts to 1668.66 Gt [106], exceeding by several orders of magnitude the plausible demand. Thus, extracted basalt quantities are constrained by the build rate for mining extraction facilities rather than resource availabilities. When basalt is crushed to produce aggregate, around 20% (up to 40-45%) of the fine materials produced are too small for usage, and are thus available for EW[108], [109]. With particle size below 63 µm, these fines require less energy for grinding than other silicate types [110]. As multiple studies warn of the potential negative impact of ultramafic silicates (*e.g.*, dunite) on soil and water pollution due to heavy metals in their composition, we do not consider this type of rock for EW. Moreover, we also consider industrial silicate residues, for which we don't account for any industrial-associated emissions. The UK production of these silicates was 86 million tonnes per year in 2012. These by-products are composed of Cement Kiln Dust (CKD), construction and demolition wastes (CDWaste) and iron and steel processing (slag). We assume that industrial by-product availability that could potentially be processed and spread over croplands is very limited due to social acceptance and considering that a high share of these by-products is already recycled. We arbitrarily assume that 0.5% of national by-product production can be used for EW in our model.

2.2.4.1 EW GHG balance

Like other CDR, the total amount of carbon removed by EW is computed as the carbon captured through the weathering process minus all emissions along the supply chain, expressed in t_{CO2} per t_{rock}:

$$CR_{EW} = CC_{EW,s,g,t} - CE_{EW,s} \quad \text{Eq. 29}$$

Where the carbon captured in the EW process, CC_{EW} is expressed as a function of both time of measurement *t*, and time of rock application *t'*:

$$CC_{EW,s,g,t} = D_{s,g,t} * R_{CO_2,s} * p_{g,d,s,t}^{weathered} \quad \text{Eq. 30}$$

where:

- $D_{s,g,t}$ is the rock *s* supply in region *g* at time *t* (in t_{CO2})
- $R_{CO_2,s}$ is the maximum CO_2 capture potential of the silicate material (in t_{CO2}/t_{rock}), indicated in Table 2.1
- $p_{g,d,s,t}^{weathered}$ is the carbonation rate, *i.e.*, the share of rock that weathers every year (in %)

The carbonation rate assumed in our study follows a shrinking core model. It is dynamic and is correlated with the weathering rate W_r:

$$p_{g,d,s,t}^{int,weathered} = \frac{d_m^3(d) - (d_m(d) - 2V_m W_r * D(t))^3}{d_m^3(d)} \quad \text{Eq. 31}$$

where:

- $d_m(d)$ is the targeted rock particle size (in μm), assumed to be 10 μm
- V_m is the molar volume $V_m = 4{,}302 * 10^{-5}$ (in $m^3 mol^{-1}$) , as indicated in [106]
- W_r is the weathering rate W_r (in $mol.m^2.s^{-1}$), depend on other parameters such as the rock's mineral, soil temperature, and soil pH described in Eq. 33
- $D(t)$ is the time between measurement t and the time the rock was spread (in seconds)

The weathering is maxed out by a maximum value $p^{max,weathered}$, assumed to be 95%, following data from [106].

$$p_{g,d,s,t}^{weathered} = \begin{cases} p_{g,d,s,t}^{int,weathered} \; if \; p_{g,d,s,t}^{int,weathered} < p^{max,weathered} \\ p^{max,weathered}, otherwise \end{cases} \quad \text{Eq. 32}$$

The weathering rate depends on multiple parameters such as the mineral composition, the soil temperature, and pH. It is calculated as a weighted average of a rock's mineral composition (*i.e.*, mineral weight fraction) weathering rates, defined as follows [111], [112]:

$$W_r = \sum_i k_i \exp\left(-\frac{E_i}{R}\left(\frac{1}{T} - \frac{1}{298.15}\right)\right) a_j^{n_i} \quad \text{Eq. 33}$$

where:

- *i* is the individual weathering agent, namely H+, H_2O, and OH-
- k_i is the rate constant of the weathering agent (namely, H+, H_2O, OH-) (in mol.m-2.s-1)
- E_i is the activation energy (kJ.mol-1) [112]
- R is the universal gas constant, equal to 8.314472 [112]
- T is the annual average soil temperature [112]
- a_j is the molar activity of weathering agent j (in mol.l-1) [112]
- n_i is the reaction order [112]

The overall carbon captured *via* various EW pathways can be found in Figure 2.13, showing the evolution of the GHG absorption (in t_{CO2} per t_{rock}, y-axis) with years (x-axis). We observe an increasing rock weathering during the assumed project duration of 40 years, with the theoretical cap of 95% of weathering reached after 25 years. Slag and cement kiln dust (CKD) particles have a higher carbon capture potential than basalt, due to their inherent rock composition, resulting in higher $R_{CO_2,s}$ values, as can be seen in Table 2.1.

Table 2.1: Rock Properties

Silicate	$R_{CO_2,s}$(t_{CO2}/t_{rock})[a]	W_s (in kWh/t_{rock}) [106]	$d_{ini}(s)$ (in μm) [113]	$elec_{s,d}^{commin1}$ (in kWh/t_{rock})[b]
	Maximum CO2 capture potential	Bond Index	Initial rock size	Electricity required for initial comminution step
Basalt	0.299	19	1000	25.22
Basalt fines	0.299	19	63	7.29
CKD	0.56	11.05	22	0

Slag	0.57	14.28	1000	18.96

[a]Values are calculated from $R_{Ca,s}$ values and computed via formula $R_{CO_2,s} = R_{Ca,s} * \omega$ from [108] and with $\omega = 1.7$

[b]Computed using Eq. 43.

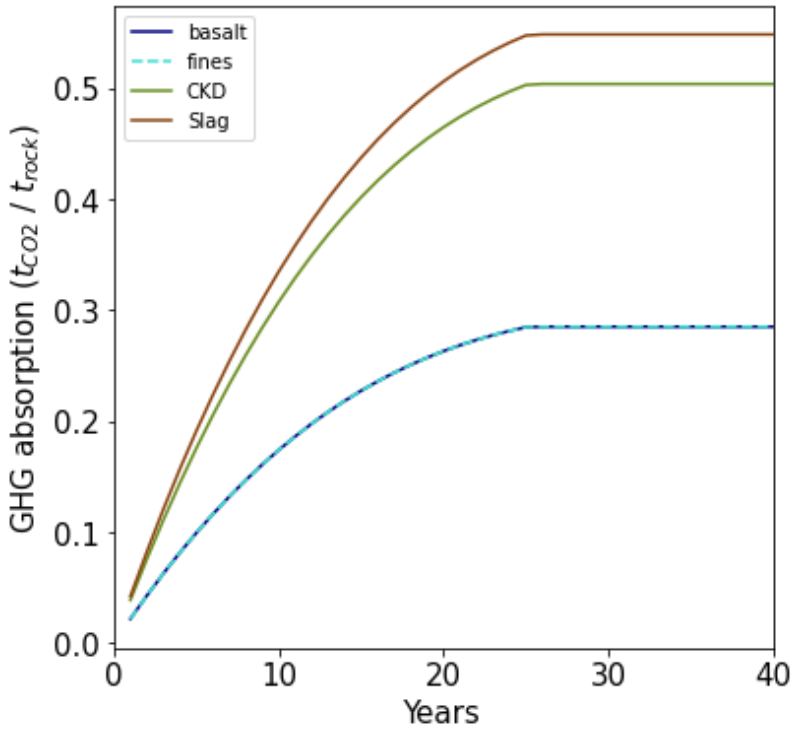


Figure 2.13: Carbon capture via Enhance Weathering considering four types of rocks, computed with targeted particle size of 10 μm.

Carbon emissions along the EW process occur while using electricity and fuel at different steps of the supply chain, expressed in t_{CO2}/t_{rock}:

$$CE_{EW,g,s} = CE^{EW}_{elec,s} + CE^{EW}_{fuel,s,g} \quad \text{Eq. 34}$$

Where emissions related to electricity use include both mining, crushing, and the comminution processes:

$$CE^{EW}_{elec,s} = GHG^{1kWh}_{elec} * \left(elec_s^{mining-crushing} + elec_s^{commin1-2}\right) \quad \text{Eq. 35}$$

where:

- GHG^{1kWh}_{elec} is the carbon footprint associated with electricity production (assumed to be similar to the carbon footprint of the UK power system in 2019, *i.e.*, 0.19 t_{CO2} per MWh [89])

- $elec_s^{mining-crushing}$ and $elec_s^{commin1-2}$ – the electricity requirements (in MWh/t_{rock}) during the mining, crushing, and comminution processes – are detailed in the *power balance subsection* below

Fuel emissions are associated with rock transport to the spreading fields and then, the spreading of rocks over croplands:

$$CE^{EW}_{fuel,s,g} = CE_{transp,s,g} + GHG^{1L}_{fuel} * fuel^{EW}_{app} \quad \text{Eq. 36}$$

where:

- $CE_{transp,s,g}$ corresponds to emissions related to inter– and intra–regional transports as defined in Eq. A 3 (in t_{CO2}/t_{rock})

- GHG^{1L}_{fuel} is the carbon footprint associated with fuel use (2.688 kg_{CO2} per litre)

- $fuel^{EW}_{app}$ is the fuel requirement for rock spreading (in litre per t_{rock})

Figure 2.14 shows the calculated GHG balance of the EW entire process, across the different rock types, expressed in kg_{CO2} per tonne of rocks. We find that the greater GHG contribution is due to the comminution process across the four different types of rock. An additional mining step is required for basalt because other rock types are residues from existing operations, and hence do not include mining. The inclusion of direct nitrous oxide emissions (using its CO_2 equivalent conversion factor of 298 kg_{CO2eq} per kg_{N2O}) resulting from the utilization of ammonium nitrate-based explosives in rock mining is accounted for. but mining emissions are low on a per t_{rock} basis, representing ~2% of all supply chain emissions. Similarly, a crushing step is required for basalt and slag, as their initial size is macroscopic (higher than 1 cm), and needs to be reduced before comminution, but crushing emissions are also low on a per t_{rock} basis, representing ~1.5% of all supply chain emissions. However, in the case of basalt fines and CKD, the initial particle size is sufficiently small (63 μm for fines and 22 μm for CKD) to skip the crushing step. Then, the energy required during comminution depends on the rock type and the initial particle size, thus differs for different rocks. For example, it is 15% higher for basalt than for basalt fines due to initial particle sizes (1000 μm versus 63 μm, see Table 2.1). Similarly, comminution energy is 6% higher for slag than for basalt fines. Emissions related to transport and spreading represent ~20% of the total carbon footprint. The overall GHG balance is slightly varying across different rock types, ranging between 58 – 68 kg_{CO2} per t_{rock}. Therefore, the optimal pathway chosen by the optimisation will rather look at other decision parameters (such as the cost, the weathering rate, or the rock availability).

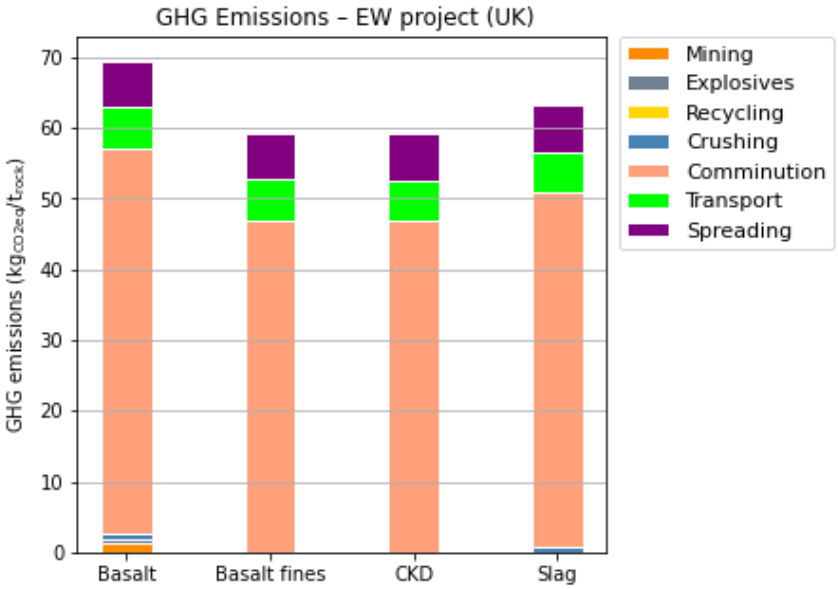


Figure 2.14: Emissions of Enhanced Weathering process considering four types of rock. The EW supply chain is decomposed into mining, comminution, transport, and application (spreading) of the rocks.

Leakage risk for EW

In this dissertation, we assume there is no leakage risk, and that the CO_2 that has been captured through the EW process is permanent. [52]

2.2.4.2 EW cost balance

Total enhanced weathering cost can be divided into CAPEX and OPEX costs, expressed in $:

$$TotCost_{EW} = \sum_{s\in S, g\in G} TotCapex_{EW,s,g} + TotOpex_{EW,s,g} \quad \text{Eq. 37}$$

Along the supply chain of EW, CAPEX investment costs related to both mining and comminution infrastructures must be included in our modelling:

$$TotCapex_{EW,s,g} = Capex_{mining,s} + Capex_{commin,s} \quad \text{Eq. 38}$$

The operational cost of EW is the sum of the fixed OPEX (*i.e.*, non-fuel OPEX), electricity, transport, and application costs:

$$TotOPEX_{EW,s,g} = Cost^{EW}_{fixOM,s} + Cost^{EW}_{elec,s} + Cost^{EW}_{transp,s,g} + Cost^{EW}_{app} \quad \text{Eq. 39}$$

The fixed operating and maintenance costs $Cost^{EW}_{fixOM}$ include the mining OPEX, recycling OPEX, comminution OPEX, and the general & administration OPEX:

$$Cost^{EW}_{fixOM,s} = Cost^{EW}_{mining,s} + Cost^{EW}_{Recycling,s} + Cost^{EW}_{Commin,s} + Cost^{EW}_{GA,s} \quad \text{Eq. 40}$$

The cost of electricity covers both the mining and the comminution processes:

$$Cost_{elec,s}^{EW} = cost_{elec}^{1kWh} * (elec_s^{mining-crushing} + elec_s^{commin1-2}) \quad \text{Eq. 41}$$

The cost of transport follows the general transport equation indicated in Eq. A 4 (Appendix), which applies to every material (biomass and rock) incorporated in this study.

Finally, the cost of rock application includes costs from the operation and maintenance of the machinery, and the fuel used to operate it:

$$Cost_{app}^{EW} = cost_{OM,app}^{EW} + cost_{fuel,app}^{EW} \quad \text{Eq. 42}$$

We provide the cost breakdown of EW pathways depending on the rock type in Figure 2.15. A higher removal cost is associated with basalt (reaching almost \$250 per t_{CO2}) and basalt fines (~\$150 per t_{CO2}), due to their relatively lower sequestration potential, as illustrated in Figure 2.13. Basalt remains more expensive than using fines, as there is no CAPEX associated with fines production, and the OPEX is restricted to the comminution OPEX (and not mining). Slag and CKD removal costs are ~ \$95 per t_{CO2}, explained by a higher maximum CO_2 capture potential (Table 2.1).

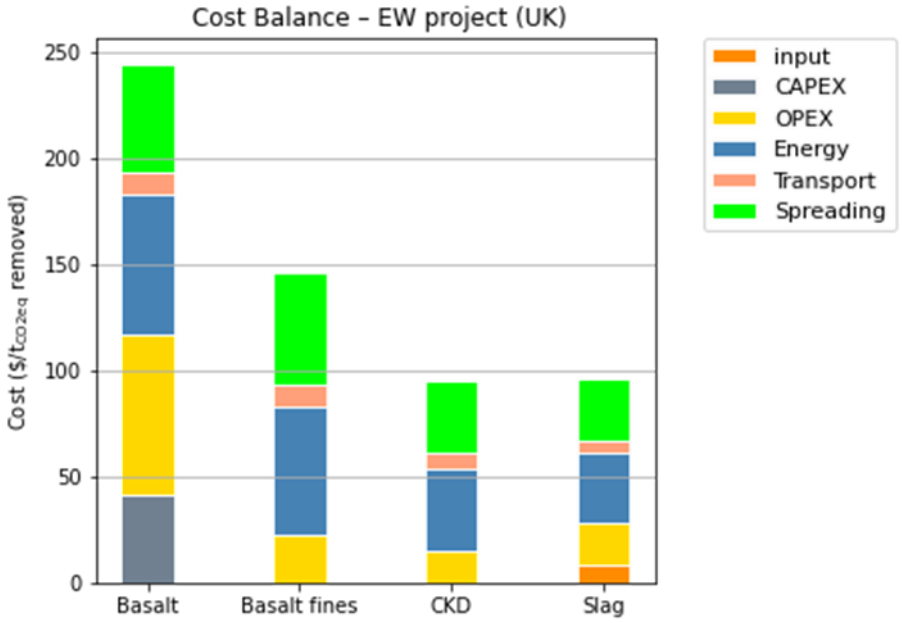


Figure 2.15: Cost of Enhanced Weathering process considering five types of rock.
The EW supply chain is decomposed into mining, comminution, transport, and application (spreading) of the rocks.

2.2.4.3 EW power balance

Like DACCS, EW requires electricity along its process, which will affect the electrical system in a scenario where EW is deployed significantly.

Electricity used to mine and crush the rock is used before comminution. Crushing is used to bring to an initial particle size of ~1,000 μm . This demand is zero for basalt fines and CKD because their initial particle size is small enough (as can be observed in Table 2.1):

$$elec_{basalt/slag}^{mining-crushing} = 8.33$$
$$elec_{fines/CKD}^{mining-crushing} = 0$$

These values have been derived from the findings of Strefler et al [114].

Then, electricity needed during the first comminution step, *i.e.*, to bring the particle to even lower sizes is computed using the following formula [115]:

$$elec_{s,d}^{commin1} = 10 * W_s * (\frac{1}{\sqrt{d_m(d)}} - \frac{1}{\sqrt{d_{ini}(s)}}) \quad \text{Eq. 43}$$

where:

- W_s is the bond index (in kWh/t_{rock}) as reported in Table 2.1.
- $d_{ini}(s)$ is the initial particle size before the comminution step (in μm)
- $d_m(d)$ is the targeted particle size after the first comminution step (in μm), assumed to be 37 μm [115]

As a final grinding step, to bring particle size to 10 μm a secondary comminution (or grinding) step is needed, requiring $elec_{s,d}^{commin2} = 150$ kWh/t_{rock}. This final step is required for all types of rocks, even for basalt fines, CKD, and CDWaste.

Bio-geophysical constraints for EW deployment

The number of mining and comminution facilities built across the optimization timeframe follows the infrastructure equation given in Eq. A 2 (Appendix, similar equation to other CDR).

The quantity of basalt sourced $P_{basalt,g,t}^{source}$ is linked to the number of operating mining facilities $ON_{g,t}^{mining}$ *via* the mining capacity:

$$P_{basalt,g,t}^{source} = Capacity^{mining}\ ON_{g,t}^{mining}, \quad \forall g \in G, \forall t \in T \quad \text{Eq. 44}$$

Similarly, the quantity of silicate produced is linked to the number of operating comminution facilities $ON_{g,t}^{commin}$ *via* the comminution capacity:

$$P_{s,g,t} = Capacity^{commin} ON_{g,t}^{commin}, \quad \forall g \in G, \forall s \in S, \forall t \in T \quad \text{Eq. 45}$$

Material balance equation

The transport balance equation – like the biomass balance equation – ensures that the amount of material produced plus the material leaving a *region g* is equal to the material used plus the material imported in that region and is expressed in Eq. A 5.

Material availability, land use equations

Rock availabilities, rock weathering rates, and rock application rates are determinant to estimate the potential of enhanced weathering in the UK.

Waste and by-product rocks are scarce and thus have a very low total CDR potential, even though they have high weathering rates). Basalt needs to be mined in existing igneous rock formations in the UK, which have large basalt quantities in theory [112]. Land used by EW includes both the mining sites where the rock is extracted for basalt, and croplands used to spread the rocks. However, it is debatable whether croplands should be included in the land footprint of EW, as they are also used for another purpose, and because rock spreading has the potential of having soil benefits, in addition to removing CO_2 (rejuvenating soils, improving yield, stabilising soil organic matter, etc.) [116]. Thus, in this dissertation, we don't consider croplands in the land use balance, as such lands are not exclusively used for enhanced weathering. Constraints and data used for rock and land availability are expressed in Eq. A 10 to Eq. A 17.

Finally, the rock application rate onto cropland is crucial to assess the global potential of enhanced weathering. It is however subject to uncertainty, and it is still not clear what are the rates that maximise carbon sequestration, without having negative effect on agricultural soils, also depending on different rock's mineral composition [116]. In this study, we assume an application rate of 30 t_{rock} per ha per year, lying in the range of 5-50 t_{rock} per ha per year found in the literature[108], [113], [116]

2.2.5 Biochar (BC)

Biochar is the process of thermochemically converting biomass using pyrolysis and applying the resulting char to agricultural soils. Carbon dioxide gets fixed into the biochar during the pyrolysis and is then released over the ensuing years [52].

The overall process energy efficiency, biochar yield, and carbon storage duration depend on the feedstock used, and the pyrolysis conditions, which are characterised by a temperature target to which biomass is heated up (between 300^{o}C and 800^{o}C), under low-oxygen conditions [52].

Biochar attracts many CDR investors given the various benefits it has on the environment, in addition to its direct carbon removal benefits. Indeed, bio-oil and gases can be used to provide energy services, similar to CHP systems and therefore abate emissions *via* fossil substitution, whereas char has many agricultural benefits when applied to soils [66], avoiding the use of fertiliser, and reducing nitrogen emissions at the same time [20].

Biochar modelling

The pyrolysis process results in biochar and primary gas (*i.e.*, volatile fraction of feedstock). A small fraction of the volatiles (typically measured as equivalent to 8% of the fuel HHV) serves as fuel for heating the pyrolysis and a larger fraction of it is combusted in a boiler, usually for domestic heat production or condensed into bio-oil for later use.

The amount of carbon sequestered, and the permanence of biochar greatly depend on the feedstock type, and pyrolysis temperature and type. The relation between these characteristics is not well understood and is the focus of much current research. Well-known trends are that wood-based feedstock results in more C sequestered in the biochar resulting in a product with lower nutrients needed by plants (*e.g.*, nitrogen (N), phosphorus (P) and potassium (K)). Manure-based biomass shows opposite behaviours and crop-based biomass results in between both[117]. Moreover, these trends are also affected by pyrolysis temperature and type. Other trends are that higher pyrolysis temperature results in more C, P, K, Ca, ash content, pH and SSA, but lower N, H and O [117]. Slow pyrolysis can produce an equivalent amount of biochar, gas and bio-oil whereas fast pyrolysis results in higher bio-oil yields [117].

The various stages considered for the biochar modelling are cropping and harvesting of the biomass, (including the fuel required, chemical input required, *e.g.*, seed, fertiliser, herbicides), drying of biomass and pyrolysis process, transport of biochar, and its application onto fields, as described by Chiquier et al.[21].

In this section, we compute the cost and GHG emission balance for biochar in the UK, for miscanthus, forestry residues, and crop residues (assumed to be wheat straw). We assume that pyrolysis processes are higher than 550^{o}C with an H/C_{org} ratio lower than 0.4, as they are more suitable and efficient for carbon sequestration purposes [117], [118]. The overall picture of biochar (BC) we assume in this dissertation is conveyed in the diagram in Figure 2.16.

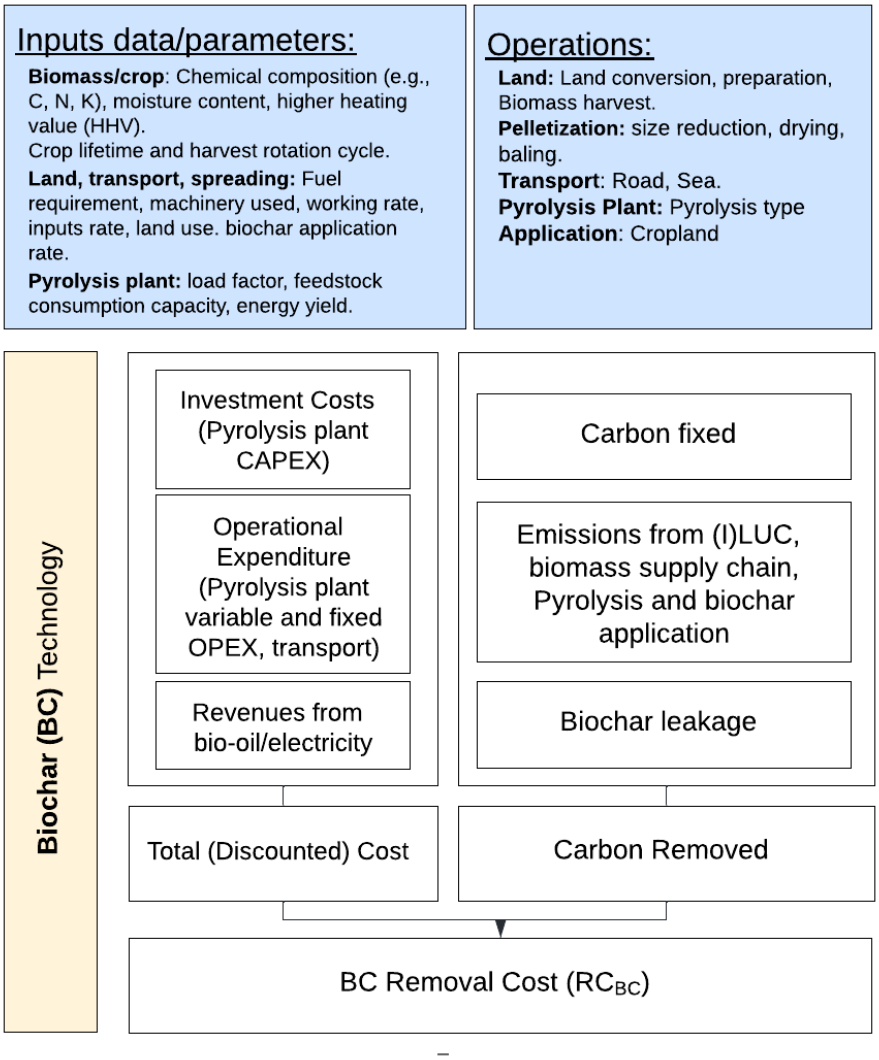


Figure 2.16: Overall picture of biochar (BC)

2.2.5.1 BC GHG balance

In the case of biochar, CO_2 capture occurs during the lifetime of the biomass crop. For similar reasons than for BECCS, BC removal immediacy is related to the land used for biomass growth, thus we only assume biomass cultivation on marginal lands or residues from existing operations (managed forests for forest residues and wheat crops for wheat straw). Our BC model is inspired by Chiquier et al.[21], and like other CDR solutions, we use the following carbon removal equation:

$$CR_{BC,i,g,C_k} = CC_{BC,i,g,C_k} - CE_{BC,i,g} \quad \text{Eq. 46}$$

Where:

- CR_{BC,i,g,C_k} is the carbon removed by a pyrolysis process (in t_{CO2} per ha of harvested land per year)

The organic carbon captured by biochar can be estimated from the pyrolysis method used and feedstock and can be expressed in t_{CO2} per ha of harvested land per year:

$$CC_{BC,i,g,C_k} = Yield_{i,g} * Cbio_i * Yield_{C\,char}(C_k) * Stable_C * \frac{44}{12}, \quad \text{Eq. 47}$$

where:

- $CC_{BC,i}$ is the CO_2 captured by the BC pathway with pyrolysis configuration C_k, and biomass *i* (in t_{CO2}/ha)

- $Yield_{i,g}$ is the biomass yield for biomass *i* in region g (in t_{DM}/ha)

- $Cbio_i$ is the carbon content of dry biomass (in t_C per t_{DM}), see Table A 2 (Appendix)

- $Yield_{C\,char}(C_k)$ is the biochar carbon yield, which is equal to 49% (in t_C in biochar/t_C in biomass) [119]. Note that the biochar carbon yield depends on the pyrolysis configurations C_k, a parameter described in 2.3.2, used to explore different scenarios, as biochar outputs contains certain degrees of uncertainty [120]. This parameter also affects the power generated from the pyrolysis process.

- $Stable_C$ is the proportion of carbon that is permanently fixed in the char

The biochar supply chain is based on biomass and therefore has many similarities with BECCS' biomass supply chain. Emissions for biochar include emissions from the biomass supply chain $CE_{biom,i,g}$, occurring before the pyrolysis, and the emissions from the biochar $CE_{char,i,g}$ occurring after the pyrolysis:

$$CE_{BC,i,g} = CE_{biom,i,g} + CE_{char,char(i),g}, \quad \forall\, i \in B, \forall g \in G, \quad \text{Eq. 48}$$

Where emissions related to the biomass supply chain are similar to the BECCS biomass supply chain (Eq. 6). Emissions occurring after the pyrolysis relate to the transport of biochar $CE^{BC}_{transp,i'',g}$, and the application of biochar on lands $CE^{BC}_{app,i'',g}$, expressed in t_{CO2} per ha of harvested land per year:

$$CE_{char,i'',g} = Yield_{i,g} * Yield_C_{char} * (CE^{BC}_{transp,i'',g} + CE^{BC}_{app,i'',g}), \quad \forall\, i'' \in BC, \forall g \in G, \quad \text{Eq. 49}$$

Akin to other material supply chains (biomass for BECCS, rocks for EW), biochar transport emissions are defined in Eq. A 4.

As observed in Figure 2.17, emissions associated with bioenergy-dedicated crops (miscanthus in this study) are much more significant than in the case of residues. This should not prevent an investor from investing in a miscanthus project, as the amount of CO_2eq captured per ha of land will also be much more significant in the case of miscanthus compared to that of wheat straw and forest residues. Most of the emissions in the case of miscanthus and wheat straw are due to inputs (seeds, lime, nitrogen, phosphorus, potash, herbicide, pesticide), farming

operations, and nitrous oxide (N_2O) emissions through fertiliser and pesticides. Most of the emissions (~90%) for forestry residues occur during residue harvesting.

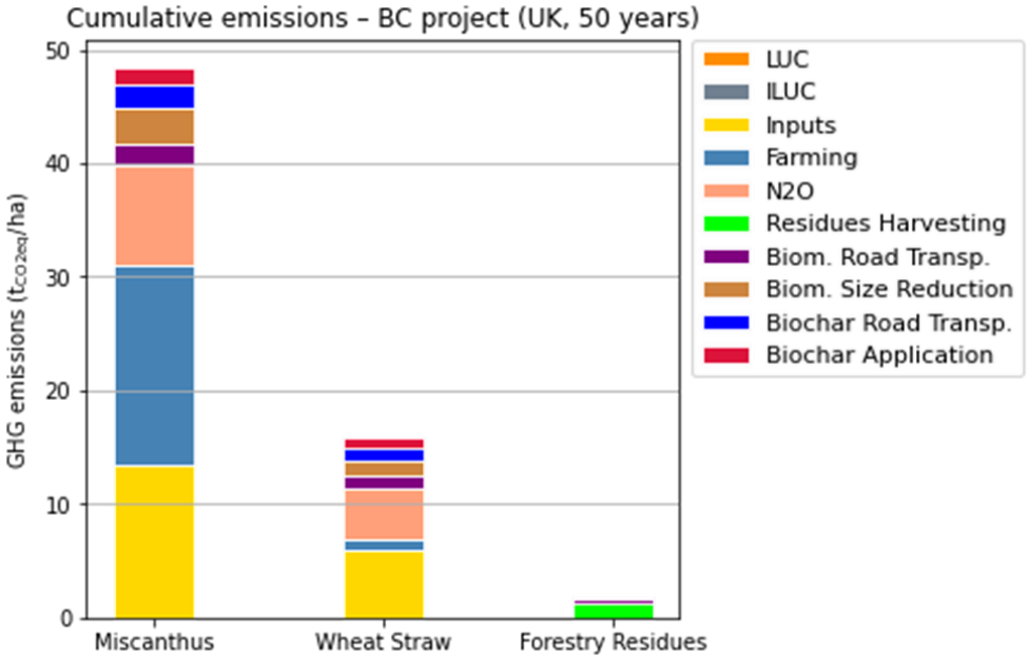


Figure 2.17: Cumulative emissions along the biochar supply chain (in t_{CO2eq} per ha)

Leakage risk for Biochar

The carbon fixed into the char during pyrolysis is often described with two different characteristics. Some fraction of that carbon (labile) will remain fixed for relatively short periods, and another fraction (recalcitrant) will remain for much longer periods. However, due to the lack of long-term biochar experiments, it is hard to predict accurate long-term biochar decay [118]. However, good estimations of the decay rate of biochar after 100 years can be made from the pyrolysis temperature or its elemental composition. Specifically, the ratio of hydrogen to organic carbon (H/C_{org}) in biochar appears to be a determinant in the decay rate of the carbon stock. Woolf et al. show there is a linear relation between the H/C_{org} ratio and the fraction of carbon remaining in biochar after 100 years (F_{perm}) [121], with higher F_{perm} values for low H/C_{org} ratios. If the H/C_{org} ratio cannot be measured, the temperature used during pyrolysis is also a possible estimate for F_{perm} with higher temperatures increasing F_{perm}.

Along this thesis, we assume a two-pool exponential decay to incorporate the potential leakage of biochar, as done in different studies and also known as the mean residence time of biochar-C[102], [119], [122]:

$$Decay_{BC}(t) = C_1 \exp\left(-\frac{ln(2)}{t_{1/2}^1}t\right) + C_2 \exp\left(-\frac{ln(2)}{t_{1/2}^2}t\right), \quad \text{Eq. 50}$$

where:

- C_1 and C_2 are respectively the labile and recalcitrant fractions of biochar [102].
- $t_{1/2}^1$ and $t_{1/2}^2$ are the labile and recalcitrant half-life (in years) [102].

In this study, we have chosen to fix the pyrolysis process to high-temperature pyrolysis (>600°C) with an H/C_{org} ratio lower than 0.4, as we aim at maximizing long-term carbon sequestration. Based on these criteria, we have averaged the decay rate coefficient from the database provided by Woolf et al. (2021) [121], resulting in the decay coefficient indicated in Table 2.2 for miscanthus, forestry residues, and wheat Straw.

Table 2.2: Decay Coefficient for different biomass types for study-specific pyrolysis conditions.

	C_1	C_2	$t^1_{1/2}$ (years)	$t^2_{1/2}$(years)	$F_{Perm,100}$	$F_{Perm,500}$
Miscanthus	0.040	0.959	19.3	468.8	0.773	0.329
Wheat Straw	0.0025	0.997	0.18	308.5	0.719	0.196
Forestry Residues	0.0015	0.998	0.0225	1381	0.928	0.694

$F_{Perm,N}$ values are usually good indicators of biochar permanence. They represent the fraction of carbon remaining after N years. They are directly deduced from coefficients C_1, C_2, $t^1_{1/2}$ and $t^2_{1/2}$. We observe that forestry residues (that are wood-based biomass) have a recalcitrant carbon fraction with a half-time (1381 years) that is much longer than for miscanthus and wheat straw, 468.8 and 308.5 years respectively. This results in higher permanence for forestry residues, with a $F_{Perm,100}$ of 92%, as opposed to 77,3% and 71.9% for miscanthus and wheat straw.

2.2.5.2 BC cost balance

Like other CDRs, biochar cost can be expressed by the following sum in $:

$$TotCost_{BC} = TotCapex_{BC} + \sum_{i \in B, g \in G} TotOpex_{BC,i,g} \quad \text{Eq. 51}$$

Where $TotCapex_{BC}$, the capital expenditure cost for the pyrolysis plant, is expressed in Eq. A 1. The data used is provided in Table A 1.

The operational costs of biochar $TotOpex_{BC,i,g}$ include the cost of pellet $Cost_{Pellet,i,g}$ (including land rent, land input, chemicals, and farming operation costs), pyrolysis non-variable operating costs $VarNFOPEX_{BC,i,g}$ (including labour and maintenance costs of the pyrolysis plant, indicated in Table A 1) and the cost of biochar application $Cost_{App,BC,i,g}$:

$$TotOpex_{BC,i,g} = Cost_{Pellet,i,g} + VarNFOPEX_{BC,i,g} + Cost_{App,BC,i,g} \quad \text{Eq. 52}$$

2.2.5.3 BC removal cost

As illustrated in Figure 2.18, we find that the removal cost of biochar is $287, $175, and $190 per t_{CO2} for miscanthus, wheat straw and forestry residues, respectively, when assuming a

permanence horizon of 100 years, and a project duration of 50 years. If revenues associated with bio-oil production were assumed with an associated electricity price of 125 $/MWh [74], respective prices were estimated to be $200, $92, and $101 per t_{CO2}.

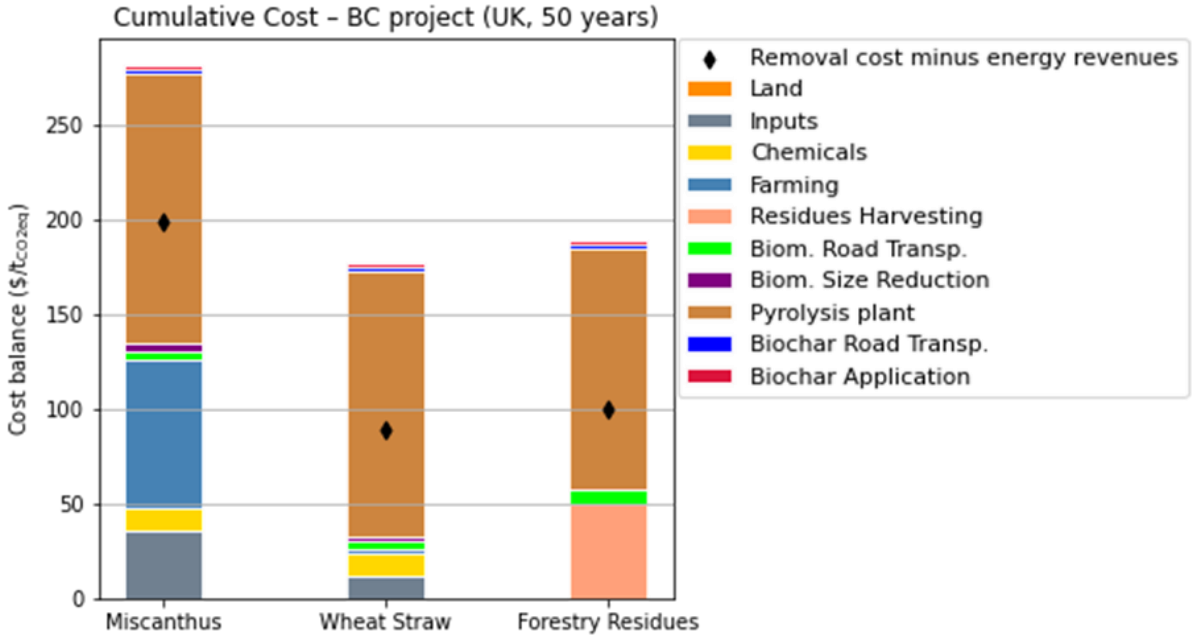


Figure 2.18: Removal cost of Biochar

2.2.5.4 BC energy balance

Through pyrolysis, the biochar process provides by-products such as bio-oil and syngas, that can be used to generate low-grade heat and power, respectively. The configuration of energy and biochar output depends on the pyrolysis conditions and can be adapted, according to pyrolysis plant needs. [19]

In a typical slow pyrolysis setting, the heat-to-power ratio is either 0 (no power produced at all) or 0.37 (typically 48% of thermal efficiency and 18% of power efficiency, where percentages are w.r.t LHV of the feedstock), assuming a pyrolysis enthalpy of 8% of the fuel HHV[19]. It is interesting to compare these efficiencies with typically combined heat and power plants which are about 70% and 33% for thermal and power efficiencies [19]. Naturally, pyrolysis loses energy in char production, resulting in lower thermal and power efficiencies.

Thus, we will consider that an oil engine is added on top of a pyrolysis process [123] the overall process can be a net electricity provider, with total electricity generated following a similar formula to BECCS':

$$P_{g,t}^{BC} = \sum_{i \in Pellet} DMR * HHV_i * \eta_{BC,C_k} * D_{i,g,t} \qquad \text{Eq. 53}$$

where:

- $P_{g,t}^{BC}$ is the total amount of electricity generated by the pyrolysis in region *g* at time *t* (in MWh per year)

- η_{BC,C_k} is the power efficiency of pyrolysis configuration C_k set to 12%, by default.

To summarise, we have suggested different pathways to model five different CDR solutions, that have been built on both recent works published in the literature [22], [53]. We have also collected suitable data with sufficient regional granularity for a UK case study. Before diving into the results, focusing on the interaction between the CDR and power sector and its broader economic and infrastructure deployment implications, we will provide some additional comparisons between CDR solutions, related to bio – and physical – constraints, energy balances, and land use.

Bio-geophysical constraints for BC deployment

Infrastructure equations – detailed in Eq. A 2 – are used for pyrolysis infrastructures.

Material balance equation

In the case of biochar, the transport balance equation – ensuring that the amount of material produced plus the material leaving a *region g* is equal to the material used plus the material imported in that region – is applied to both biomass and biochar and is expressed in Eq. A 5.

In the next section, we will focus on metrics such as 1) energy services & requirements, 2) removal costs and 3) land use.

2.3 Comparative assessment of CDR

2.3.1 Characteristics of CDR deployment in the UK

As developed in the above subsections, there is a wide range of potential CDR pathways – engineered and nature-based – that could be deployed to meet a given CDR target or requirement.

Build rate and land availability constraints

The role that each option can play will be constrained by several considerations, including capital and operating costs, but also land requirements, and – importantly – the rate at which a given pathway can be deployed.

One can arguably plant trees faster than one can build direct air capture facilities, for example. It is also important to consider that the deployment rate of a given CDR pathway is not fixed, but rather will evolve with time. As a given sector of the economy builds capacity, its possible rate of expansion also increases, similar to what has been observed in the context of wind or solar capacity, for example [124].

Thus, the rate at which a given CDR pathway can be deployed is constrained by a build-or-expansion rate and land availability, detailed in Table 2.3. We use a build rate multiplier (BRM) formulation for new technologies, allowing them to have an increasing build rate with increasing adoption [125].

Table 2.3: Deployment rates and land availability constraints

	Build rate multiplier (BRM)[a]	Initial capacity built allowed (/year)	Land availability[b,c] (Mha)
Afforestation	1	40 kha[d]	10.4 [126]
BECCS	2	200 MW – 1.39 Mt_{CO2}[e] [127]	2.1 [56], [57]
DACCS	2	1.5 Mt_{CO2}[f] [128]	-
EW	1	1 Mt_{CO2}[g] [129]	2.66 [130]
BC	2	0/15/30 MW – 0.01/0.03/0.06 $MtCO_2$[h]	2.1 [56], [57]

[a]The BRM provides the factor by which the installed capacity of a CDR can be multiplied every 5 years, allowing potentially groundbreaking technology to exponentially increase. We assign a BRM of 2 for BECCS and DACCS, as both are in early commercialization stages, with greater potential than other CDR solutions. We assign 1 to EW due to its large-scale unknown impacts on soil health and still being at the research level. Similarly, the assumption on rock application rate is conservative (30 t_{rock}/ha/yr). The possibilities of a high EW deployment in a national CDR portfolio are out of the scope of this study. Given historical data, it is reasonable to assume a BRM of 1 for Afforestation, in the UK.

[b]Marginal lands and water stress maps[57] have been combined to compute land availability for virgin biomass production and afforestation. The potential overlap between land used for AF and biomass production is considered in our model such that the same land can be used only once.

[c]For EW, we assume 25% of UK cropland availability for rock powder application, in line with cropland areas needed for reaching CDR goals in European countries[112].

[d]The Sixth Carbon Budget (CCC)[89] indicates the UK government has committed to a forest expansion rate of 30 kha per year until 2035 and plans to increase it to 50 kha per year thereafter. A mean value of 40 kha per year was assumed.

[e]Using the assumption that worldwide, over 2 Mt_{CO2}/yr are currently captured from biogenic sources, of which half is stored in dedicated storage.

[f]According to the IEA, 1 Mt_{CO2}/yr capture plants are currently under development.

[g]We approximate the starting capacity for EW from Undo's co-founder ambition of removing a cumulative 1 bn tonne of CO_2 by 2030, and dividing it by 2^{10}, corresponding to our BRM of 2.

[h]Multiple values are given for the three configurations in the order C_{CO2}/ C_{med}/ C_{pow}.

Because MONET is a least-cost optimisation problem, it is primarily driven by the cost of CDR solutions and is constrained by several other parameters, such as build rates, or upper bound on deployment where, *e.g.*, land use, or material (biomass, rocks) constraints are reached. Other system-wide constraints are discussed in the next section.

2.3.2 Energy services and requirements

In the above sections, each CDR solution, except afforestation, has a non-negligible interaction with the power sector, either by producing power – in the case of BECCS and

biochar –, or by consuming it – EW, and DACCS. In this context, we found it relevant to compare the different energy services or needs of each CDR, as illustrated in Figure 2.19.

In this context, we explore multiple biochar configurations, inspired by Azzi et al. [19] and Woolf et al. [119] that result in different power efficiency (η), and biochar yield ($Yield_C_{char}$):

- The high-CO_2 configuration C_{CO2}: $\eta = 0\%$, $Yield_C_{char} = 49\%$.
- The balanced configuration C_{med}: $\eta = 12\%$, $Yield_C_{char} = 35\%$.
- The high-power configuration C_{pow}: $\eta = 18\%$, $Yield_C_{char} = 21\%$.

The yield value $Yield_C_{char} = 49\%$ is sourced from a study conducted by Woolf et al. [119], as indicated in Eq. 47. Power efficiencies η values and biochar yield $Yield_C_{char}$ for balanced and high-power configurations are derived from Azzi et al. [19].

Biochar – in some configurations – and BECCS, provide energy with values ranging from 0.6 to 1.8 MWh per t_{CO2} captured, for biochar with configurations C_{med} and C_{pow}, respectively. BECCS lies in that range, with approximately 0.9 MWh per t_{CO2} captured for miscanthus, forest residues and wheat straws. We find that the high-power biochar configuration (C_{pow}) has a higher energy balance than BECCS, due to its low biochar efficiency ($Yield_C_{char} = 21\%$.) and unit chosen for the graph (MWh per t_{CO2} removed). Ultimately, BECCS is more efficient on a %-HHV basis (30% for BECCS versus 18% for BC-C_{pow}).

Biochar with configuration C_{CO2} has no power production, nor has power needs. Among consumers, DACCS with solid sorbent is the more power-intensive CDR with a requirement of 0.7 MWh per t_{CO2} captured. Overall, enhanced weathering-based CDR and DACCS with liquid solvent have an electricity footprint in the range of 0.2 – 0.5 MWh per t_{CO2} captured, proving that in theory, given sufficient proximity between installations, BECCS and biochar pathways could well satisfy power needs from a DACCS plant, or mining and comminution facilities in the case of EW.

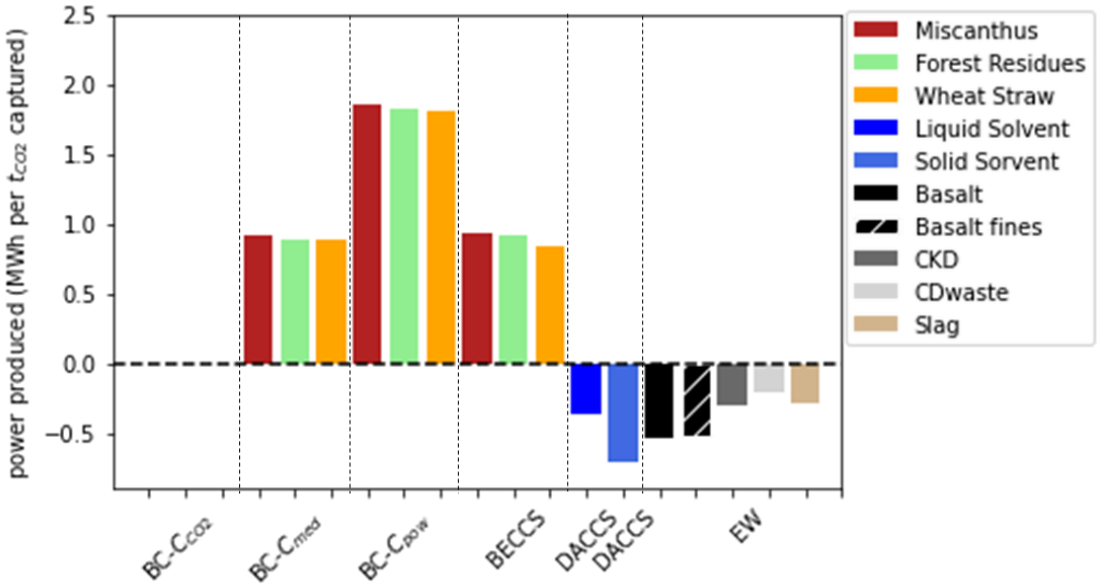


Figure 2.19: Energy requirements for various CDR pathways.

2.3.3 Electricity price variation

Throughout this dissertation, we will study the effect of considering different electricity prices and will determine how an optimal CDR portfolio qualitatively evolves. The model presented in the next section will iteratively optimise the power system (thus determining electricity prices), which will, in turn, affect the subsequent optimization of a CDR portfolio, itself depending on the cost of CDR, therefore on the electricity prices. To better understand these trends, we look at the evolution of CDR modelling costs when considering a range of electricity prices. For example, we know in advance that BECCS and some biochar configurations will be rewarded and that DACCS and EW will be penalised by increasing power revenues. We illustrate the impact on CDR removal costs (in $/$t_{CO2}$) in Figure 2.20, for electricity prices varying between 50 and 180 $/MWh.

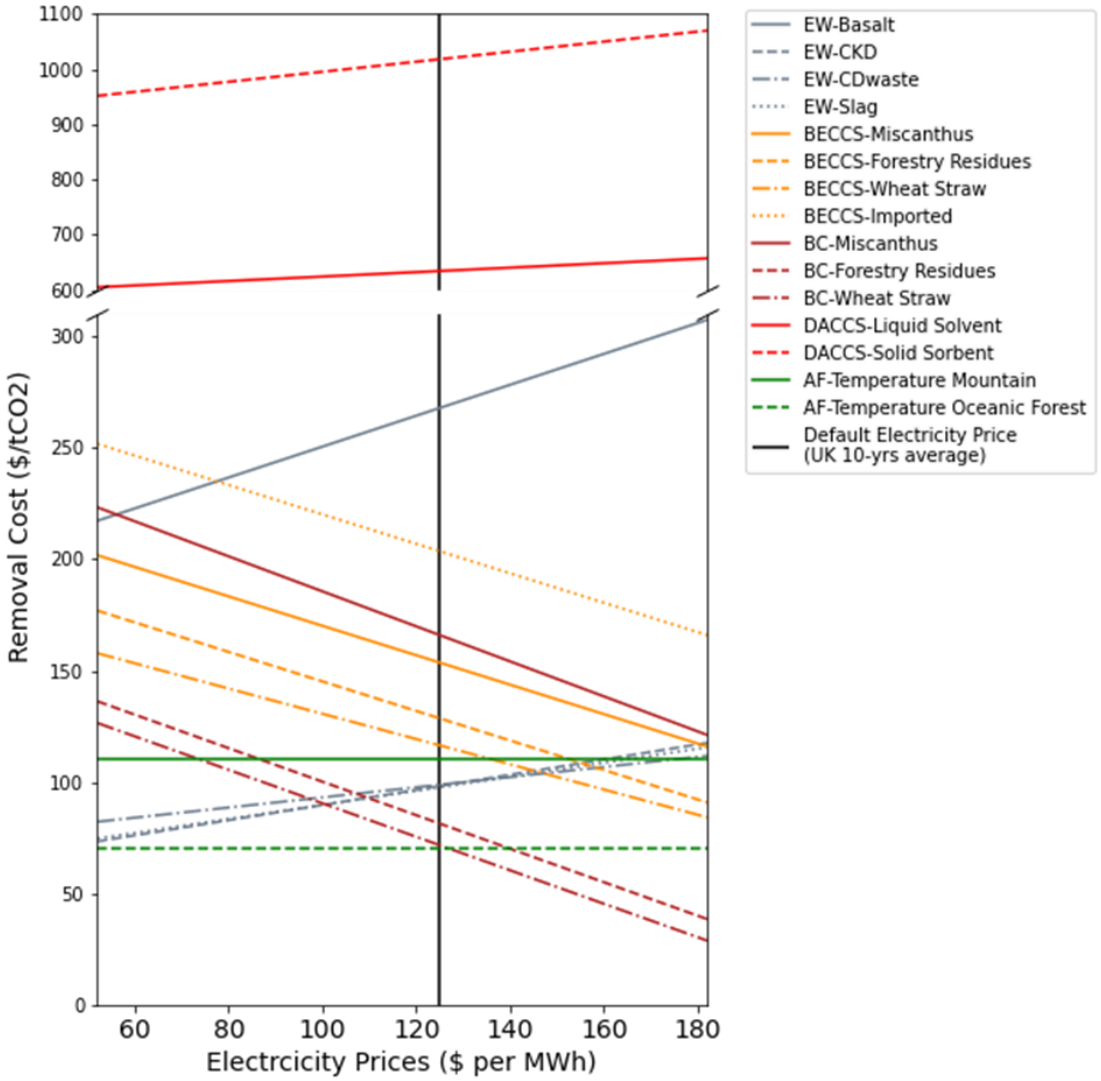


Figure 2.20: CDR removal cost variations with different electricity prices.
In our default scenario electricity price is set to 125 $/MWh, the calculated average annual non-domestic electricity price in the UK in the period 2010-2021 [74]

In Figure 2.20, we find significant cost variations across different CDRs. For example, BECCS and biochar pathways using forestry residues and wheat straw becoming cheaper than AF, at different electricity price levels. BECCS with forestry residues and wheat residues becomes more cost-effective than AF in temperate mountain zones when electricity prices surpass 80-90 $/MWh, and than AF in temperate oceanic forests when prices surpass 130-140 $/MWh. Similarly, BECCS and biochar pathways using forestry residues and wheat straw become cheaper than EW with CKD and Slag, at price levels around 110 and 160 $/MWh for BECCS and biochar, respectively. However, BECCS with miscanthus and imported biomass, as well as biochar with miscanthus, remain more expensive than AF in temperate mountains, when electricity levels remain lower than 180 $/MWh.

Moreover, we note that if electricity prices were to become lower, this would be at the expense of BECCS and biochar. In particular, with prices lower than 60 $/MWh, biochar with miscanthus becomes more expensive than EW with basalt.
Thus, electricity price levels could affect, in the future the deployment of CDR, and their profitability.

On the one hand, the order of CDR costs varies with different electricity prices for the most affordable solutions (AF, EW with rock residues, biochar and BECCS with biomass residues). On the other hand, the most expensive CDR solutions (other BECCS and BC pathways, EW with basalt, and DACCS) order remains almost unchanged, except for EW with basalt, which becomes cheaper than BC with miscanthus, and BECCS with imported pellet, for prices lower than 60 and 80 $/MWh, respectively.

Even though the ranking of CDR based on cost changes for the cheapest solutions, it has no impact on the final optimization, because these solutions also have the lowest potential [66], which makes them always deployed at full potential by the optimisation. Indeed, some are limited by the amount of forestry residues, and wheat straw produced annually, others by the availability of slag, cement kiln dust (CKD) and construction and demolition wastes. In the case of AF, its deployment is limited by the plantation rate assumption, in line with UK government targets.

Finally, due to the low availability of cheap CDR pathways (limited biomass and rock residues, limited plantation rate or AF), we will see that electricity price variations caused by different power mix outcomes are not significant enough to lead to a quantitative change in the outcome of CDR portfolio deployment.

2.3.4 Land use efficiency

The efficiency of CDR per land used is key to determining the future CDR portfolio, as many controversies point to land use and contradictions with a growing world population.

For this analysis, we account for various land use, *i.e.*, (1) marginal lands for CDR pathways using miscanthus, (2) forests for those using forestry residues, (3) cropland for those using wheat straw, and (4) land used for the mining of basalt. The size of each plant (DACCS, BECCS, pyrolysis, and mining) is also included. For biochar, we only include the land used for biomass growth, and not for biochar application given that lands, where pyrolyzed biochar is spread,

have other purposes than that of hosting biochar. A similar argument holds for EW with basal, where only the area used for mining is included. We ignore other EW pathways in this analysis, as they use by-products of existing industries and don't use additional land that is not currently used. Thus, the ignored CDR pathways can be considered the most efficient CDR solution, compared to those included in this graph. However, as we highlighted in the previous subsection, these pathways are strongly restricted by material availability.

We find that the most land-efficient CDR is DACCS and EW with basalt. DACCS with liquid solvent has a land efficiency in the range of 10^4 t_{CO2} per ha, EW with basalt of 10^5 t_{CO2} per ha, and DACCS with solid sorbent of 10^6-10^7 t_{CO2} per ha.

BECCS with miscanthus reaches a removal efficiency of 1,600 t_{CO2} per ha, whereas both BECCS with wheat straw and biochar with miscanthus are twice less efficient. The reason why biochar is less efficient relative to BECCS with the same biomass type is due to the loss of energy occurring during pyrolysis.

Afforestation and enhanced weathering both have smaller CO_2 removal efficiencies. Afforestation's removal efficiency increases with similar rates to BECCS and BC in the first 20-30 years, but rapidly stagnates, as the forest has reached maturity and slows down its CO_2 sequestration rate.

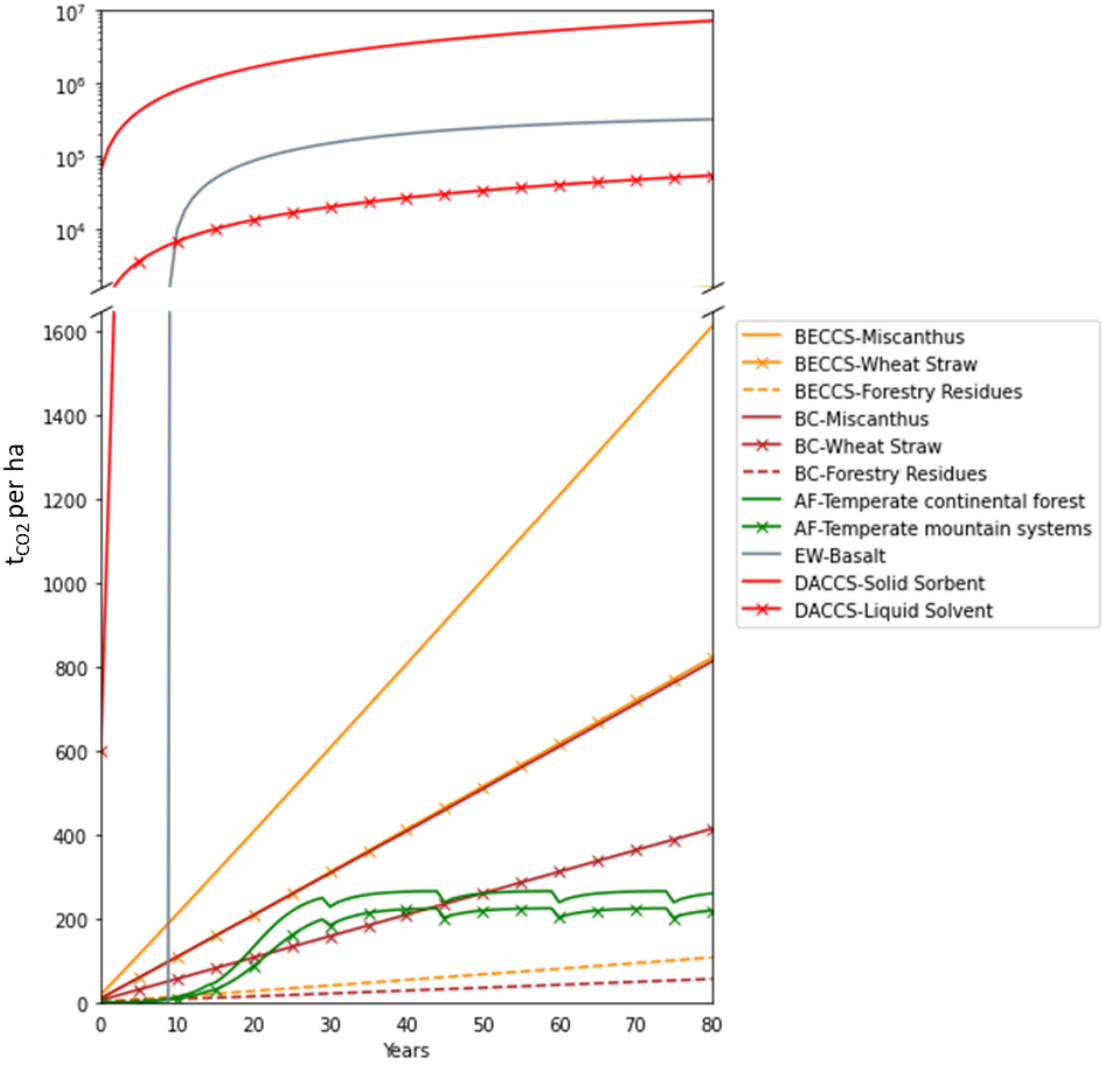


Figure 2.21: Land-use efficiency of CDR solutions

Before diving into the core of this dissertation, we will determine what a CDR portfolio would look like if optimised independently.

2.4 MONET optimisation

For CDR portfolio optimization, we use a MILP-based model, also known as MONET [21]–[25] (Modelling and Optimisation of Negative Emission Technology). MONET has been adapted for this work by adding CDR solutions (BC, EW) and increasing the data granularity to the UK NUTS1 regions for optimisation.

In this framework, we minimise the total system cost (Eq. 54), such that the CDR removal constraint (Eq. 55) is satisfied. Bio-geophysical CDR-specific constraints expressed in previous subsections are also incorporated in the optimisation but are not repeated here.

$$\min f(x) = \left(\sum_{CDR_i \in CDR, t \in T} Cost_{CDR_i}(t) \right) + penalty_{CO2} * slack(t) \quad \text{Eq. 54}$$

s.t.

$$\left(\sum_{i \in CDR,} TCR_i(t)\right) + slack(t) \geq RemTarget(t), \forall t \in T \quad \text{Eq. 55}$$

The reader will observe a cost penalty added to the system cost if it fails to remove the amount of CO_2 required by the $RemTarget(t)$ parameter. We conservatively assumed a cost penalty $penalty_{CO2}$ of \$1,000 per t_{CO2}, in the higher range of social cost of carbon estimations, a metric used to measure the expected economic damages of carbon dioxide emissions [131]. In the optimisation, the cost penalty is assumed to be paid by the system for each tonne of CO_2 that was not removed by CDR solutions – due to lack of resource availabilities, build rate limitations, or proposed removals more expensive than the cost penalty. The chosen carbon removal target parameter $RemTarget(t)$ is as provided by BEIS [12] and provided in Table 2.4. It is assumed that CDR in the UK will start in 2030 and increase to a total of 90 Mt_{CO2}/yr removed in 2050, with an exponential increase in removal rate assumed (Table 2.4).

Table 2.4: Carbon budgets and finances

	Annual CDR target[a] [12] (Mt_{CO2}/yr)	Reference electricity carbon footprint[b] (g_{CO2} / kWh)	Carbon Tax[c] [132] (\$/t_{CO2})
2020	0	220	27
2025	0.1	-	71
2030	5	50	122
2035	23	10	173
2040	36	-	223
2045	57	-	275
2050	90	2	324

[a] No data was found for carbon budgets in 2040 and 2045, hence we extrapolated with an exponential function for missing values, of the form $f(x) = \alpha \exp(\beta x)$.
[b] Values are based on the Balanced Pathway of the Sixth Carbon Budget (CCC, 2020) [89].
[c] Values come from BEIS projections, then extrapolated, and converted from £ to \$ using the 2021 average exchange rate of 1.3757.

Figure 2.22 shows the optimal CDR portfolio deployment in the timeframe 2025-2050 when a low and high amount of biomass is available to the system. Given the suggested objective function (Eq. 54), we deduce that the cost-optimal CDR portfolio deployment will choose the lowest cost CDR solutions, until one of the constraints is reached, before choosing the second lowest CDR, etc. This logic is compatible with what would occur in a liberal market economy. Although these results are a practical view of future CDR deployment, they are not a prediction of the future of CDR. We also note that the removal costs assumed in this analysis,

are based on exogenous assumptions of heat, and electricity prices, and thus need to be considered with scrutiny.

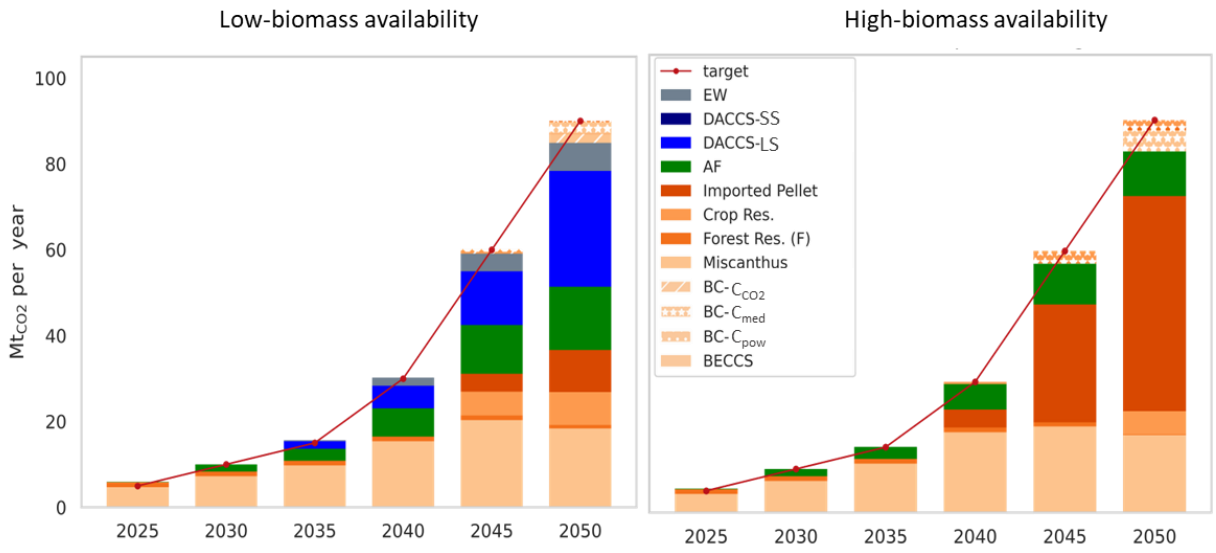


Figure 2.22: NETs deployment in the UK with CCC's 2050 target.
Low-biomass and high-biomass availability scenarios are shown.

In both scenarios (low-biomass and high-biomass availability), we assume indigenous biomass can be used up to its maximal potential (*i.e.*, *via* marginal lands, forestry residues and wheat straw availabilities). In the low-biomass availability scenario, we assume that imported biomass is limited to 36 million tonnes per annum (Mtpa) in 2030 and 7 Mtpa in 2050, as suggested by Ricardo Energy & Environment [133]. In the high-biomass availability scenario, we relax the limitation on imported biomass.

In both scenarios, we find a mix of CDR solutions deployed and meeting the target at each time step from 2025 to 2050, meaning that the system manages to find an optimal portfolio, in line with build rate, material availability, land availability, and water stress constraints, without having to make use of the slack variable (priced at 1,000 \$/t_{CO2}).

In the low-biomass availability scenarios, the optimisation results in a linear deployment of BECCS and afforestation deployment across the half-century; with 6 Mt_{CO2}/yr of BECCS removal by 2025, and 2 Mt_{CO2}/yr of AF removal by 2030. By 2050, they reach 35 and 17 Mt_{CO2}/yr, respectively, representing more than 50% of national CDR needs. Afforestation linear deployment is logical due to the linearity of the plantation rate, made in the assumptions. BECCS deployment is not constrained by a linear build rate, like afforestation, but by a build rate multiplier (BRM) (assumptions, Table 2.3). The justification for relaxing this constraint lies in the pivotal role BECCS has in contemporary global projections, alongside its high TRL level. However, it is constrained by the amount of biomass available. Enhanced weathering removals start from 2035 increasing to 10 Mt_{CO2}/yr by 2050. Similarly to afforestation, a linear build rate was presumed for EW, attributed to its relatively low TRL and the uncertainty associated with soil toxicity. Given the low potential of EW with by-products (*i.e.*, slag, CKD, CDWaste) of less than 0.5 Mt_{CO2}/yr, the average cost of EW is mainly determined by EW with basalt, making EW the second most-expensive CDR, after DACCS.

Thus, the optimal output does not deploy EW before 2035, as the target is already met by the other options. EW deployment is also limited by geo-physical constraints (application rate, cropland availability constraint, linear build rate), as per our assumptions (Table 2.3).

DACCS with liquid solvent and biochar with miscanthus and forestry residues complete the CDR mix, with a high build rate in the last five years of the represented timeframe (2045-2050), in order to meet the 90 Mt_{CO2} target in 2050, as all other options have reached their maximum potential.

In the high-biomass availability, all removals previously from DACCS and EW have been replaced by BECCS with imported pellets, with BECCS now removing 70 Mt_{CO2}/yr by 2050. This is explained by the fact that BECCS with imported pellets is cheaper than EW, or DACCS removal in 2050, based on the cost estimations that we have detailed in Chapter 2. Thus, the system optimisation chooses this pathway, as the resource limitation (imported pellet availability, in that case) has been relaxed in that scenario.

It is important to note that assumptions regarding CDR deployment differ across different CDRs, and are a major driver for our optimisation results, as delineated earlier. While certain assumptions are derived from official government projections, such as the afforestation rate in the UK, others entail a degree of subjectivity, albeit rooted in scientific considerations. Therefore, these results must be understood as a realistic projection given different scenarios, and a set of assumptions stated beforehand. In the following section, we will explore the impact that such deployments may have on the power sector.

Chapter 3

3 Power sector model and interaction with MONET

In this section, we introduce a unit commitment and capacity expansion model of the electricity system, namely the Electricity System Optimisation (ESO) model [6], which is used to investigate the value of power technologies and supports decision-making in the power sector. ESO finds the optimal power system design and hourly unit-wise operational strategy, including a range of power generating technologies: conventional (nuclear, coal, combined – and open–cycle gas turbine with or without CCS), intermittent electricity generation technologies (onshore wind, offshore wind, solar), electricity import and negative emission technologies (BECCS). This work will focus particularly on the deployment and the value of BECCS, as it provides both low carbon dispatch power and atmospheric CO_2 removal.

In this chapter, we will first describe the power sector model (ESO) (3.1.), and then optimise it without consideration of its interaction with the broader CDR landscape (3.2). Then, using CDR targets taken from the BEIS net zero strategy report [12], we finally consider the coupled

CDR-power system and evaluate how it evolves distinctly from what might be anticipated if one considers each sector independently (3.3).

3.1 Electricity System Optimisation

Similarly to MONET (the optimisation model for CDR), ESO has a MILP formulation. It minimises the total system cost (described by the sum of the levelised capital and operational expenditure costs) subject to different constraints:

- Capacity constraints: initial capacity, build rate, maximum capacity, lifetime.
- System-wide constraints: supply meeting the demand, minimum inertia requirement, minimum reserve capacity, environmental constraint (carbon emission target, land use availability for solar and wind).
- Technology-specific constraint: reserve and inertia potential, flexibility, ramping times, and carbon emissions of each power technology.

The mathematical equations used in this work are the same as presented in [28]. Like in MONET, we use a 5-year time resolution between today and 2050.

Electricity System Optimisation (ESO) assumptions

The optimal power mix deployment between today and 2050, resulting from optimisation, is mainly driven by initial assumptions and constraints used in the optimisation model [27], [28].

In particular, amongst system-wide constraints (as mentioned above), the assumed electricity demand trajectory during the given period, and the carbon emission target associated with the power sector, are determinant parameters that will strongly affect the optimal output. Also, technological costs (both CAPEX, and non-variable OPEX), power plant parameters (such as ramp-up, ramp-down rates, efficiencies, and renewable availabilities), fuel costs, or environmental constraints (limiting the deployment of wind and solar) are crucial input parameters.

Different trajectories can be foreseen for the electricity demand level that is consistent with meeting net zero emissions across the whole economy [12]. According to the UKITMES (UKTM) model [134], indicative levels for 2040 and 2050, are 495 TWh, and 596 TWh, respectively, as reported in the Net Zero low electrification scenario, where road transport is mostly electrified *via* hydrogen production. Such a scenario includes higher levels of hydrogen for heating in the building sector, hence reducing the power demand compared to the high electrification scenario. In the Net Zero high electrification scenario, indicative levels for 2040 and 2050 are estimated to be 578 and 792 TWh, respectively.

In this work, we will consider baseline power demand values computed from the low electrification scenario. Because of the nature of our optimisation model, additional power demand – from DACCS and EW – will be added, substantially increasing the baseline power demand.

However, some model constraints that are not hit in the current scenario could be reached if power demand from the high-electrification scenario was used, resulting in additional trends we cannot see in the present results. This limitation should be considered when analysing our outputs.

Equivalently, the carbon emission constraint assigned to the system is an estimation of power sector emission trajectories and is implemented as a soft constraint, for which a cost penalty of $1,000 is applied per additional t_{CO2}. According to different commitments, the power sector carbon emissions need to decrease by 72-75% by 2030 (Nationally Determined Contribution), 83% by 2035 (6th UK carbon budget, [89]), and 98% by 2050 (Net Zero objectives [12]). The emission target that is applied to the system can be found in Table 3.1. Using an end-point constraint speeds up the power sector optimisation running-time. In this work, we are mostly interested in meeting the target in 2050, and not necessarily meeting the intermediate carbon budget – or, nationally recommended pathways –, hence we only use an end-point constraint, in 2050.

Table 3.1: National Emission Target for the power sector in the UK [89]

	National Emission Target for the electricity system (compared with today in %)
2022	100%
2025	
2030	-
2035	-
2040	-
2045	-
2050	0%

In the following section, we will explore the possibility of having a net negative electricity sector by 2050 in the UK. This would require a significant rise in biomass use in the power sector, as well as the deployment of CCS technology combined in thermal power plants (coal, gas-fired power plants), and biomass power plants (BECCS). Considering this new perspective, First, a description of some biomass uses in today's electricity systems will be provided, to better understand the challenges of increasing bioenergy electricity generation.

Example of biomass use for electricity in the US and Europe

The utilization of biomass in power sectors has been a longstanding practice. Today, its share reaches 15% of the global electricity generation [18] and even represents the highest energy source in some countries, like in the UK [135]. The UK has been actively promoting the use of biomass for renewable energy production, particularly through the conversion of coal-fired power plants to biomass-fired plants.

The utilization of biomass for electricity generation in the United States demonstrates a diverse range of sources and methods, as highlighted by the data from the US Energy Information Administration (EIA) [135]. The USA has biomass electricity generators installed in 40 states and generated 2% of total US electricity consumption in 2018, according to the US Energy Information Administration (EIA) [136]. In line with the US EIA data, 30% of this electricity production comes from wood solid biofuels, and 28% from black liquor, a wood-derived fuel and by-product of pulp mills. However, 20% of biomass –and waste–generated electricity comes from Municipal Solid Waste (MSW), which is not incorporated in this research. MSW can indeed be a significant source of biomass-derived energy, as it can be incinerated or used in waste-to-energy facilities to generate electricity.

Woody biomass comes from forests, mainly in the southeast and the northeast, that are managed using different approaches (thinning frequency, harvesting, passive owners) depending on their owner's choices, as they are mostly private-owned [137].

More generally, biomass represents 5% of primary energy in the USA; however, this is only half of the share that it represents in Europe (10%), according to the European Commission. European policy regulation plays an important role in this large share of biomass in the energy mix. The latest Renewable Energy Directive 2018/2001 has recently changed the status of large-scale biomass plants producing electricity and heat; now, they are considered renewable energy if these projects fulfil specific criteria, joining the same category as biofuels and bioliquids for transport. Many criticize the use of forestry biomass; for instance, the atmospheric impact can be worse than that of fossil fuel, in some cases accelerating climate change in the short and medium term, as warned by 500 scientists [138]. Some concerns have been raised by scientists regarding the use of certain types of forestry biomass, which could have a negative climate impact depending on factors such as sourcing, sustainability, and carbon emissions. It's worth noting that the environmental impact of biomass can vary depending on various factors, including the type of feedstock, land use practices, emissions from combustion, and overall sustainability of the biomass supply chain.

This supports the need to have a robust model that encompasses biomass supply chain emissions, from land-use change to biomass pelletisation, as provided by MONET presented in Chapter 2.

Similarly, in the UK, bioenergy is today the second largest source of renewable energy. It generates ~13% of the total UK electricity supply in 2021 [139], showing the important role that biomass may play in the UK energy outlook. In particular, this opens the possibility of having a net-negative power sector – *via* the deployment of CCS infrastructure – which would have profound implications for the design and operation of electricity systems [47]. In the next section, we will describe a reference scenario for the power system installed capacity and power generation in the UK between today and 2050.

3.2 ESO first results

First considering the power system in isolation, we constrain it to transition to net zero by 2050, in line with the CCS's Sixth Carbon Budget [89], and also including a carbon tax [140]

(Table 2.4) to further disincentivize carbon-emitting power technologies. This scenario will serve as the ESO-reference scenario for future comparisons.

Figure 3.1 shows (A) the installed generation capacity (B) the power to demand (left axis), and the carbon intensity of electricity generated (right axis). Driven primarily by an increasing carbon tax, CO_2 emissions from the electricity system are observed to reduce by 75% in 2025 and by 90% in 2030.

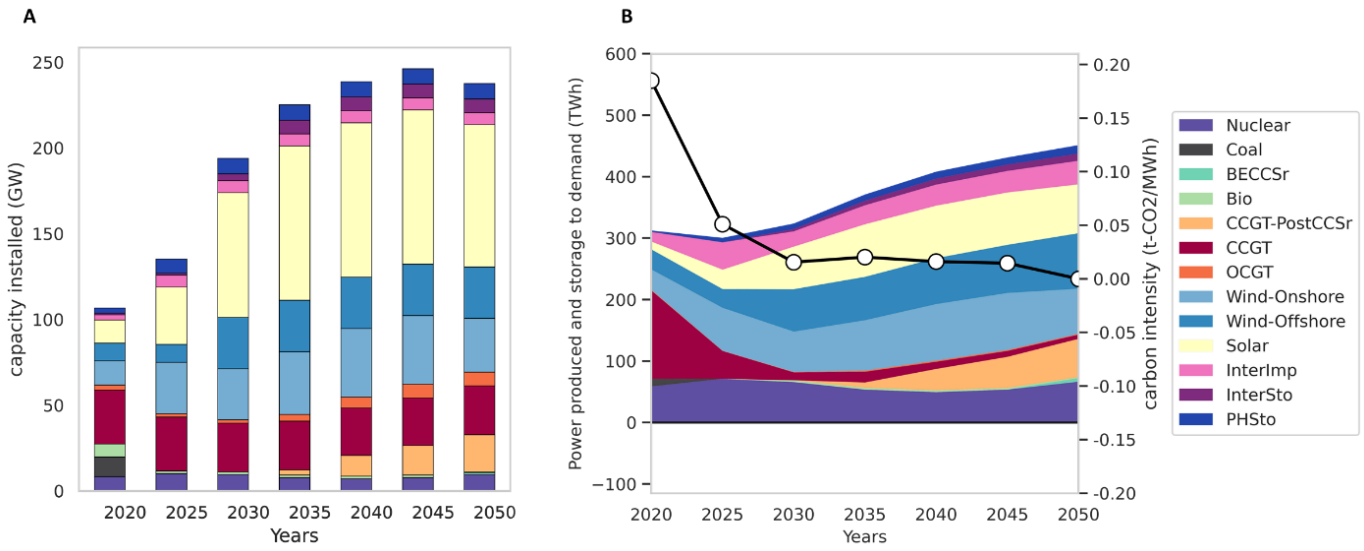


Figure 3.1: Least-cost evolution of the UK electricity system from 2020 to 2050 to net zero*

*Abbr. BECCS retrofit (BECCSr), Biomass power (Bio), combined cycle gas turbine (CCGT), open cycle gas turbine (OCGT), interconnection imports (InterImp), interconnection storage (InterSto), Pumped hydro storage (PHSto).

(A) *Capacity expansion*. The decarbonized electricity system results in a diverse generation mix (conventional, renewable, and storage) in line with the government's Ten Point Plan[141]: Offshore wind capacity reaches 40 GW by 2030, nuclear capacity is stable and reflects national goals of investing in modern nuclear technologies (small and advanced modular reactors). Moreover, onshore wind and solar reach maximal capacity expansion at 40 GW and 90 GW respectively, as constrained by land use [89]. Coal capacity is retired by 2025, while non-abated CCGT capacity is preserved, and CCGT-CCS is built from 2030 onwards.

(B) *Electricity generation/carbon intensity*. As reflected by the installed capacity in (A), coal generation reaches zero in 2025. CCGT generation decreases drastically reaching almost zero by 2040 but is replaced by CCGT with CCS, making natural gas constantly used until 2050. Renewable generation share is rapidly increasing until 2030 (+180% compared to today's level) and keeps increasing with a lower gradient from 2030 to 2050 (+27%).

The decarbonisation of the electricity system is primarily achieved through the deployment of renewable capacity (54% of the generation in 2050) and firm low-carbon generation (including nuclear, combined-cycle gas turbine (CCGT) with CCS, and interconnection with neighbouring countries) to compensate for the intermittency of wind and solar power. In the first decade, we observe a reduction of unabated fossil fuel generation, replaced by renewable energy. Coal power is anticipated to be entirely phased out by 2025 due to growing carbon prices, in line with the UK national coal phase-out commitment[142]. However, it is important to note that this projection might be disrupted by the increasing prominence of

energy security[143]. By 2030, unabated gas-fired power stations contribute only 1.5% relative to 46% today.

This reduction in unabated thermal power generation is balanced by a significant expansion in renewable power generation, increasing from 78 TWh today to 204 TWh in 2030. Offshore wind remains the cornerstone of the UK's renewable power system, reaching 40 GW of installed capacity by 2030, as anticipated by the government's Ten Point Plan[141]. From 2030 we observe an increase in firm low-carbon capacity beginning with electricity produced from biomass without CCS from 2030 and CCGT with CCS from 2035 onwards. After 2030, the contribution of renewable power increases from 204 TWh in 2030 to 243 TWh in 2050, meeting 63% and 54% of the electricity demand, respectively. Owing to ecological concerns, we limit land use of onshore wind and solar to 3,300 km^2 and 2,000 km^2, corresponding to a capacity of 40 GW and 90 GW, respectively[89]. This consequent renewable generation results in curtailment levels of 30 TWh in 2030, and 5 TWh in 2050. Nuclear provides baseload power, with capacity deployment between 7-10 GW depending on plant decommissioning. Finally, BECCS deployment only reaches 1 GW, which corresponds to two BECCS plants and meets 2% of electricity generation. This will generate up to 4 $MtCO_2$ of negative emissions by 2050, enough to balance residual emissions and meet the net zero emissions target for the power sector. This is, however, insufficient to cover potential CDR needs from other sectors, such as the industry, agriculture, and aviation[144]. Overall, these changes allow the electricity system to meet an increasing energy demand (with 2050 levels 33% higher than today's) while reducing its carbon footprint.

This reference scenario shows that, owing to a steadily increasing carbon price, the electricity sector is almost entirely decarbonised by 2030, well ahead of the 2050 net-zero target. We also observed the prominent role of renewable power and the necessity of nuclear providing low-carbon and baseload power generation. Natural gas-powered generation technologies (CCGT, then CCGT-CCS) are operated flexibly to balance renewable intermittency. Finally, the relatively small amount of CO_2 removal that is required for the power sector to reach net zero is achieved via the deployment of BECCS.

3.3 The joint ESO-MONET (EM) framework

In this section, we first present the ESO-MONET (EM) framework used for our analysis. Then, we show what a least-cost transition to a 2050 carbon-neutral electricity system would look like without explicit spatiotemporal modelling of the CDR sector, paying particular attention to the capacity that is either decommissioned or installed for the transition. We then discuss the cost of the various CDR pathways and consider the composition of a least-cost CDR portfolio designed to meet the UK's CDR targets. We then investigate the impact of deploying different CDR portfolios on the design, operation, and total costs of the electricity system. Finally, we perform a comprehensive sensitivity analysis to provide insight as to which system parameters have the highest impact on the role and value of different CDR pathways.

3.3.1 Convergence and constraints of EM framework

Model convergence

As illustrated in Figure 1, the EM framework determines the least-cost system $Cost_{EM}$ (*i.e.,* ESO and MONET-UK), in the UK at the NUTS1 level, between 2020-2050, with a five-year time step, defined as follows:

$$Cost_{EM} = Cost_{ESO} + Cost_{MONET} \quad \text{Eq. 56}$$

The optimization includes constraints from both MONET and ESO respectively, during each model-independent optimization. As illustrated in Figure 3.2, the EM framework successively optimises ESO and MONET, until a convergence criterion is satisfied, as follows:

$$\frac{\sum_{t,i \in power\ technologies} |\mathrm{CAP}(i,t,l) - \mathrm{CAP}(i,t,l-1)|}{\sum_{t,i \in power\ technologies} \mathrm{CAP}(i,t,l-1)} \leq \varepsilon \quad \text{Eq. 57}$$

where $\mathrm{CAP}(i,t,l)$ is the capacity installed of power technology *i* at time step *t*, after *l* iterations of the EM framework. The default value used for ε is 1%. The list of $power\ technologies$ considered is shown in Figure 3.2.

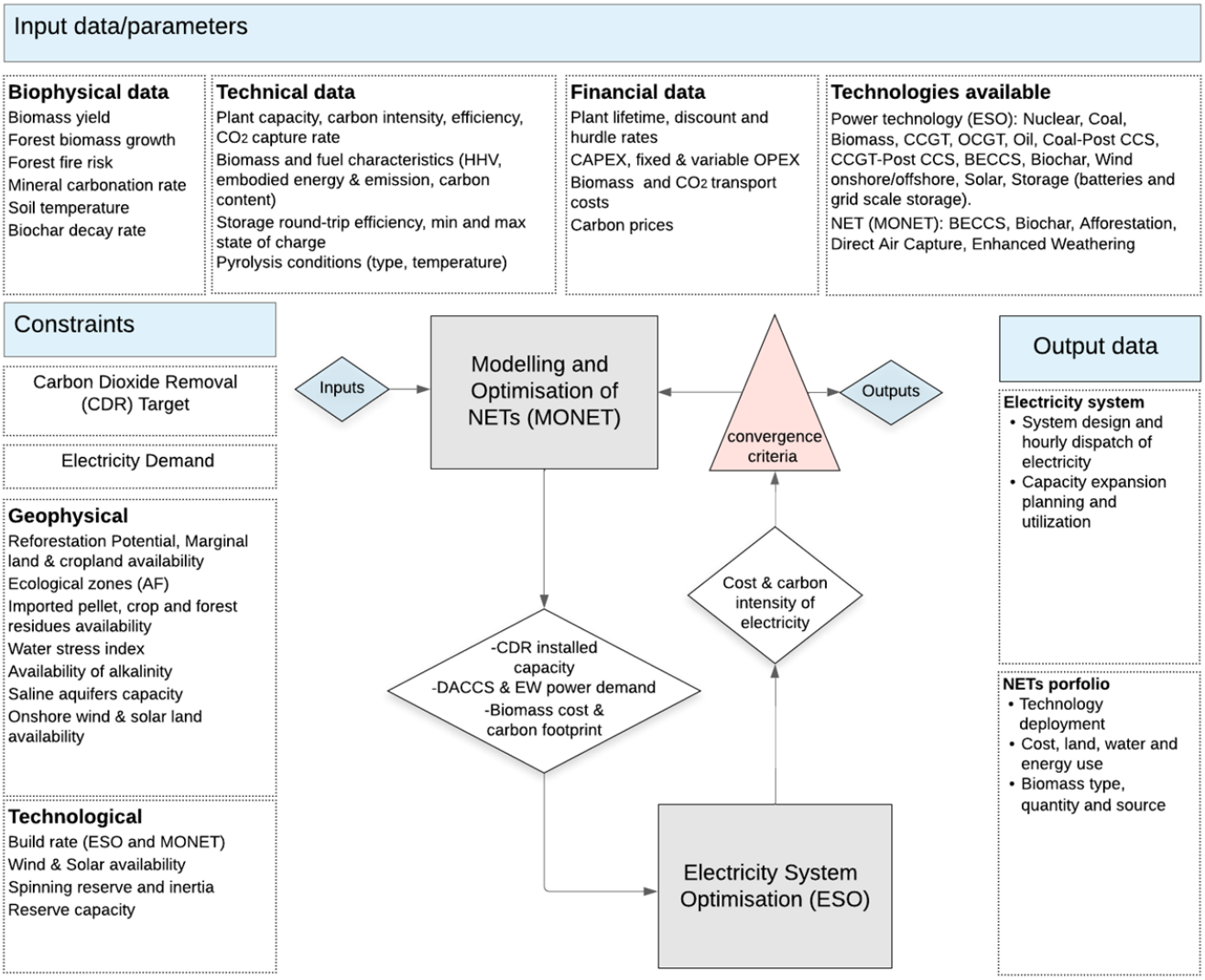


Figure 3.2: ESO-MONET Joint-System framework

This figure illustrates the interaction between the Electricity System Optimisation (ESO) model and the Modelling and Optimisation of Negative Emission Technologies (MONET) model within the ESO-MONET framework. The CDR target (for MONET) and the electricity demand (for ESO) are the key constraints of the EM optimisation framework. Other bio-geophysical constraints include lands with reforestation potential[126] for AF, marginal lands used to grow biomass crops for BECCS and BC, and biomass import availability for BECCS[56], as well as water stress index used to filter out water-stressed lands, igneous rock (basalt) formations locations and capacities for EW, and underground CO_2 storage capacities for BECCS and DACCS.

Model constraints and parameter transfer

During the first iteration, ESO transfers the price and carbon footprint of electricity to MONET-UK. MONET-UK in turn calculates DACCS power demand and biomass cost and carbon footprint, both transferred to ESO. These parameters are key in the iteration process because CDRs use electricity in their process (DACCS) or along their supply chain (BECCS, EW) and because biomass characteristics (used for BECCS and biomass power) and power demand resulting from DACCS and EW deployment are important for the electricity system optimisation. The loop (*i.e.*, ESO followed by MONET optimisation) iterates until Eq. 57 is

satisfied. Overall, the EM is optimised to meet the UK CDR targets between 2020-2050 (see Table 2.4). It is important to note that, given the ESO formulation, BECCS and BC are included in the power-generating technologies, and they are therefore recognized as providing CDR services, generating negative carbon electricity, and providing ancillary grid services. However, as it is understood that the most valuable service delivered by BECCS is that of carbon removal[145], ESO is constrained to the same level of BECCS as that deployed in the MONET CDR portfolio.

In other words, the carbon removal constraint assigned to the model is 90 Mt_{CO2} per year in 2050 for the emission of both ESO and MONET. In addition, the electricity system model (ESO) is constrained to reach at least zero emissions by 2050 (as discussed in ESO constraints section) but is allowed to become carbon negative (*i.e.*, removing CO_2, using CDR *via* BECCS and BC). It is important to note that both BECCS and BC's negative emissions are accounted for in the power sector emission balance.

Once the convergence criterion is met, the EM framework provides over the period 2020-2050: 1) an optimal electricity system design, including a capacity expansion planning and electricity generation mix (from ESO), and 2) an optimal CDR portfolio (from MONET-UK), along with technology-specific deployment information such as the type of biomass, areas, and locations of land-use for biomass, forest, and number and locations of BECCS and DACCS plants.

We note that carbon prices are assumed to be an exogenous parameter in this study, equal to BEIS carbon price projections (Table 2.4). Yet, this neglects potential carbon price dynamics that could affect the price of power technologies deployment. However, the EM optimization does incorporate competition between low and zero-carbon power generating and CDR technologies, establishing an implicit carbon price defined by technology cost modelling.

3.3.2 Impact of CDR deployment on the electricity system

Having first considered the evolution of the power and CDR sectors in isolation, the next step is to study the co-evolution of both sectors in an integrated fashion. Ultimately, the key question is if a material change in the outcome can be identified, implying that this kind of "sector coupling" is, in fact, important. Conversely, if only minor quantitative perturbations to each sector are observed, perhaps this sector coupling is insufficiently important to warrant the additional complexity.

We perform this investigation *via* a scenario-based approach and compare power system outputs with those of the reference scenarios (in section 3.2) where the power system has been optimised in isolation.

We first consider the impact of having only one CDR pathway available at a time, *i.e.*, just BECCS, just DACCS, or just AF is available at any point in time. These scenarios help us understand the maximal potential of each CDR and its direct impact on the electricity system.

Then, owing to the prominent role of BECCS in many IAMs, but recognizing the controversy over the competition with food production, we investigate the implications of seeking to meet a CDR target without the option of using biomass, *i.e.*, only AF, DACCS and EW are available.

Finally, in the last two scenarios, all CDRs are available (AF, BECCS, BC, DACCS and EW) and we allow for low and high biomass. Here, we use Ricardo Energy and Environment's projections on imported biomass availability, where imports are limited to 36 Mtpa in 2030 and 7 Mtpa in 2050 [133].

3.3.3 Only one CDR available

In the *BECCS-only* scenario, BECCS deployment is constrained by national land availability (2.1 Mha) and biomass imports are limited to 7 Mtpa. This value is comparable to the 9 Mtpa of wood pellets imported into the UK in 2020[146]. Miscanthus on dedicated land, forest, and crop residues are used as domestically sourced, and the allowed quantity of pellets is imported. This results in CDR deployment of 47 Mt_{CO2}/yr in 2050. This falls approximately 42 Mt_{CO2}/yr short of the 90 Mt_{CO2}/yr estimated by the CCC to be required in 2050[47].

To remove 90 Mt_{CO2}/yr using only BECCS technology, not only would all available marginal lands, *i.e.*, 2.1 Mha, need to be set aside for bioenergy cultivation, but biomass imports would need to increase to 83 Mtpa by 2050. Not only would this require significant expansion of associated infrastructure, *e.g.,* ports and associated handling and distribution infrastructure, but would lead to significant exposure to a currently illiquid bioenergy market. This emphasizes the need to invest in the development and deployment of alternative CDRs.

In the *AF-only* scenario, CDR reaches a maximum limit of 15 Mt_{CO2}/yr in 2050, owing to the rate at which afforestation can expand. Forest expansion rates should increase to 450 kha/yr to deliver 90 Mt_{CO2}/yr. This is more than 10 times the currently anticipated expansion rate by the CCC[89]. This scenario is expected to have no impact on the electricity system compared to the ESO-reference scenario, as there is no BECCS deployed.

Finally, the *DACCS-only* scenario meets the national 2050 CDR target, with an ambitious DACCS deployment rate of 3.6 Mt_{CO2} of additional capacity per year starting from 2025, which is more than 4 times greater than BEIS expectations[16]. Consequently, DACCS power demand resulting from such DACCS deployment would reach 115 TWh per year in 2050, which increases the national power demand by 24% in 2050 compared to the ESO-reference scenario.

3.3.4 No Biomass and different levels of biomass available

In the No-Biomass scenario, AF and EW are deployed to their maximum potential of 15 and 6 Mt_{CO2}/yr in 2050 respectively (see Figure 3.3a). Therefore, DACCS is deployed to make up the shortfall – with an average deployment rate of 0.3 Mt_{CO2}/yr of new capacity during the period 2022-2030 and building 7 Mt_{CO2}/yr of new capacity in the period 2045-2050, allowing the removal of 70 Mt_{CO2}/yr by 2050. The associated power demand increases by 21% by 2050 compared to the ESO-reference scenario. This demand is met with an additional 18GW (+12% relative to the reference scenario) of renewable capacity accounting for 50% of the power

supply in 2050, a stable nuclear generation (12% of the power supply in 2050), as well as a dispatchable thermal capacity doubling the CCGT-CCS fleet to 46GW providing 14% of the supply in 2050. After 2030, the intermittency of renewable generation will be addressed in the short term through storage technologies such as battery storage (GenSto), pumped hydro storage (PHSto), and a substantial capacity of CCGT-CCS.

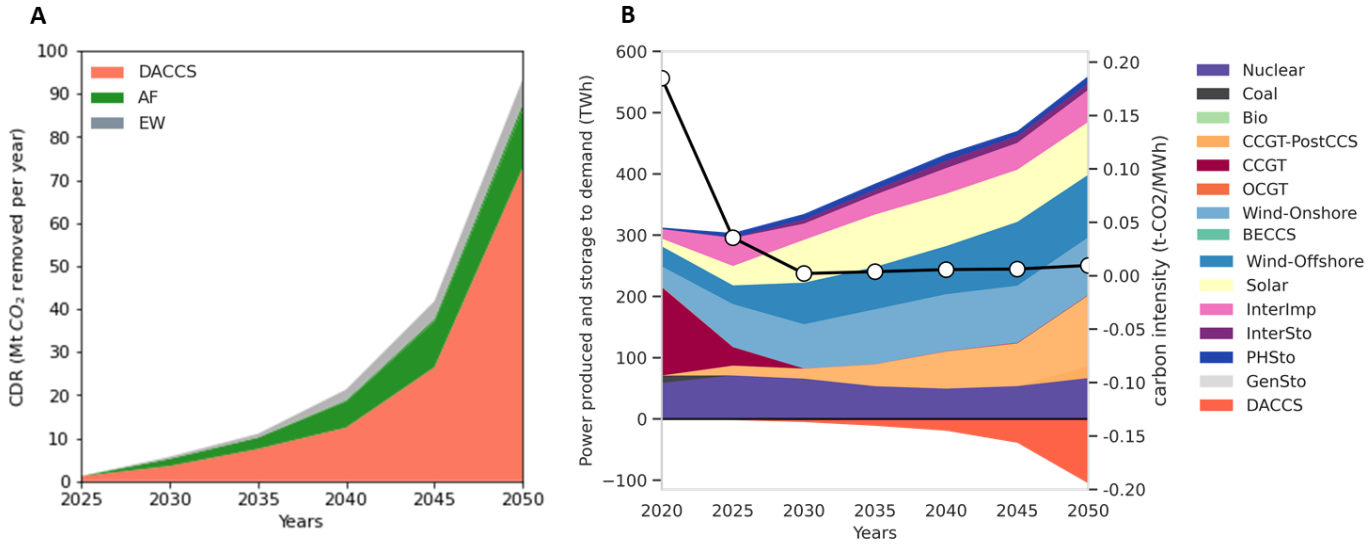


Figure 3.3: ESO-MONET Optimisation in No-Biomass Scenario (2020-2050)
CDR portfolio (A) and electricity production (B) resulting from the ESO-MONET optimisation.
We use all CDRs except BECCS and Biochar. As AF and EW are both limited by geophysical constraints, DACCS is required to meet the 90 Mt_{CO2}/yr target by 2050. The carbon intensity of electricity is computed as the average emission factor of all power-generating technologies (including BECCS, and BC).

In the *All-Low-bio* scenario, the CDR portfolio includes all five technologies (Figure 3.4a). All biomass available, *i.e.*, both indigenous and imported biomass is distributed between BECCS and BC, reaching respectively a removal of 21 and 22 Mt_{CO2}/yr by 2050, reaching about half the CO_2 removal budget in 2050. Afforestation is deployed as early as 2020 to remove up to 14 Mt_{CO2}/yr in 2050, whereas EW is only deployed from 2035 up to 9 Mt_{CO2}/yr in 2050. This is because EW is more expensive than AF, but still cheaper than DACCS. AF, EW, as well as BECCS are deployed up to their maximum potential, and, over the last decade DACCS is therefore required to meet CDR targets, ultimately removing 23 Mt_{CO2}/yr by 2050. This corresponds to an annual rate of 1.5 Mt_{CO2}/yr after 2035, which is comparable to the roll-out rates indicated in the BEIS report (2 Mt_{CO2}/yr)[16], described as “feasible but ambitious”.

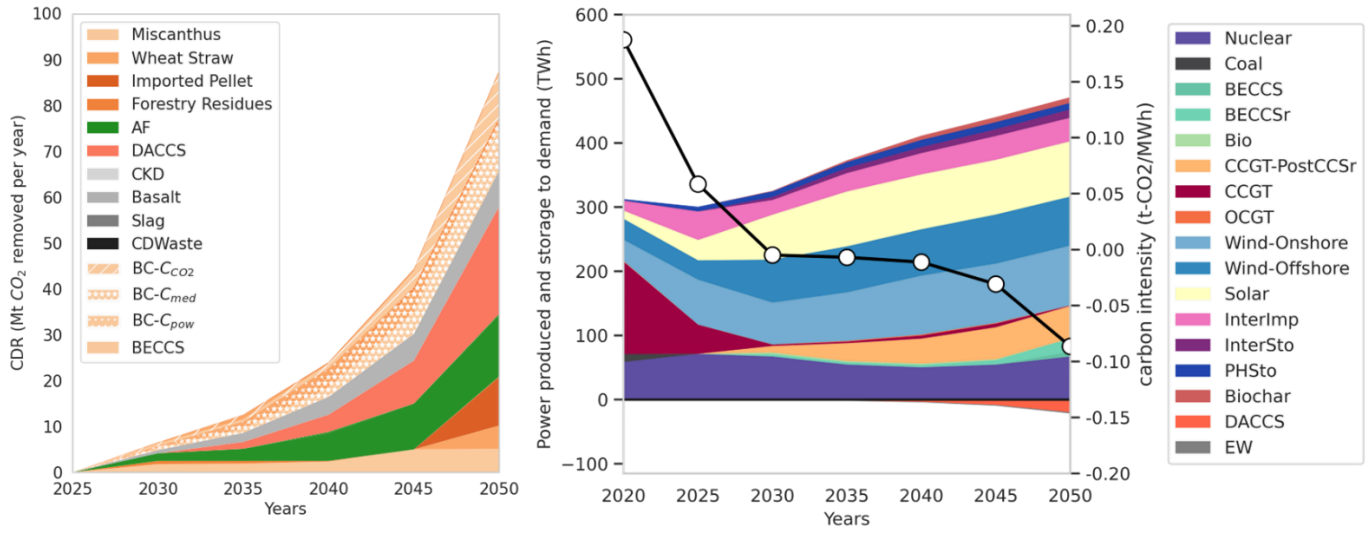


Figure 3.4: ESO-MONET Optimisation in All-Low-bio Scenario (2020-2050)
CDR portfolio (left) and electricity production (right) resulting from the ESO-MONET optimisation. All CDRs are considered. A limitation is assumed on biomass import, restricting BECCS and biochar deployment. The carbon intensity of electricity is computed as the average emission factor of all power-generating technologies (including BECCS, and BC).

Therefore, the electricity system reaches net zero emissions as early as 2030 and has a negative carbon footprint of -0.09 t_{CO2}/MWh in 2050, (compared to 0.20 t_{CO2}/MWh in 2020, Figure 3.4b). Akin to the ESO-reference scenario, coal generation reaches zero by 2025 and unabated natural gas (CCGT) generation is drastically reduced, but little generation is still needed to meet peak demand. BECCS capacity reaches 4 GW by 2050, equivalent to an average rate of ~400 MW plants every two years from 2030 to 2050. This capacity with that of pyrolysis units meets 8% of total electricity generation in 2050 and runs in a baseload fashion such that it impacts the remaining electricity mix. Nuclear clean and baseload electricity supply remains stable over the century and is similar to the ESO reference scenario. Generation share from CCGT-CCS is importantly reduced by 22% relative to the ESO reference scenario but still provides 50 TWh of flexible electricity by 2050. Renewables are deployed massively throughout the half-century with solar and wind, overall meeting 54% of electricity production in 2050, increasing by 6% relative to the ESO reference scenario. This is driven by the additional power demand from DACCS and EW deployment and results in comparable curtailment levels in 2030 (compared to ESO reference) but more than three times higher (18 TWh) in 2050. Such an increase can be justified by a combined increase in intermittent renewable, due to rising demand, and unflexible BECCS generation. As BECCS and biochar provide both energy and CDR services, they are observed to provide 8% of the UK's power demand in 2050, and half the annual CDR required in the UK by 2050.

In the *All-High-bio* scenario (Figure 3.5), DACCS and most of the EW removals are both replaced by BECCS using imported pellets. In this scenario, about 80 Mt_{CO2}/yr are removed by BECCS and biochar by 2050, with a further 10 Mt_{CO2}/yr removed *via* Afforestation. Deploying this quantity of BECCS and biochar has a significant impact on the electricity sector. We observe 12 GW of BECCS installed in 2050, implying an average deployment rate of 600 MW/yr in the period 2030 to 2050. Similarly, biochar generates 13 TWh of baseload electricity, meeting 3% of the power national demand. As in the *All-Low-bio* scenario, the electricity sector reaches net zero emissions in 2030, but this time has a negative carbon

footprint of -0.18 t_{CO2}/MWh in 2050 (versus -0.09 t_{CO2}/MWh for *All-Low-bio,* Figure 3.5b). This amount of BECCS and biochar generation reduces power generation of both nuclear and renewable capacity by 18% and 13% in 2050, respectively. Curtailment levels are akin to the ESO reference scenario in 2030. 18 TWh in the All-Low-Bio scenario). Curtailment levels in 2050 are tripled to 14 TWh, slightly decreasing compared to the 18 TWh of the All-Low-Biomass scenario, due to the reduction in wind power generation. The share of CCGT-CCS is also reduced by 55% relative to the ESO reference scenario.

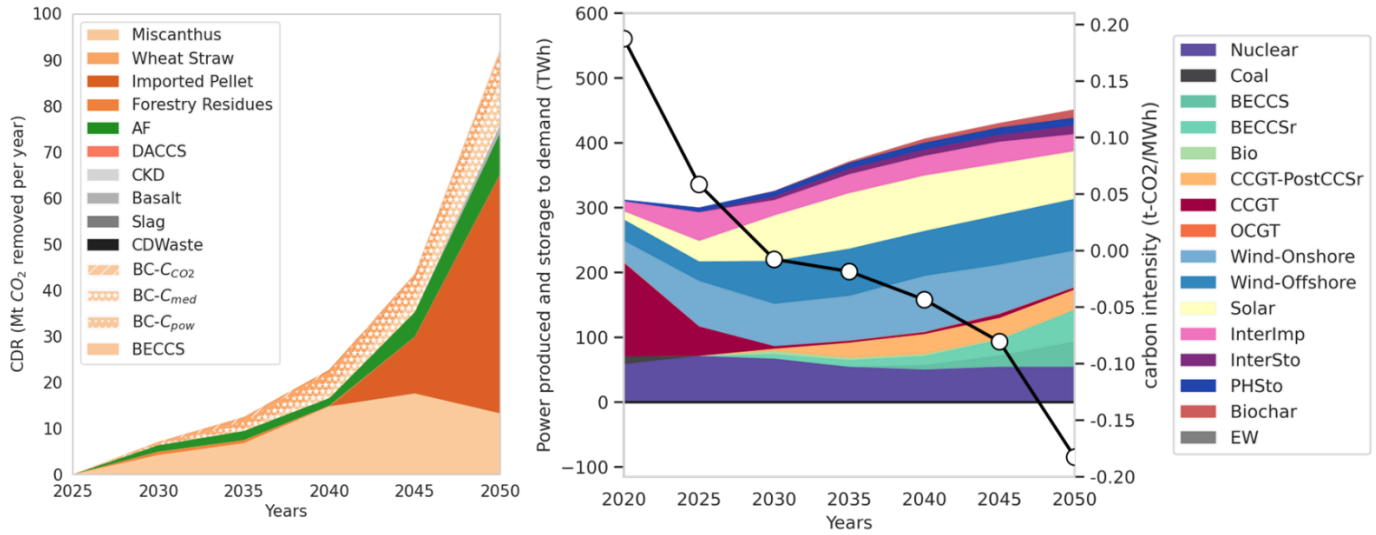


Figure 3.5: ESO-MONET Optimisation in All-High-bio Scenario (2020-2050)
CDR portfolio (left) and electricity production (right) resulting from the ESO-MONET optimisation. All CDRs are considered. No limitation is assumed on biomass import. The carbon intensity of electricity is computed as the average emission factor of all power-generating technologies (including BECCS, and BC).

Finally, we show the system costs (normalized to the *All-Low-bio* costs scenario) in Figure 3.6. Even though the electricity system (ESO) cost is 10 % higher for scenarios meeting the CCC removal target, thus offsetting other sectors' emissions, there are no major differences between the total ESO system costs of the various scenarios. This observation is driven by the fact that BECCS investments and operating costs represent less than 10% of the total electricity system cost across all the scenarios. This results in a marginal cost impact when deploying large-scale BECCS, as it also reduces investments in other power technologies (Gas-CCS, renewables). However, we find a larger discrepancy in CDR operating costs. The average cost per tonne of carbon removed is observed to vary between \$150-550/t_{CO2}, driven primarily by the availability of BECCS and biochar.

Using the *All-Low-bio* scenario as a reference, where BECCS and BC are unavailable, total system costs are observed to be 30% higher in the *No-Biomass* scenario, and 10% lower in *All-High-bio*. This serves to highlight the potential benefit related to scenarios with higher biomass availability.

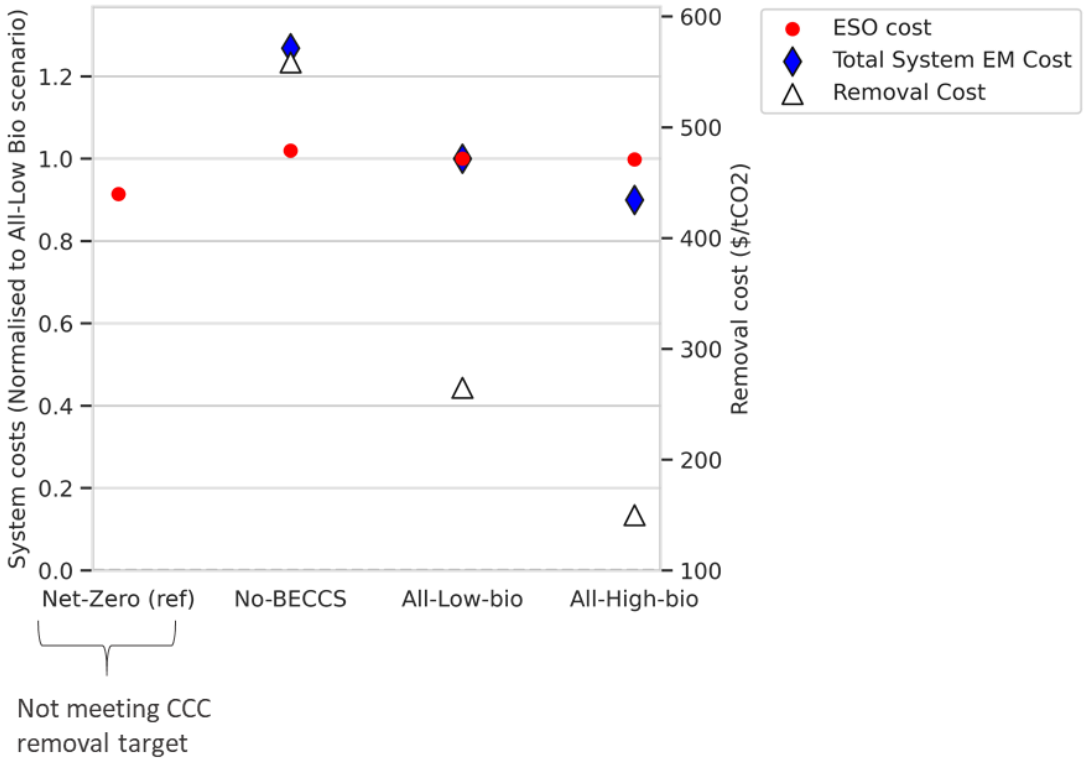


Figure 3.6: ESO-MONET scenario's cumulative costs

To summarise, the EM framework provides a least-cost pathway for meeting both electricity system constraints (total demand, reserve requirement, regulation services, frequency control) and negative emission requirements to mitigate other sectors' emissions. A key observation is that BECCS and BC are strong candidates for significant deployment nationwide subject to biomass availability, along with a limited afforestation deployment, due to expansion rate constraints.

We recognise that, in practice, BECCS and DACCS deployment will also be limited by proximity to CO_2 storage, and availability of CO_2 transport and storage infrastructure, which is not incorporated in this section. We will bring possible answers in Chapter 5.

Based on the cost and bio – and geo–physical bounds assumed in this study, a power system with a high installed capacity of BECCS (1) is complementary, to a certain extent, to flexible generation (such as CCGT with or without CCS), as it provides baseload power, (2) is deployed along with more than 50% of renewable generation, (3) competes with nuclear generation after a certain point, as both BECCS and nuclear provide a baseload power supply, (4) results into higher power system costs due to the increase curtailment levels, but overall decrease the total power-CDR system cost.

However, these results do not consider technological learning for early-stage deployment solutions like DACCS. Such an assumption could bring DACCS cost closer to BECCS, EW, BC and AF, therefore changing the expected power-CDR future deployments and costs. If DACCS becomes a competitive technology compared to BECCS, BC and EW in the next 25 years, and given AF bio –and geo– physical limits, DACCS would be the best candidate for deployment. This would bring the No-Biomass scenario (which massively uses DACCS) to lower costs than

current scenarios with biomass (All-Low and All-High). In such a case, it is crucial that the pace of DACCS deployment matches with enough additional power to support it. This is especially important because building new power generation sources need anticipation, and in some cases, decades of investments. The burning question of which power technology to use to power DACCS will be more explored in the next subsection.

Whilst the *All-High-bio* scenario is the most attractive financially, having the UK's CDR requirements rely so heavily on one material – 88% of removals observed to be delivered by biomass-based CDR solutions– could introduce an element of risk to the portfolio. Conversely, a system composed of a diversity of suppliers, using biomass sourced from several activities (residues, indigenous and imported) and from different parts of the world (50% of pellets are imported), can provide some security to the overall system.

3.4 ESO-MONET Sensitivity Analysis to the availability of imported pellet and AF expansion rate

As pointed out in scenarios *All-Low-bio* and *All-High-bio* in the above section, greater biomass availability increases BECCS' and biochar's contribution to meeting CDR targets, and therefore increases their penetration within the electricity system. This has the consequence of displacing other assets from the grid. Simultaneously, more biomass-based CDR in the system also implies less DACCS, adding a second dynamic in the system variation. To understand both dynamics, we evaluate the variation of power technologies with different levels of BECCS and DACCS in the system, ignoring BC for the sake of simplicity, and due to the role BECCS has in scientific and policy discussions. The results are presented in Figure 3.7 below. In this analysis, AF constitutes a proxy for nature-based solutions and their potential impact on the adoption of engineered CDR solutions. Finally, we run a sensitivity analysis on biomass availability and afforestation expansion rate to investigate variations in the CDR portfolio and the electricity system by 2050.

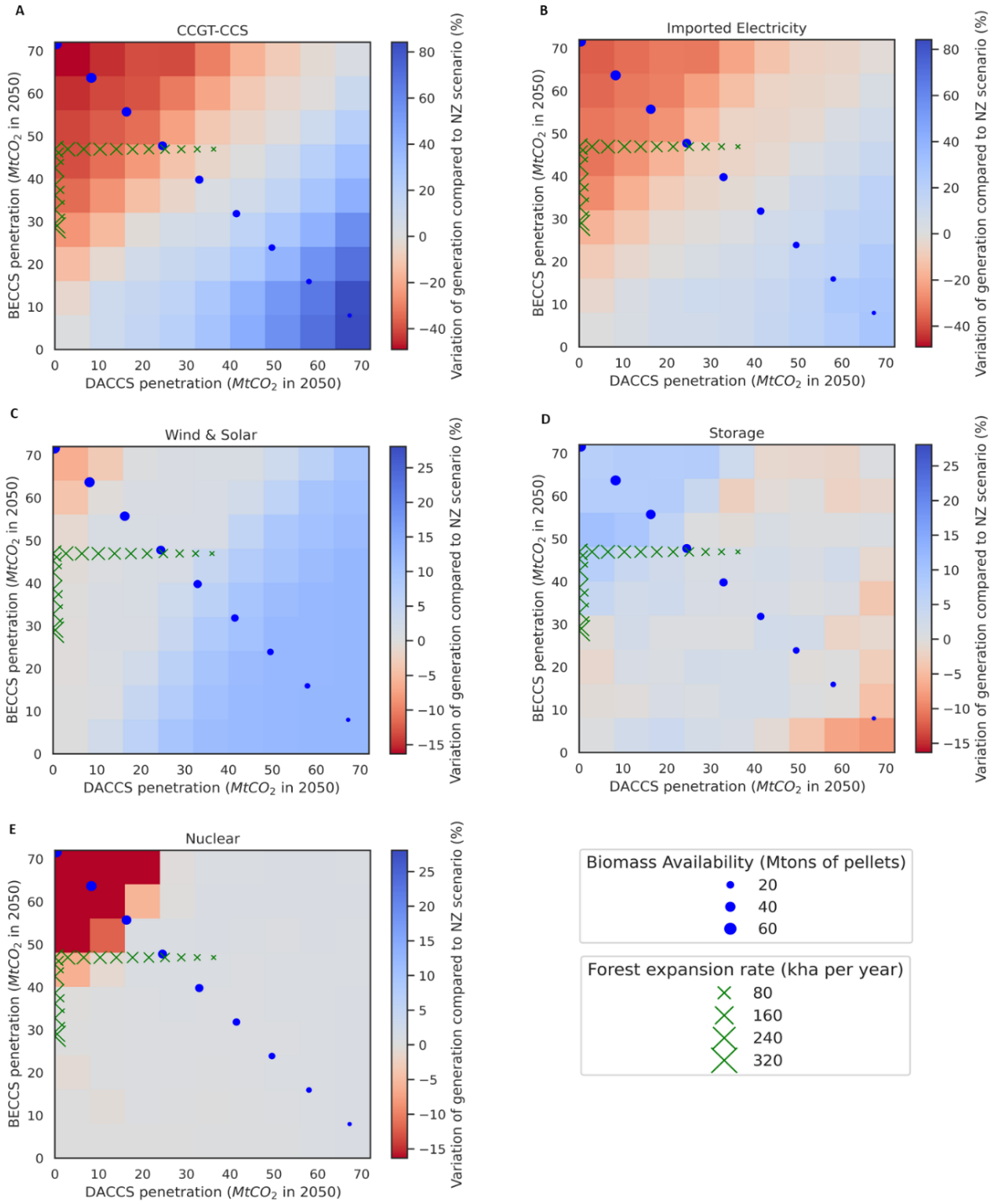


Figure 3.7: Power technology variations compared to their generation share in the ESO reference scenario

As can be observed from Figure 3.7a, b, and c, CCGT-CCS imported electricity, and wind & solar exhibit similar behavior in response to perturbations in the availability of BECCS and DACCS.

We find that for CCGT-CCS and imported electricity, the zero line follows the perfect diagonal (1:1), meaning that for the same deployment of BECCS and DACCS, both generations will not vary compared to the ESO reference scenario. This means that in an idealized system, a

surplus of DACCS removals would be powered by a surplus of BECCS, and other power technologies, except CCGT-CCS, or imported electricity.

The zero line of wind and solar is located slightly above the perfect diagonal, meaning that for the same deployment of BECCS and DACCS, wind and solar will increase their share to power some DACCS deployment.

The insight provided by the variation of electricity storage is that a high level of BECCS in the system will result in more storage, giving more flexibility to the system *via* BECCS-to-storage.

Nuclear share does not fluctuate much and is the only technology–with electricity storage– that does not power additional DACCS when BECCS level is fixed. However, with a high BECCS deployment (> 40 Mt_{CO2}) and DACCS removing 0 – 30 Mt_{CO2}, BECCS increase will significantly displace nuclear, reducing its share up to -15%.

This discussion reflects the implications of having cheaper DACCS available (due to technological learning costs, in particular). We find that more DACCS in the system needs an increase in power generation from wind and solar first, and CCGT-CCS second. Moreover, DACCS can also be partially supported by power generated by BECCS, as indicated by the diagonal shapes in Figure 3.7.

A more detailed representation of where the system optima lies can be found through the green and blue dots, providing the level of deployment of each technology, given the deployment level of both BECCS and DACCS, concatenating the information in 3 values (i.e., three dimensions of the graph). The combination of these 3 values is uniquely determined by varying key assumptions in our model input.

As shown by the blue dots (Figure 3.7), increasing biomass availability simultaneously increases BECCS and decreases DACCS deployment, following a top left direction. It is worth noting that if no biomass is available, we would see a significant increase in the use of DACC. This scenario is similar to what might happen if DACCS cost were to become cost-competitive with other CDR solutions. An increase in CCGT-CCS, wind and solar, and imported electricity generation would be required, in such a case. The effect of allowing more AF in the system by increasing the forest expansion rate can be observed in Figure 3.7 (green dots). Interestingly, AF reduces DACCS and then, BECCS share, following consecutively two orthogonal directions. Because of appearing symmetries in the case of CCGT-CCS, imported electricity and wind & solar, this reflects a possible fungibility between expensive engineered CDR and lower-cost AF removals for these power-generating technologies.

For the sake of compactness, we show in Figure 3.8a the evolution of a 2050 CDR portfolio and in Figure 3.8b a 2050 electricity system varying with biomass availability.

The observed effect of increasing biomass availability is the reduction of first CCGT-CCS, then imported electricity (InterImp), and finally wind and solar. These reductions occur at the same time as that of DACCS, proving these technologies are used specifically to power DACCS. Once biomass availability exceeds 60 million tonnes per year, BECCS displaces nuclear power as the

additional CDR service provided by BECCS reduces the relative cost of the associated baseload generation.

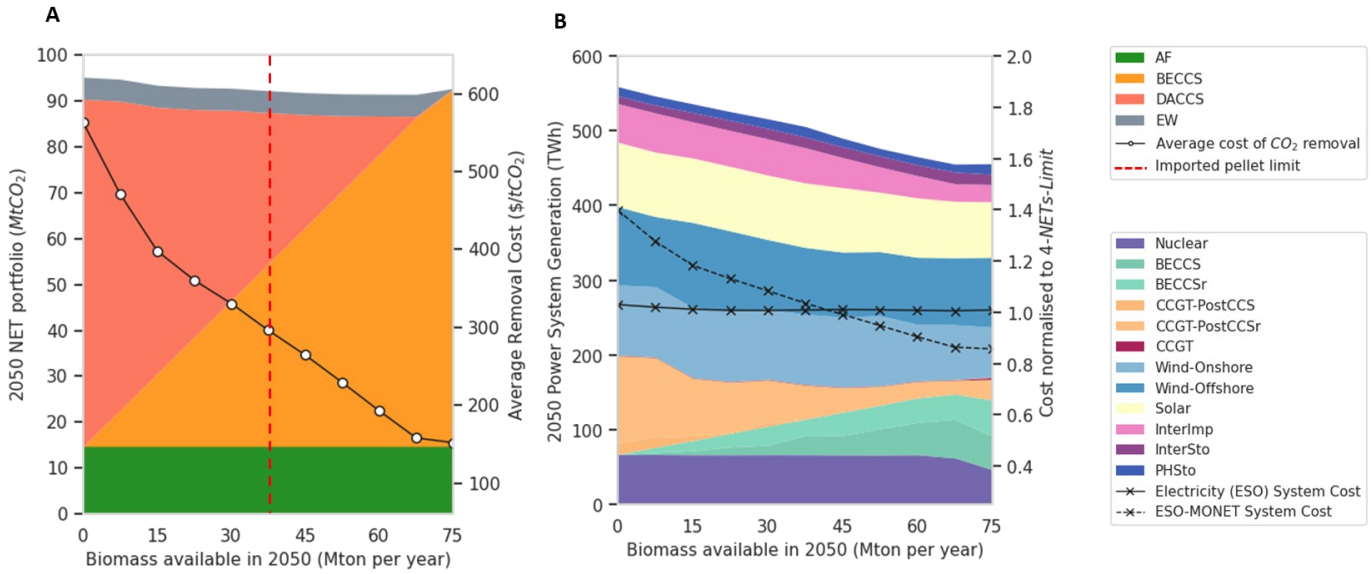


Figure 3.8: ESO-MONET System (EM) evolution in 2050 imported biomass availability
(A) *Evolution of the CDR portfolio in 2050.* More BECCS allowed in the system decreases DACCS share, as well as the average cost of CO_2 removal. AF expansion rate increase has a similar effect. The case where national bioenergy crops and biomass pellet imports are limited to 7 million tonnes in 2050[133], is shown by a red dotted line in Figure 9a.
(B) *Evolution of the electricity system.* The evolution of power technologies with more BECCS allowed in the system (left, centre). BECCS deployment impacts the electricity system by shrinking gas generation first. Secondly, intermittent renewable (solar, onshore and offshore wind) share decreases with higher BECCS deployment.

When biomass availability increases, the average removal cost decreases by up to a factor of three (Figure 3.8a), leading to a reduction in overall EM System cost (Figure 3.8b). We note that DACCS and EW are eliminated from the CDR portfolio when the pellet availability surpasses 70 million tonnes per year. Specifically, more than 80% of CDR in 2050 in the system is achieved with high BECCS availability scenarios. Inversely, prohibiting the use of biomass results in the most expensive CDR portfolio (~500 $/$t_{CO2}$ removed).

Finally, when biomass becomes highly available, the associated electricity system will tend to substitute gas generation and imported electricity first, then displacing renewable and nuclear supply, as shown in the sensitivity analysis. This highlights one dilemma that the UK electricity system will face regarding fuel use for its power generation. When no biomass power is present in the electricity system, it heavily relies on gas (combined with CCS) mainly used to power a massive DACCS deployment, required to meet national carbon budgets. Whilst some biomass can be sourced indigenously, beyond a certain amount of BECCS deployment, biomass imports would be required.

In a world where there are increased demands for bioenergy, this currently relatively illiquid market could come under strain. Since approximately June of 2021, EU energy prices have been significantly higher than historical precedent, spiking first in December 2021 and again in March 2022 owing to a combination of factors, including low wind speeds and Russia's

invasion of Ukraine. Thus, policymakers will need to be cautious about introducing new fragilities into the energy system.

In this section, we have presented the potential qualitative impact of CDR solution on the power sector, considering different biomass availabilities, and incorporating bio-geophysical bounds, such as marginal land, cropland, land with reforestation potential, silicate and biomass residues availabilities. In the next section, we will explore a different aspect of CDR solutions: their permanence.

Chapter 4

4 Permanence considerations

In light of the latest IPCC report (AR6 [3]), which underscores the imperative of integrating robust emission reductions with carbon dioxide removal (CDR) technologies, both through engineering and nature-based solutions, the emergence of carbon removal credits on voluntary markets has become a focal point. Today, these credits are subject to stringent verification processes and trade within established frameworks such as the Verified Carbon Standard (VCS).

Today, carbon removal credits are verified and traded on the voluntary carbon markets and are subject to a set of rules (*e.g.*, *via* the Verified Carbon Standard (VCS)). Existing standards mandate that removals be (1) verifiable (2) additional, and (3) permanent [147].

However, the advent of a global CDR market raises profound economic and ethical questions, particularly concerning the comparability of credits derived from different CDR solutions. [148]. This debate, illustrated by the differing timescales and ecological impacts of engineering versus nature-based solutions, underscores the complexity of evaluating removal costs, especially concerning permanence. Furthermore, understanding the intricate interactions between CO_2 and the biosphere is paramount in accurately assessing the impact of surplus emissions or removal deficits on the atmospheric CO_2 balance [30].

In this light, it is essential to accurately value the impact of temporary removal with respect to that of permanent removal. Studies have proposed different approaches to value temporary removal [144]–[146]. The majority of approaches outlined in the literature rely on CO_2 impulse response functions (IRFs) obtained from carbon cycle models to better simulate the effects of CO_2 emissions on the atmosphere. For example, Cherubini et al. applies this method to biomass combustion, usually assumed to be carbon neutral, notably in LCA studies of bioenergy systems. In this study, they examine the effects of shorter biomass rotation on the atmospheric CO_2 concentration and suggest the use of a coefficient between 0 and 1 to alter the global warming potential (GWP) of CO_2 in LCA studies [149]. The IRF approach used in their study is similar to our approach (presented in section 4.2) but is limited to biomass combustion and CO_2 emissions (not removals). We aim to provide a universal framework that can be applied across all types of CDR.

On a different vision, Kim et al. explore permanence discounting factors for land-based carbon sequestration, using the economic-based approach of differentiated goods [150].

Some studies have also explored the long-term tendencies of carbon leakage (thousands of years). For example, Lyngfelt et al., using CO_2 IRF functions, showed that both the quantity and the leakage rate of sequestered carbon have a determinant role in long-term CO_2 atmospheric concentrations, in the context of meeting global climate targets [152]. The study concluded that if 80% of CDR was permanently stored, and that the 20% remaining would leak with a mixture of leakages of 300, 1,000, and 10,000 years, the impact of leakage would not damage, or significantly change, global temperature trajectories.

However, there is a lack of frameworks generalisable to all CDR solutions. In this novel contribution, we present a general framework that combines an existing approach—the Lashof method [153]—with a long-term response of different carbon pools, as this is key for valuing the atmospheric impact of short and long-term temporary removals. This impact is quantified and described through a metric called the *Climate Repair Value* (CRV), detailed in section 4.2.

In the following section, we will distinguish between permanent CO_2 sinks, predictably leaky and unpredictably leaky CO_2 sinks [154]. The permanent and predictably leaky sinks can be estimated with some certainty. However, unpredictably leaky sinks, such as afforestation, are more complicated to anticipate. These sinks' leakiness can still be estimated, yet with more uncertainty than for other types of sinks.

This section will provide, first, a study case of a predictably leaky CDR (4.1). The meaning and definition of Climate Repair Values (CRV) will be then expanded (4.2). How CRV values will be used in the context of CDR solutions, and, in particular, their role in the computation of carbon balance, and removal cost, will be explained in the formulation of the Cost of Permanent Removal (CPR) (4.3). Finally, the results of CPR for different CDR solutions – both engineering and nature-based –, are analysed (4.4)

4.1 The case of predictably leaky CDR

In this subsection, we use biochar as a study case to motivate our permanence exploration which is a substantial part of this dissertation.

4.1.1 The BC example

As assumed in Eq. 50, the biochar decay rate can be approximated by a two-pool exponential decay that is given by $DecayBC(t)$.

In addition to some uncertainty, there is some variation in biochar decay rates, as it depends on the pyrolysis process, and the type of biomass, chosen for biochar production. Given these uncertainties, we will base our current study case on three scenarios that represent two extreme cases (pessimistic and optimistic), and a medium-range case, inspired by [119]. The three scenarios' leakage curves are provided in Figure 4.1.

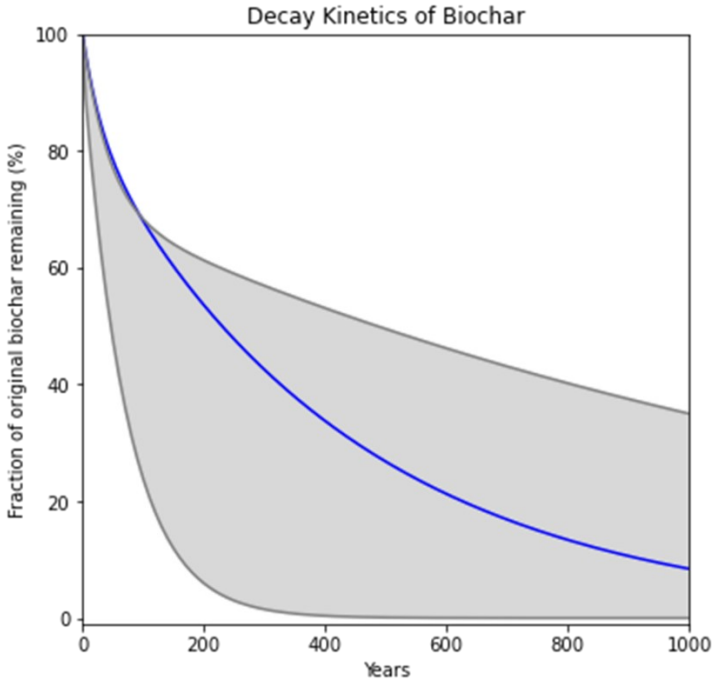


Figure 4.1: Decay Kinetics of Biochar

We assume that the pyrolysis plant outputs the same amount, of *T* tonnes of biochar (t_{BC}) every year containing the same total quantity of carbon C (in t_{CO2}). Based on the decay rate equation, we can determine the carbon dynamic profile $C_{t,t_{app}}$ of *T* t_{BC} of biochar applied at year t_{app} over time t:

$$C_{t,t_{app}} = C * DecayRate(t - t_{app}) \qquad \text{Eq. 58}$$

This represents the evolution of carbon or cumulative stock associated with *T* t_{BC} of biochar applied at year t_{app}.

We choose to write the decay as a sum of sub-decays $\alpha_i > 0$, where each α_i determines the decrement of the decay from the year *i* to year *i+1.* The expression of the decay is given as follows:

$$DecayRate(t) = 1 - \sum_{i=1}^{t} \alpha_i \qquad \text{Eq. 59}$$

From an annual perspective, the carbon fixed in the biochar will leak progressively over time (more or less rapidly, depending on the assumption made on the decay). Thus, it will remove carbon in the first year (when pyrolysis happens) and will emit carbon back into the atmosphere every year, in the following years.

Given that a pyrolysis plant produces *T* t_{BC} of biochar each year over its lifetime, its annual carbon sequestration at year *N* equals the sequestration at year N of biochar applied at year *N* (C) minus the emissions at year N from decaying biochar applied at year N-1 ($E_{N,N-1}$), minus

the ones from decaying biochar applied at year N-2 ($E_{N,N-2}$), *etc., minus* the ones from decaying biochar applied at year 1 ($E_{N,1}$) of the pyrolysis lifetime:

$$AnC_N = C - E_{N,N-1} - E_{N,N-2} - \cdots - E_{N,1} \quad \text{Eq. 60}$$

where emissions can be computed as the difference of the carbon profile of biochar applied at year t_{app} between years *N* and *N-1*:

$$E_{N,t_{app}} = C_{N,t_{app}} - C_{N-1,t_{app}} \quad \text{Eq. 61}$$

Which can be rewritten, using Eq. 58 and Eq. 59, as follows:

$$E_{N,t_{app}} = C * DecayRate(N - t_{app}) - C * DecayRate(N - 1 - t_{app}), \quad \text{Eq. 62}$$

$$= C * \left(1 - \sum_{i=1}^{N-t_{app}} \alpha_i\right) - C * \left(1 - \sum_{i=1}^{N-1-t_{app}} \alpha_i\right)$$

$$= C * \left(\sum_{i=1}^{N-t_{app}} \alpha_i\right) - C * \left(\sum_{i=1}^{N-1-t_{app}} \alpha_i\right)$$

$$= C * \alpha_{N-t_{app}}$$

$$E_{N,t_{app}} = C * \alpha_{N-t_{app}} \quad \text{Eq. 63}$$

Thus, we find that emissions at year N from biochar applied at year t_{app} can also be expressed as the sub-decay fraction $\alpha_{N-t_{app}}$ of C, which is an intuitive result.

Combining Eq. 60 with Eq. 63, we can express the annual carbon sequestration of a pyrolysis plant at year N as follow:

$$AnC_N = C - C * \alpha_1 - C * \alpha_2 - \cdots - C * \alpha_{N-1}$$

$$= C(1 - \sum_{i=1}^{N-1} \alpha_i)$$

$$= C * DecayRate(N - 1)$$

$$AnC_N = C_{N,1} \quad \text{Eq. 64}$$

Thus, the *annual* sequestration of a pyrolysis plant (producing *T* t_{BC} every year) at year N is equal to the carbon dynamic profile of *T* t_{BC} of biochar applied at year 1 over N years.

We have first described the carbon profile of *T* t_{BC} as a sum of decay. Then, we found that the *annual* removal of a pyrolysis plant producing *T* t_{BC} per year is identical to the carbon profile of *T* t_{BC} applied at year 1. Let us express the *cumulative* removal profile of a pyrolysis plant. It is equal to the sum of annual removals of the pyrolysis plant:

$$CC_N = \sum_{t=1}^{N} AnC_t$$

Thus, using Eq. 64, we can express it as a sum of carbon profiles of T t_{BC} applied at year 1:

$$CC_N = \sum_{t=1}^{N} C_{t,1}$$

$$= \sum_{t=1}^{N} C * DecayRate(t)$$

$$= C * \sum_{t=1}^{N} \left(1 - \sum_{i=1}^{t} \alpha_i\right)$$

$$CC_N = C * N - C * \sum_{t=1}^{N} \sum_{i=1}^{t} \alpha_i \quad \text{Eq. 65}$$

This formula provides some insight into the trend and shape of a pyrolysis plant's cumulative carbon balance. As the pyrolysis project lifetime increases, more carbon is sequestered in the biochar that has been produced ($C * N$). However, at the same time more carbon leaks too ($C * \sum_{t=1}^{N} \sum_{i=1}^{t} \alpha_i$). At this point, the cumulative carbon removal cannot be negative because:

$$C * N \geq C * \sum_{t=1}^{N} \sum_{i=1}^{t} \alpha_i$$

In other words, there cannot be more carbon leaking than what has been sequestered in the first place.

Let us now investigate the total carbon balance of a biochar project, considering supply chain emissions, as described in Chapter 2.

Naturally, the annual carbon balance at year t of a biochar project, CB_t can be computed as the difference between the supply chain emission E_{SC} and the annual biochar sequestration of CO_2 at year t AnC_t:

$$CB_t = E_{SC} - AnC_t$$

Thus, the cumulative carbon balance of a biochar project at year N can be expressed as a sum of annual carbon balances:

$$CCB_N = \sum_{t=1}^{N} CB_t = \sum_{t=1}^{N} E_{SC} - AnC_t$$

$$= N * E_{SC} - CC_N, \quad \text{Eq. 66}$$

By combining equations Eq. 65 and Eq. 66, we can compute the cumulative carbon balance of a biochar project. Note that parameter N, corresponds to the lifetime of the BC project, and is an uncertain parameter, as we cannot predict how long a BC project will be deployed, or whether the BC business will thrive, or collapse. Thus, we study explore two approaches.

(1) $N = 20$ *the pyrolysis plant operates for 20 years (i.e., the lifetime of the plant) and is then left for another purpose or abandoned.*
(2) $N = \infty$ *the biochar project operates for an undetermined duration. When the pyrolysis plant comes to its life end, the same business owner retrofits the pyrolysis plant and keeps operating it.*

These two different approaches enable us to explore the potential carbon balance of BC deployment if BC is deployed for a short-term period (*e.g.*, one pyrolysis plant lifetime, that is 20 years), or whether it is deployed forever (in this case, defined to be 1,000 years). Even though none of these timescales might happen, they encompass a range of likely situations. Therefore, the qualitative trends, rather than the exact results will be discussed in this section. Noteworthy, all data assumptions on carbon sequestration during the pyrolysis process and biochar supply chain carbon emissions are the same as we have detailed in Chapter 2.

Figure 4.2 illustrates the annual carbon balance of a biochar project for both approaches across the three decay scenarios (pessimistic, medium, and optimistic) if we assume a pyrolysis plant keeps producing T t_{BC} per year every year throughout the lifetime of the project.

In **case 1**, the biochar project captures CO_2 during the 20 years of its lifetime but stops capturing CO_2 after 20 years ($C = 0$ in Eq. 60). However, after the end of the project lifetime, carbon keeps being emitted due to biochar leakages (the negative terms in Eq. 60).

In **case 2**, we find that in all the cases, annual removals from the pyrolysis plant decreases with different speeds depending on the leakage assumptions. In the optimistic case, it is divided by 4 after 1,000 years. Annual removals become null after 1000 years in the medium case and negative after less than 200 years in the pessimistic case. A negative annual removal means that the biochar project is a carbon emitter along that specific year, but not necessarily overall. Looking back at Eq. 60, this can be justified by the fact that carbon sequestered at a specific year N, is lower than emissions from biochar produced during the previous years. In mathematical terms:

$$C < E_{N,N-1} - E_{N,N-2} - \cdots - E_{N,1},$$

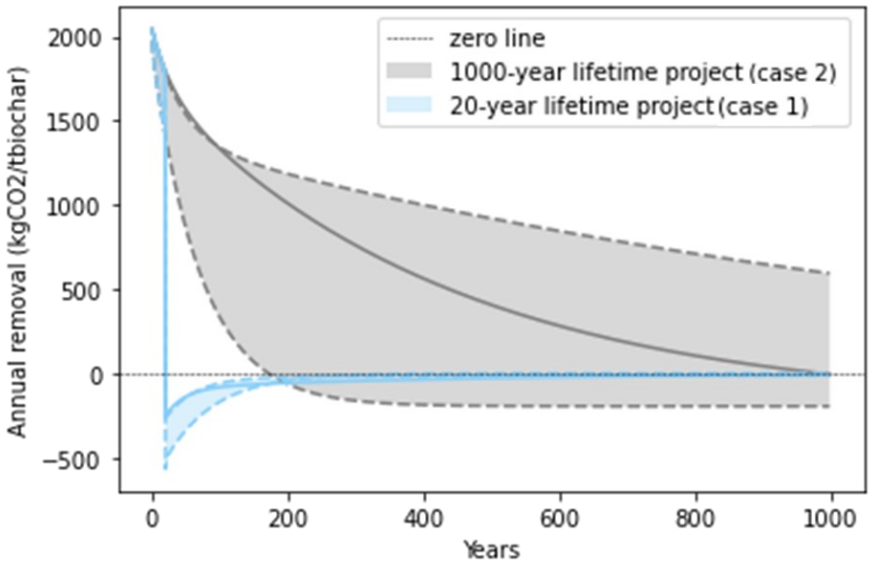


Figure 4.2: Annual Sequestration of a predictably leaky CDR

In Figure 4.3, we look at the cumulative sequestration of a biochar project for both approaches across the three decay scenarios (pessimistic, medium, and optimistic). This offers insight into the comprehensive carbon footprint associated with a project.

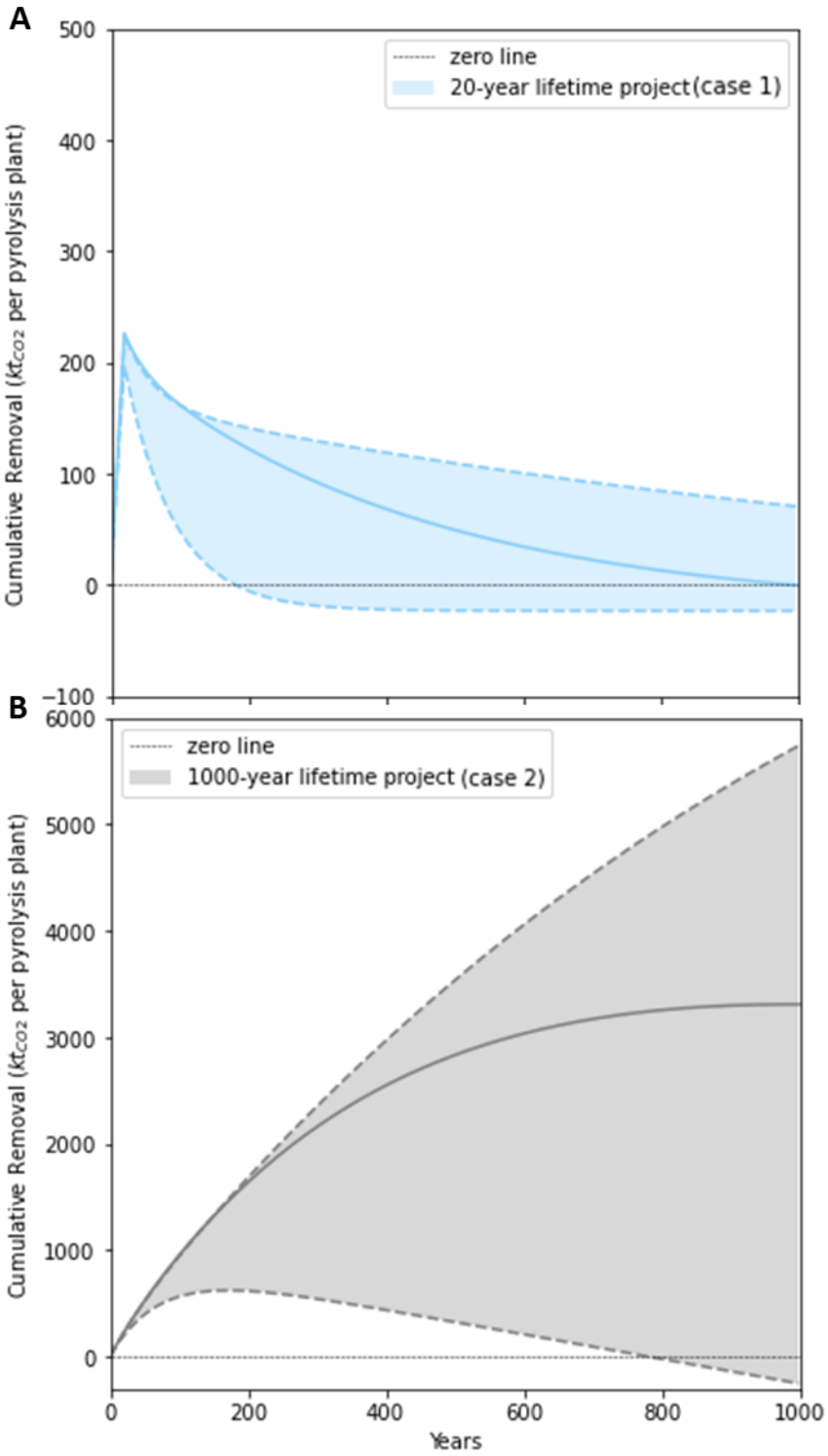


Figure 4.3: Cumulative Sequestration of a predictably leaky CDR
(A) Case 1: 20-year lifetime project
(B) Case 2: 1000-year lifetime project

We logically observe that the cumulated carbon stock is higher when the pyrolysis plant operates for longer periods, with the carbon stock approximately proportional to the lifetime of the project (**case 2** ~ 50 times higher, as it operates 50 times longer than **case 1**).

In **case 1**, similarly to the annual removal in Figure 4.2, we observe in Figure 4.3 a decreasing carbon stock after 20 years. In the pessimistic trajectory – where most of the carbon leaks 200 – 400 years after it gets fixed within the char – the total carbon stock becomes negative after 200 years, *i.e.*, even before all the carbon sequestered has leaked, due to supply chain emissions occurring in the first 20 years. In the medium trajectory, the carbon stock becomes negative after 1,000 years. A negative carbon stock removal means that the biochar project is overall a carbon emitter and, hence, should not be considered in the first place, unless there are good reasons to think that the value brought by temporary removals compensates for future neutral or negative outcomes.

In **case 2**, the difference lies in the fact that every year, even after 20 years, more carbon is sequestered during the pyrolysis plant operation, along with emissions from biochar leakage and the biochar supply chain, resulting in a wider range of outputs. In the trajectory where CO_2 in biochar leaks within 200 – 400 years after it gets captured (pessimistic scenario), the carbon negativity of the project is pushed back until 800 years (versus 200 years in **case 1**), showing the beneficial effect of operating a predictably leaky CDR (biochar here) for long periods, rather than for a short period. In the trajectory where most of the CO_2 in biochar leaks within 1,000 years (medium scenario), we observe an increasing carbon stock that resembles a parabola, reaching an asymptote between 800 – 1,000 years, that coincides with the biochar leakage timeline of that scenario. In this case, a predictably leaky CDR shows similarities with an everlasting, non-flammable (*i.e.*, non-leaky) forest that captures carbon during its growth, but that reaches a maximum carbon stock capacity, limited by physical bound (available area and tree density for forests). Yet, a natural/sustainable forest requires no, or very little human activity to maintain its carbon stock, once it has reached its maximum capacity (*i.e.*, referred to as the asymptote in mathematical terms) when biochar projects need to keep operating at full capacity. This concept can be illustrated by someone filling a leaky bucket continuously so that the quantity of water in the bucket remains the same. Such a concept is illustrated in Figure 4.4. Finally, in the optimistic scenario, the carbon stock increase starts the slow down after 1,000 years, but it has not reached the asymptote, yet.

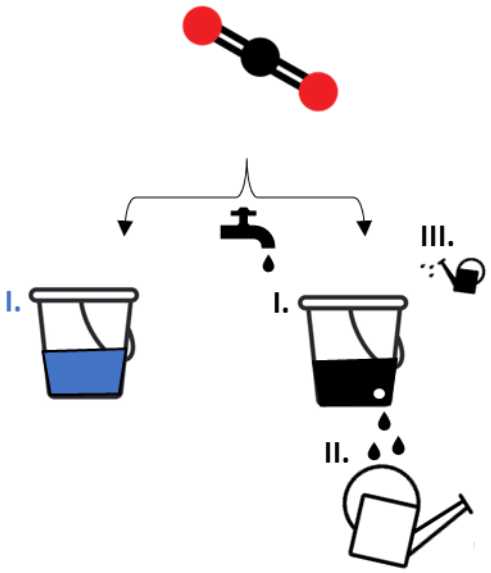


Figure 4.4: Graphical representation of permanent (blue numbering) versus temporary removal (black numbering)

Such observations warn us towards the deployment of a predictably leaky CDR project, as they might lock us into a future we don't want. Using the example of biochar as a proxy for predictably leaky CDR, with three different leaking scenarios, we conclude that one should not deploy such solutions for short periods, as they would result in carbon emissions, which is worse than doing nothing in the first place. Instead, we should deploy them *forever,* or for long periods, being careful with their leakage rate, as a pessimistic leakage (200 –400 years, here) would also result in a negative outcome, that has just been pushed back in time.

However, this study only considers the total balance of carbon, disregarding the potential value brought by temporary storage, which must be investigated.

This study case has attracted interest towards the integration of permanence considerations into the above-described CDR-power model. In the next section, a novel approach will be presented that values temporary carbon removals, using a carbon pool approach.

4.2 Climate Repair Value (CRV)

In calculating the CRV of a given CDR pathway, we start from the premise of "removed damage", *i.e.,* given that the main purpose of CDR is to compensate for net-positive emissions to the atmosphere, the question then becomes "what fraction of the environmental damage that would have otherwise occurred can be effectively (and permanently) removed via a given CDR pathway?"

In addressing this question, we compare the behaviour of the initial CO_2 emission and then consider how that would be modified by an equivalent CDR of arbitrary durability.

Presented in Eq. 67 below, and alternatively known as Green's function, or the impulse response function (IRF), the $IRF_{CO_2}(t)$ describes the fraction of CO_2 emissions remaining in the atmosphere at time *t*.

$$IRF_{CO_2}(t) = A_0\left(\sum_{j=1}^{3} B_j\, e^{-\frac{t}{\gamma_j}}\right) + \sum_{i=1}^{3} A_i\, e^{-\frac{t}{\tau_i}} \qquad \text{Eq. 67}$$

The IRF approximates the reabsorption of emitted CO_2 into the earth system's major carbon reservoirs via the combination of two exponential decay terms. The parameters A_i and $B_j \in [0, 1]$ represent the relative importance of a given reservoir, they are determined such that they sum up to 1. Exponential decays are characterised by τ and γ, the mean lifetime (sometimes called the half-life) of carbon related to a given reservoir's capacity. Here the first term represents the reabsorption of CO_2 into the slow carbon cycle, *i.e.,* weathering of carbonate or silicate rocks, and the second term describes the decay of CO_2 into the fast carbon cycle, *i.e*., land and oceans [152], [155], [156]. The characteristic parameters used to describe the IRF_{CO_2} are presented in Table 4.1. This study focuses exclusively on CO_2, and has not considered other GHGs, which will have their own unique IRF. However, the generality of our method stands, and these other IRFs could be implemented in the approach presented here.

The integral of $IRF_{CO_2}(t)$ over a given time horizon is considered to quantify the damage done by CO_2 whilst it persists in the atmosphere. As can be observed in Figure 4.5, $IRF_{CO_2}(t)$ will decay relatively rapidly in the early decades, but then is followed by a millennium-scale tale. To evaluate the integral of $IRF_{CO_2}(t)$, we must truncate $IRF_{CO_2}(t)$ at a given time, TP, *i.e.,* the point in time after which the residual damage is considered to be negligible. In this contribution, we use a static horizon approach, widely used in the literature to value temporary removals[153], [157], [158], noting that they are equivalent to inaction in the long term, with their value resting on assumptions regarding tipping points, and human behaviour. Alternative approaches with an exponentially decreasing discount function as an envelope to allow evaluation of the integral with infinite TP[157], [159] have not been explored, however, we provide in the result section, an interpretation of our results in the context of this approach.

Table 4.1: Coefficients and timescales representing the earth system removals.
Coefficient adjustments for long-term removals ($\boldsymbol{B_j}$) are taken from Lyngfelt et al[152].

i,j	0	1	2	3
A_i (unitless)[155]	0.2173	0.2763	0.2824	0.224
τ_i (mean lifetime in years)[155]	-	4.3	36.54	394.4
B_j (unitless)[156]	-	0.54	0.14	0.32

γ_j (mean lifetime in years)[156]	-	5.5k	8.2k	200k

This allows us to specify the total environmental damage done by a given emission to be $D_0 = \int_0^{TP} IRF_{CO_2}(t)dt$. This approach is consistent with several previous studies[149], [152], [153], [157], [160], and is illustrated in Figure 4.5.

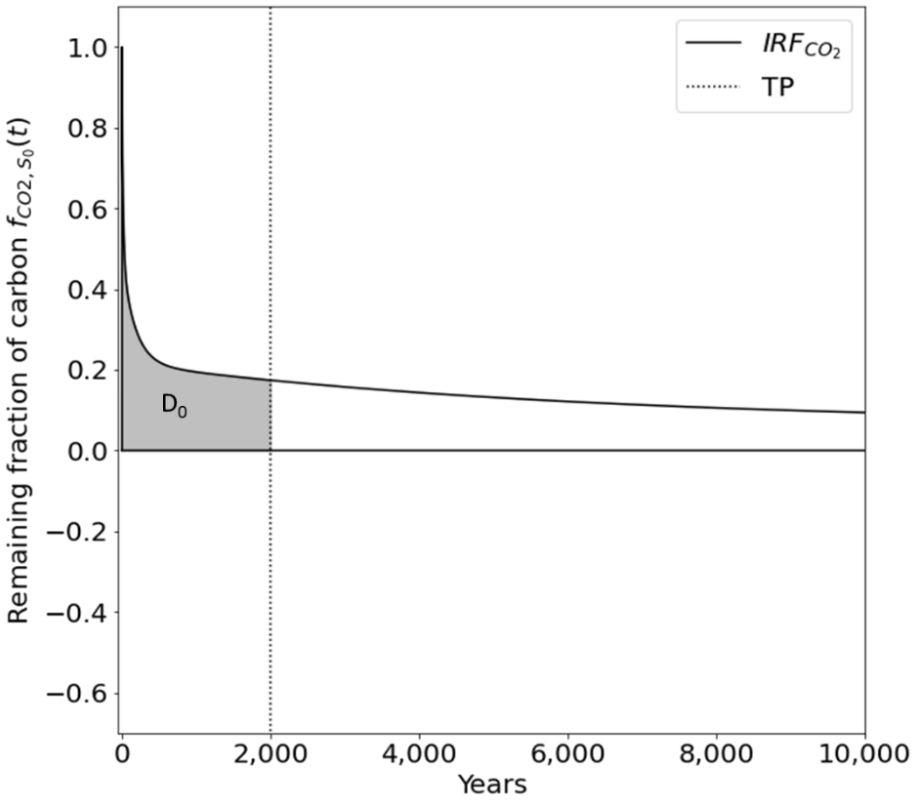


Figure 4.5: Illustration of the climate damage caused by an unmitigated emission.

As can be observed from Equation 1, this function will asymptotically approach zero, with the residual atmospheric CO_2 concentration reduced to 2% of the original pulse after 200,000 years, consistent with the observation of Archer et al[161]. In the example demonstrated here, TP is specified as 2,000 years. D_0 represents only a fraction of the total climate damage incurred by the original emission. However, in practice, there is a balance to be struck between specifying a TP that is coherent with what can be reliably predicted, and contracted for, and what is required by the earth system to effect climate repair.

The various CDR pathways can either remove or release CO_2 as a function of time[102]. For example, afforestation or enhanced weathering will take up CO_2 gradually, and biochar will release it gradually. However, given that we are interested in a time scale of millennia in this study, we model removals and emissions at the time *i* by a Dirac delta function $\pm\delta_i$,. Thus, in order to describe CDR, we define the following scenarios S_i:

1. an emission without any subsequent removal: $S_0 = \delta_0$
2. an emission immediately followed by a permanent removal: $S_1 = \delta_0 - \delta_0 = 0$

3. an emission immediately followed by a non-permanent removal, with an associated leakage t_{leak} years later: $S_2 = \delta_0 - \delta_0 + \delta_{t_{leak}} = \delta_{t_{leak}}$
4. an emission followed by a permanent removal t_{rem} years later $S_3 = \delta_0 - \delta_{\mathrm{t_{rem}}}$
5. an emission followed by a non-permanent removal t_{rem} years later, and a subsequent leakage at year t_{leak} $S_4 = \delta_0 - \delta_{\mathrm{t_{rem}}} + \delta_{\mathrm{t_{leak}}}$

Then, the remaining fraction of CO_2 in the atmosphere at time *t* for a given scenario $f_{CO_2,S_i}(t)$, is calculated by convoluting scenario S_i with $IRF_{CO_2}(t)$:

$$f_{CO_2,S_i}(t) = S_i * IRF_{CO_2}(t). \quad \text{Eq. 68}$$

Note that a convolution between any function and a delta function δ_i is equal to the same function shifted by a delay *i*. If this function is defined in the shifted domain, we can compute the CO_2 remaining in the atmosphere for different scenarios.

$$f_{CO_2,S_0}(t) = \delta_0 * IRF_{CO_2}(t) = IRF_{CO_2}(t), \quad \text{Eq. 69}$$
$$f_{CO_2,S_1}(t) = 0, \quad \text{Eq. 70}$$
$$f_{CO_2,S_2,t_{leak}}(t) = \delta_{t_{leak}} * IRF_{CO_2}(t) = IRF_{CO_2}(t - t_{leak}), \quad \text{Eq. 71}$$
$$f_{CO_2,S_3}(t) = IRF_{CO_2}(t) - IRF_{CO_2}(t - t_{rem}), \quad \text{Eq. 72}$$
$$f_{CO_2,S_4}(t) = IRF_{CO_2}(t) - IRF_{CO_2}(t - t_{rem}) + IRF_{CO_2}(t - t_{leak}). \quad \text{Eq. 73}$$

In scenario S_0, the remaining fraction of carbon in the atmosphere is equal to the IRF_{CO_2}, and the damage caused is illustrated in Figure 4.5 by area D_0. The different levels of damage caused by other scenarios, illustrated by shaded areas in Figure 4.6, demonstrate the distinct climate repair value, and in particular, the impact arising from temporary (S_2 and S_4), and permanent removals (S_1 and S_3).

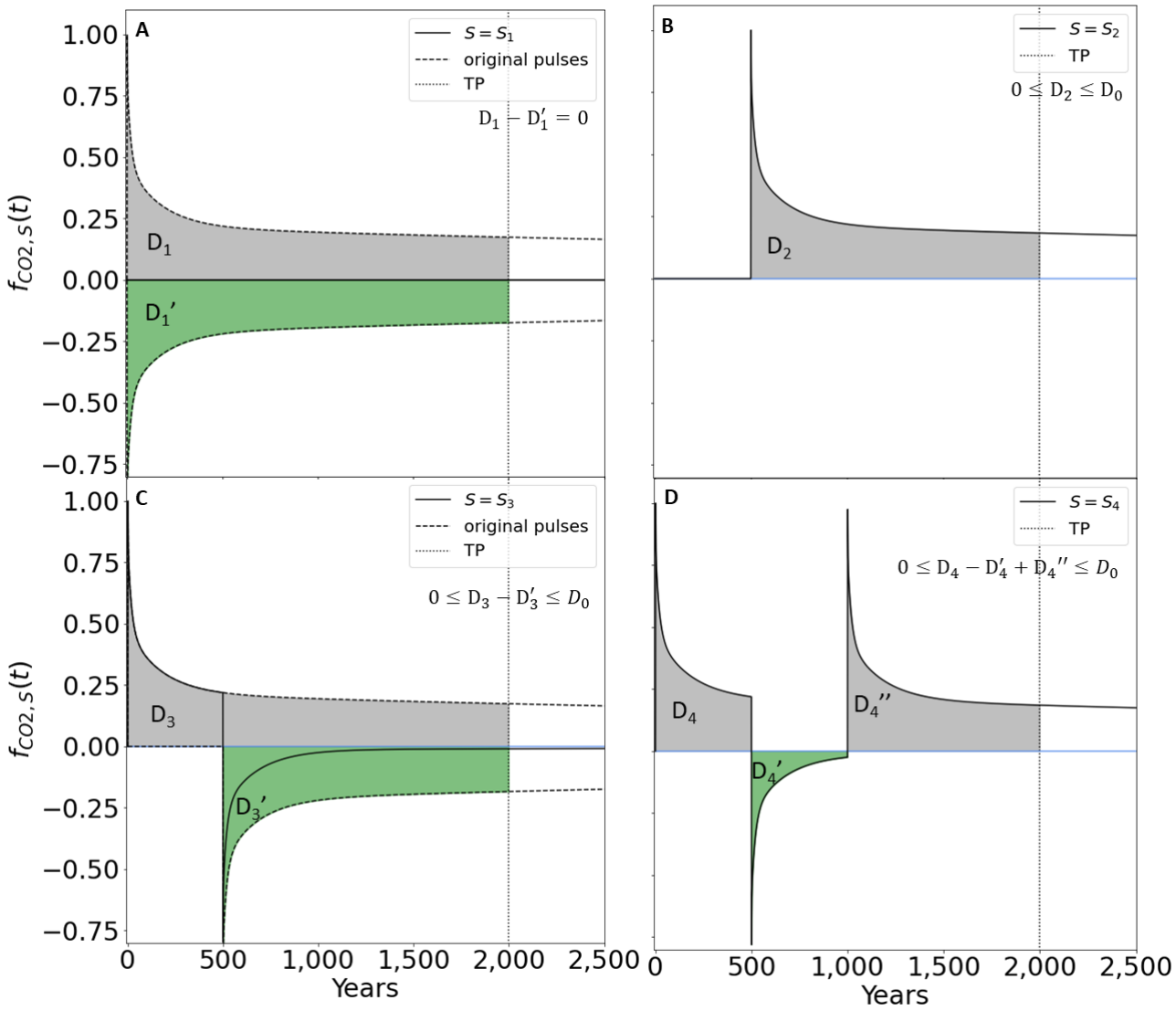


Figure 4.6: Carbon remaining in the atmosphere, under a variety of temporary or permanent removal scenarios.

As can be observed, aside from S_1, the total climate damage is non-zero for all scenarios.

(A) S_1, an emission immediately followed by a permanent removal

(B) S_2, an emission immediately followed by a removal, leaking 500 years later

(C) S_3, an emission followed 500 years later by a permanent removal

(D) S_4, an emission followed 500 years later by a removal that lasts 500 years, before it leaks

As can be observed from Figure 4.6, the optimal form of CDR is one where both emission and permanent removal occur concurrently, *i.e.,* S_1, and thus the climate damage of the emission is negated by the removal.

In S_2, the emission is non-permanently removed, and thus the climate damage is simply "moved forward in time", with $D_2 = D_0$ over the very long term. Hence, the value of a contemporaneous non-permanent removal is a highly uncertain function of what choices humanity makes in terms of broader emission mitigation. If S_2 results in the re-emission of CO_2 after peak warming, there will be some positive value associated with this strategy. If, however, the re-emission occurs at or before the point of peak warming then the non-

permanent removal may cause more harm than had the original emission not been "removed" in the first place.

In S_3, a historic emission, E_H, is subsequently compensated for by a permanent removal. In this context, the damage done is substantially repaired. However, to entirely compensate for the damage done by the original emission, it will be necessary to remove somewhat more than the original quantity, *i.e.*, $E_H\left(\frac{D_0}{D_3{}'}\right)$, though in most practical circumstances $\left(\frac{D_0}{D_3{}'}\right) \cong 1$ as $D_0 \cong D_3{}'$.

Finally, in S_4, where a historic emission is compensated for by a non-permanent removal, one introduces the jeopardy associated with S_2 and does not repair the original damage done.

In general, S_1 and S_2 represent the majority of the activity in the context of contemporary efforts on carbon removal. For this reason, we focus on S_2 for the balance of this study, noting that $S_2 = S_1$ where $t_{leak} > TP$.

Thus, the Climate Repair Value ($CRV_{t_{leak},TP}$) of a temporary removal leaking at t_{leak} years, with an assumed time of permanence *TP* is defined as the quotient of damage caused by S_2 and that caused by an emission alone (S_0), both defined by integrals between 0 and *TP*:

$$CRV_{t_{leak},TP} = 1 - \int_0^{TP} f_{CO_2,S_2,t_{leak}}(t)dt \,/\, \int_0^{TP} f_{CO_2,S_0}(t)dt. \qquad \text{Eq. 74}$$

The result of evaluating CRV for S_2 using multiple t_{leak} and *TP* values are illustrated in Table 4.2.

Table 4.2: Results for Climate Repair Values (CRV).
An evaluation of $CRV_{t_{leak},TP}$ values for S_2 with a leakage date t_{leak} and time of permanence *TP*. As can be observed, if 1,000 years is taken as TP and a given sink lasts for 200 years, this is equivalent to a CRV of 0.15, *i.e.*, only 15% of the damage has been removed.

TP (years) ---------- Leakage year t_{leak}[a]	10	50	100	200	500	1,000	2,000	5,000	10,000
0	0	0	0	0	0	0	0	0	0
10	1	0.14	0.06	0.03	0.012	0.007	0.003	0.001	0.0005
50	1	1	0.4	0.18	0.07	0.037	0.02	0.007	0.003
100	1	1	1	0.4	0.14	0.075	0.04	0.015	0.006
200	1	1	1	1	0.3	0.15	0.08	0.03	0.013
500	1	1	1	1	1	0.4	0.2	0.075	0.03
1,000	1	1	1	1	1	1	0.41	0.15	0.07
2,000	1	1	1	1	1	1	1	0.32	0.14
5,000	1	1	1	1	1	1	1	1	0.38
10,000	1	1	1	1	1	1	1	1	1

[a]This method provides results that are in good agreement with those obtained via Lashof's method[153].

As can be observed from Table 4.2, whilst non-permanent removals do have a non-zero value, the total value is modest. For example, if TP is required to be 1,000 years, then removing the CO_2 for 200 years will compensate for only 15% of the damage. After 500 years, this increases to 40%. The CRV of non-permanent removals may also be observed to decrease with an increasing time horizon. The characteristics of the CRV can thus be conveyed in four rules:

1- $CRV_{i,TP}$ is increasing and strictly monotonic for all *TP*, *i.e.*, the effectiveness of a temporary removal increases with an increasing date of leakage *i*.
2- $CRV_{i=0,TP} = 0$ for all *TP*.
3- $CRV_{i \geq TP,TP} = 1$ for all *TP*.
4- $CRV_{i,TP} < \frac{i}{TP}$, for $i \in [0, TP]$.

The first three rules indicate that the value of temporary removal $CRV_{i,TP}$ is increasing between 0 and 1 for increasing *i*, for every value of *TP*. The fourth rule claims it remains lower than the linear line between 0 and *TP*, *e.g.*, meaning that for a carbon removal leaking at half the time of permanence TP, the CRV assigned will be less than 50%. For example, $CRV_{500,1000} = 0.4 < 0.5$.

The climate repair values for other scenarios have also been evaluated, providing insight into the utility of permanently removing an emission t_{rem} years after its initial pulse (S_3), and temporarily removing an emission t_{rem} years after its initial pulse until it leaks at t_{leak} (S_4). We find an equivalence between delaying a permanent removal from X years and shortening an immediate temporary removal by X years. Further, we find that temporarily removing an emission in the future is always less valuable relative to immediate temporary removal and that delaying this removal further will only decrease CRV values. These results are presented in detail in Figure A 7 and Figure A 8.

4.3 Cost of Permanent Removal (CPR)

We next seek to relate the cost of a removal to its effectiveness in implementing climate repair. For ease of use, we follow a normal “levelised cost” approach.
We explicitly account for three separate time horizons:

1. the economic lifetime of the project, *NE*,
2. the duration for which a given project will operate, NP, and,
3. the duration for which monitoring, reporting, and verification (MRV) efforts must continue for a given carbon sink, until the sink can be closed, and the project completed, TC.

For example, in the case of a BECCS or DACCS project in the USA, this project can claim 45Q for 12 years under current legislation, but it might reasonably expect to operate for 20 – 30 years, and the MRV operations of the geological store may be expected to continue for several years beyond the date at which active injection ceases.

Note that TC *could* be equivalent to the aforementioned TP, or a lesser period, equivalent to the duration for which the carbon sink must be monitored until it can be demonstrated to be behaving predictably. This equivalence will vary for different CDR pathways.

The Cost of Permanent Removal (*CPR*) is therefore a function of the time of permanence *TP,* the economic lifetime, *NE*, and the physical lifetime, *NP*, of the CDR project.
It is necessary to distinguish each time as CO_2 leakage may occur after the normal economic lifetime of the project, and it is assumed that there will be some liability for these future emissions:

$$CPR_{TP,NP,NE,TC} = \frac{TC_{TC,NP,NE}}{\widehat{CB}_{TP,NP}} = \frac{I\frac{(1+i)^{NE}}{(1+i)^{NE}-1} + \sum_{t=1}^{NP}\frac{OM_t - Rev_t}{(1+r)^t} + \sum_{t=1}^{TC}\frac{MRV_t}{(1+r)^t}}{\sum_{t=1}^{NP} CS_t - \sum_{t=1}^{TP} CE_t + CL_t * \left(1 - CRV_{t,TP}\right)} \quad \text{Eq. 75}$$

Thus, the cost of permanent removal is the ratio of the total cost TC over the total carbon balance $\widehat{CB}$. Total cost TC includes the investment cost I, and revenues Rev from secondary products, such as electricity in the case of power BECCS, or timber products in the case of managed forest carbon sinks. Whilst O&M costs are anticipated to last for the physical lifetime of the project, allowance is made for the possibility that MRV operations may continue for a distinct, possibly longer, period.

The weighted average cost of capital, *i*, is used to calculate the annualised cost for the CDR facility, and a discount rate, *r,* is used to express a time preference for money.
Total carbon balance $\widehat{CB}$ includes the carbon stored CS during the physical lifetime of the CDR project. Carbon emissions from the supply chain at year *t,* CE_t, are considered during the physical lifetime *NP* (*e.g.*, fuel, transport emissions) and the time of permanence *TP* (e.g., emissions from MRV operations). Carbon leaked at year *t*, CL_t, is included in the carbon balance, and is multiplied by the climate repair value $1 - CRV_{t,TP} \in [0,1]$ measuring the removed damage associated with a temporary removal. In this formulation, we recognise that we have elected not to assign a discount factor to future emissions. This is a deliberate choice, with which others may disagree, and we note that the formulation is readily modified to account for this.

4.4 Permanence assessment of CDR

Using CDR leakage models as defined above, we apply our framework to the following CDR pathways: afforestation, BECCS, DACCS, enhanced weathering, and biochar.
In principle, no CDR pathway can be claimed to be 100% free of risk of reversal. Geological stores can leak, biochar will decay, and forests are exposed to a range of risks including fire, pests, and disease. These multiple leakage curves associated with each CDR pathway, as defined in CDR-specific subsections (Chapter 2), are presented in Figure 4.7.

For forests, we follow the approach of Hurteau et al.[102], [162] to quantify the probability of a wildfire event occurring during a given period, and to estimate the potential loss of carbon in the forest sink. Assigning a probability of reversal associated with the incidence of pest or disease is left for future work.

Once biochar has been applied to soils, the carbon is gradually released into the atmosphere following a decay rate, determined by a sum of two exponential decays, described by the pyrolysis temperature, the moisture content, and the composition of the biomass used.

BECCS and DACCS both rely upon geological storage and are subject to the same level of leakage risk. Here, we adopt the approach proposed by Alcalde et al.[68] by a linear leakage rate estimating the probability of carbon leak out of a well-regulated reservoir. Biochar is assumed to leak in a manner described by its decay, and afforestation is assumed to be subject to sudden catastrophic reversal, *i.e.*, a forest fire.

For each CDR pathway, the assumed *real* leakage is the cumulative sum of annual leakages $L_{real}(t) = \sum_{t_{leak}=1}^{t} CL_{t_{leak}}$, defined by each leakage curve.

On this basis, the CRV metric can be used to assess the true impact of atmospheric carbon, incorporating the short and long-term non-linear cycles of the earth system's major carbon reservoirs.

To do so, we mitigate each *real* leakage curve by assigning a value between 0 and 1 t_{CO2} for each t_{CO2} that is temporarily stored. This is particularly important for, *e.g.*, the case of biochar, where leakage occurs relatively slowly over time, as opposed to as a direct pulse. The resulting *modified* leakage curve is the cumulative sum of weighted annual leakages as expressed in the denominator of Eq. 75: $L_{TP}(t) = \sum_{t_{leak}=1}^{t} CL_{t_{leak}} * (1 - CRV_{t_{leak},TP})$.

These curves are shown in Figure 4.7 [37] for different *TP* values. Here, the solid lines represent the physical rate leakage predicted for each CDR pathway, *i.e.*, the leakage that we assume will occur, for *real*.

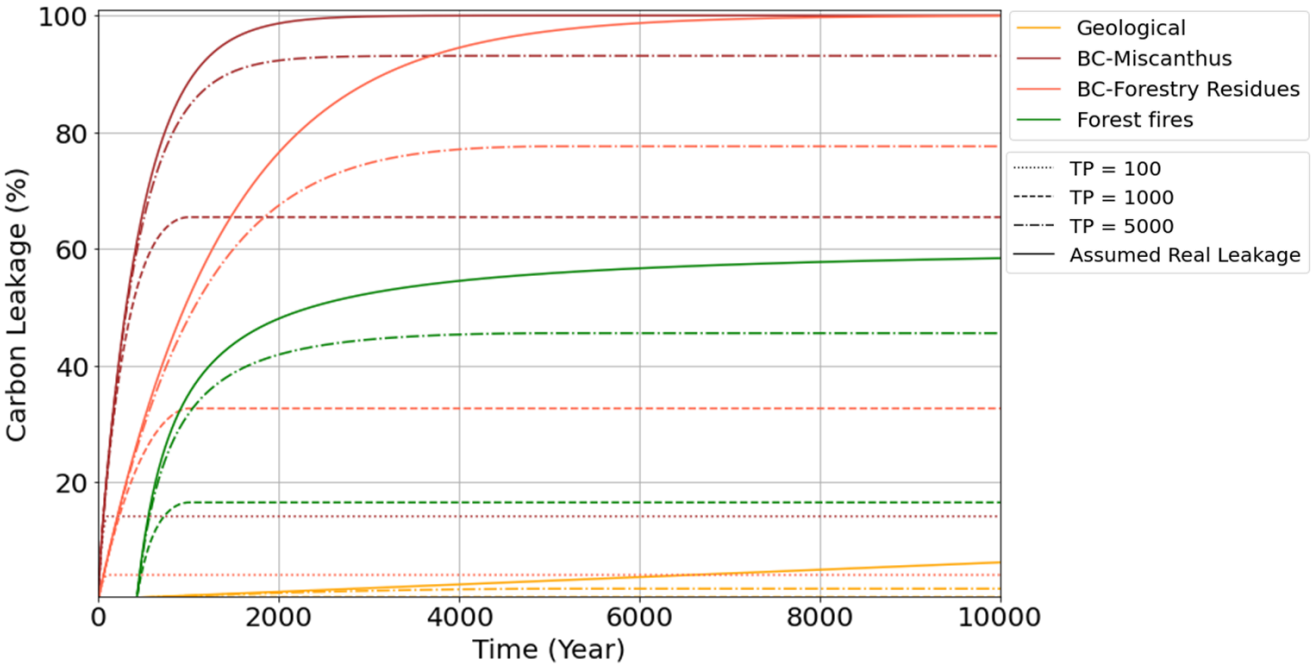


Figure 4.7: CO_2 leakage curves for diverse types of sequestration and times of permanence TP.

The dashed lines demonstrate how the impact of this leakage is attenuated by the CRV of temporary storage, *via* the climate repair values. As can be observed, the level of attenuation is a function of *TP*. Importantly, for large *TP* values, such that $CRV_{j,TP}, = 0$ for all *j*, *i.e.*, with no reward associated with temporary storage, the resulting leakage will equate to the *real* leakage: $L_{TP},(t) = L_{real}(t)$. Conversely, if TP = 0, *i.e.,* the most short-sighted horizon for permanence, corresponding $CRV_{j,0} = 1$, for all *j*, hence valuing with maximum value temporary storage regardless of its duration, and suggesting no leakages are considered: $L_0(t) = 0$ for all t. Thus, as can be observed, both the choice of TP and the description of store reversal have a significant impact on the CRV of a given CDR pathway.

Finally, Figure 4.8 shows the cost of permanent removal (CPR) with respect to *TP* values for different CDR solutions, following equation (1), with no discount rate. We assume that CDR projects stop operating when reaching the end of their physical lifetime *NP*, *i.e.*, they no longer capture CO_2. However, the CO_2 already captured remains sequestered provided it does not leak. After *NP* years, there are no additional costs except for fixed MRV operation costs. Owing to a lack of data, MRV operations are assumed to cost 5% of the total investment for all CDR solutions, although we acknowledge that MRVs might have different costs depending on the CDR pathway. We chose not to display costs below 100 years of permanence times, as they do not provide meaningful information, and because we assume that 100 years of permanence must be a minimum requirement, for every CDR, to be defined as a CDR.

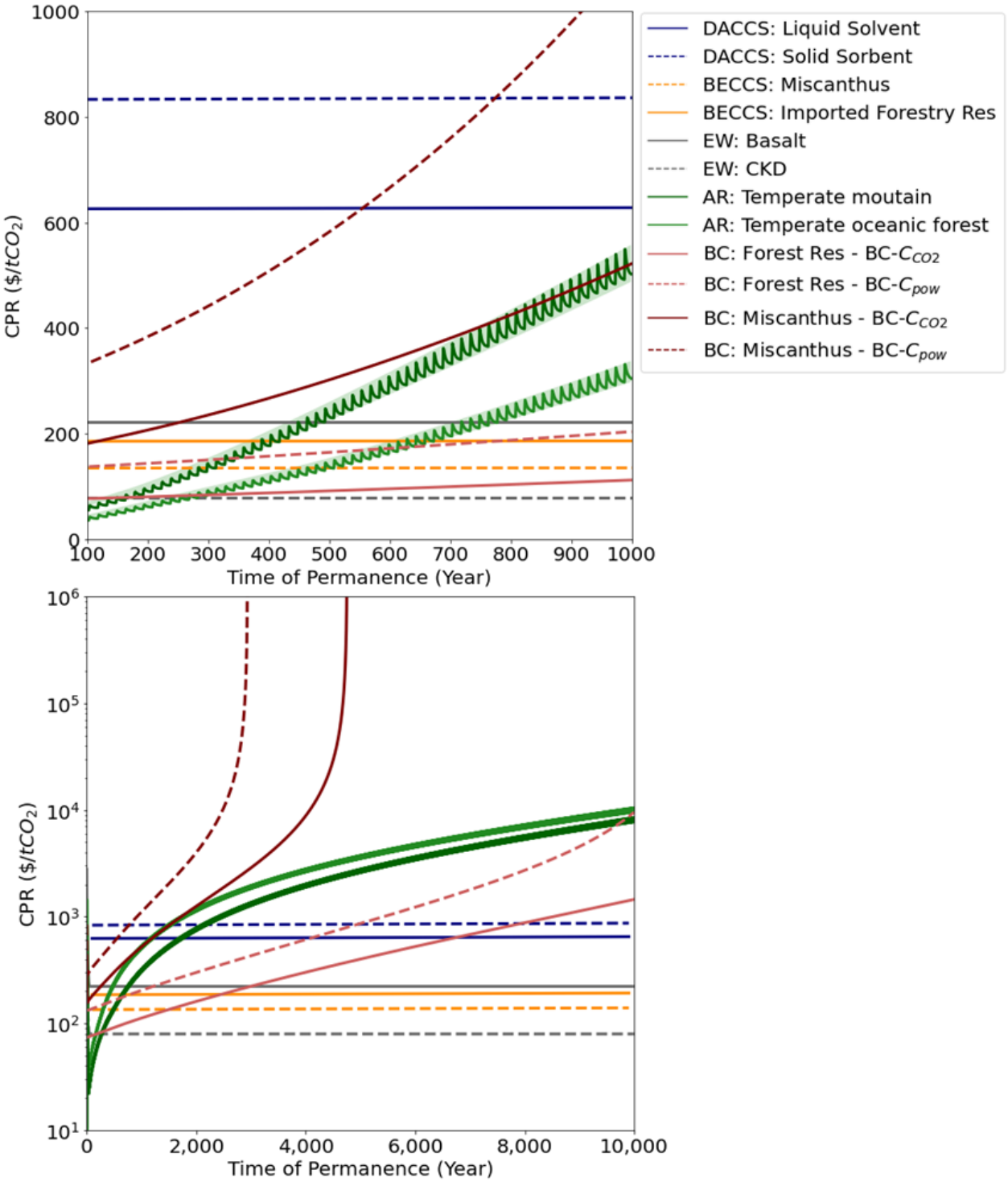


Figure 4.8: Cost of permanent removal for a range of CDR pathways as a function of TP. Subplot A illustrates the CPR of CDR pathways with between 0 and 1,000 years of permanence with an emphasis between 0 and 100 years. Crosses represent the end of the lifetime of different CDR projects. Except for AR, we assume an economic lifetime of 30 years for each CDR solution[22], [163], [164]. Subplot B presents the CPR of CDR solutions between 0 and 10,000 years of permanence. As can be observed, over the long term, almost any form of permanent removal will emerge as being economically preferable to a short-term solution.

As can be readily observed from Figure 4.8, the merit order of carbon removal technologies is a strong function in the definition of permanent removal.

< than 1,000 years TP

If the definition of permanent removal is held to be less than 200 years, AR is the cost-optimal choice at \$50-100/t_{CO2} – a comparable value to what is typically reported in the literature[52] and marketplace[10], [165] (See also Figure A 9). Although the cost of AR is initially low, it rapidly becomes uncompetitive compared to BECCS where a durability of greater than 300 years is required, and to DACCS for *TP*s greater than 750 years.

This increasing cost trend is due to a combination of sink saturation – once established, the CDR rate of a given forest will approach a maximum, and then plateau. Conversely, the risk of store reversal *via*, *e.g.*, forest fire, pests, and disease, tends to increase with time, as does the political risk associated with governance. Moreover, ongoing forest management costs persist, and over time tend to increase the costs of afforestation-based carbon removal.

Similarly, biochar with forestry residues has a low cost for low permanence times, with a low-cost increase in the first 1,000 years, as the pyrolysis conditions assumed in this study (high temperature and low H/C_{org} ratio) result in low leakage in that period. Using a different biomass type (miscanthus here) can greatly affect the CPR, as the initial cost of removal is higher, and the leakage is faster, due to biomass composition. Indeed, the cost of permanent removal associated with biochar with miscanthus is multiplied by about 3 for a TP of 1,000 years, reaching a removal cost comparable with what is assumed here for DACCS for both configurations (C_{pow} & C_{CO2}), becoming the costliest CDR solution where store durability of greater than 1,000 years is required.

> than 1,000 years TP

In Figure 4.8b, we also observe the cost of permanence over longer timescales. The CPR of some biochar configurations and afforestation exponentially increase with time, reaching more than 10,000 \$/t_{CO2} in the very long term.

These high costs associated with biochar and afforestation are a result of the combination of a high probability of store reversal – forest fires occur with more than 50% probability after 100 years, and after 1,000 years, some biochar configurations decay almost entirely. Set against this, the cost of permanent removal associated with BECCS, DACCS, and enhanced weathering is observed to be constant, regardless of the required horizon for removal. Interestingly, biochar using miscanthus and forestry residues behave very differently, as their decays do. Biochar with forestry residues only reach costs comparable to DACCS' for permanence assumptions of 5,000 and 8,000 years, for a carbon yield of 21% (C_{pow}) and 36% (C_{CO2}), respectively.

All of this speaks to the importance of monitoring, reporting, and verification (MRV) of CO_2 sinks to guard against store reversal[166], even though we only use a common estimate for MRV cost across CDR solutions. Future CDR carbon accounting projects may well show

differences in MRV costs across CDR solutions, favouring a certain storage type, but this is out of the scope of this study.

By not considering any carbon removal discount over time, these results overlook the potential short-term benefits of deploying BC, or AF, which could buy us time to deploy more durable CDR and other climate change mitigation solutions. However, this incentivises a delay in permanently addressing climate change. Finally, a discounted approach with infinite TP for CRV calculations would also result in temporary removals being less advantageous than permanent's but would reduce the exponential gap and depend on assumptions like discount rates.

Findings

CDR at scale is recognised as an indispensable complement to mitigation in meeting climate change goals. At the time of writing, many pathways for CDR are being explored. Broadly speaking, these can be decomposed into permanent and non-permanent removal pathways. It is understood that CO_2 emissions cause harm owing to both the global warming potential associated with CO_2 and also the longevity of CO_2 in the atmosphere; once emitted it persists for many tens of millennia. In this context, it is manifest that short-lived removals with durations of either decades or centuries are not fungible with an emission.

Similarly, mechanisms for the commercial deployment of CDR are being actively explored in both voluntary– and compliance-based paradigms. One key challenge for the inclusion of all CDR pathways has, hitherto, been the lack of an approach for their quantitative comparison. Thus, in this contribution, we present a generally applicable framework to address this lacuna. From a climate repair standpoint, the contemporaneous and permanent removal of CO_2 is consistently observed to be the best way to fully compensate for emissions that are too costly to directly abate.

We have considered three other possible scenarios, *id est*, where emissions are contemporaneously and temporarily removed, where they are permanently removed after a delay, and where they are temporarily removed after a delay.

Where temporary removals are relied upon, we risk doing more harm than good, with the climate repair value of temporary removals a strong function of the collective decisions of society in the future. Importantly, whilst temporary removals may appear to be more cost-effective in the short term, over the long term, and accounting for the probability of reversal and ongoing MRV costs, almost all forms of permanent removal will emerge as economically preferable. Given this logic, permanent solutions must be favoured compared to predictably leaky, or unpredictably leaky CDR sinks. In the case of biochar, scrutiny is needed to ensure that pyrolysis conditions and biomass choices are made to maximise the permanence of sequestration.

Finally, we recognise that many elements will contribute to the durability of non-permanent stores, such as forests and biochar. We further recognise that there are many lenses through which the various CDR pathways may be viewed and compared. Similarly, political risk is

particularly important and can be expected to vary substantially over time and with the location. This is difficult to quantify, however.

Chapter 5

5 CDR-power sector interaction, permanence, and final thoughts

In this final section, we first run a sensitivity analysis providing insight into various assumptions of permanence horizons. This will provide an answer to the question of the optimal CDR portfolio, and the least cost power mix transition if we consider the CRV-adjusted price of CDR solutions based on the permanence framework described in Chapter 4.

Then, we will explore a series of more practical scenarios, considering multiple time availabilities for CO_2 transport and storage infrastructures, given the uncertainty lying around the timing of such infrastructures. This provides the less costly CDR & power portfolio for a spectrum of possible futures.

Finally, we will discuss how these new insights counterbalance with previous conclusions, *i.e.*, the important role of biomass in the power transition, the unchanged role of nuclear, the rise of renewables and the use of gas through unabated and abated CCGT.

5.1 Permanence perspectives on the integration of CDR in the power sector

In the following figure (Figure 5.1), we illustrate the evolution in the CDR mix, considering different assumptions on permanence horizons (in years), and the associated effect on the power sector, in terms of power generation, and system costs.

We obtained these results *via* multiple optimisations of the E-M framework, by updating CDR cost assumptions, based on the Cost of Permanent Removal (CPR) methodology [37]. We use similar assumptions for the *All-low-bio* scenario, except for the permanence horizon that was fixed to 100 years in the *All-low-bio* scenario.

First, when considering permanence horizons of hundreds to thousands of years, results are similar to the All-low-bio scenario described in section 3.3.4, but not the same. In this section, a different assumption is made for the EW application rate which has been increased to 50 t_{rock} per ha per year [106], as opposed to 30, which is still in the range of 10-50 t_{rock} per ha per year found in the literature[108], [113], [116]. Thus, the potential of EW is increased (from 10 to 23 Mt_{CO2}/yr), partially displacing the removals from DACCS. The rationale behind this novel assumption is to have a more optimistic vision of what EW deployment could be, in the context of studying the importance of parameters such as permanence and CO_2 transport and

storage infrastructure availabilities. Even though absolute values are changed, this does not affect the conclusions of this study.

Biochar and afforestation are cost-effective solutions. They are deployed up to 25 and 14 Mt_{CO2}/yr by 2050, respectively. BC is only deployed *via* miscanthus pathways, its cheapest option. BECCS removes 18 Mt_{CO2}/yr in 2050 using crop residues, forest residues and imported pellets, DACCS liquid solvent pumps 11 Mt_{CO2}/yr and EW 23 Mt_{CO2}/yr. This results in 3.5 GW of BECCS installed capacity and 24 TWh of power generated in the power mix. The power generated in 2050 by nuclear, CCGT-CCS, and renewables amounts to 67, 45, and 250 TWh, respectively, alike baseline scenarios for 2050 projections.

For assumed permanence horizons higher than 400 years, removals from biochar *via* miscanthus and certain afforestation pathways become more expensive than geological storage solutions. Thus, we observe a reduction from 25 to 4.5 Mt_{CO2}/yr of biochar removals, and from 14 to 7 Mt_{CO2}/yr for AF. BECCS and DACCS' installed capacity and operations double, compensating for these reductions.

After 2,500 years of permanence assumed, all afforestation removals and the majority of BC removals become more expansive than their geological storage alternatives. Thus, AF is not deployed at all, and BC is reduced to 0.8 Mt_{CO2}/yr. This reduction in removals is substituted by a 25% increase in DACCS removals, reaching 29 Mt_{CO2}/yr.

Biochar pathways with forestry residues are shown to stock carbon in the char for permanent timescales (Figure 4.8) and thus remain in the CDR portfolio even when longer permanence times are assumed. This shows the possibility of combining biochar pathways and high permanence requirements if specific pyrolysis conditions and biomass choices are considered, *i.e.*, slow-pyrolysis, high pyrolysis temperature, low H/C_{org} ratio, and forestry biomass feedstocks.

Moreover, the power system shows very little variation except for the reduction in BC, the sharp rise of BECCS share after 400 years of assumed TP, and the two-step increase of DACCS demand – at first at 400 years, then at 2,500 years. Although the first DACCS demand

increase (at 400 years) seems to be powered largely by BECCS, the second is fuelled by a 5% increase in solar generation (+ 5%).

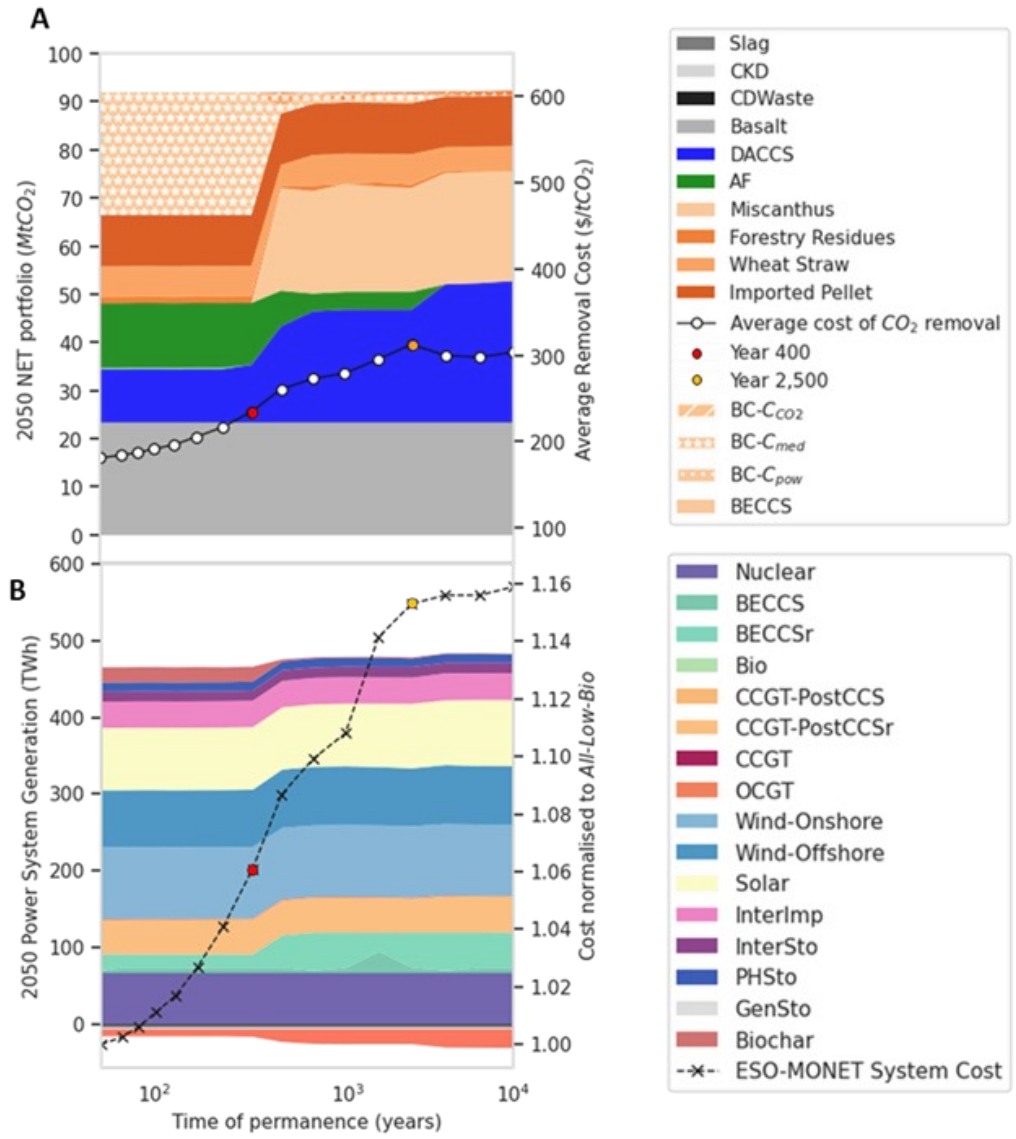


Figure 5.1: Evolution of the 2050 CDR portfolio and power generation mix with different times of permanence
(A) 2050 CDR portfolio evolution and average removal cost
(B) 2050 power generation mix and total ESO-MONET system cost

As we adjust CDR costs with the climate repair value metric removal costs jump from $200 per t_{CO2} to $350 per t_{CO2}, and total E-M system cost increases by 16%.

Finally, although we find that the CDR mix is much impacted by different permanence horizons *via* the CPR metric, non-CDR power-generating technologies are not much affected in the power mix. Only small changes in power generation are observed for high permanence horizons (>1,000 years), the greater being a 5% increase in solar generation.

5.2 CO_2 transport and storage availability

In the following figure (Figure 5.2), we illustrate the evolution in the CDR mix considering different CO_2 transport and storage availabilities (from 2025 to 2055), and the associated effect on the power sector, in terms of power generation, and system costs.

We obtained these results by consecutively optimising the E-M framework, with different CCS availabilities timelines, including its use for CDR (BECCS, DACCS) and abatement purposes in the power sector (Gas-CCS). In this study, we assume a default permanence horizon of 100 years.

It appears that different CCS availabilities significantly affect both the CDR and power sectors. We first remark that AF and EW remain stable across all CCS availability dates. By definition, they are not affected by T&S infrastructures. AF offers a cheap, long-term– if permanence is assumed to be 100 years – and sustainable removal, however, is limited by the national forest plantation rate (Table 2.3). Similarly, EW is permanent and does not need much space to get deployed, except croplands area used to spread the crushed rocks. If we assume a spreading rate of 50 t_{rock} per ha per year [106] on the equivalent of 40% of UK croplands (*i.e.*, 2.5 Mha), EW is limited to 19 Mt_{CO2}/yr of removal.

The CDR mix remains stable if CO_2 T&S infrastructures are delayed until 2035, showing that the system barely uses them by this date. However, if they are delayed after 2035, BECCS and DACCS deployments do not follow the required deployment pace, according to our build rate constraints (Table 2.3).

In the power sector, BC plays an important role – all the more so when BECCS is less available, *i.e.* when CCS infrastructure is delayed to 2045, and later. For T&S availabilities between 2025 to 2040, BC generates 19 TWh of electricity and removes 25 Mt_{CO2}/yr – using only miscanthus. For later T&S availabilities, BC increases its generation by an additional 5 TWh and its removal capacity by 6 Mt_{CO2}/yr, *via* crop and forest residue pathways, as their BECCS alternative is not available. Note that we do not allow for BC pathways with imported pellets.

When T&S infrastructure becomes available later than 2040, we also observe a decrease in CCGT-CCS power generation in the power sector (from 45 TWh to zero), compensated with more wind-offshore (+130%) and solar (+5%). The significant renewable increase requires additional storage technologies (5 GW of battery storage (GenSto) installed) to allow more flexible use of intermittent electricity and results in a quadrupling of curtailment levels (109 vs 20 TWh, for T&S availability later than 2040, and before 2040, respectively).

Finally, we find that BECCS negative power generation is replaced by biomass without CCS, resulting in low–instead of negative–carbon power generation. The increase in total system cost is most and foremost due to the failure to reach the CDR target, which is penalised by a cost set to \$1,000 per t_{CO2} in our study. This reveals how CCS-dependent our future CDR portfolio is to meet ambitious CDR targets without surpassing bio and – geo–physical

bounds. This also highlights the urgent need for investment in developing industrial-scale CO_2 T&S infrastructure.

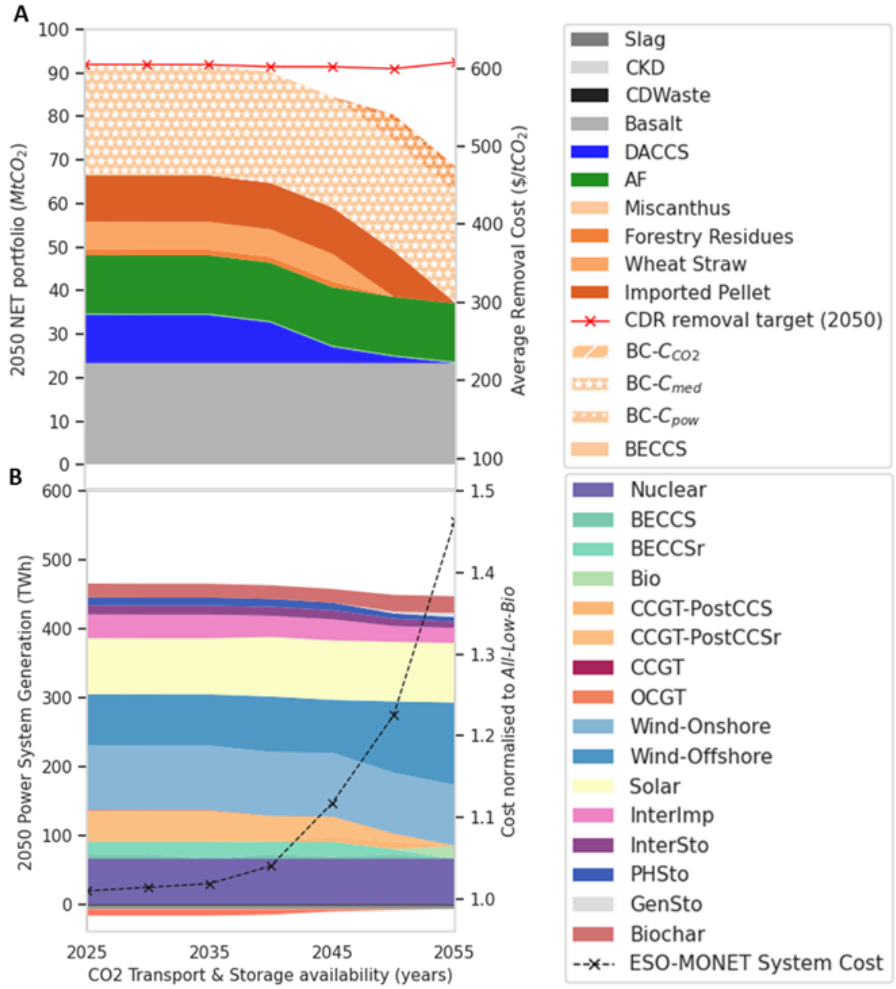


Figure 5.2: Evolution of the 2050 CDR portfolio and power generation mix with different CO_2 T&S infrastructure availabilities.
(A) 2050 CDR portfolio evolution and average removal cost
(B) 2050 power generation mix and total ESO-MONET system cost

This study has raised the question of the timing of CO_2 T&S infrastructure. Interestingly, the two subsections result in paradoxical conclusions, that need to be further discussed and incorporated into scientific and policy discussions (Table 5.1).

Table 5.1: Impact in CDR power mix depending on permanence assumptions, and T&S availabilities

CDR	Higher permanence horizons	Later T&S infrastructure availabilities
BECCS	+	-
DACCS	+	-
AF	-	+
BC	-	+
EW	+	+

Although BECCS and DACCS are favoured if higher permanence horizons are assumed, they are uncertain given the potential unavailability of T&S infrastructures. Provided that T&S infrastructures are developed in a timely fashion, and with similar roll-outs than BECCS and DACCS' needs, they are the best CDR solution.

Inversely, nature-based CDR solutions like AF and BC are very sensitive to permanence considerations, but are not dependant on CCS infrastructures, making them a good candidate for significant deployments, if 1) forests are carefully managed through long-term fire risk management for AF, and 2) appropriate pyrolysis conditions and biomass types are used for BC.

Finally, EW seems to be an important candidate as it is insensitive to both parameters. However, other challenges need to be weighed for EW: having a robust removal quantification method, rock type choice, and avoiding negative impacts such as soil and water pollution due to heavy metals. Moreover, we assumed that rock spreading is limited due to eligible land for such operations, thus limiting EW deployment to 23 Mt_{CO2}/yr. Although this is already an ambitious estimation (requiring the use of 40% of available croplands in the UK), this ignores other types of land, that may be less constraining, such as sand beaches, or grasslands.

Chapter 6

6 Conclusion

6.1 Key conclusions and contributions made

In the present dissertation, we introduce an innovative framework designed to integrate the optimization of two Mixed-Integer Linear Programming (MILP)-based problems. This integration facilitates a perspective on the prospective deployment of CDR solutions, in conjunction with investments within the power sector, with a specific focus on the United Kingdom from the current period extending to the year 2050. Such a framework has been analysed through the lenses of different permanence assumptions. For this, we present a novel built-in algorithm whose goal is to reward temporary CO_2 storage, based on the benefits they bring to the atmosphere compared with that of permanent storage, using a ton-year accounting approach. These new tools have been specifically developed to answer the following questions: (1) What is the optimal CDR portfolio deployment in the UK to meet a given CDR removal target, given the country's bio – and geo–physical bounds? (2) What are the different bio – and geo–physical bounds that are reached by the system, when meeting the target? (3) What is the anticipated CDR portfolio and power system capacity expansion and scheduled generation, when considering a national CDR target? (4) What is the impact of considering limitations on CDR deployment? For example, on biomass availability? (5) What is the impact of exploring a range of permanence assumptions?

Throughout our answers to these questions, a key message that emerges is the significance of considering the broader economic perspective in both modelling studies and policymaking. The deployment of Carbon Dioxide Removal (CDR) technologies can have implications beyond

their direct environmental impact, potentially influencing the electricity sector and, more generally, the energy landscape. In this dissertation, we delve into the question of how likely it is for Bioenergy with Carbon Capture and Storage (BECCS) or biochar to affect the current electricity mix, particularly by mitigating the challenges posed by intermittent renewables. However, it is crucial to recognize that the impacts on the electricity sector may not materialize if BECCS and biochar are not sufficiently deployed or if their deployment serves different purposes, such as BECCS for hydrogen production, or biochar for biogas generation. In such cases, other sectors will experience consequences. This research contributes to a more comprehensive discussion that emphasizes the necessity of considering inter-sectoral trends and adopting a regionally focused approach to comprehend the local implications and technological barriers involved.

Besides this global perspective, our investigation highlights indicators of potential future limitations of CDR large-scale deployment. Within this context, public perception and acceptability will play a key role but also will drive investments into infrastructures such as CO_2 transport and storage. The uncertainty around CO_2 T&S availability presents a notable challenge for modellers, yet concurrently offers a potential advantage for early investors, given the prospect of carbon markets. These markets are forecasted to experience a substantial increase in value, with projections estimating a range from $10 to $40 billion by the year 2030 (i.e., at least five-fold compared to 2021), as delineated in a report by the Boston Consulting Group. Furthermore, these solutions are likely to provide highly permanent CDR services, for thousands to tens of thousands of years. Such durability positions them as potentially preferable alternatives to more transient solutions like biochar (BC) and afforestation (AF). The latter, while beneficial for their lack of necessity for supplementary infrastructure to facilitate CO_2 transportation, may not offer the long-term carbon sequestration potential of their more permanent counterparts. Finally, we discuss the case of Enhanced Weathering (EW), facing challenges to ensure the CO_2 absorption is well monitored and that soil toxicity is well understood and circumvented. Enhanced Weathering is distinguished by its dual benefit: it not only offers a mechanism for permanent Carbon Dioxide Removal (CDR) but also obviates the need for CO2 Transportation and Storage (T&S) infrastructure.

This section provides a summary of the dissertation's findings and delves into the potential enhancements, limitations, and further research inquiries that can be explored with the joint ESO-MONET framework and the cost of permanent removal (CPR) formulation.

6.1.1 Optimal CDR portfolio in the UK (today-2050)

The CDR portfolio optimization (modelling and optimisation of Negative Emission Technologies, or MONET), led in this work is based on a cost-minimisation objective function, resulting in an algorithm that deploys the cheapest solutions satisfying system-wide constraints (technology, land, resource, environmental, and carbon constraints). In particular, the system is constrained to meet a net carbon removal target of 90 $MtCO_2$ per year by 2050, as anticipated by the Climate Change Committee in the UK (Sixth Carbon Budget, 2020 [89])

Therefore, the modelled removal costs are crucial in the determination of the CDR portfolio evolution between today and 2050. In MONET, the removal cost of each CDR is dependent

on a set of data assumptions, such as market energy costs (power, gas), and carbon footprints. Some of these parameters are exogenous to our system, such as natural gas, fuel, and biofuel prices. Others, such as power prices and carbon footprint are derived from the power sector model (Electricity System Optimisation, ESO [27], [28]) when both models are coupled. Otherwise, we assume a default electricity price of 125 $/MWh [74] and a decreasing carbon footprint going from 0.19 t_{CO2} per MWh today to 0.01 t_{CO2} per MWh in 2050 [89]. Equivalently, assumptions made on cost technological learning are crucial, as they influence the CDR costs order. In consequence, a conservative approach was adopted, assuming no technological learning would occur for any CDR solution.

Similarly, the decision on what products to value as revenues for each CDR has a significant impact on each cost balance. In this regard, we assume that BECCS and Biochar earn extra-revenues through the production of electricity, and biochar only via gas production.

In the computations derived from our modelling, we find that the most expensive solution is DACCS with solid sorbent with a removal cost of $837 per t_{CO2}, followed by DACCS with liquid solvent reaching $640 per t_{CO2} when assuming decarbonized electricity. EW *via* basalt reaches a cost of ~$250 per t_{CO2}, making it the third most expensive CDR whereas basalt fines ($150 per t_{CO2}), and CKD and slag (~$100 per t_{CO2}) pathways are much cheaper.

BECCS removal with imported biomass is identified as the fourth more expensive CDR option, costing $210 per t_{CO2}, whereas miscanthus (~160 per t_{CO2}), wheat straw (~160 per t_{CO2}) and forest residues (~140 per t_{CO2}) are cheaper.

Finally, biochar with miscanthus is found to be the fifth most expensive option costing $200 per t_{CO2}. Biochar pathways with wheat straw and forestry residues respectively cost $92 and $101 per t_{CO2}.

Besides the respective costs, the optimal deployment planning of CDR solutions is also constrained by a set of biophysical and geophysical constraints, such as land use, material availability, and build rate constraint, for which specific assumptions have been made for all CDR types. These assumptions play a key role in the mixed-integer linear optimization. Indeed, some of the constraints are “reached” by the optimization, limiting further deployment of a specific CDR.

For DACCS, land requirements assumed are small enough so that they never restrict its deployment, even in DACCS-optimistic scenarios. It is worth noting that our DACCS land use assumption only includes the size of the plant and not the land required by the additional installed power capacity needed to power DACCS operation. The assumption on build rate (allowing a doubling of DACCS capacity every five years) is not constraining DACCS deployment neither. As DACCS is the most expensive CDR solution, we deliberately relaxed its build rate, to allow the model to use DACCS as a last-resort solution to meet the target. Moreover, no special material resource is constraining DACCS deployment.

For enhanced weathering pathways, basalt silicate resources in the UK, as suggested by Renforth [106] are not a binding constraint in the optimisation. However, by-products such as slag, cement kiln dust (CKD), and construction and demolition wastes (CDWaste) are

limited resources, resulting in a small removal potential for EW *via* these pathways (0.25, 0.11, and 0.02 Mt_{CO2}/yr, respectively). However, both the rock application rate onto croplands (30 t_{rock} per ha per year) and the linear build rate, are restrictive assumptions that will limit the deployment of EW in the optimization.

BECCS and BC both use biomass as a main resource. They are both limited, on the one hand, by marginal land availability (used for miscanthus growth), limited to 2.1 Mha in the UK, and on the other hand by limited national availability of crop and forest residues. For BECCS, imported pellets are also limited to 36 million tonnes per annum (Mtpa) in 2030 and 7 Mtpa in 2050, following a prediction from Ricardo Energy & Environment [133]. This constraint is also binding, in the low-biomass scenario, whereas it is relaxed in the high-biomass scenario. For BC, we made the conservative assumption that it can only use indigenous and not imported biomass.

In summary, biomass-based CDRs are limited by available biomass resources. Akin to DACCS, a build rate multiplier formulation is used for BECCS and BC, allowing a rapid expansion of its capacity. However, the build rate constraint is not reached in the case of BECCS and BC.

For afforestation, we assume a land use constraint (*i.e.*, the reforestation potential area), and a linear expansion rate of 50 kha of newly planted forests per year (as recommended per CCC's sixth carbon budget [89]). Because the UK has a very large reforestation area (11 Mha), the restrictive assumption during the optimisation is the expansion rate.

In the low-biomass scenario, the ultimate CDR portfolio is composed of 29 and 17 Mt_{CO2}/yr removed by BECCS and AF, respectively. Enhanced weathering removes 10 Mt_{CO2}, DACCS 25 Mt_{CO2}, and BC 9 Mt_{CO2}/yr. Importantly, this reveals that given national bio – and geo–physical and build rate bounds, all five CDR solutions will be needed to meet the ambitious 90 Mt_{CO2} removal capacity needed in the UK by 2050.

6.1.2 The optimal power system in the UK (today-2050)

This section uses the Electricity System Optimisation (ESO) model, an existing framework, to determine an optimal power mix evolution (both capacity installed and power generation) meeting current power system decarbonization targets between today and 2050.

Like MONET, ESO has a mixed integer linear programming (MILP) formulation and minimises the total cost of the system given technology, system-wide (meeting the national demand, minimum reserve capacity, and inertia requirements), environmental (i.e., land-use) and carbon constraints. Given a national decarbonisation target for the electricity sector aiming at 100% emission reduction by 2050 (as per CCC's sixth carbon budget recommendation [89]), we find that the optimal 2050 power generation mix is composed of 54% intermittent renewable, 14% of CCGT-CCS, and 15% nuclear. Little generation from unabated CCGT is deployed (1.7%) along with small BECCS generation (1.6%) to compensate for the residual power sector emissions. Reserve capacity requirements are mainly met through unused unabated CCGT capacity. Wind offshore has a curtailment level of 5-30% of the total demand in 2030-2050, whereas wind onshore and solar are not curtailed.

Although these results are not a forecast of the power mix evolution, they are a possible representation of a net-zero power sector scenario, given a set of practical assumptions on power generation cost and power system constraints. This scenario will be set as a baseline scenario and will be compared to more advanced scenarios in the next sections, to better understand underlying key parameters driving the optimisation.

6.1.3 How does the power-CDR system integration change the optimal CDR, and power sector in the UK?

We provide a multi-sectoral approach, adjusting the perspectives and deployment anticipated in the power and the CDR sector presented in subsections 2.4 and 3.2 (and summarised in 6.1.1 and 6.1.2).

In other words, this section explores different behaviours of the power and CDR sectors, if considered within a broader whole-economy perspective. For this, we propose a novel joint ESO-MONET framework that combines the two models presented above (ESO for the power, and MONET for the CDR sector). We ensure the system meets the model's convergence criteria via an objective function based on total installed capacity in the power sector. The joint system shows quick convergence (2 optimisation loops at maximum) and provides close similarities – in terms of complexity, running time (15-20 minutes), and outcome – with a system that optimises both ESO and MONET equations simultaneously through one solver statement.

Our results show that constraining the deployment of carbon dioxide removal (CDR) technologies *via* a national removal target (set to balance with hard-to-abate sector emissions) will have a significant impact on energy systems. As per our assumptions, BECCS can provide energy services, while DACCS and EW consume them. From our combined model optimisation results, we find that the availability of biomass is the main driver for BECCS and BC deployment and that planting rates limit the potential of forests to sequester carbon by 2050. When biomass is abundant, BECCS and BC can play a major role in achieving a net-zero carbon target but are limited by the above-mentioned resource availability. In the context of substantial BECCS deployment, the use of natural gas with CCS and intermittent renewable energy sources will be reduced, by up to 55% and 13% respectively, compared to the reference power system scenario studied in section 3.2 (and summarised in 6.1.2).

Optimal outputs prove that BECCS and BC remove up to 43 Mt_{CO2}/yr by 2050, as per our limited biomass scenario. Afforestation and EW remove 14 and 8 Mt_{CO2}/yr by 2050, respectively. DACCS is used as a last resort to meet the target when other CDRs reach their maximum potential.

In addition, the power sector is also impacted by the need for CDR in the limited biomass scenario, compared to the reference scenario: BECCS and BC both provide 8% of the power generation by 2050, as opposed to 1.5% in the ESO-reference scenario, renewable generation is increased due to risen power CDR demand (DACCS and EW). Moreover, renewable curtailment levels tripled, and CCGT-CCS flexible generation is reduced by 22%.

As highlighted in the All-High-Biomass scenario and a sensitivity analysis on biomass availability, the power sector changes are accentuated by higher biomass availability, with even higher BECCS and BC generation share (22%), further reduced CCGT-CCS and nuclear, simultaneously with less demand from other CDR, thus drastically reducing the renewable share (-13%). Such scenarios are unlikely, given the quantity of biomass required, but worth being explored.

Finally, a sensitivity analysis reveals that gas combined with CCS (CCGT-CCS), wind, solar, and imported electricity is the preferred option to power DACCS, unlike nuclear.

Also, a biomass versus gas dilemma is underscored by our results. When biomass is not available, the system significantly deploys DACCS and relies on gas with CCS, which is largely deployed to power it.

Finally, we also explore a future where neither BECCS nor DACCS is part of the CDR portfolio, as part of the same sensitivity analysis. By observing the variation of CCGT-CCS, wind, solar and imported electricity throughout different expansion rate scenarios, the sensitivity analysis results exhibit a fungibility between lower-cost AF and more expensive BECCS removals. Indeed, we find an equivalence in power generation, between a scenario that depends on engineered-based CDR, and one that prioritises nature-based CDR solution.

6.1.4 How do permanence assumptions change the cost of removal and, thus the optimal CDR portfolio?

In the scientific community, time horizons for the permanence of carbon sequestration are not debated much. This parameter has been assumed to be 100 years in inter-governmental reports [3] and most studies [150], [159], as it is short enough from a policy perspective to make a decision based on the foreseeable future. Moreover, it guarantees, to a certain extent, the persistence of a CO_2 storage solution for a minimum duration of one hundred years, notwithstanding the inherent uncertainties. Indeed, the future societal landscape, particularly concerning technological advancements and reliance on fossil fuels, remains an area of profound uncertainty, with no definitive foresight available.

In addition, such a vision disregards the long-term effect of the carbon and other greenhouse gases emitted by humans since the industrial revolution, which have repercussions over thousands, to hundreds of thousands of years. Ideally, each CDR unit can compensate for a unit of fossil CO_2 emissions. However, removing CO_2 and storing it in non-permanent sinks with a risk of reversal or with natural durability lasting decades or centuries does not meet this requirement, given the long-lasting nature of CO_2 in the atmosphere.

Conversely, even non-permanent CDR pathways play a role in repairing the climate, yet less efficient than a permanent CDR solution.

To quantify this value, we have presented in Chapter 4 an analytical framework that calculates the climate repair value (CRV) of a CDR pathway of any permanence. First using a definition of permanent removal as lasting 1,000 years, we show that a carbon sink with an average durability of 200 years can only mitigate 15% of the damage caused by the original emission,

assuming it was left unmitigated. We also observe a non-linear relationship between store durability and CRV and show that removing CO_2 for 500 years can deliver a CRV of 40%.

Additionally, we suggest that temporary removals have the potential to create a moral hazard and may end up doing more harm than good. To account for this, we incorporate the CRV concept into a conventional levelised cost of removal analysis that includes monitoring, reporting, and verification (MRV) of a given store.

Finally, this framework is applied to the CDR solutions included in the ESO-MONET framework. CDR solutions can be divided into permanent, predictably leaky, and unpredictably leaky solutions. Amongst the predictably leaky solutions, we explore different carbon decay rates of biochar, depending on the pyrolysis types and temperature, biomass choice. We find out that specific BC configurations can result in permanent removals (time horizons higher than 1,000 years). This is the case of forestry residue, with slow pyrolysis, high temperature (>700 ^{o}C) and with H/C_{org} ratio lower than 0.4. BC pathways with miscanthus or crop residues are much less permanent, which is reflected in the Cost of Permanent Removal (CPR) metric.

To summarise, our analysis shows that, once the impacts of reversal and ongoing MRV costs are considered, the cost of permanent removal is generally lower than that of non-permanent removal.

6.1.5 Optimal CDR-power sector deployment given practical assumptions

6.1.5.1 Permanence horizon assumption

In this section, we present the impact of different permanence assumptions – using the CPR formulation presented in Chapter 4 (and summarised in 6.1.4) – on the ESO-MONET framework. We highlight the differences in power systems and CDR mixes, with a particular focus on 2050. These findings warrant further discourse and emphasis within the scientific community and among governmental bodies, given that permanence is a key parameter in the determination of the optimal composition of CDR strategies.

We find, as a logical follow-up of Chapter 4, that the definition of permanence is very important in the resulting optimal CDR and power mixes. Permanence horizons of 400 and 2,500 years mark a frontier across which the cost rankings of various technologies diverge. The higher the permanence, the more the CDR portfolio relies on CCS and EW solutions, instead of nature-based solutions such as AF and BC. Drastic changes in the CDR sector result in small modifications in the power sector, as additional BECCS seems to be powering the additional demand from DACCS, resonating with the conclusions of chapter 3 (summarised in 6.1.3). Only a 5% increase in solar generation is observed to fuel a marginal increase in DACCS' demand for high permanence times.

6.1.5.2 CCS infrastructure availability

Finally, we provide insight into potential changes in behaviours based on different CCS availability trajectories.

This section present findings that contrast with results from section 5.1 (summarised in 6.1.5.1) providing contrary outcomes. We have seen that geological storage solutions (BECCS and DACCS) and EW show cost robustness against permanence considerations, meanwhile, nature-based solutions such as BC and AF offer low-cost solutions only if low-permanence times are assumed. On the contrary, if we suppose CO_2 transport and storage infrastructure do not follow anticipated roll-out rates, it may become a bottleneck that will reduce our chances to meet our net zero targets, even if all other removal services are pushed to their maximum potential limits, as per our constraint definitions.

This suggests that biochar and afforestation might be reconsidered, either as a transition solution before CO_2 T&S becomes available or as a second-resort solution, if unforeseen obstacles are faced when building CO_2 transport pipelines, or unexpected CO_2 leakage at storage sites, for example. Moreover, as we will further develop in the limitation section, BC and afforestation, bring other benefits than that of sequestrating carbon such as nature, and biodiversity conservation, that are not considered in this study.

6.2 Limitations and future work

In this last section, the limitations of this work will be discussed, followed by future work suggestions.

6.2.1 Limitations

This dissertation presents some limitations regarding the exogenous nature of some parameters. For example, carbon dioxide removal (CDR) targets, power demand associated with the power system, carbon prices (penalizing the cost of polluting power technologies), price and carbon footprint of gas, CAPEX and OPEX for CDR (infrastructures and operations), but also power generation technologies (Nuclear, CCGT, Biomass, Coal, Wind, Solar, Storage, CCS). Determining these parameters falls beyond the scope of this study, which is solely focused on the CDR sector.

For example, carbon prices could be endogenous *via* the price of carbon removal (computed through MONET), but this would only be representative of carbon removals, ignoring other mitigation activities. A carbon market pricing model could help to accurately monitor carbon prices, and help determine various future carbon price trajectories, but this was out of the scope of this dissertation.

Then, no fluctuation in the costs of technology and fuel was considered. The robustness of such a coefficient could be tested using a Monte Carlo-type analysis but would be very inefficient if a high number of runs are needed, as one run of the E-M framework takes ~ 15 minutes. More research is needed in this area.

Also, technology cost learning rates over time have not been considered in our study, as we try to be conservative in the future cost of technologies, both in the power and in the CDR sector. Potentially, it could be interesting to compare current *conservative* results with other cost-learning assumptions, such as *learning-by-doing*, thus providing *cost-optimistic*

pathways. In particular, the future cost of DACCS could be drastically lowered. As a consequence, DACCS would become cost-efficient compared to other CDR solutions. In such a scenario, the evolution of the CDR portfolio and power systems would be impacted significantly. Such pathways are worth being better explored in future works, although some conclusions can already be drawn from current work, *i.e.*, DACCS is likely to be mainly powered by gas with CCS, and wind and solar.

Finally, a substantial number of papers call for a more comprehensive approach to evaluate CDR options, since the implementation of CDR options could exhibit environmental side-effects, such as their impact beyond carbon, land occupation, water consumption, or material utilization.

In this work, we aim to encompass as many parameters as possible, including land, material use, and water use limitations. The MONET framework considers a water footprint model [22], [53] for each CDR solution, but anticipated CDR portfolios are not explicitly constrained by water use in this work. However, they are implicitly constrained *via* the land availability, for AF, BECCS and BC, which has been adjusted to only account for lands with a low water stress index, according to the Aqueduct index [57].

In the literature, life cycle assessments (LCAs) are often used for comprehensive environmental studies and sustainability research. Typically, having a broader perspective than only focusing on the carbon footprint of CDR options could fit into our current model. Such an extension could explore life cycle GHG emissions and extend the analysis to include other environmental burdens.

Similarly, the permanence section of this dissertation focuses on CO_2, by only using the impulse response function of CO_2. Standard LCA methodologies employ CO_2-equivalent factors to account for the impacts of various greenhouse gases (GHGs) beyond CO_2. Therefore, one possibility would be to convert all GHGs into CO_2-equivalent and apply the CRV methodology. Another more in-depth solution would be using the impulse response function of each GHG. For example, methane's IRF can be described by a simple exponential decay (versus a sum for CO_2) [32]:

$$IRF_{CH_4}(t) = e^{-t/\tau}$$

However, when accounting for the atmospheric impact (estimated using an integral) of methane the effects on ozone (f_1) and on stratospheric H_2O (f_2) need to be incorporated, which modifies the IRF, as follows [32]:

$$IRF'_{CH_4}(t) = (1 + f_1 + f_2) * e^{-t/\tau}$$

Where f_1 and f_2 are scalar parameters, due to effects on ozone and stratospheric H_2O, respectively.

Based on such observations, the study of CDR permanence can be more comprehensive, including more GHGs by using their specific atmospheric impact, and provide more robust outputs.

6.2.2 Future work

6.2.2.1 What is the role of CDR solutions, in a larger economy-wide setting, to meet net-zero targets?

The power mix variation between the reference scenario (*i.e.*, optimised in isolation) versus the All-Low-Bio scenario shows the importance of exploring the synergies between different sectors. Indeed, the deployment of CDR solutions can indisputably influence the evolution of the power mix, by changing the need for renewable, abated gas, and nuclear's installed capacity.

This framework facilitates an understanding of how key factors in the CDR sector, like biomass availability, affect the necessary investments in the power sector, such as the capacity of wind and solar installations over a certain timeframe. It also offers policy recommendations from a more comprehensive viewpoint than an analysis focused solely on individual sectors, including the identification of CDR and power-generating technologies and specific construction rates required to achieve national climate goals.

This framework could be, in future work, replicated to account for more sectors, such as heavy industries, aviation, and heating. In a recent study from Mersch et al. [167] (2022), an integrated approach, similar to ours, is used to investigate the role of CCS solutions across three sectors simultaneously: power, hydrogen and heating.

This shows the potential for further sector-coupling works, to cover as many relevant sectors as possible while keeping the regional granularity of these models. Spatial temporality allows for the exploration of regional drivers, which is essential for making policy decisions at the regional level.

Because a CDR-power joint model has been proposed in this dissertation, and Mersch et al. [167] have built a power-hydrogen-heat framework at the UK scale, suggesting that future works focus on a joint CDR-power-hydrogen-heat which could provide more practical views on the deployment of CDR. In particular, Mersch et al. have highlighted the role of DACCS in scenarios with low gas prices and low biomass costs. Incorporating more CDR solutions (EW, BC, and AF) could also bring value to this work.

6.2.2.2 Investigate the regional deployment of CDR solutions: the ESONE-MONET framework

MONET provides meaningful spatial information on CDR deployment, *i.e.*, the location of CDR infrastructure, and transport of material. However, we don't explore the location of the optimal outputs of the model. There is no need to investigate them, *per se*, to draw some conclusions: optimising BECCS power pants location is equivalent to finding a middle ground between harvested land and CO_2 storage sites, *i.e.*, by the seaside. Pyrolysis plants need to find compromises to be at reasonable distances between harvested lands and croplands where biochar is spread. Comminution and mining facilities must be directly constructed (if not existing already) on mining sites for silicate rocks, and close to industrial plants for CKD, or slag. Afforestation should be incentivised in a region with greater carbon sequestration

potential – in temperate oceanic zones *i.e.*, mainly in the South West, Wales, Scotland and Northern Ireland (350 t_{CO2}/ha for temperate oceanic versus 200 for temperate mountain zones). We remarked that regional disparities are not significant enough to make a significant difference in the UK (also explained by the fact that 98% of the land with reforestation potential is in temperate oceanic zones) but could be decisive in a global context.

Even though MONET is a spatial model, ESO – the power mix model we use – is not spatially explicit and does not optimise transmission infrastructures, nor the flow of power through these infrastructures. Yet, such a model, ESONE [168], exists.

Given the interactions that some CDR solutions might have in the power system, it would be interesting to explore the optimal locations of CDR infrastructure in the UK, especially their proximity to transmission lines versus that of biomass resources, in the case of BECCS and BC. As BECCS plants are already constrained by their distance to harvested land and geological storage, adding the transmission line component might restrict them to very specific locations. In their study, Aziz et al. [19] analyse the climate benefits of pyrolysis plants providing heat and power to Stockholm's district heating network and power grid. A future study could explore, the optimal deployment of pyrolysis plants at the national scale. Pyrolysis plants with large capacities could provide energy *via* existing network infrastructures and be located close to transmission lines, and smaller pyrolysis would benefit from proximity to biomass harvest, or lands for biochar application, and could provide energy locally. The ESONE-MONET framework could provide an optimal design choice for biochar deployment, given existing transmission infrastructures and biomass resources.

6.2.2.3 What are the risks of investing in CDR solutions at a global scale?

Future investments are primordial to developing CDR projects, all the more so in the current context of the emerging carbon market, in which rules are still being determined [33]. Investors will seek to maximise their ROI while ensuring that their project meets the criteria needed by the voluntary carbon market. For example, the carbon core principles (CPP) state, amongst others, the need for a) robust independent third-party validation and verification, b) additionality, and c) permanence. One possible answer to the question of permanence has been suggested *via* the CPR formulation (Chapter 4, subsection 4.3).

Article 6 of the Paris Agreement [4] reveals the ambition to build a financial environment enabling international transactions, *i.e.*, countries with no CDR resources to buy credits or develop CDR projects in countries having them. In this context, models must consider the financial risks associated with investments in a given country. This risk can indisputably affect the return rates (IRR), and thus the cost of removal of a given store. Along with the notion of permanence – that we have seen can greatly impact the removal cost – the notion of corruption, as well as uncertainties related to conflicts and political instabilities, must be investigated in a broader future work, at the global scale, on CDR market price determination [169].

References

[1] G. S. Callendar, “The artificial production of carbon dioxide and its influence on temperature,” *Q. J. R. Meteorol. Soc.*, vol. 64, no. 275, pp. 223–240, Apr. 1938, doi: 10.1002/QJ.49706427503.

[2] Z. the P. of P. C. M. P. Hausfather, H. F. Drake, T. Abbott, and G. A. Schmidt, “Evaluating the Performance of Past Climate Model Projections,” *Geophys. Res. Lett.*, vol. 47, no. 1, p. e2019GL085378, Jan. 2020, doi: 10.1029/2019GL085378.

[3] H.-O. Pörtner *et al.*, “IPCC, 2022: Climate Change 2022: Impacts, Adaptation, and Vulnerability. Contribution of Working Group II to the Sixth Assessment Report of the Intergovernmental Panel on Climate Change,” *Cambridge Univ. Press. Cambridge Univ. Press. Cambridge, UK New York, NY, USA, 3056 pp.*, 2022, Accessed: Oct. 10, 2022. [Online]. Available: https://www.ipcc.ch/sr15/.

[4] UNFCCC, “Paris Agreement,” 2015.

[5] United Nation Environment Program (UNEP), “Emissions Gap Report 2022,” 2022. Accessed: Jan. 03, 2023. [Online]. Available: https://www.unep.org/resources/emissions-gap-report-2022.

[6] J. Rogelj, P. M. Forster, E. Kriegler, C. J. Smith, and R. Séférian, “Estimating and tracking the remaining carbon budget for stringent climate targets,” *Nat. 2019 5717765*, vol. 571, no. 7765, pp. 335–342, Jul. 2019, doi: 10.1038/s41586-019-1368-z.

[7] H. D. Matthews, N. P. Gillett, P. A. Stott, and K. Zickfeld, “The proportionality of global warming to cumulative carbon emissions,” *Nature*, vol. 459, no. 7248, pp. 829–832, Jun. 2009, doi: 10.1038/NATURE08047.

[8] H. D. Matthews and A. J. Weaver, “Committed climate warming,” *Nat. Geosci. 2010 33*, vol. 3, no. 3, pp. 142–143, Mar. 2010, doi: 10.1038/ngeo813.

[9] H. Naegele and A. Zaklan, “Does the EU ETS cause carbon leakage in European manufacturing?,” *J. Environ. Econ. Manage.*, vol. 93, pp. 125–147, Jan. 2019, doi: 10.1016/J.JEEM.2018.11.004.

[10] “CORC Supplier Listing.” https://puro.earth/CORC-co2-removal-certificate/ (accessed Sep. 05, 2022).

[11] “Carbon removal you can trust.” https://www.carbonfuture.earth/ (accessed Apr. 18, 2023).

[12] Department for Business Energy & Industrial Strategy, “Net Zero Strategy: Build Back Greener,” 2021. Accessed: Dec. 17, 2021. [Online]. Available: https://www.gov.uk/government/publications/net-zero-strategy.

[13] D. J. van de Ven, M. González-Eguino, and I. Arto, “The potential of behavioural change for climate change mitigation: a case study for the European Union,” *Mitig. Adapt. Strateg. Glob. Chang.*, vol. 23, no. 6, pp. 853–886, Aug. 2018, doi: 10.1007/S11027-017-9763-Y/TABLES/11.

[14] V. Masson-Delmotte *et al.*, “IPCC, 2018: Global warming of 1.5°C,” 2018. Accessed: May 06, 2021. [Online]. Available: www.environmentalgraphiti.org.

[15] The Royal Society, “Greenhouse gas removal,” 2018.

[16] Vivideconomics, “Greenhouse Gas Removal (GGR) policy options,” 2019.

[17] “EU action to address the energy crisis.” https://commission.europa.eu/strategy-and-policy/priorities-2019-2024/european-green-deal/eu-action-address-energy-crisis_en#diversifying-our-supply (accessed Mar. 18, 2023).

[18] “Renewable Electricity – Analysis - IEA.” https://www.iea.org/reports/renewable-electricity (accessed Mar. 18, 2023).
[19] E. S. Azzi, E. Karltun, and C. Sundberg, “Prospective Life Cycle Assessment of Large-Scale Biochar Production and Use for Negative Emissions in Stockholm,” 2019, doi: 10.1021/acs.est.9b01615.
[20] J. Lehmann *et al.*, “Biochar in climate change mitigation,” *Nat. Geosci. 2021 1412*, vol. 14, no. 12, pp. 883–892, Dec. 2021, doi: 10.1038/s41561-021-00852-8.
[21] S. Chiquier, M. Fajardy, and N. Mac Dowell, “CO_2 removal and 1.5 °C: what, when, where, and how?,” *Energy Adv.*, 2022, doi: 10.1039/D2YA00108J.
[22] M. Fajardy and N. Mac Dowell, “Can BECCS deliver sustainable and resource efficient negative emissions?,” *Energy Environ. Sci.*, vol. 10, no. 6, pp. 1389–1426, 2017, doi: 10.1039/c7ee00465f.
[23] D. Zhang, M. Bui, M. Fajardy, P. Patrizio, F. Kraxner, and N. Mac Dowell, “Unlocking the potential of BECCS with indigenous sources of biomass at a national scale,” *Sustain. Energy Fuels*, vol. 4, no. 1, pp. 226–253, 2019, doi: 10.1039/c9se00609e.
[24] N. Mac Dowell and M. Fajardy, “Inefficient power generation as an optimal route to negative emissions via BECCS?,” *Environ. Res. Lett.*, vol. 12, no. 4, p. 045004, 2017, doi: 10.1088/1748-9326/aa67a5.
[25] M. Fajardy, S. Chiquier, and N. Mac Dowell, “Investigating the BECCS resource nexus: Delivering sustainable negative emissions,” *Energy Environ. Sci.*, vol. 11, no. 12, pp. 3408–3430, 2018, doi: 10.1039/c8ee01676c.
[26] C. F. Heuberger, I. Staffell, N. Shah, and N. Mac Dowell, “Quantifying the value of CCS for the future electricity system,” *Energy Environ. Sci.*, vol. 9, no. 8, pp. 2497–2510, Aug. 2016, doi: 10.1039/c6ee01120a.
[27] C. F. Heuberger, I. Staffell, N. Shah, and N. Mac Dowell, “A systems approach to quantifying the value of power generation and energy storage technologies in future electricity networks,” *Comput. Chem. Eng.*, vol. 107, pp. 247–256, Dec. 2017, doi: 10.1016/j.compchemeng.2017.05.012.
[28] C. F. Heuberger, E. S. Rubin, I. Staffell, N. Shah, and N. Mac Dowell, “Power capacity expansion planning considering endogenous technology cost learning,” *Appl. Energy*, vol. 204, pp. 831–845, 2017, doi: 10.1016/j.apenergy.2017.07.075.
[29] Climate Change Committee, “Business use of offsets risks delaying Net Zero.” https://www.theccc.org.uk/2022/10/13/business-use-of-offsets-risks-delaying-net-zero/ (accessed Jan. 03, 2023).
[30] S. Fankhauser *et al.*, “The meaning of net zero and how to get it right,” *Nat. Clim. Chang.*, vol. 12, no. 1, pp. 15–21, 2022, doi: 10.1038/s41558-021-01245-w.
[31] R. Lal, “Managing soils and ecosystems for mitigating anthropogenic carbon emissions and advancing global food security,” *Bioscience*, vol. 60, no. 9, pp. 708–721, Oct. 2010, doi: 10.1525/BIO.2010.60.9.8.
[32] “Anthropogenic and Natural Radiative Forcing — IPCC.” https://www.ipcc.ch/report/ar5/wg1/anthropogenic-and-natural-radiative-forcing/ (accessed Feb. 08, 2023).
[33] “High Quality Voluntary Carbon Credits Principles.” https://icvcm.org/the-core-carbon-principles/ (accessed Mar. 22, 2023).
[34] “Revealed: more than 90% of rainforest carbon offsets by biggest certifier are worthless, analysis shows | Carbon offsetting | The Guardian.” https://www.theguardian.com/environment/2023/jan/18/revealed-forest-carbon-

offsets-biggest-provider-worthless-verra-aoe (accessed Feb. 08, 2023).
[35] J. Fuhrman, H. McJeon, S. C. Doney, W. Shobe, and A. F. Clarens, “From Zero to Hero?: Why Integrated Assessment Modeling of Negative Emissions Technologies Is Hard and How We Can Do Better,” *Front. Clim.*, vol. 1, p. 11, Dec. 2019, doi: 10.3389/fclim.2019.00011.
[36] “CO2 Transport and Storage – Analysis - IEA.” https://www.iea.org/reports/co2-transport-and-storage (accessed Feb. 18, 2023).
[37] A. Prado and N. Mac Dowell, “The cost of permanent carbon dioxide removal,” *Joule*, Apr. 2023, doi: 10.1016/J.JOULE.2023.03.006.
[38] “Energy System Modelling Environment - Energy Systems Catapult.” https://es.catapult.org.uk/tools-and-labs/our-national-net-zero-toolkit/energy-system-modelling-environment/ (accessed Apr. 17, 2023).
[39] L. Göransson, J. Goop, M. Odenberger, and F. Johnsson, “Impact of thermal plant cycling on the cost-optimal composition of a regional electricity generation system,” *Appl. Energy*, vol. 197, pp. 230–240, Jul. 2017, doi: 10.1016/J.APENERGY.2017.04.018.
[40] Carbon Market Watch, “EU’s new carbon removal framework in danger of camouflaging climate inaction.” https://carbonmarketwatch.org/2022/11/30/eus-new-carbon-removal-framework-in-danger-of-camouflaging-climate-inaction/ (accessed Jan. 02, 2023).
[41] W. Rickels, A. Proelß, O. Geden, J. Burhenne, and M. Fridahl, “Integrating Carbon Dioxide Removal Into European Emissions Trading,” *Front. Clim.*, vol. 3, p. 62, Jun. 2021, doi: 10.3389/FCLIM.2021.690023/BIBTEX.
[42] “A European Green Deal.” https://commission.europa.eu/strategy-and-policy/priorities-2019-2024/european-green-deal_en (accessed Jan. 03, 2023).
[43] “Fit for 55 - The EU’s plan for a green transition - Consilium.” https://www.consilium.europa.eu/en/policies/green-deal/fit-for-55-the-eu-plan-for-a-green-transition/ (accessed Jan. 03, 2023).
[44] F. Schenuit and O. Geden, “Carbon Dioxide Removal: Climbing up the EU Climate Policy Agenda 1.”
[45] “Climate Change Act 2008.”
[46] “Tree planting rates to treble by end of this Parliament - GOV.UK.” https://www.gov.uk/government/news/tree-planting-rates-to-treble-by-end-of-this-parliament (accessed Dec. 30, 2022).
[47] Committee on Climate Change, “Net Zero - The UK’s contribution to stopping global warming Committee on Climate Change,” 2019. Accessed: Feb. 26, 2021. [Online]. Available: www.theccc.org.uk/publications.
[48] “Enhanced Rock Weathering in Soil Puro Standard Methodology.” https://puro.earth/articles/enhanced-rock-weathering-in-soil-methodology-public-consulta-788 (accessed Mar. 18, 2023).
[49] J. Lezaun, P. Healey, T. Kruger, and S. M. Smith, “Governing Carbon Dioxide Removal in the UK: Lessons Learned and Challenges Ahead,” *Front. Clim.*, vol. 3, p. 89, Aug. 2021, doi: 10.3389/FCLIM.2021.673859/BIBTEX.
[50] J. Young *et al.*, “The cost of direct air capture and storage: the impact of technological learning, regional diversity, and policy.,” Nov. 2022, doi: 10.26434/CHEMRXIV-2022-DP36T-V3.
[51] C. S. Galik, “A continuing need to revisit BECCS and its potential,” *Nature Climate Change*, vol. 10, no. 1. Nature Research, pp. 2–3, Jan. 01, 2020, doi: 10.1038/s41558-

019-0650-2.
[52] S. Fuss *et al.*, “Negative emissions—Part 2: Costs, potentials and side effects,” *Environ. Res. Lett*, vol. 13, no. 6, 2018, doi: 10.1088/1748-9326/aabf9f.
[53] S. M. Chiquier, “The implications of the Paris Agreement on carbon dioxide removal (CDR) - techno-economics, potential, efficiency and permanence of CDR pathways,” Imperial College London, 2022.
[54] C. R. Stoof *et al.*, “Untapped Potential: Opportunities and Challenges for Sustainable Bioenergy Production from Marginal Lands in the Northeast USA,” *Bioenergy Res.*, vol. 8, no. 2, pp. 482–501, Jun. 2015, doi: 10.1007/S12155-014-9515-8.
[55] D. for Energy Security and N. Zero, “Biomass Strategy 2023,” 2023, Accessed: Dec. 24, 2023. [Online]. Available: www.gov.uk/official-documents.
[56] X. Cai, X. Zhang, and D. Wang, “Land availability for biofuel production,” *Environ. Sci. Technol.*, vol. 45, no. 1, pp. 334–339, Jan. 2011, doi: 10.1021/es103338e.
[57] “Aqueduct – World Resources Institute.” https://www.wri.org/aqueduct/ (accessed Nov. 09, 2021).
[58] Department for Environment Food & Rural Affairs, “Crops Grown for Bioenergy in the UK: 2019,” 2020.
[59] M. Guo, W. Song, and J. Buhain, “Bioenergy and biofuels: History, status, and perspective,” *Renew. Sustain. Energy Rev.*, vol. 42, pp. 712–725, Feb. 2015, doi: 10.1016/J.RSER.2014.10.013.
[60] H. A. Daggash, C. F. Heuberger, and N. Mac Dowell, “The role and value of negative emissions technologies in decarbonising the UK energy system,” *Int. J. Greenh. Gas Control*, vol. 81, no. July 2018, pp. 181–198, 2019, doi: 10.1016/j.ijggc.2018.12.019.
[61] A. H. Truong, P. Patrizio, S. Leduc, F. Kraxner, and M. Ha-Duong, “Reducing emissions of the fast growing Vietnamese coal sector: The chances offered by biomass co-firing,” *J. Clean. Prod.*, vol. 215, pp. 1301–1311, Apr. 2019, doi: 10.1016/J.JCLEPRO.2019.01.065.
[62] F. Creutzig, C. Breyer, J. Hilaire, J. Minx, G. P. Peters, and R. Socolow, “The mutual dependence of negative emission technologies and energy systems,” *Energy Environ. Sci.*, vol. 12, pp. 1805–1817, 2019, doi: 10.1039/c8ee03682a.
[63] M. Lehtveer and A. Emanuelsson, “BECCS and DACCS as Negative Emission Providers in an Intermittent Electricity System: Why Levelized Cost of Carbon May Be a Misleading Measure for Policy Decisions,” *Front. Clim.*, vol. 0, p. 15, Mar. 2021, doi: 10.3389/FCLIM.2021.647276.
[64] W. J. Sagues, S. Park, H. Jameel, and D. L. Sanchez, “Enhanced carbon dioxide removal from coupled direct air capture-bioenergy systems,” *Sustain. Energy Fuels*, vol. 3, no. 11, pp. 3135–3146, 2019, doi: 10.1039/c9se00384c.
[65] M. Fajardy and N. Mac Dowell, “The energy return on investment of BECCS: Is BECCS a threat to energy security?,” *Energy Environ. Sci.*, vol. 11, no. 6, pp. 1581–1594, 2018, doi: 10.1039/c7ee03610h.
[66] A. Prado, S. Chiquier, M. Fajardy, and N. Mac Dowell, “Assessing the impact of carbon dioxide removal on the power system,” *iScience*, vol. 26, no. 4, p. 106303, Apr. 2023, doi: 10.1016/J.ISCI.2023.106303.
[67] P. Brandl, M. Bui, J. P. Hallett, and N. Mac Dowell, “Beyond 90% capture: Possible, but at what cost?,” *Int. J. Greenh. Gas Control*, vol. 105, p. 103239, Feb. 2021, doi: 10.1016/J.IJGGC.2020.103239.
[68] J. Alcalde *et al.*, “Estimating geological CO_2 storage security to deliver on climate

mitigation," doi: 10.1038/s41467-018-04423-1.
[69] C. Zahasky and S. M. Benson, "Evaluation of hydraulic controls for leakage intervention in carbon storage reservoirs," *Int. J. Greenh. Gas Control*, vol. 47, pp. 86–100, Apr. 2016, doi: 10.1016/J.IJGGC.2016.01.035.
[70] E. Smith, J. Morris, H. Kheshgi, G. Teletzke, H. Herzog, and S. Paltsev, "The cost of CO2 transport and storage in global integrated assessment modeling," *Int. J. Greenh. Gas Control*, vol. 109, Jul. 2021, doi: 10.1016/J.IJGGC.2021.103367.
[71] "Project - Porthos." https://www.porthosco2.nl/en/project/ (accessed Jan. 12, 2024).
[72] M. Bentham, T. Mallows, J. Lowndes, and A. Green, "CO2 STORage evaluation database (CO2 Stored). The UK's online storage atlas," in *Energy Procedia*, Jan. 2014, vol. 63, pp. 5103–5113, doi: 10.1016/j.egypro.2014.11.540.
[73] "PORTHOS CCS-TRANSPORT AND STORAGE (T&S) TARIFF REVIEW The Dutch Ministry of Economic Affairs and Climate Policy Disclaimer Notice Contents," Accessed: Jan. 12, 2024. [Online]. Available: www.xodusgroup.com.
[74] HM Government, "Gas and electricity prices in the non-domestic sector." https://www.gov.uk/government/statistical-data-sets/gas-and-electricity-prices-in-the-non-domestic-sector (accessed Jan. 14, 2022).
[75] M. Bui, M. Fajardy, and N. Mac Dowell, "Bio-Energy with CCS (BECCS) performance evaluation: Efficiency enhancement and emissions reduction," *Appl. Energy*, vol. 195, pp. 289–302, 2017, doi: 10.1016/j.apenergy.2017.03.063.
[76] M. C. Fajardy, "Developing a framework for the optimal deployment of negative emissions technologies," 2020, doi: 10.25560/80691.
[77] G. F. Nemet *et al.*, "Negative emissions—Part 3: Innovation and upscaling," *Environ. Res. Lett*, vol. 13, no. 6, p. 063003, May 2018, doi: 10.1088/1748-9326/AABFF4.
[78] A. Marcucci, S. Kypreos, and E. Panos, "The road to achieving the long-term Paris targets: energy transition and the role of direct air capture," *Clim. Change*, vol. 144, no. 2, pp. 181–193, Sep. 2017, doi: 10.1007/S10584-017-2051-8.
[79] J. Strefler, N. Bauer, E. Kriegler, A. Popp, A. Giannousakis, and O. Edenhofer, "Between Scylla and Charybdis: Delayed mitigation narrows the passage between large-scale CDR and high costs," *Environ. Res. Lett.*, vol. 13, no. 4, p. 044015, Mar. 2018, doi: 10.1088/1748-9326/AAB2BA.
[80] G. Realmonte *et al.*, "An inter-model assessment of the role of direct air capture in deep mitigation pathways," *Nat. Commun.*, vol. 10, no. 1, pp. 1–12, Dec. 2019, doi: 10.1038/s41467-019-10842-5.
[81] J. Fuhrman *et al.*, "Food-energy-water implications of negative emissions technologies in a +1.5 °C future," *NatCC*, vol. 10, no. 10, pp. 920–927, Oct. 2020, doi: 10.1038/S41558-020-0876-Z.
[82] P. Smith *et al.*, "Biophysical and economic limits to negative CO2 emissions," *Nature Climate Change*, vol. 6, no. 1. Nature Publishing Group, pp. 42–50, Jan. 01, 2016, doi: 10.1038/nclimate2870.
[83] R. Hanna, A. Abdulla, Y. Xu, and D. G. Victor, "Emergency deployment of direct air capture as a response to the climate crisis," *Nat. Commun. 2021 121*, vol. 12, no. 1, pp. 1–13, Jan. 2021, doi: 10.1038/s41467-020-20437-0.
[84] "New IEAGHG report: Global Assessment of DACCS Costs, Scale and Potential - BLOG." https://ieaghg.org/ccs-resources/blog/new-ieaghg-report-global-assessment-of-daccs-costs-scale-and-potential (accessed Feb. 20, 2023).
[85] "The next step towards a climate-positive world: Orca!"

https://climeworks.com/roadmap/orca (accessed Nov. 09, 2021).
[86] M. Fasihi, O. Efimova, and C. Breyer, “Techno-economic assessment of CO_2 direct air capture plants,” *J. Clean. Prod.*, vol. 224, pp. 957–980, Jul. 2019, doi: 10.1016/j.jclepro.2019.03.086.
[87] D. W. Keith, G. Holmes, D. St. Angelo, and K. Heidel, “A Process for Capturing CO_2 from the Atmosphere,” *Joule*, vol. 2, no. 8, pp. 1573–1594, Aug. 2018, doi: 10.1016/j.joule.2018.05.006.
[88] “Direct air capture technology and carbon removal.” https://climeworks.com/direct-air-capture (accessed Oct. 17, 2022).
[89] Climate Change Committee, “The Sixth Carbon Budget - The UK’s path to Net Zero,” 2020. Accessed: Feb. 25, 2021. [Online]. Available: www.theccc.org.uk/publications.
[90] C. Chen and M. Tavoni, “Direct air capture of CO_2 and climate stabilization: A model based assessment,” *Clim. Change*, vol. 118, no. 1, pp. 59–72, May 2013, doi: 10.1007/S10584-013-0714-7/FIGURES/5.
[91] D. Brack and R. King, “Managing Land-based CDR: BECCS, Forests and Carbon Sequestration,” *Glob. Policy*, vol. 12, no. S1, pp. 45–56, Apr. 2021, doi: 10.1111/1758-5899.12827.
[92] J. McKechnie, S. Colombo, J. Chen, W. Mabee, and H. L. MacLean, “Forest bioenergy or forest carbon? Assessing trade-offs in greenhouse gas mitigation with wood-based fuels,” *Environ. Sci. Technol.*, vol. 45, no. 2, pp. 789–795, Jan. 2011, doi: 10.1021/ES1024004/SUPPL_FILE/ES1024004_SI_001.PDF.
[93] T. Buchholz, M. D. Hurteau, J. Gunn, and D. Saah, “A global meta-analysis of forest bioenergy greenhouse gas emission accounting studies,” *GCB Bioenergy*, vol. 8, no. 2, pp. 281–289, Mar. 2016, doi: 10.1111/GCBB.12245.
[94] T. Kuramochi *et al.*, “Greenhouse gas mitigation scenarios for major emitting countries Analysis of current climate policies and mitigation commitments: 2018 update,” 2018, Accessed: Jan. 13, 2023. [Online]. Available: http://newclimate.org/publications/.
[95] “Treeconomy | Unlock Nature’s Value.” https://www.treeconomy.co/about (accessed Jan. 16, 2024).
[96] Fao, “FOOD AND AGRICULTURE ORGANIZATION OF THE UNITED NATIONS Rome.”
[97] U. Bohn, C. Hettwer, and G. Gollub, “Application and Analysis of the Map of the Natural Vegetation of Europe,” 2001, Accessed: Mar. 22, 2022. [Online]. Available: https://www.researchgate.net/profile/Nugzar-Zazanashvili/publication/275580442_Application_of_the_Map_of_the_Natural_Vegetation_of_Europe_in_Developing_a_Protected_Areas_Network_in_the_Caucasus_Ecoregion/links/553f883d0cf23e796bfb6432/Application-of-the-M.
[98] A. H *et al.*, “Chapter 4 - Forest Land in Volume 4: Agriculture, Forestry and Other Land Use - IPCC Guidelines for National Greenhouse Gas Inventories,” 2006.
[99] “2006 IPCC Guidelines for National Greenhouse Gas Inventories — IPCC.” https://www.ipcc.ch/report/2006-ipcc-guidelines-for-national-greenhouse-gas-inventories/ (accessed Oct. 14, 2022).
[100] M. D. Hurteau, B. A. Hungate, and G. W. Koch, “Accounting for risk in valuing forest carbon offsets,” *Carbon Balance Manag.*, vol. 4, pp. 1–5, 2009, doi: 10.1186/1750-0680-4-1.
[101] “LANDFIRE Program: Home.” https://www.landfire.gov/ (accessed Oct. 13, 2022).
[102] S. Chiquier, P. Patrizio, M. Bui, N. Sunny, and N. Mac Dowell, “A comparative analysis

of the efficiency, timing, and permanence of CO2 removal pathways," *Energy Environ. Sci.*, 2022, doi: 10.1039/D2EE01021F.
[103] W. Seifritz, "CO2 disposal by means of silicates," *Nat. 1990 3456275*, vol. 345, no. 6275, pp. 486–486, 1990, doi: 10.1038/345486b0.
[104] K. S. Lackner, C. H. Wendt, D. P. Butt, E. L. Joyce, and D. H. Sharp, "Carbon dioxide disposal in carbonate minerals," *Energy*, vol. 20, no. 11, pp. 1153–1170, Jan. 1995, doi: 10.1016/0360-5442(95)00071-N.
[105] "Project Carbdown's next step: We will set up a large scale greenhouse experiment with hundreds of pots — Carbon Drawdown Initiative." https://www.carbon-drawdown.de/blog/2022-11-15-project-carbdowns-next-step-we-will-set-up-a-large-scale-greenhouse-experiment-with-hundreds-of-pots (accessed Feb. 20, 2023).
[106] P. Renforth, "The potential of enhanced weathering in the UK," *Int. J. Greenh. Gas Control*, vol. 10, pp. 229–243, Sep. 2012, doi: 10.1016/J.IJGGC.2012.06.011.
[107] F. J. R. Meysman and F. Montserrat, "Negative CO_2 emissions via enhanced silicate weathering in coastal environments," *Biol. Lett.*, vol. 13, no. 4, p. 20160905, Apr. 2017, doi: 10.1098/RSBL.2016.0905.
[108] P. Renforth, "The negative emission potential of alkaline materials," *Nat. Commun. 2019 101*, vol. 10, no. 1, pp. 1–8, Mar. 2019, doi: 10.1038/s41467-019-09475-5.
[109] P. Renforth, C. L. Washbourne, J. Taylder, and D. A. C. Manning, "Silicate production and availability for mineral carbonation," *Environ. Sci. Technol.*, vol. 45, no. 6, pp. 2035–2041, Mar. 2011, doi: 10.1021/es103241w.
[110] A. Sanna, M. Dri, M. R. Hall, and M. Maroto-Valer, "Waste materials for carbon capture and storage by mineralisation (CCSM) – A UK perspective," *Appl. Energy*, vol. 99, pp. 545–554, Nov. 2012, doi: 10.1016/J.APENERGY.2012.06.049.
[111] J. Strefler, T. Amann, N. Bauer, E. Kriegler, and J. Hartmann, "Potential and costs of carbon dioxide removal by enhanced weathering of rocks," *Environ. Res. Lett.*, vol. 13, no. 3, p. 034010, Mar. 2018, doi: 10.1088/1748-9326/AAA9C4.
[112] D. J. Beerling *et al.*, "Potential for large-scale CO_2 removal via enhanced rock weathering with croplands," *Nature*, vol. 583, 2020, doi: 10.1038/s41586-020-2448-9.
[113] D. Lefebvre *et al.*, "Assessing the potential of soil carbonation and enhanced weathering through Life Cycle Assessment: A case study for Sao Paulo State, Brazil," *J. Clean. Prod.*, vol. 233, pp. 468–481, Oct. 2019, doi: 10.1016/j.jclepro.2019.06.099.
[114] J. Strefler, T. Amann, N. Bauer, E. Kriegler, and J. Hartmann, *Potential and costs of carbon dioxide removal by enhanced weathering of rocks*, vol. 13, no. 3. IOP Publishing, p. 034010.
[115] S. J. T. Hangx and C. J. Spiers, "Coastal spreading of olivine to control atmospheric CO_2 concentrations: A critical analysis of viability," *Int. J. Greenh. Gas Control*, vol. 3, no. 6, pp. 757–767, 2009, doi: 10.1016/j.ijggc.2009.07.001.
[116] D. J. Beerling *et al.*, "Farming with crops and rocks to address global climate, food and soil security," *Nat. Plants 2018 43*, vol. 4, no. 3, pp. 138–147, Feb. 2018, doi: 10.1038/s41477-018-0108-y.
[117] J. A. Ippolito *et al.*, "Feedstock choice, pyrolysis temperature and type influence biochar characteristics: a comprehensive meta-data analysis review," *Biochar*, vol. 2, no. 4, pp. 421–438, Dec. 2020, doi: 10.1007/S42773-020-00067-X/TABLES/6.
[118] H. P. Schmidt *et al.*, "Biochar in agriculture – A systematic review of 26 global meta-analyses," *GCB Bioenergy*, vol. 13, no. 11, pp. 1708–1730, Nov. 2021, doi: 10.1111/GCBB.12889.

[119] D. Woolf, J. E. Amonette, F. A. Street-Perrott, J. Lehmann, and S. Joseph, “Sustainable biochar to mitigate global climate change,” *Nat. Commun. 2010 11*, vol. 1, no. 1, pp. 1–9, Aug. 2010, doi: 10.1038/ncomms1053.
[120] R. Arvidsson *et al.*, “Environmental Assessment of Emerging Technologies: Recommendations for Prospective LCA,” *J. Ind. Ecol.*, vol. 22, no. 6, pp. 1286–1294, Dec. 2018, doi: 10.1111/JIEC.12690.
[121] D. Woolf, J. Lehmann, S. Ogle, A. W. Kishimoto-Mo, B. Mcconkey, and J. Baldock, “Greenhouse Gas Inventory Model for Biochar Additions to Soil,” *Cite This Environ. Sci. Technol*, vol. 55, pp. 14795–14805, 2021, doi: 10.1021/acs.est.1c02425.
[122] Y. Fang, B. Singh, and B. P. Singh, “Effect of temperature on biochar priming effects and its stability in soils,” *Soil Biol. Biochem.*, vol. 80, pp. 136–145, Jan. 2015, doi: 10.1016/J.SOILBIO.2014.10.006.
[123] G. Perkins, “Techno-economic comparison of the levelised cost of electricity generation from solar PV and battery storage with solar PV and combustion of bio-crude using fast pyrolysis of biomass,” *Energy Convers. Manag.*, vol. 171, pp. 1573–1588, Sep. 2018, doi: 10.1016/J.ENCONMAN.2018.06.090.
[124] E. I. Konstantinidis and P. N. Botsaris, “Wind turbines: current status, obstacles, trends and technologies,” *IOP Conf. Ser. Mater. Sci. Eng.*, vol. 161, no. 1, p. 012079, Nov. 2016, doi: 10.1088/1757-899X/161/1/012079.
[125] Y. W. Pratama and N. Mac Dowell, “Carbon capture and storage investment: Fiddling while the planet burns,” *One Earth*, vol. 5, no. 4, pp. 434–442, Apr. 2022, doi: 10.1016/J.ONEEAR.2022.03.008.
[126] B. W. Griscom *et al.*, “Natural climate solutions,” *Proc. Natl. Acad. Sci. U. S. A.*, vol. 114, no. 44, pp. 11645–11650, Oct. 2017, doi: 10.1073/pnas.1710465114.
[127] IEA, “Bioenergy with Carbon Capture and Storage – Analysis.” https://www.iea.org/reports/bioenergy-with-carbon-capture-and-storage (accessed May 05, 2023).
[128] IEA, “Direct Air Capture – Analysis.” https://www.iea.org/reports/direct-air-capture (accessed May 04, 2023).
[129] “Enhanced rock weathering can help decarbonise the atmosphere.” https://www.energymonitor.ai/tech/carbon-removal/speeding-up-rock-weathering-can-help-decarbonise-the-atmosphere/ (accessed May 04, 2023).
[130] “Dataset Record: MCD12Q1 - MODIS/Terra+Aqua Land Cover Type Yearly L3 Global 500m SIN Grid.” https://catalogue.ceda.ac.uk/uuid/2bdeefa63a234a18a8fd0fabd4fa62b0 (accessed Jan. 04, 2022).
[131] K. Ricke, L. Drouet, K. Caldeira, and M. Tavoni, “Country-level social cost of carbon,” doi: 10.1038/s41558-018-0282-y.
[132] Department for Business Energy & Industrial Strategy, “Updated short-term traded carbon values used for UK public policy appraisal: 2018,” 2019. Accessed: May 12, 2021. [Online]. Available: https://www.gov.uk/government/publications/carbon-valuation-in-uk-policy-appraisal-a-.
[133] Ricardo Energy & Environment, “Biomass Feedstock Availability,” 2017.
[134] H. E. Daly and B. Fais, “UK TIMES MODEL OVERVIEW,” 2014, Accessed: Feb. 13, 2024. [Online]. Available: http://www.ukerc.ac.uk/support/Energy+Systems.
[135] “A burning issue: biomass is the biggest source of renewable energy consumed in the UK - Office for National Statistics.”

https://www.ons.gov.uk/economy/environmentalaccounts/articles/aburningissuebiomassisthebiggestsourceofrenewableenergyconsumedintheuk/2019-08-30 (accessed Mar. 24, 2023).
[136] "U.S. Energy Information Administration - EIA - Independent Statistics and Analysis." https://www.eia.gov/biofuels/biomass/ (accessed Feb. 19, 2023).
[137] "Forest Bioenergy 101: Generation and Emissions." https://www.rff.org/publications/explainers/forest-bioenergy-101/ (accessed Feb. 19, 2023).
[138] "Scientist Letter to Biden, von der Leyen, Michel, Suga & Moon Re. Forest Biomass (February 11, 2021).pdf." https://www.dropbox.com/s/hdmmcnd0d1d2lq5/Scientist Letter to Biden%2C von der Leyen%2C Michel%2C Suga %26 Moon Re. Forest Biomass %28February 11%2C 2021%29.pdf?dl=0 (accessed Feb. 19, 2023).
[139] A. Booth and J. Wentworth, "Biomass for UK energy," 2023. Accessed: Mar. 24, 2023. [Online]. Available: https://post.parliament.uk/research-briefings/post-pn-0690/.
[140] Department for Business Energy & Industrial Startegy WRONG ONE, "Updated short-term traded carbon values used for UK public policy appraisal: 2018," 2019. Accessed: Jun. 18, 2021. [Online]. Available: https://www.gov.uk/government/publications/carbon-valuation-in-uk-policy-appraisal-a-.
[141] HM Government, "The Ten Point Plan for a Green Industrial Revolution," 2020.
[142] HM Government, "End of coal in sight as UK secures ambitious commitments at COP26 summit." https://www.gov.uk/government/news/end-of-coal-in-sight-as-uk-secures-ambitious-commitments-at-cop26-summit (accessed Jan. 03, 2022).
[143] Bloomberg, "UK Energy Crisis: War Derails Plan to Ditch Coal After Johnson Led COP26." https://www.bloomberg.com/news/articles/2022-06-19/uk-energy-crisis-war-derails-plan-to-ditch-coal-after-johnson-led-cop26 (accessed Aug. 10, 2022).
[144] S. Paltsev, J. Morris, H. Kheshgi, and H. Herzog, "Hard-to-Abate Sectors: The role of industrial carbon capture and storage (CCS) in emission mitigation," *Appl. Energy*, vol. 300, p. 117322, Oct. 2021, doi: 10.1016/J.APENERGY.2021.117322.
[145] R. G. Prinn *et al.*, "The economics of bioenergy with carbon capture and storage (BECCS) deployment in a 1.5°C or 2°C world," *Glob. Environ. Chang.*, vol. 68, p. 102262, 2021, Accessed: Apr. 26, 2022. [Online]. Available: http://globalchange.mit.edu/.
[146] Statista, "Wood pellet imports by major country 2020," 2020. https://www.statista.com/statistics/477057/imports-of-wood-pellets-volume-by-key-country/ (accessed Aug. 10, 2022).
[147] "Rules & Requirements - Verra." https://verra.org/project/vcs-program/rules-and-requirements/ (accessed Jun. 20, 2022).
[148] J. Strefler, N. Bauer, F. Humpenöder, D. Klein, A. Popp, and E. Kriegler, "Carbon dioxide removal technologies are not born equal," *Environ. Res. Lett.*, vol. 16, no. 7, p. 074021, Jul. 2021, doi: 10.1088/1748-9326/AC0A11.
[149] F. Cherubini, G. P. Peters, T. Berntsen, A. H. Strømman, and E. Hertwich, "CO_2 emissions from biomass combustion for bioenergy: Atmospheric decay and contribution to global warming," *GCB Bioenergy*, vol. 3, no. 5, pp. 413–426, 2011, doi: 10.1111/J.1757-1707.2011.01102.X.
[150] M. K. Kim, B. A. McCarl, and B. C. Murray, "Permanence discounting for land-based carbon sequestration," *Ecol. Econ.*, vol. 64, no. 4, pp. 763–769, Feb. 2008, doi:

10.1016/J.ECOLECON.2007.04.013.
[151] G. Marland, K. Fruit, and R. Sedjo, “Accounting for sequestered carbon: the question of permanence,” *Environ. Sci. Policy*, vol. 4, no. 6, pp. 259–268, Dec. 2001, doi: 10.1016/S1462-9011(01)00038-7.
[152] A. Lyngfelt, D. J. A. Johansson, and E. Lindeberg, “Negative CO_2 emissions - An analysis of the retention times required with respect to possible carbon leakage,” *Int. J. Greenh. Gas Control*, vol. 87, pp. 27–33, Aug. 2019, doi: 10.1016/J.IJGGC.2019.04.022.
[153] P. M. Fearnside, D. A. Lashof, and P. Moura-Costa, “Accounting for time in Mitigating Global Warming through land-use change and forestry,” *Mitig. Adapt. Strateg. Glob. Chang. 2000 53*, vol. 5, no. 3, pp. 239–270, 2000, doi: 10.1023/A:1009625122628.
[154] N. Mac Dowell, D. M. Reiner, and R. S. Haszeldine, “Comparing approaches for carbon dioxide removal,” *Joule*, Sep. 2022, doi: 10.1016/J.JOULE.2022.09.005.
[155] D. Shindell *et al.*, “Anthropogenic and Natural Radiative Forcing Supplementary Material,” 2013.
[156] D. Archer, H. Kheshgi, and E. Maier-Reimer, “Multiple timescales for neutralization of fossil fuel CO_2,” *Geophys. Res. Lett.*, vol. 24, no. 4, pp. 405–408, Feb. 1997, doi: 10.1029/97GL00168.
[157] Z. Parisa, E. Marland, B. Sohngen, G. Marland, and J. Jenkins, “The time value of carbon storage,” *For. Policy Econ.*, vol. 144, p. 102840, Nov. 2022, doi: 10.1016/J.FORPOL.2022.102840.
[158] R. Korhonen, K. Pingoud, I. Savolainen, and R. Matthews, “The role of carbon sequestration and the tonne-year approach in fulfilling the objective of climate convention,” *Environ. Sci. Policy*, vol. 5, no. 6, pp. 429–441, Dec. 2002, doi: 10.1016/S1462-9011(02)00091-6.
[159] H. Herzog, K. Caldeira, and J. Reilly, “AN ISSUE OF PERMANENCE: ASSESSING THE EFFECTIVENESS OF TEMPORARY CARBON STORAGE,” 2003.
[160] F. Joos *et al.*, “Carbon dioxide and climate impulse response functions for the computation of greenhouse gas metrics: A multi-model analysis,” *Atmos. Chem. Phys.*, vol. 13, no. 5, pp. 2793–2825, 2013, doi: 10.5194/ACP-13-2793-2013.
[161] D. Archer, E. Kite, and G. Lusk, “The ultimate cost of carbon,” *Clim. Change*, vol. 162, no. 4, pp. 2069–2086, Oct. 2020, doi: 10.1007/S10584-020-02785-4/TABLES/5.
[162] M. D. Hurteau, B. A. Hungate, and G. W. Koch, “Carbon Balance and Management Accounting for risk in valuing forest carbon offsets,” 2009, doi: 10.1186/1750-0680-4-1.
[163] F. W. Wellmer and R. W. Scholz, “What Is the Optimal and Sustainable Lifetime of a Mine?,” *Sustain. 2018, Vol. 10, Page 480*, vol. 10, no. 2, p. 480, Feb. 2018, doi: 10.3390/SU10020480.
[164] T. Terlouw, K. Treyer, C. Bauer, and M. Mazzotti, “Life Cycle Assessment of Direct Air Carbon Capture and Storage with Low-Carbon Energy Sources,” *Environ. Sci. Technol.*, vol. 55, no. 16, pp. 11397–11411, Aug. 2021, doi: 10.1021/ACS.EST.1C03263/SUPPL_FILE/ES1C03263_SI_002.ZIP.
[165] “Stripe’s first carbon removal purchases.” https://stripe.com/blog/first-negative-emissions-purchases (accessed Sep. 05, 2022).
[166] “Monitoring, reporting and verification of greenhouse gas removals (GGRs): Task and Finish Group report - GOV.UK.” https://www.gov.uk/government/publications/monitoring-reporting-and-verification-of-ggrs-task-and-finish-group-report (accessed Oct. 13, 2022).

[167] M. Mersch, C. N. Markides, and N. Mac Dowell, “The Role and Value of CCS in Integrated Heat and Power Systems of the UK,” *SSRN Electron. J.*, Nov. 2022, doi: 10.2139/SSRN.4273913.
[168] C. F. Heuberger, P. K. Bains, and N. Mac Dowell, “The EV-olution of the power system: A spatio-temporal optimisation model to investigate the impact of electric vehicle deployment,” *Appl. Energy*, vol. 257, p. 113715, Jan. 2020, doi: 10.1016/J.APENERGY.2019.113715.
[169] “2021 Corruption Perceptions Index - Explore the… - Transparency.org.” https://www.transparency.org/en/cpi/2021 (accessed Apr. 16, 2023).
[170] British Geological Survey (BGS), “United Kingdom Minerals Yearbook 2020,” 2021. Accessed: Apr. 05, 2022. [Online]. Available: https://www.bgs.ac.uk/download/united-kingdom-minerals-yearbook/.
[171] T. A. Branca *et al.*, “Reuse and Recycling of By-Products in the Steel Sector: Recent Achievements Paving the Way to Circular Economy and Industrial Symbiosis in Europe,” *Met. 2020, Vol. 10, Page 345*, vol. 10, no. 3, p. 345, Mar. 2020, doi: 10.3390/MET10030345.
[172] HM Government, “BEIS Electricity Generation Costs (2020).” https://www.gov.uk/government/publications/beis-electricity-generation-costs-2020 (accessed Nov. 10, 2021).
[173] Department for Business Energy & Industrial Strategy, “Investable commercial frameworks for Power BECCS Prepared by Element Energy and Vivid Economics,” 2021.
[174] S. Shackley, J. Hammond, J. Gaunt, and R. Ibarrola, “The feasibility and costs of biochar deployment in the UK,” *https://doi.org/10.4155/cmt.11.22*, vol. 2, no. 3, pp. 335–356, Jun. 2014, doi: 10.4155/CMT.11.22.
[175] S. Wye Energy Agency, “Greenhouse gas removal: Mersey Biochar - executive summary.”
[176] “Fossil fuel price assumptions: 2019 - GOV.UK.” https://www.gov.uk/government/publications/fossil-fuel-price-assumptions-2019 (accessed Oct. 17, 2022).
[177] P. Balcombe, K. Anderson, J. Speirs, N. Brandon, and A. Hawkes, “The Natural Gas Supply Chain: The Importance of Methane and Carbon Dioxide Emissions,” *ACS Sustain. Chem. Eng.*, vol. 5, no. 1, pp. 3–20, Jan. 2017, doi: 10.1021/ACSSUSCHEMENG.6B00144/ASSET/IMAGES/MEDIUM/SC-2016-00144C_0015.GIF.

Appendix

A. MONET optimisation equations

CAPEX formula

For each CDR solution, the total levelised CAPEX cost is determined by the number of specific-CDR plants $N_{g,t}^{CDR}$ built in region *g* at each time *t* and is discounted over time by discount rate r:

$$TotCapex_{CDR} = \sum_{g \in G} \sum_{t \in T} \frac{CAPEX^{CDR} N_{g,t}^{CDR}}{(1+r)^t} \quad \text{Eq. A 1}$$

Where $TotCapex_{CDR}$is expressed in $.

Infrastructure equation

This equation links the number of operating CDR-specific infrastructures, with the number of newly built CDR units:

$$ON_{g,t}^{CDR} = ON_{g,t-1}^{CDR} + N_{g,t}^{CDR}, \forall\, t \in T \quad \text{Eq. A 2}$$

Where $ON_{g,2025}^{CDR} = 0, \forall g \in G$, *i.e.*, we impose that no plant can be operating in the first-time step (2025) of the optimisation.

Such an equation is applied to CDR including infrastructures: BECCS, DACCS, pyrolysis (BC), mining (EW) and comminution (EW) facilities.

Material transport GHG and cost equations

Emissions due to the transport of material (biomass, rock) are the sum of all emissions caused by inter-regional and intra-regional transport. The inter-regional distance $Dist(g, g')$ is an estimate between different regions in the UK, based on the shortest distance between two regions.

The intra-regional transport corresponds to the distance $Dist_{intra}(g)$ for the material type (*i.e.*, pellet in the case of BECCS, BC and rock in the case of EW) to reach the facilities (BECCS, pyrolysis plant or cropland used to spread the rock for EW), and is estimated as the average distance between any two points within a region. The intra-regional transport is assumed to be processed by a truck as considered to be more flexible than trains to reach specific locations.

The overall formula is expressed in t_{CO2} per $t_{material}$:

$$CE_{transp,i,g}(g', l) = GHG_{i,l}^{transp} * Dist(g, g') + GHG_{i,truck}^{transp} * Dist_{intra}(g'), \quad \forall g' \in G, \forall l \in L \quad \text{Eq. A 3}$$

Finally, like for the GHG balance, the cost of transporting material from pellet facilities – respectively comminution – to BECCS plants – respectively, croplands – is divided between inter-regional and intra-regional components with similar estimates used for distances. Total cost at time *t* for material *i* can be expressed as follow, in $ per $t_{material}$:

$$Cost_{transp,i,g}(g', l) = UTC_{i,l} * Dist(g, g') + UTC_{i,truck} * Dist_{intra}(g), \quad \text{Eq. A 4}$$

$$\forall\, g' \in G, \forall\, l \in L$$

In the case of BECCS and BC, the pellet facility is assumed to be near the land where the biomass is harvested. Thus, the impact of such transport is considered negligible and not accounted for. Similarly, in the case of non-residual material for EW, we assume that both mining and comminution facilities are at the same location, thus omitting this transport component in both previous equations.

Material balance equation

The equation balancing material transfer between regions ensures the amount of material produced plus the material leaving a *region g* is equal to the material used plus the material imported in that region:

$$P_{i,g,t} + \sum_{l \in L} \sum_{g' \in G} Q_{ig'glt} = D_{i,g,t} + \sum_{l \in L} \sum_{g' \in G} Q_{igg'lt}\,, \forall g \in G, \forall t \in T, \forall i \in I \qquad \text{Eq. A 5}$$

Such an equation is applied to multiple material types: biomass for both BECCS and BC and rock material for EW.

Biomass and land use for BECCS and BC

As biomass is used for both BECCS through power generation and BC through pyrolysis, the biomass and land-use constraints are common to both solutions.

Production of bioenergy-dedicated crops within one region is equal to the marginal land area used multiplied by the biomass yield, in t_{DM} per year:

$$P_{i,g,t} = Yield_{i,g} * Area_{used}{}_{i,g,t}, \qquad \text{Eq. A 6}$$
$$for\ i \in \{miscanthus, poplar\}, g \in G, t \in T$$

The total area used for biomass growth (miscanthus or poplar) is limited by the land availability per region $Landa_{g,t}$, as follow:

$$Area_used_{miscanthus,g,t} + Area_used_{polar,g,t} \leq Landa_{g,t} \qquad \text{Eq. A 7}$$

We illustrate this equation in Figure A 1 showing the marginal land availability in the UK, using the NUTS3 region partition, extracted from a global land availability dataset [56]. Most marginal lands lie in the north of England, Scotland, and Northern Ireland, adding up to 2.1 Mha. We use the water index map from the World Resource Institute [57] to filter out all lands with an index higher than 3, which precludes most of the regions in the southeast of England. There is 2.1 Mha of marginal land. These land areas will be used as an upper bound for BECCS deployment.

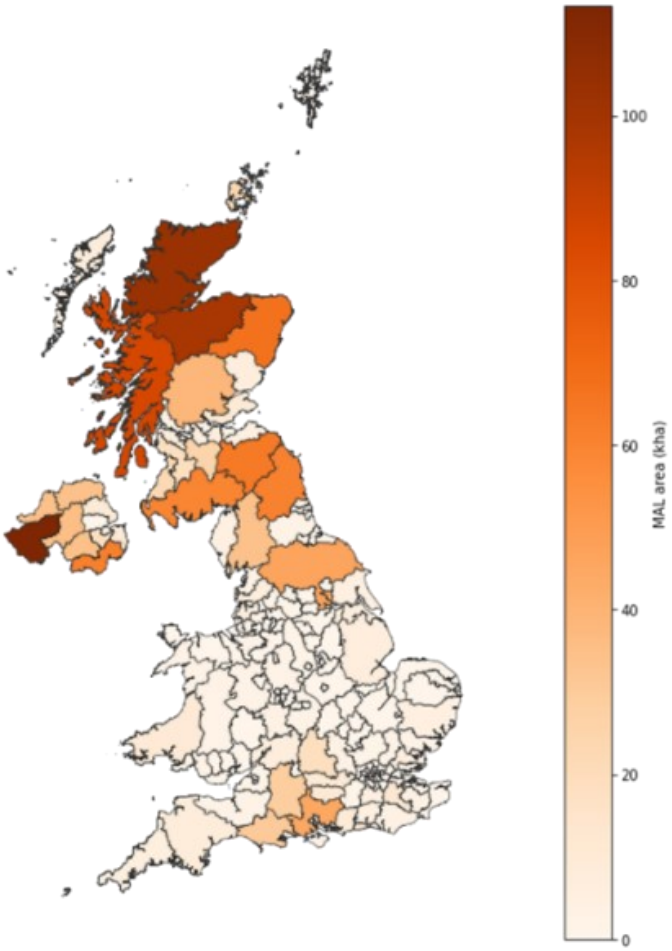


Figure A 1: Availability of marginal land in the UK for bioenergy feedstock production [56]

Biomass residues (in this study forest and crop residues) are limited based on residues national production available for bioenergy use $BA_{i,g}^{max}$:

$$P_{i,g,t} \leq BA_{i,g}^{max}, \quad for\ i \in \{crop\ resiudes, forest\ resiudes\}, g \in G, t \in T \qquad \text{Eq. A 8}$$

Forest and crop residues are assumed to be limited respectively to 1'358 and 8'247 kt per year [58].

Finally, imported pellets are limited by Ricardo's projected imported pellet availability $BA_{Imported}^{max}$ [133]:

$$\sum_{g' \in G} Q_{pel(Imp),out,g',ship,t} \leq BA_{Imp}^{max}, \quad for\ t \in T \qquad \text{Eq. A 9}$$

Here, we use Ricardo Energy and Environment's projections on imported biomass availability [133], where imports are limited to 36 Mtpa in 2030 and 7 Mtpa in 2050.

Rock availability for EW

We consider basalt, basalt fines, slag, cement kiln dust (CKD) and construction and demolition wastes (CDWaste). For basalt, the amount of rock extracted needs to satisfy the total regional availability $Rocka_{basalt,g}$:

$$\sum_{g \in G} P^{source}_{basalt,g,t} \leq Rocka_{basalt,g} \quad \text{Eq. A 10}$$

For basalt rocks that are extracted from mining sites, we estimated the number of available rocks in the UK using data from Renforth et al. (2012), corresponding to a theoretical maximum of extractable rocks in multiple UK igneous rock formations [106]:

$$Rocka_{basalt,g} = total_{mass,g} * \mathrm{p}_{\mathrm{acceptability}} * \mathrm{p}_{basaltic} \quad \text{Eq. A 11}$$

where:

- $total_{mass,g}$ is the data found in [106]
- $\mathrm{p}_{\mathrm{acceptability}}$ is the proportion of rock that could be allocated for EW purposes (as per our assumption, 1%)
- $\mathrm{p}_{basaltic}$ is the proportion of basaltic rock in igneous rock formations (as per our assumption, 50%)

For residues or by-products extracted from existing operations, we estimate the amount of annual production at the national scale and assume that a proportion could be allocated to EW operations, resulting in the following constraint:

$$\sum_{g \in G} P^{recycle}_{s,g,t} \leq Rocka_{s,g}, \text{ for } s \in \{\text{fines, slag, CKD, CDWaste}\} \quad \text{Eq. A 12}$$

The material availabilities are different for different silicate types (Eq. A 13 – Eq. A 16) :

$$Rocka_{fines,g} = P^{source}_{basalt,g,t} * p_{fines} \quad \text{Eq. A 13}$$

where:

- $p_{fines} = 20\%$ [106]

$$Rocka_{slag,g} = P_{Steel} * p_{slag} * p_{Slag-NR} \quad \text{Eq. A 14}$$

where:

- Steel production in the UK P_{Steel} (in tonne)
- The proportion of slag from steel production $p_{slag} = 11\%.7$ [170]
- The proportion of slag that is not recycled $p_{Slag-NR} = 14\%$ [171]

$$Rocka_{CKD,g} = P_{Cement} * p_{CKD-NR} \quad \text{Eq. A 15}$$

- Cement production in the UK P_{Cement} (in tonne) [170]
- The proportion of CKD not recycled $p_{CKD-NR} = 7‰$ [170]

$$Rocka_{CDWaste,g} = P_{Cement} * P_{CDWaste-NR} 1\% \quad \text{Eq. A 16}$$

- Cement production in the UK P_{Cement} (in tonne) is the same as above [170]
- The proportion of CDWaste not recycled $P_{CDWaste-NR} = 1\%$ (own assumption)

We illustrate the rock availability per region in Figure A 2. This shows both the amount of rock availability per region and the share of each rock type per region. Basalt is mostly available in the northern regions, due to the presence of mining sites[106], where the number of rocks available reaches up to 3,690 Mt_{rock} in Scotland, and 2,625 Mt_{rock} in Northern Ireland, following Eq. A 11.

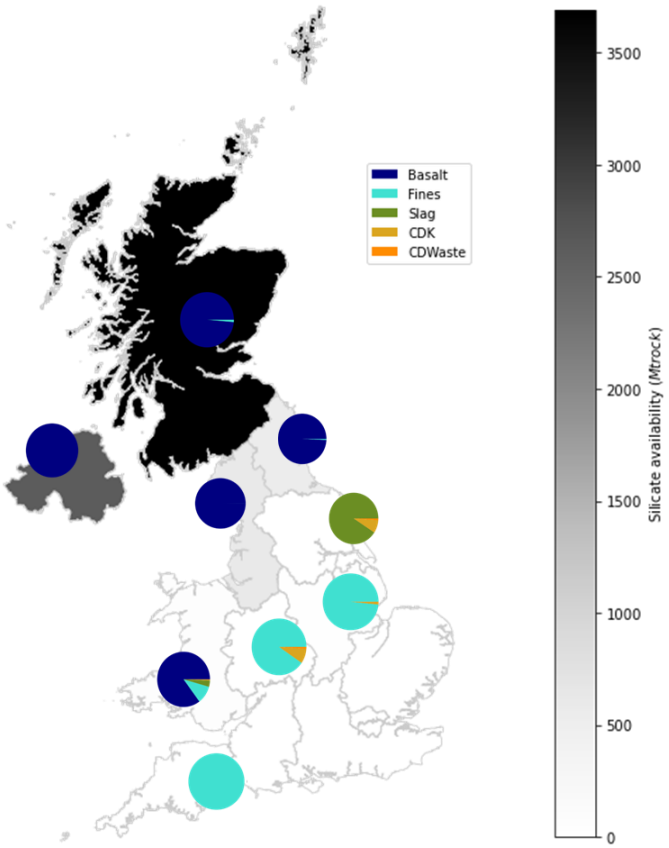


Figure A 2: Rock availability in the UK (Mt_{rock})

Finally, the amount of cropland used to spread rock particles is limited by the cropland availability that we assume corresponds to 20% of total croplands available $Cropa_g$ per region *g* in the UK (as per our assumption). We express this constraint as follows:

$$D_{s,g,t} \leq 0.2 * Cropa_g * application_rate_max, \quad \text{Eq. A 17}$$

$$\forall g \in G, \forall s \in S, \forall t \in T$$

The application rate assumed is 30 t_{rock} per ha per year, which is in the range 10-50 t_{rock} per ha per year found in the literature[108], [113], [116].

The available cropland is illustrated with a map in Figure A 3.

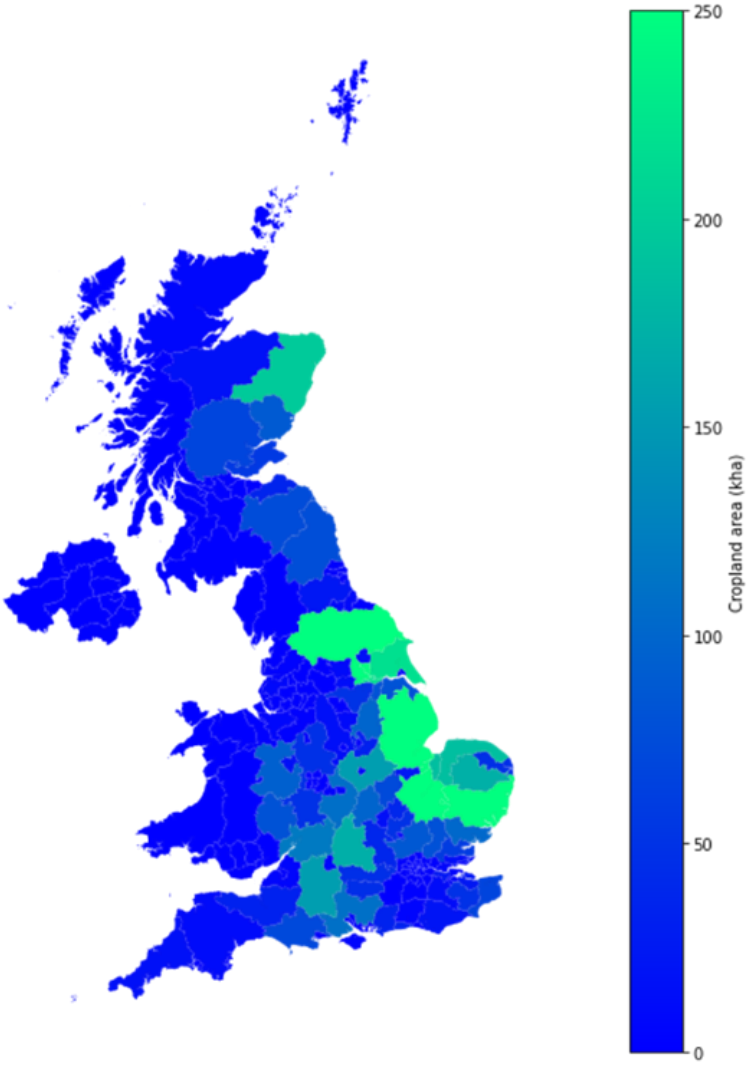


Figure A 3: Cropland availability in the UK (20% of which will be available for rock spreading)

CO_2 Transport and Storage Cost

Smith et al.[70], provide a CO_2 transport and storage analysis, giving insight into CO_2 T&S costs variations. In particular, important decision parameters to determine T&S costs are the distance of transport and the flow rate of CO2 that is transported through these pipelines. Such cost variations are illustrated in Figure A 4.

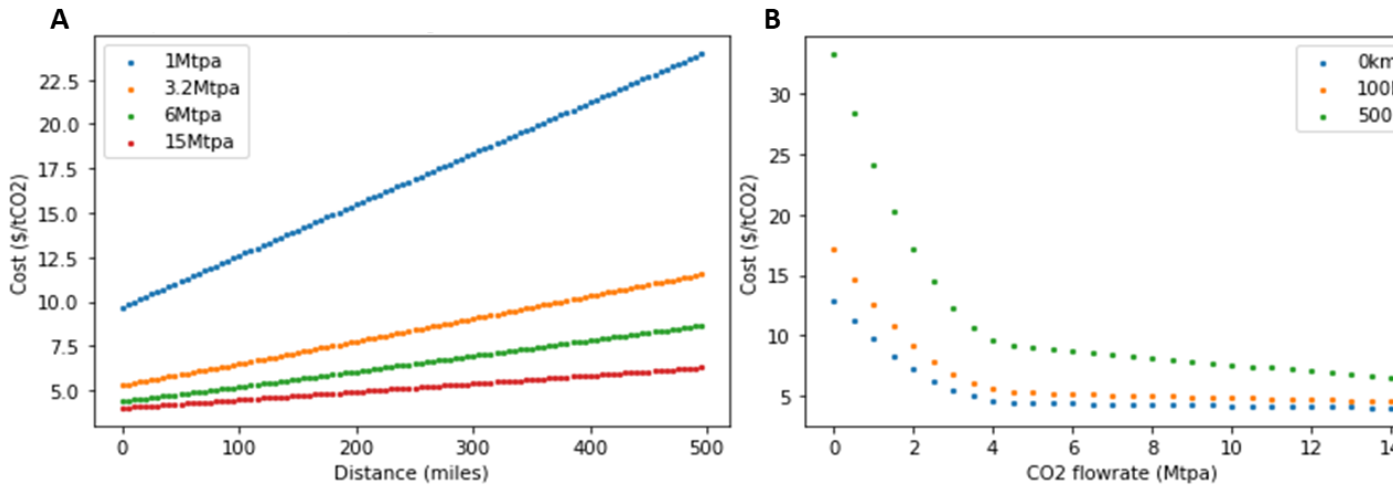


Figure A 4: CO_2 transport and storage costs depending on (A) the distance, extrapolated from [70].

Availability of CO_2 storage for the UK

The "CO_2 Stored" website provides an open-source dataset gathering data from 500 potential storage sites around the UK (*i.e.*, offshore)[72], illustrated in Figure A 5. Considering the 85 storage sites of the dataset, the cumulative potential reaches a cumulative 17.1 Gt_{CO2}, which appears to be higher than what is required by the UK, even in most optimistic scenarios (less than 1 Gt_{CO2}). Thus, this does not appear to be a constraining factor in our optimisation. However, scenarios, where other European countries use the CO2 storage resources that are in the North Sea, are likely.

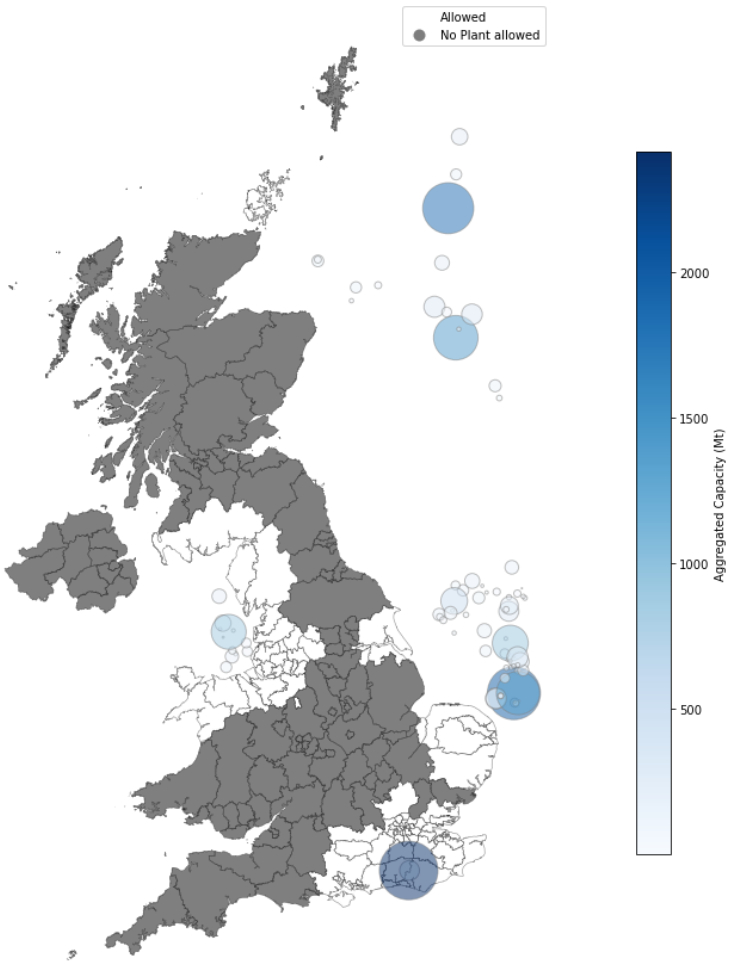


Figure A 5: Offshore storage sites and cumulative potential in the UK (Mt_{CO2})

B. Permanence results

Designed Experiments

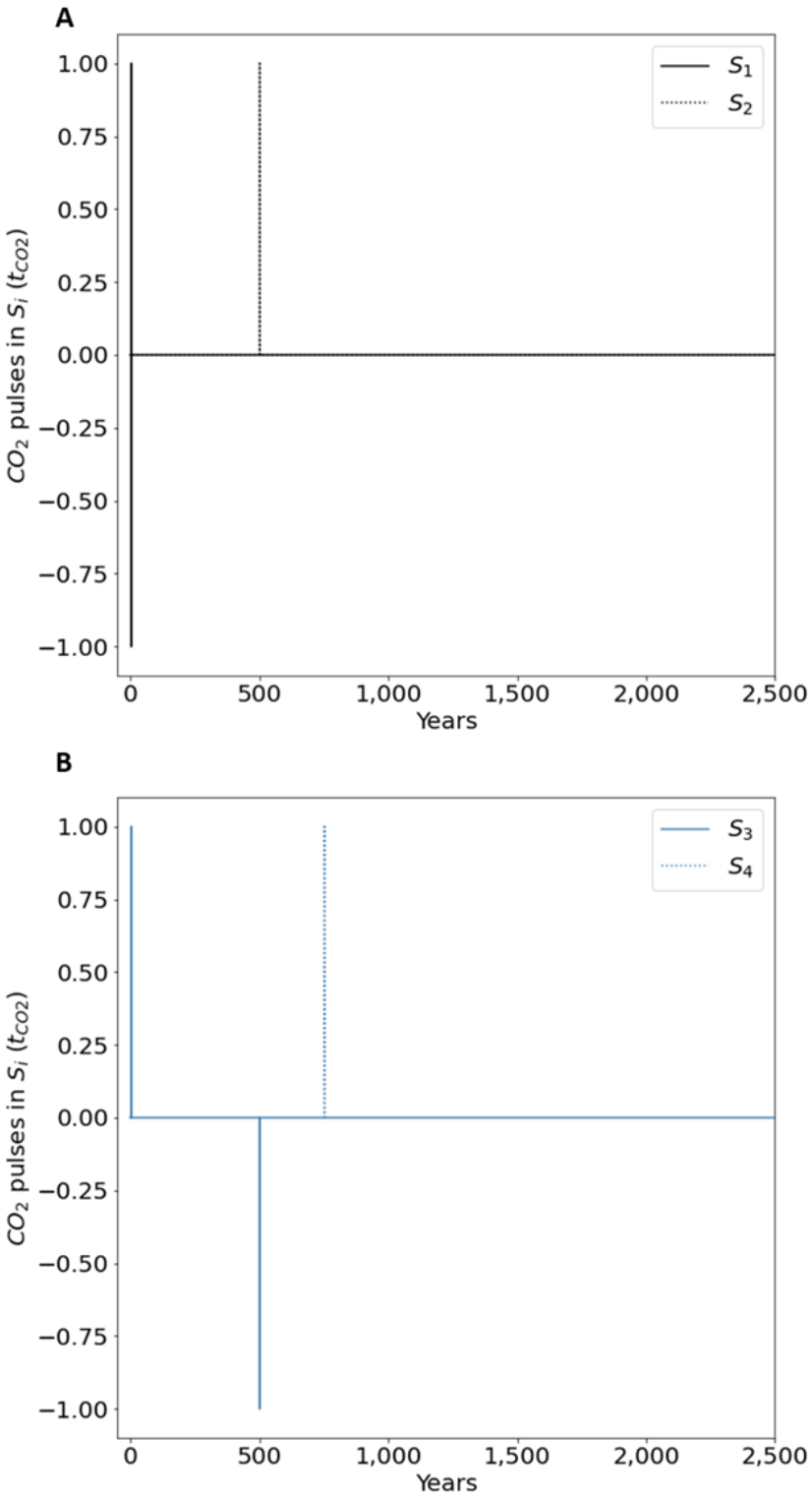


Figure A 6: Designed Experiment for four scenarios (S_1-S_4)

Climate Repair Values in the case of S_2 and S_3

We provide CRV results for both scenarios S_2 and S_2 and multiple TP assumptions in Figure A 7. Not that the values for S_2 correspond to the ones obtained *via* the Lashof method. We find that both scenarios result in correlated results:

$$CRV_{S_2,t_{leak},TP} = 1 - CRV_{S_3,t_{rem},TP}, \text{ if } t_{leak} = t_{rem}.$$

This shows the benefit of delaying the leakage date for temporary removals, is the same as hasting the permanent removal of an emission.

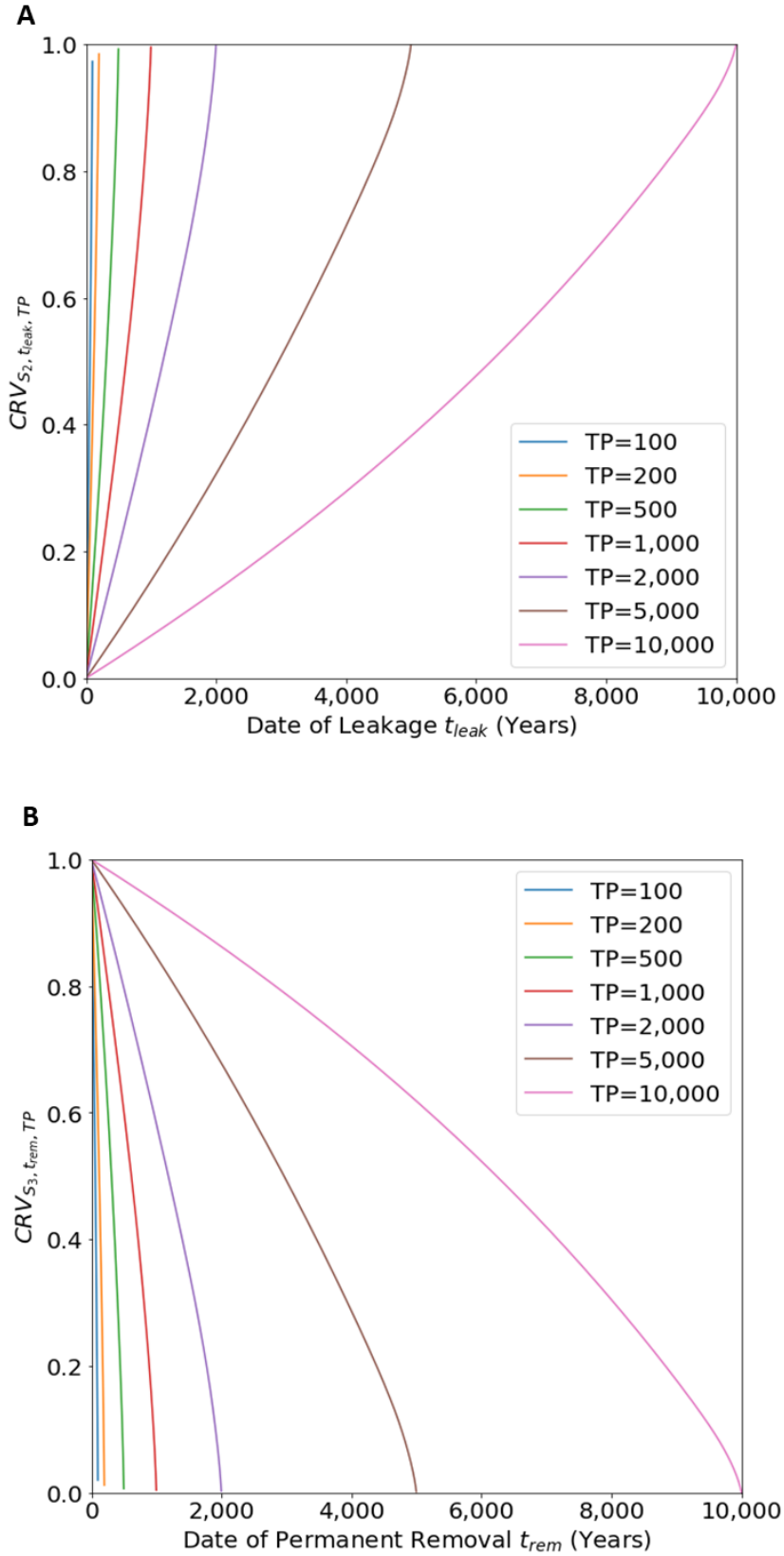


Figure A 7: Climate Repair Values (CRV) for scenario S2 and S3

(A) as a function of the date of leakage t_{leak} for scenarios S_2 and (B) as a function of the date of permanent removal t_{rem} for scenario S_3.

Climate Repair Values in the case of S_2 and S_4

In Figure A 8, we compare the CRV results for scenarios S_2 and S_4, multiple TP assumptions, and 3 different t_{rem} values for S_4, 100, 500 and 3,000 years. In this study, we aim at measuring the avoided damages of temporary removals, with different leakages dates. This corresponds to scenario S_2 presented in the Climate Repair Value (CRV) subsection of the result section. Here, we comment and conclude similar measures associated with scenario S_4: an emission at t_0, followed by a non-permanent removal t_{rem} years later, and a following leakage at year t_{leak}. For each individual TP value, we display four CRV lines to provide the evolution of the avoided damage (between 0 and 1) for different leakage dates t_{leak}. The solid line is for scenario S_2, as discussed in Figure S2.A. The three others are for scenario S_4 and for different t_{rem} values, *i.e.*, delaying the non-permanent removal date. We find that for a fixed date of leakage t_{leak}, delaying the removal date decreases the repaired damage associated with scenario S_4. This is justified because the duration of the temporary removal $t_{leak} - t_{rem}$ is shortened, as t_{leak} is fixed.

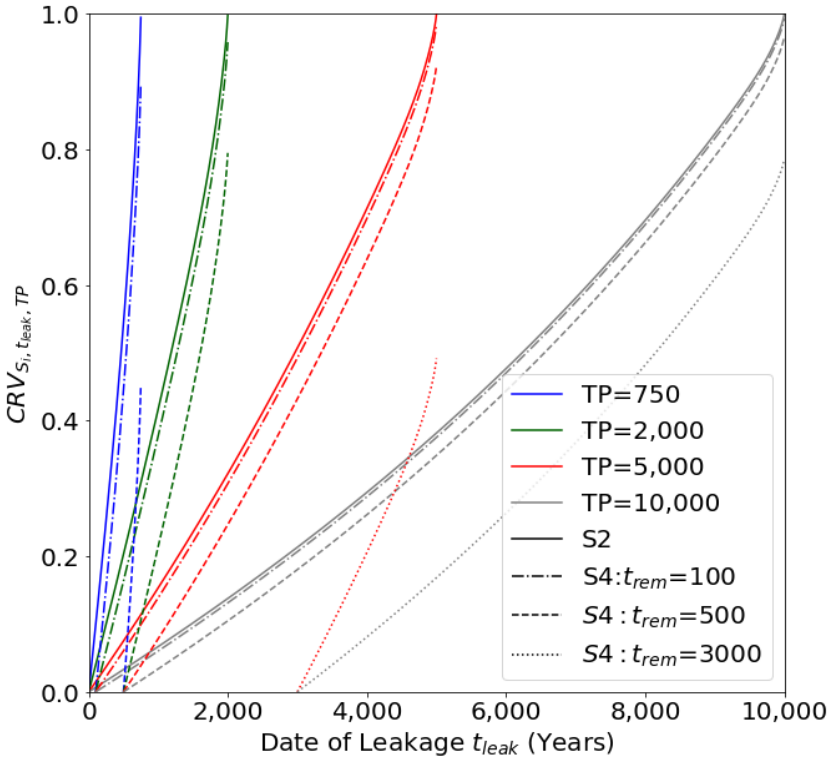


Figure A 8: Climate Repair Values (CRV) for scenarios S2 and S4
CRV values are explored as a function of the date of leakage t_{leak} for scenario S_2 and S_4.

Permanence data for current CDR market projects

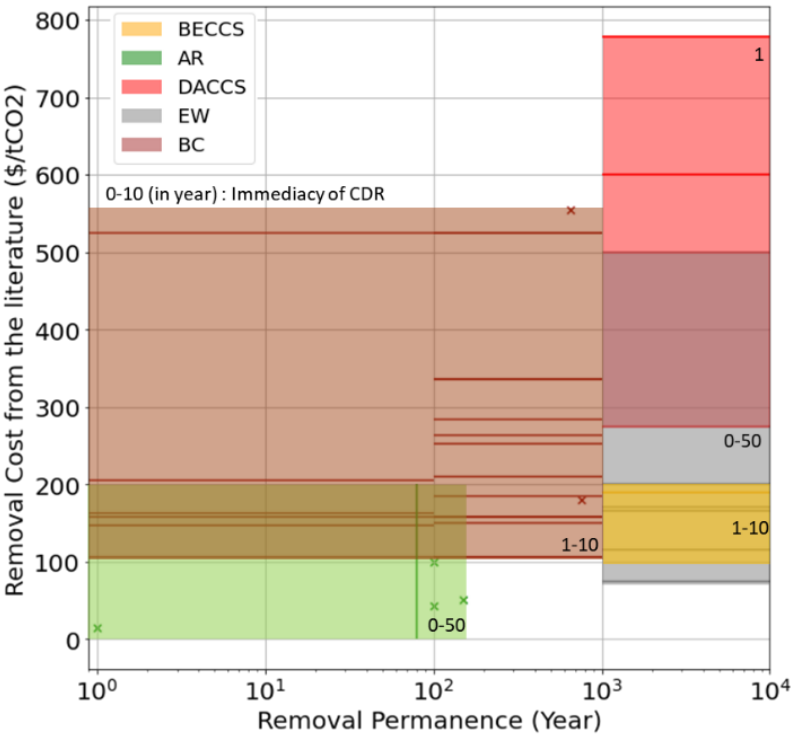


Figure A 9: Market costs versus claimed permanence.
Current market[10], [165] and literature[52] removal costs, compared to their claimed permanence. We also display the immediacy of CDR solutions, describing the duration over which the CO_2 capture occurs.

Table A 1: CDR infrastructure data

	CAPEX	non-variable OPEX	Hurdle Rate	Revenues[b]
BECCS plant	4,180 $/kW[172][,a]	5 $/MWh[172][,a]	9%[173]	Power
DACCS plant - Liquid Solvent	1,600 $/$t_{CO2}$[87]	116 $/$t_{CO2}$[87]	15%[c]	-
DACCS plant - Solid Sorbent	1,814 $/$t_{CO2}$[88]	361 $/$t_{CO2}$[88]	15%[c]	-
Pyrolysis plant - Biochar	9.5717 M$[174]	505,104 $/year[174]	9%[175]	Bio-Oil
Mining & comminution facility - Enhanced Weathering	5 $/$t_{rock}$/year[111]	21.64 $/$t_{rock}$[111]	-[d]	-

[a]We use a conversion of 1£~1.2$. [b]We consider no revenues from carbon sequestration in this study. [b]Own assumptions. [c]No hurdle rate is given because CAPEX values provided by the reference are already levelised.

Table A 2: Pellet and biomass data ([22], [23])

	$Cbio_i$, Carbon Content (t_C per t_{DM}) [22]	Embodied Emissions (t_{CO2} per t_{DM})[23]	Energy Density (MJ per t)[23]
Miscanthus	0.478	0.272	18,400
Crop residues	0.48	0.224	18,700
Forest residues	0.4	0.268	15,120
Imported pellets	0.4181	0.224	18,700

Table A 3: Pellet cost and conversion rate

	Unit production cost of pellets UPC_i (£/t_{pellet})[a] [23]	Pellet conversion rate (%) [23]
Miscanthus	49	83.7
Crop residues	60	83.7
Forest residues	20	83.7

[a]Currency considered is 2019£.

Table A 4: Fuel Data

	Price	Carbon Footprint
Power	100 $/MWh[74]	19 t_{CO2}/MWh[a]
Compressed Natural Gas (CNG)	0.009 $/MJ[176]	11 g_{CO2}/MJ[177]
Miscanthus	59 $/t[23][,b]	47 tC/t[22]
Forestry Residues	24 $/t[23][,b]	42 tC/t[22]

[a]2021 carbon footprint of the UK power system [b]We use a conversion of 1£~1.2$

Table A 5: DACCS assumptions

	CO_2 Captured (t_{CO2}/hr/plant-module)	Input Heat (GJ EC/hr/plant-module)	Input Power (kWh EC /hr/plant-module)	Land Footprint (ha/t_{CO2} captured) [86]
DACCS-Liquid Sorbent	110.74[87]	587[87]	40921[87]	1.37*1e-3
DACCS-Solid Sorbent	0.21[a]	1.6[a]	143[a]	1*1e-5

[a]Our own calculations from [88]